

Structure and Bonding 156

Series Editor: D.M.P. Mingos

David Scheschkewitz *Editor*

Functional Molecular Silicon Compounds II

Low Oxidation States

 Springer

156

Structure and Bonding

Series Editor:

D.M.P. Mingos, Oxford, United Kingdom

Editorial Board:

F.A. Armstrong, Oxford, United Kingdom

X. Duan, Beijing, China

L.H. Gade, Heidelberg, Germany

K.R. Poeppelmeier, Evanston, IL, USA

G. Parkin, New York, USA

M. Takano, Kyoto, Japan

For further volumes:

<http://www.springer.com/series/430>

Aims and Scope

The series *Structure and Bonding* publishes critical reviews on topics of research concerned with chemical structure and bonding. The scope of the series spans the entire Periodic Table and addresses structure and bonding issues associated with all of the elements. It also focuses attention on new and developing areas of modern structural and theoretical chemistry such as nanostructures, molecular electronics, designed molecular solids, surfaces, metal clusters and supramolecular structures. Physical and spectroscopic techniques used to determine, examine and model structures fall within the purview of *Structure and Bonding* to the extent that the focus is on the scientific results obtained and not on specialist information concerning the techniques themselves. Issues associated with the development of bonding models and generalizations that illuminate the reactivity pathways and rates of chemical processes are also relevant

The individual volumes in the series are thematic. The goal of each volume is to give the reader, whether at a university or in industry, a comprehensive overview of an area where new insights are emerging that are of interest to a larger scientific audience. Thus each review within the volume critically surveys one aspect of that topic and places it within the context of the volume as a whole. The most significant developments of the last 5 to 10 years should be presented using selected examples to illustrate the principles discussed. A description of the physical basis of the experimental techniques that have been used to provide the primary data may also be appropriate, if it has not been covered in detail elsewhere. The coverage need not be exhaustive in data, but should rather be conceptual, concentrating on the new principles being developed that will allow the reader, who is not a specialist in the area covered, to understand the data presented. Discussion of possible future research directions in the area is welcomed.

Review articles for the individual volumes are invited by the volume editors.

In references *Structure and Bonding* is abbreviated *Struct Bond* and is cited as a journal.

David Scheschkewitz
Editor

Functional Molecular Silicon Compounds II

Low Oxidation States

With contributions by

B. Blom • M. Driess • S. Ishida • T. Iwamoto • C. Präsang •
E. Rivard • D. Scheschkewitz • M. Unno

 Springer

Editor
David Scheschkewitz
Chair of General and Inorganic Chemistry
Saarland University
Saarbrücken
Germany

ISSN 0081-5993 ISSN 1616-8550 (electronic)
ISBN 978-3-319-03733-2 ISBN 978-3-319-03734-9 (eBook)
DOI 10.1007/978-3-319-03734-9
Springer Cham Heidelberg New York Dordrecht London

Library of Congress Control Number: 2014931517

© Springer International Publishing Switzerland 2014

This work is subject to copyright. All rights are reserved by the Publisher, whether the whole or part of the material is concerned, specifically the rights of translation, reprinting, reuse of illustrations, recitation, broadcasting, reproduction on microfilms or in any other physical way, and transmission or information storage and retrieval, electronic adaptation, computer software, or by similar or dissimilar methodology now known or hereafter developed. Exempted from this legal reservation are brief excerpts in connection with reviews or scholarly analysis or material supplied specifically for the purpose of being entered and executed on a computer system, for exclusive use by the purchaser of the work. Duplication of this publication or parts thereof is permitted only under the provisions of the Copyright Law of the Publisher's location, in its current version, and permission for use must always be obtained from Springer. Permissions for use may be obtained through RightsLink at the Copyright Clearance Center. Violations are liable to prosecution under the respective Copyright Law.

The use of general descriptive names, registered names, trademarks, service marks, etc. in this publication does not imply, even in the absence of a specific statement, that such names are exempt from the relevant protective laws and regulations and therefore free for general use.

While the advice and information in this book are believed to be true and accurate at the date of publication, neither the authors nor the editors nor the publisher can accept any legal responsibility for any errors or omissions that may be made. The publisher makes no warranty, express or implied, with respect to the material contained herein.

Printed on acid-free paper

Springer is part of Springer Science+Business Media (www.springer.com)

Preface

Due to its unique properties, elemental silicon is a pivotal material in modern society. Even though a few other semiconductors, e.g., gallium arsenide, rival silicon in some performance indicators such as electron mobility, none of them can equally meet the technological and economic demands of current microprocessor technology: Electronic grade silicon is available at relatively low cost and its native oxide as an insulator is predisposed to effectively separate the conducting zones of microprocessors [1]. In this arguably most important application, silicon is thus present both in the elemental state (oxidation No. 0) and in its most highly oxidized form (oxidation No. +IV). In view of the prominent role of molecular silicon compounds in related industrial processes, this volume of *Structure&Bonding* is devoted to *Functional Molecular Silicon Compounds* with silicon in various oxidation states. It is divided into two sub-volumes: the first covers topics associated to silicon compounds in the “regular” oxidation state of +IV, while the second concerns compounds in lower oxidation states.

All industrial chemical processes involved in the production/purification/transformation of silicon in its elemental form have in common that silicon in lower oxidation states is prevalent in short-lived intermediates such as silylenes and larger unsaturated aggregates [2]. The chapter by Burgert Blom and Matthias Driess (Technical Universität Berlin, Germany) summarizes recent advances in the chemistry of stable silylenes, molecular compounds in the formal oxidation state +II (Volume 2, chapter titled “Recent Advances in Silylene Chemistry: Small Molecule Activation En-Route Towards Metal-Free Catalysis”). Saturated and unsaturated silicon clusters are several steps further on the way towards elemental silicon. Recent years have seen important progress with regard to the functionalization of stable derivatives of such clusters as well as the realization of surprising new structural motifs. In chapter titled “Substituted Polyhedral Silicon and Germanium Clusters” of Volume 2 Masafumi Unno (Gunma University, Kiryu, Japan) gives an account of the developments in this area. It is probably just a question of time before silicon clusters will be routinely connected to extended systems with exciting new properties as novel materials. Oligosilane chains are predisposed as linking

units for such an endeavor. Christoph Marschner (University of Graz, Austria) updates comprehensively on the preparation and functionalization of oligosilane systems in chapter titled “Oligosilanes” of Volume 1.

Initially, the research into molecular silicon compounds was driven by the mostly academic question of how much the chemistry would parallel that of its lighter cousin carbon. Naturally, the stability of unsaturated derivatives was at the center of attention. Frederic Stanley Kipping – generally considered to be one of the most influential pioneers of organosilicon chemistry – eagerly pursued the synthesis of “silico ethylenes” [3] and “silicones” [4] – the heavier analogues of alkenes and ketones, respectively. The first reliable reports on stable compounds with heavier double bonds to silicon, however, only appeared in 1981. Since these milestone achievements on compounds with Si=Si (West et al.) [5] and Si=C bonds (Brook et al.) [6], the chemistry of molecular silicon compounds has matured considerably. Especially during the first decade of the new millennium the focus has shifted from the replication of well-known carbon motifs from organic chemistry to the introduction and tolerance of functional groups. The contribution by Takeaki Iwamoto and Shintaro Ishida (Tohoku University, Sendai, Japan) gives an overview of recent developments regarding Si=Si double bonds (Volume 2, chapter titled “Multiple Bonds with Silicon: Recent Advances in Synthesis, Structure, and Functions of Stable Disilenes”).

With the powerful concept of stabilization of reactive main group species by strongly σ -donating *N*-heterocyclic carbenes pioneered inter alia by Greg Robinson [7], some of Kipping’s initial targets are now available as derivatives stabilized by coordination of *N*-heterocyclic carbenes. Eric Rivard (University of Alberta, Edmonton, Canada) summarizes this emerging new field from the point of view of low valent silicon chemistry in chapter titled “Recent Advances in the *Heterocyclic Carbene-Supported Chemistry of Silicon*” of Volume 2. Interestingly, however, *N*-heterocyclic carbenes were initially employed by Kuhn et al. for the expansion of the coordination sphere of molecular silicon compounds beyond the usual four substituents [8]. Since it is now well established that this expansion does not entail hypervalency, low valent compounds with higher coordination numbers are one possible approach to increase the functionality of hypercoordinate silicon species. The various aspects of higher coordinate silicon compounds are comprehensively reviewed by Jörg Wagler, Uwe Böhme, and Edwin Kroke (Technical University Bergakademie Freiberg, Germany) in chapter titled “Higher-Coordinated Molecular Silicon” of Volume 1.

Having been unsuccessful in the original tasks, Kipping became disillusioned regarding any commercial value of his discoveries towards the end of his career [9]. As Thomas Edison said, however, “just because something doesn’t do what you planned it to do does not mean it’s useless” (As quoted in: [10]). Kipping’s discoveries indeed laid the foundations for the nowadays ubiquitous application of polysiloxanes (colloquially known as silicones) in daily life. Silsequioxanes – already mentioned by Kipping as formally having the empirical formula of an anhydride $(R_2SiO)_2O$ [9] – are increasingly being used as precursors for sophisticated hybrid materials involving polysiloxanes. In his chapter, Guido Kickelbick (Saarland University, Saarbrücken,

Germany) gives an overview of the fundamental sciences and high-end applications of silsesquioxanes (Volume 1, chapter titled “Silsesquioxanes”).

Finally, two chapters are devoted to the most extreme of functionalization: ionization. The generation of silyl cations and anions provides valuable synthons, e.g., for the further extension of the silicon scaffold. In chapter titled “Silylium Ions” of Volume 1, Thomas Müller (University of Oldenburg, Germany) summarizes the many applications of silylium cations in catalysis and discusses recent trends towards low valent silicon cation chemistry thus completing the full circle to other chapters that are more explicitly devoted to low valent silicon species. Finally, the chemistry of silyl anions is summarized in chapter titled “Silyl Anions” of Volume 2.

Initially, only one volume was envisaged for the topic of functional molecular silicon chemistry, but it rapidly became clear that with the dedicated hard work and enthusiasm of all authors two volumes would be needed to accommodate the vast progress in that area during the last 10 years: the field keeps growing in an exponential manner. The ready availability of this exiting element at very low cost paired with the inquisitiveness and passion of organosilicon chemists will ensure that this trend continues for a long time to come.

Saarbrücken, Germany
September 2013

David Scheschkewitz

References

1. Meindl JD, Chen Q, Davis JA (2001) Limits on silicon nanoelectronics for terascale integration. *Science* 293:2044
2. Ravasio S, Masi M, Cavalotti C (2013) Analysis of the gas phase reactivity of chlorosilanes. *J Phys Chem A* 117:5221
3. Kipping FS (1911) Derivatives of silicoethane and silicoethylene. *Proc Chem Soc* 27:143
4. Kipping FS, Lloyd LL (1901) XLVII.-Organic derivatives of silicon. Triphenylsilicic and alkyloxysilicon chlorides. *J Chem Soc Trans* 79:449
5. West R, Fink MJ, Michl J (1981) Tetramesityldisilene, a stable compound containing a silicon–silicon double bond. *Science* 214:1343
6. Brook AG, Abdesaken F, Gutekunst B, Gutekunst G, Kallury RK (1981) A solid silaethene: isolation and characterization. *J Chem Soc Chem Commun* 191
7. Wang Y, Robinson GH (2011) Carbene stabilization of highly reactive main-group molecules. *Inorg Chem* 50:12326
8. Kuhn N, Kratz T, Blaeser D, Boese R (1995) Derivate des Imidazols, XIII. Carben-Komplexe des Siliciums und Zinns. *Chem Ber* 128:245
9. Kipping FS (1937) The Bakerian lecture. Organic derivatives of silicon. *Proc R Soc Lond A* 159:139
10. Finn C (2001) Artifacts: an archaeologist’s year in silicon valley first. MIT, Boston, p 90

Contents

| | |
|--|-----|
| Silyl Anions | 1 |
| Carsten Präsang and David Scheschkewitz | |
| Substituted Polyhedral Silicon and Germanium Clusters | 49 |
| Masafumi Unno | |
| Recent Advances in Silylene Chemistry: Small Molecule Activation En-Route Towards Metal-Free Catalysis | 85 |
| Burgert Blom and Matthias Driess | |
| Multiple Bonds with Silicon: Recent Advances in Synthesis, Structure, and Functions of Stable Disilenes | 125 |
| Takeaki Iwamoto and Shintaro Ishida | |
| Recent Advances in the <i>N</i>-Heterocyclic Carbene-Supported Chemistry of Silicon | 203 |
| Eric Rivard | |
| Index | 229 |

Silyl Anions

Carsten Präsang and David Scheschkewitz

Abstract The last 10 years have witnessed tremendous advances in the field of silyl anion research. New methods for the synthesis of alkali metal silanides have been added to the toolboxes of organic, inorganic, and materials chemistry and further established their important role as protecting groups, building blocks, and useful reagents. The sheer number of recent publications in high-ranking journals alone demonstrates a pronounced interest in these species by the scientific community. Particularly, the isolation and complete characterization of highly reactive silyl anions and dianions, previously considered merely as fleeting intermediates, have been the starting point for a rich and exciting chemistry with the prospect of many more outstanding contributions from synthetic, theoretical, and materials chemistry.

Keywords Cluster compounds · Silicon · Silyl anions · Silylenoids

Contents

| | | |
|-----|--|----|
| 1 | Introduction | 2 |
| 2 | Acyclic and Cyclic Silyl Anions | 4 |
| 2.1 | Monosilanyl to Oligosilanyl Anions | 4 |
| 2.2 | Chiral Silyl Anions | 10 |
| 2.3 | Zwitterionic Silyl Anions | 14 |
| 2.4 | α -Functionalized Silyl Anions: Silylenoids | 17 |
| 3 | Silyl Dianions | 22 |
| 3.1 | Geminal Silyl Dianions | 22 |
| 3.2 | Silole Monoanions and Dianions | 25 |
| 4 | Unsaturated Systems, Small Rings, and Clusters | 25 |
| 5 | Soluble Zintl Anions | 35 |
| 6 | Conclusion | 37 |
| | References | 38 |

Abbreviations

| | |
|-----------------|---|
| [2.2.2]cryptand | 4,7,13,16,21,24-Hexaoxa-1,10-diazabicyclo[8.8.8]hexacosan |
| Ar | Aryl |
| Bn | Benzyl |
| Bu | Butyl |
| Cp | Cyclopentadienyl |
| Cp* | Pentamethylcyclopentadienyl |
| DME | 1,2-Dimethoxyethane |
| ee | Enantiomeric excess |
| Et | Ethyl |
| HMPA | Hexamethylphosphoric triamide |
| i-Pr | Isopropyl |
| LDA | Lithium diisopropylamide |
| LTMP | Lithium 2,2,6,6-tetramethylpiperidide |
| Me | Methyl |
| Mes | Mesityl, 2,4,6-trimethylphenyl |
| Np | 1-Naphthyl |
| Ph | Phenyl |
| PMDTA | <i>N,N,N',N',N''</i> -pentamethyldiethylenetriamine |
| Pr | Propyl |
| rt | Room temperature |
| SET | Single electron transfer |
| Tbt | 1,3,5-Tris(bis(trimethylsilyl)methyl)phenyl |
| <i>t</i> -Bu | <i>Tert</i> -butyl |
| THF | Tetrahydrofuran |
| Tip | 2,4,6-Tri(<i>isopropyl</i>)phenyl |
| TMEDA | <i>N,N,N',N'</i> -tetramethyl-1,2-ethylenediamine |
| TMP | 2,2,6,6-Tetramethylpiperidyl |
| Tol | 4-Methylphenyl |

1 Introduction

Silyl anions, also referred to as silanides, are anionic silicon species with a lone pair of electrons at the silicon center. The negative charge is compensated by a counter cation. As in the case of well-known carbanions this cation might (1) be directly coordinated to the anionic center (**I**) or (2) be separated from the latter by coordinating solvent molecules (**II**) or suitable intramolecular donor sites (**III**) (Fig. 1). Donor-stabilized silicon(**II**) species (**IV**) are not included in this chapter because the ylidic charges at the silicon center and the donor group are only formal. Important recent contributions to this field are summarized in Chaps. 5 and 10 of this volume.

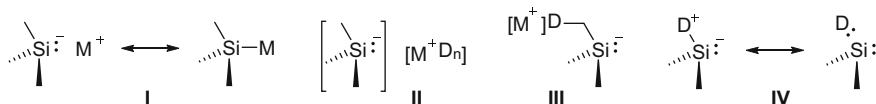


Fig. 1 Silyl anions **I–III** and a donor-stabilized silicon(II) compounds **IV**

Table 1 Frequently used functional groups for the synthesis of silyl anions and the prevalent methods of transformation, $E^{IV} = \text{Si, Ge, Sn}$

| | functional group | common methods |
|--------------|------------------|-------------------------------------|
| V | X = Cl, Br | direct synthesis |
| | H | metalation, deprotonation |
| | M' | transmetalation |
| | Ph | reductive cleavage |
| | $E^{IV}R_3$ | transmetalation, reductive cleavage |

The first organosilicon compound was prepared as early as 1863 by Friedel and Crafts via salt metathesis reaction of silicon tetrachloride and carbon nucleophiles, the very type of reaction still utilized today most frequently for silicon–carbon bond formation at the laboratory scale [1]. In contrast, it took until the 1930s for the first reports on successful generation and derivatization of silyl anions to appear [2, 3]. At that time, the overall progress in organosilicon chemistry was far from encouraging, prompting a rather pessimistic outlook on its prospects by Kipping as one of the pioneers of the field in his famous Bakerian lecture [4]. Against the backdrop of the seminal discoveries of Müller and Rochow regarding the Direct Process [1] for the industrial production of methyl chlorosilanes, the work by Gilman and others [5, 6] served to spark new interest in silyl anions as well. It became more and more obvious that anionic silicon reagents are excellent building blocks for the synthesis of novel organosilanes, thus providing valuable precursors for, e.g., organic, inorganic, and materials chemistry.

The majority of silyl anions studied to date exhibit a trigonal pyramidal geometry at the anionic silicon center with a high degree of pyramidalization due to the increased *s*-character of the Si lone pair compared to carbanions. Silyl anions with an almost trigonal planar geometry can be obtained primarily by employing very bulky, electropositive substituents. The bonding between the metal cation and the silyl anion will be depicted as formalized Lewis structures throughout most of this chapter for the sake of clarity, even though the interactions can vary from somewhat covalent to purely ionic in nature. The coordination numbers of anionic silicon centers in solution are quite often unknown and depend inter alia on the nature of the solvent and the respective metal cation. Illustrative examples will be presented throughout this review.

Silyl anion research focused on the generation and simple transformations of these species for many decades. A considerable and still increasing number of methods has been developed for the transformation of various functional groups into silicon centered anions (Table 1).

Commercially available organosilicon compounds **V** quite often exhibit more than one substituent **X** that can readily be converted to a silicon–metal bond (Table 1; **X** = halide, hydride, phenyl, etc.). The functional group tolerance of reaction conditions has therefore to be taken into account to avoid undesired side reactions. While the range of employed solvents includes simple hydrocarbons such as heptane as well as highly polar systems such as HMPA, the majority of silyl anions have been prepared in THF and DME solution. Several reviews covering the chemistry of silyl anions as a whole or certain of its aspects have been published in recent years [7–15]. As a consequence, in this chapter we will mainly focus on contributions from the last decade, but will include older publications where appropriate.

2 Acyclic and Cyclic Silyl Anions

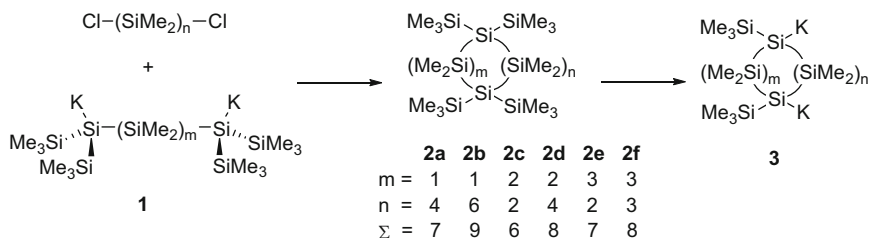
2.1 Monosilanyl to Oligosilanyl Anions

Reliable, straightforward, and high yielding synthetic steps are crucial for the successful implementation of complex and economic syntheses. Although the generation of silyl anions by cleavage of Si–Si bonds in disilanes and oligosilanes with alkali metal alkoxides has in principle been known for a long time [16, 17], it has recently developed into a versatile tool for the generation of silyl anions. Silyl ethers are systematically produced as byproducts in these reactions, which are usually to unreactive to interfere with subsequent transformations and – in addition – are readily removed if required. In particular, for silyl potassium compounds this route is one of the methods of choice and is routinely applied for the synthesis of branched and cyclic oligosilanes.

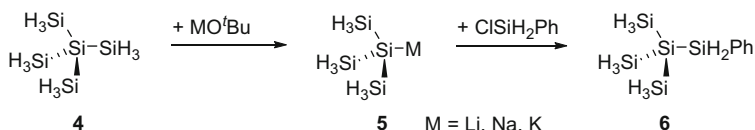
Oligosilanes are attractive synthetic targets for materials chemistry in view of their σ -bond delocalization. α,ω -(Hypersilyl)silanes (hypersilyl = tris(trimethylsilyl)silyl) turned out to be ideal starting materials for the synthesis of monocyclic and bicyclic silanes as well as for α,ω -(cyclosilyl)silanes. The former were transformed into dipotassium α,ω -silandiides **1** in THF, DME, or toluene/18-crown-6 solution with potassium *tert*-butoxide and subsequently cyclized with dichlorosilanes (Scheme 1) or by oxidation with 1,2-dibromoethane [18–20].

Cyclosilanes **2a–f** exhibit two endocyclic Si(SiMe₃)₂ moieties that are suitable for the generation of cyclic dianions **3** under conditions similar to the synthesis of dianions **1**. Successive reactions of dianions **3** gave access to various bicyclosilanes and other derivatives. The 1,1'-ferrocenylene unit [21] and SiH₂/SiBr₂ moieties [22] have also been incorporated into oligosilanes.

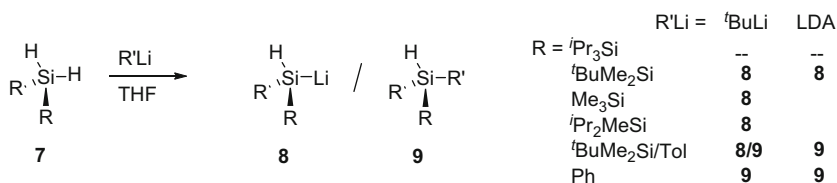
Silicon hydrides are of special interest for the deposition of elemental silicon films. As Stueger et al. reported, the cleavage of SiH₃ groups by alkoxides can equally well be utilized for the synthesis of perhydrogenated oligosilyl anions [23].



Scheme 1 Synthesis of cyclosilanes **2a–f** from α,ω -dipotassium silanides **1** and α,ω -dichlorosilanes, Σ = ring size of cyclosilanes **2a–f**



Scheme 2 Cleavage of neopentasilane with alkali metal *tert*-butoxides and synthesis of phenylsilane **6** from silanide **5**

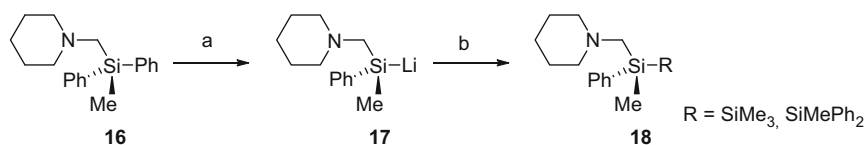


Scheme 3 Reaction of dihydrosilanes **7** with *tert*-butyllithium and LDA to yield silyl anions **8*** and substitution products **9**, “*” analyzed as R₂SiHMe after quenching with MeI

Neopentasilane, **4**, reacted cleanly in coordinating solvents with alkali metal *tert*-butoxides (M = Li, Na, K) and with LDA under cleavage of one Si–Si bond to give the corresponding silyl anion salts **5**. Reaction of **5** with chlorosilanes yielded new pentasilanes, e.g., phenylpentasilane **6** from silyl anion **5**·Li and chlorophenylsilane (Scheme 2). More details on the topic of oligosilanes can be found in Chap. 8 of this volume.

Deprotonation of silanes is not very common and was generally limited to cases where the polarity of the Si–H bond had been reversed by electronegative substituents on silicon. As had been observed before in the case of potassium hydride [24], *tert*-butyllithium and LDA react with dihydrosilanes by nucleophilic substitution at the silicon center [25, 26]. However, proton abstraction is a competing reaction and the preference of a given dihydrosilane depends mostly on its substitution pattern.

The sterically most hindered dihydrosilane (R = ⁱPr₃Si) did not react with *tert*-butyllithium or LDA at –40°C in THF solution (Scheme 3). The least hindered



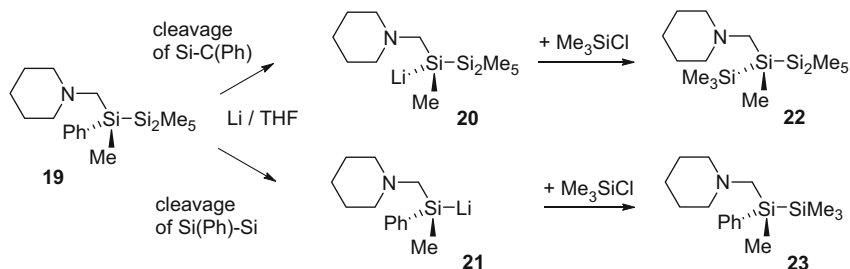
Scheme 6 Selective cleavage of a Si–C(phenyl) bond in diphenylsilane **16** and synthesis of disilanes **18**. (a) Li, THF, -50°C ; (b) +RCl, $-\text{LiCl}$

Silyl anions **14** and **15** were neither isolated nor analyzed by spectroscopic methods, but reacted with dimethyl sulfate, trimethylsilyl chloride, or sources of H^+/D^+ and characterized as the corresponding trapping products instead. Computations on simplified model compounds (methyl instead of aryl substituents at silicon) predict two resonance structures **15** (Scheme 5): a boratasilene with a short B–Si bond and a somewhat planar Si center and a borylsilyl anion (boron-stabilized silyl anion) with a longer Si–B bond and a more pyramidalized Si center. π -Donating substituents on boron favor a borylsilyl anion structure that exhibits a smaller rotational barrier around the Si–B bond and high-field ^{11}B and ^{29}Si NMR chemical shifts. The computations agree well with experimental data of the first structurally characterized boratasilene reported earlier by Sekiguchi et al. [29]. The same group also reported the generation of a silyl anion by 1,2-addition of methyllithium to a disilene [30].

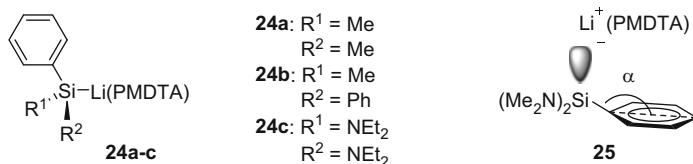
The reductive cleavage of Si–Si bonds with alkali metals in polar solvents such as THF requires at least one phenyl substituent on silicon. Therefore, trialkylsilyl anions cannot be prepared from the corresponding trialkyl(halo)silanes directly, because the intermediate hexaalkyldisilanes are inert toward further reduction under these conditions. A known side reaction during the treatment of phenylsilanes with lithium metal in polar solvents is the reductive cleavage of phenyl–silicon bonds [31]. Strohmman et al. were able to show that this reaction can be utilized for the conversion of diphenylsilane **16** to silyl anion **17** and eventually the syntheses of disilanes **18** in high yield (Scheme 6) [32]. They extended this method to the generation of enantiomerically enriched silanes via chiral lithiosilanes [33] (see also Sect. 2.2).

In a subsequent paper, Strohmman et al. showed that reductive cleavage of Si–Si and Si–C(phenyl) bonds can be competing in phenyl substituted disilanes. Reaction of disilanes **19** with lithium metal in THF followed by silylation with chlorotrimethylsilane yielded a mixture of tetrasilane **22** and disilane **23** (Scheme 7) [34].

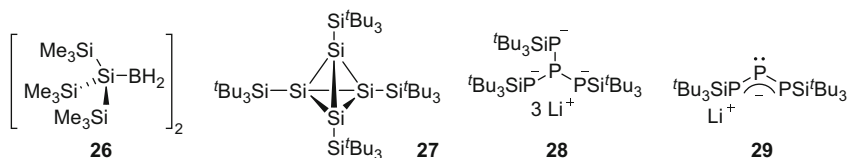
A kinetic study revealed that the formation of silyl anion **20** is favored over silyl anion **21** at lower temperatures and the product ratio of silanes **22:23** changed from 60:40 at 45°C to 85:15 at -78°C . Quantum chemical calculations for several of the disilanes and trisilanes under investigation show that their LUMO and the SOMO of the corresponding radical anions are mostly located within the aromatic phenyl substituent. A SET to the phenyl group, which is believed to be the initial step of the bond cleavage, weakens the Si–Si and Si–C(phenyl) bonds.



Scheme 7 Competing cleavage of Si-Si and Si-C(phenyl) bonds in trisilane **19** and synthesis of disilane **23** and tetrasilane **22** via silyl anions **20**, **21**



Scheme 8 Lithium silanides **24a-c** with bent phenyl substituents and model compound **25**

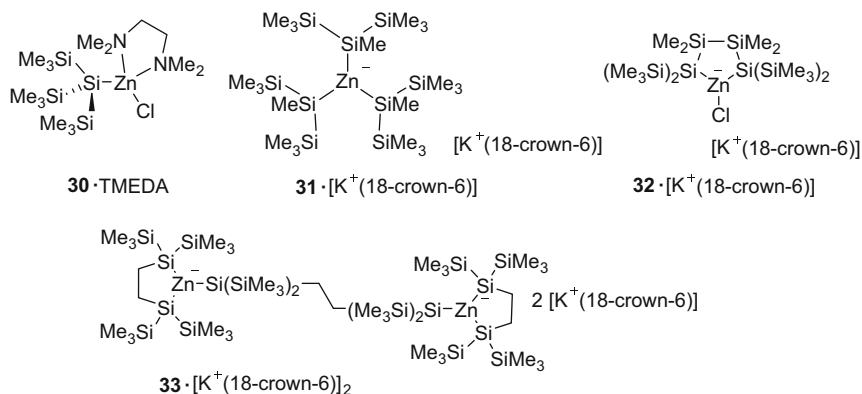


Scheme 9 Main group compounds **26-29** (groups 13-15) synthesized with the aid of silyl anions

An unexpected bending of one phenyl substituent was observed in the X-ray crystal structures of three lithium (phenyl)silanides **24a-c** [35]. Silanides **24a-c** were designed by Strohmann et al. to exhibit monomeric structures in the solid state by aid of the tridentate ligand *N,N,N',N',N''*-pentamethyldiethylenetriamine (PMDTA) (Scheme 8).

The torsion angles Si-C_{*i*}-C_{*o*}-C_{*m*} or dihedral angles α, respectively, with values of 170-176° are significantly smaller than the expected 180°. The same phenomenon had been observed for other phenyl substituted heavier group 14 anions and even isoelectronic group 15 compounds. An explanation for such angular deviations was found by quantum chemical calculations of bis(amino)silyl anion **25** and two additional model compounds. Pauli repulsion between the HOMO (silicon lone pair) and the HOMO-1/HOMO-3 (HOMO of the phenyl moieties) is minimized by bending of the phenyl substituent.

Silyl anions have been employed for the syntheses of many hitherto unknown main group compounds and transition metal complexes in recent years (Scheme 9). A complete review of this topic is beyond the scope of this chapter and only a



Scheme 10 Monomeric silylzinc chloride **30**·TMEDA and silylzincates **31**–**33**

selected number of examples is shown in the following. The first silylborane R_3Si-BH_2 **26** without coordination of an external Lewis base to the boron center was reported in 2010 by Marschner et al. [36]. Compound **26** is accessible from potassium hypersilanide and borane triethylamine complex and exhibits a dimeric diborane(6) structure in the solid state with two bridging hydrogen atoms. A one-pot procedure for the synthesis of Wiberg's tetrasilatetrahedrane **27** [37] from trichlorosilane and sodium supersilanide $[NaSi(Si^tBu_3)_3]$ was published in 2009 [38]. The activation of white phosphorous with silyl anions has been studied extensively during the last 10 years [39]. Among others, tetraphosphane trianion **28** was isolated from the reaction of P_4 and lithium supersilanide [40] and converted to previously reported triphosphene monoanion **29** [41] and an elaborate chemistry was developed around these compounds [42–44].

The syntheses, reactivities, and structures of alkali metal [45–47] and alkaline earth metal silanides [48–51, 52N] have been topic of several important studies in the last decade. Silylzinc compounds are known since the 1960s [53] and today they are very important silyl transfer agents with many applications in synthesis and catalysis. Investigations into their structures, however, are scarce. Symmetrical bis(silyl)zinc compounds with very bulky substituents exhibit a linear or almost linear arrangement of the central Si_2Zn unit and can be prepared by reaction of zinc halides with alkali metal silanides [54–57] or from hydrosilanes and dialkylzinc compounds [58]. Moreover, structures of one tetrameric silylzinc bromide with a $[Zn_4Br_4]$ -heterocubane core [55] and two dimeric silylzinc chlorides with additional coordinating THF molecules were reported [59]. Utilization of the bidentate ligand TMEDA allowed for the structural characterization of the monomeric (hypersilyl)zinc chloride complex **30**(TMEDA) with a tetrahedrally coordinated zinc center (Scheme 10) [57].

Bis(silyl)zinc centers tend to increase their coordination number by complex formation with halides, solvent molecules [21], or additional equivalents of silanides to form zincates if the steric demand of the substituents is not too high

or the Si–Zn–Si moiety is forced to an unusual small angle due to ring strain. The exclusive formation of tris(silyl)zincate **31**·[K⁺(18-crown-6)] was observed in the reaction between zinc chloride and the corresponding potassium silanide. The chloro zincate **32**·[K⁺(18-crown-6)] can be regarded as a KCl complex of a cyclic bis(silyl)zinc compound [57]. Similar observations had been reported some years earlier with the preferential synthesis of bis(zincate) **33**·[K⁺(18-crown-6)]₂ from an ethylene-bridged potassium bis(silanide) and zinc chloride [60]. Zincates **32** and **33** exhibit approximately trigonal planar coordination spheres at the zinc center in the solid state.

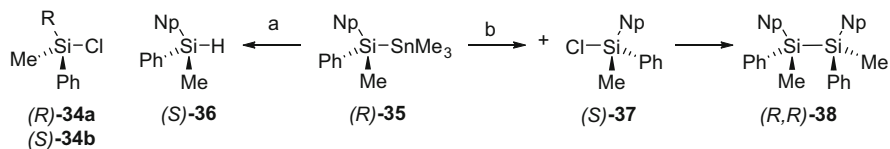
2.2 Chiral Silyl Anions

Optically active silyl anions are potentially useful reagents for organic synthesis and materials chemistry. Due to the significant higher inversion barrier of silyl anions in solution in comparison to carbanions, configurational stability might be expected even at ambient temperature. Research in this area started in the 1960s and 1970s [61, 62]. In principle, all synthetic methods suitable for the generation of achiral silyl anions are also applicable to the preparation of chiral silanides even though inversion of configuration or even racemization occasionally occurs.

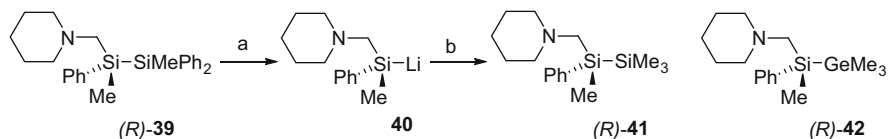
Kawakami et al. investigated several promising reactions starting from enantiomerically enriched (*R*),(*S*)-chlorosilanes **34a,b** [63]. The direct conversion by reaction with lithium metal in THF turned out to be unsuitable and led either to a mixture of products ((*R*)-**34a**) or racemization ((*S*)-**34b**) (Scheme 11).

Experiments employing less vigorous conditions for the generation of chiral silyl anions, however, were more successful. The cleavage of Si–Si bonds with lithium metal and Si–Sn bonds with methyllithium yielded optical active products after hydrolysis with only little to moderate racemization. Stannylsilane (*R*)-**35** (ee = 90%) was converted at low temperature to silane (*S*)-**36** (ee = 88%) via the corresponding silyl anion with almost no loss of chiral information. Racemization of chiral silyl anions increases with temperature and already takes place at –78°C. The same starting material and experimental conditions were used for the synthesis of disilanes and tetrasilanes with two chiral centers. Cleavage of stannylsilane (*R*)-**35** with methyllithium and subsequent reaction with chlorosilane (*S*)-**37** yielded disilane (*R,R*)-**38** with an overall ee of 40% [64]. An inversion of configuration of the chiral chlorosilane (*S*)-**37** during coupling with the chiral silyl anion was assumed.

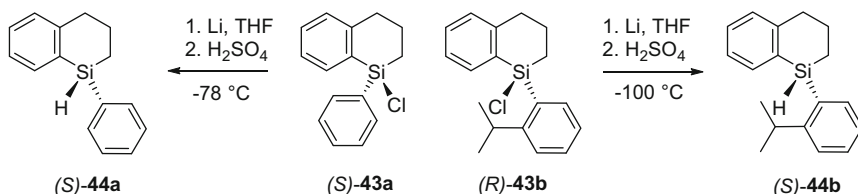
As reported by Strohmman et al. disilane (*R*)-**39** was transformed into the corresponding chiral silyl anion **40** with lithium metal in THF at –70°C. However, no assumption concerning the absolute configuration of anion **40** was made. Reaction with chlorotrimethylsilane to yield disilane (*R/S*)-**41** under variable conditions revealed that a very high ee of 98% can be obtained if solutions of anion **40** are prepared immediately before use. Furthermore, racemization of lithium silanide **40** is suppressed almost completely even at ambient temperature



Scheme 11 Chiral chlorosilanes **34a,b** and conversion of stannylsilane (*R*)-**35** to enantiomerically enriched silane (*S*)-**36** and disilane (*R,R*)-**38**, **34a**: R = 1-naphthyl, **34b**: R = ⁿBu. (a) +eLi, hydrolysis; (b) +MeLi



Scheme 12 Synthesis of disilane (*R*)-**41** from disilane (*R*)-**39** via lithio silanide **40**. (a) Li, THF, -78°C ; (b) +Me₃SiCl

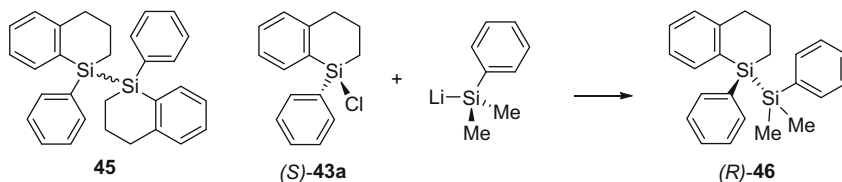


Scheme 13 Conversion of enantiomerically enriched chlorosilanes **43a,b** to silanes **44a,b** by reduction with lithium metal and subsequent protonation

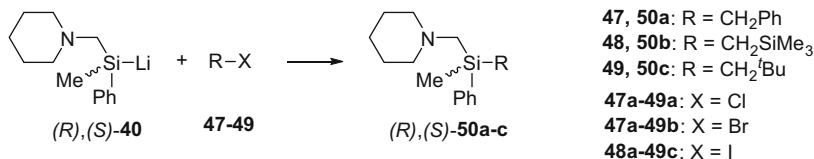
by transmetalation with magnesium bromide (Scheme 12) [33, 65, 66]. The generation of silyl anions by reductive cleavage of Si–Ph bonds in enantiomerically enriched phenyl substituted disilanes can also yield products with high ee values [32, 33].

In further studies, the Strohmann group found that excellent ee values are obtained by partially substituting silicon with germanium. The Si–Ge bond of trimethylgermylsilane (*R*)-**42** (ee = 96%) is cleaved in a similar way to eventually yield an enantiomerically enriched trisilane (ee = 96%) after trapping of the intermediate lithosilane with a chlorosilane [67].

The stereoselective conversion of chiral chlorosilanes to chiral lithio silanides has the distinct advantage that no reactive organometallic byproducts in stoichiometric amounts are formed. A detailed study by Oestreich et al. concerning the generation and racemization of silyl anions prepared via this route allows for some fundamental insights [68]. Enantiomerically enriched cyclic chlorosilanes (*S*)-**43a** (ee = 92%) and (*R*)-**43b** (ee = 98%) react with lithium at low temperatures to yield silanes (*S*)-**44a** (inversion, ee = 10%) and (*S*)-**44b** (retention, ee = 42%), respectively, after protonation of the initially formed silyl anions with sulfuric acid (Scheme 13).



Scheme 14 Disilane intermediate **45** with undefined stereochemistry and reaction of chlorosilane **(S)-43** with lithium dimethyl(phenyl)silane to yield disilane **(R)-46** with inversion of configuration



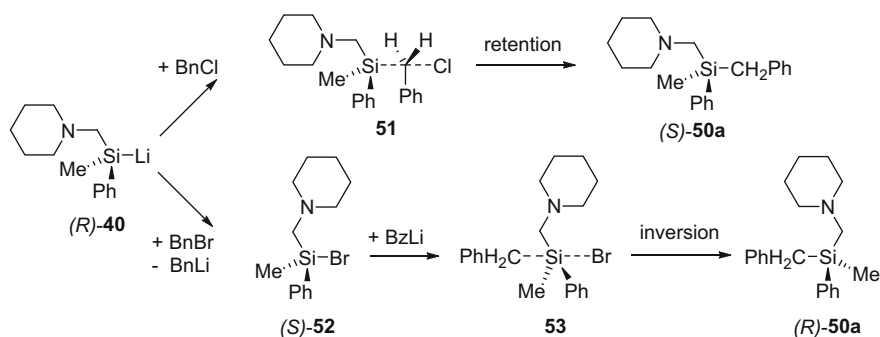
Scheme 15 Synthesis of enantiomerically enriched silanes **50a-c** from silyl anions **(R),(S)-40** and carbon electrophiles **47-49**

Two important reasons for the almost complete to moderate racemization of compounds **44a,b** were identified by Oestreich and co-workers. The presence of lithium chloride that arises from the reaction in stoichiometric amounts causes a considerable loss of chiral information even at -78°C (**43a**) or -20°C (**43b**), respectively. The increased steric hindrance around the silicon center of chlorosilane **(R)-43b** reduces racemization, which is believed to proceed via a chloride-induced pseudorotation involving a pentacoordinate silicon center. The absolute configurations of silanes **(R)-43b** and **(S)-44b** were confirmed by single crystal X-ray diffraction analyses.

The non-stereospecific formation of disilanes **45** as intermediates in the synthesis of silane **(S)-44a** also causes a decrease of the enantiomeric excess for silane **44a**. Notably, no such disilane intermediate was observed during the reduction of chlorosilane **(R)-43b**.

The nucleophilic substitution of chlorosilane **(S)-43a** (ee = 92%) with dimethyl(phenyl)silyl lithium to yield disilane **(R)-46** (ee = 84%) proceeds under inversion of the chiral silicon center (Scheme 14) [68].

Substitution reactions of enantiomerically enriched lithium silanide **(R),(S)-40** (Scheme 12) and sp^3 hybridized halocarbon nucleophiles **47-49** can involve either an inversion or retention at silicon (Scheme 15) [69, 70]. According to Strohmam et al. the preferred pathway depends on the nature of the halogen substituent. Chloro compounds **47a-49a** yielded product mixtures with excesses of the corresponding enantiomers **50a** under retention of configuration at the silicon centers. In contrast, bromo electrophiles **47b-49b** and iodo electrophiles **48c,49c** gave excesses of the enantiomers **50b** and **50c**, respectively, with inverted silicon centers (Scheme 15).



Scheme 16 Formation of chiral silanes $(R),(S)$ -**50a** from lithium silanide (R) -**40** and benzylhalides via transition states **51**, **53** and bromosilane (S) -**52**

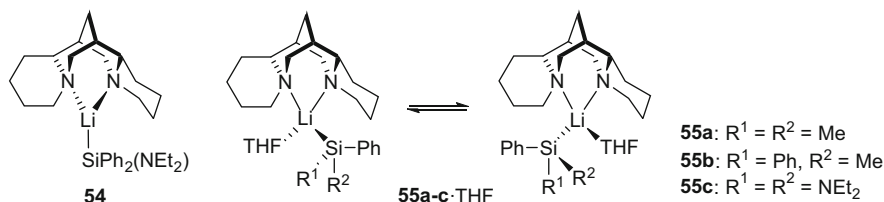
In most cases chloro electrophiles **47a–49a** gave higher selectivities than bromo and iodo electrophiles **47b,c–49b,c**. Reaction of silyl anion (R) -**40** with benzylchloride (product: (S) -**50a**, ee = 88%) and benzylbromide (product: (R) -**50a**, ee = 90%) as well as reaction of silyl anion (S) -**40** with (chloromethyl) trimethylsilane, **48a**, (product: (R) -**50b**, ee = 100%) gave the overall best results. Supported by computations, mechanisms for the observed stereoselectivities were suggested.

As demonstrated for the reaction of lithium silanide (R) -**40** with benzylchloride and benzylbromide (Scheme 16), two different transition states, **51/53**, are involved. The coupling of silyl anion (R) -**40** with benzylchloride proceeds via transition state **51** and formal inversion of the benzyl methylene moiety. Therefore, the product, silane (S) -**50a**, has the same configuration as silyl anion (R) -**40**. The first step of the reaction between silanide (R) -**40** and benzylbromide is a metal-halogen exchange to yield bromosilane (S) -**52** and benzyllithium. The latter attacks bromosilane (S) -**52** from the backside and yields silane (R) -**50a** with inversion of configuration at the silicon center via transition state **53**.

Main byproducts of the above reactions are disilanes $(R),(S)$ -**39** (Scheme 12), originating from the coupling of halosilanes of type **52** and lithium methyl (diphenyl)silanide, which is generated in equimolar amounts during synthesis of $(R),(S)$ -**40**.

Utilization of bidentate ligand $(-)$ -sparteine for the induction of chirality into nonchiral lithium alkyls is an established method. Four different complexes of $(-)$ -sparteine with silyl anions (**54**, **55a–c**·THF) have been isolated and characterized by single crystal X-ray diffraction in the Strohmamm group (Scheme 17) [71, 72].

Complexes **55a–c**·THF exhibit an additional chiral center due to the coordination of one molecule of THF to the lithium center in the solid state. In each case, only one diastereomer was detected in solution by NMR spectroscopy even though DFT calculations predict only small energy differences between the isomers. Detailed ^{29}Si NMR studies suggest that the Si–Li bonds of all complexes persist in solution on the NMR time-scale.



Scheme 17 Chiral (–)-sparteine complex **54** and diastereomeric complexes **55a–c**-THF

2.3 Zwitterionic Silyl Anions

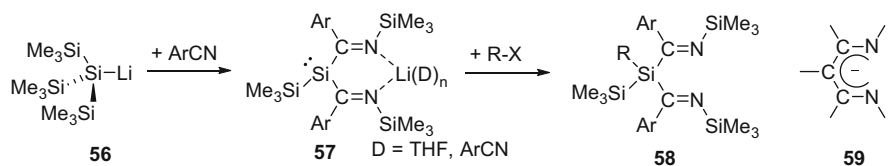
Silyl anions described in Sects. 2.1 and 2.2 exhibit either short silicon–metal contacts (contact ion pairs) or they are solvent separated ion pairs. Alternatively, the coordination of the metal cation of silanides with internal donor groups offers certain advantages: (1) the silicon lone pair is uncoordinated and therefore directly available for complexation of, e.g., transition metal centers or other substrates and (2) the solubility in nonpolar solvents is higher in comparison to solvent separated ion pairs.

The first such compound was obtained by Lappert et al. through reaction of hypersilyl lithium, **56**, with 2,6-dimethylbenzocnitrile (Scheme 18) [73]. Formal dual insertion of nitrile functionalities into Si–Si bonds via 1,2-addition of lithium silanide **56** to a C–N triple bond and subsequent 1,3-silyl shift yields zwitterionic compounds **57**. Amount and type of additional donor molecules D depend on reaction conditions and workup.

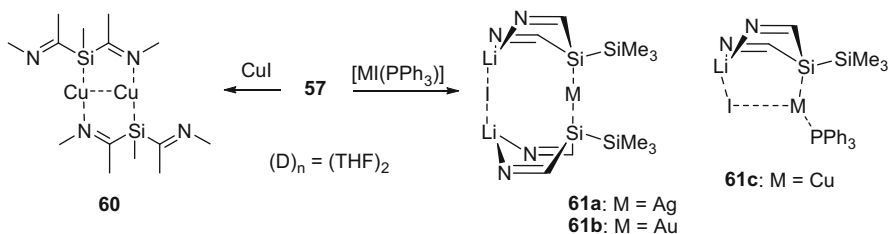
A single crystal X-ray diffraction study revealed that silyl anion **57** ($D_n = (\text{ArCN})_2$) is strongly pyramidalized at the silicon center and exhibits C–N double and Si–C single bonds. In contrast, the widely used β -diketiminato ligands **59** feature a planar C_3N_2 central core with a delocalized π -system. Other alkali metal silanides obtained in the Lappert group through transmetallation of zwitteranion **57** ($(D)_n = 2 \text{ THF}$) with alkali metal *tert*-butoxides ($M = \text{Na}, \text{K}, \text{Rb}$), however, exhibit dimeric structures with short intermolecular Si–M distances in the solid state [74]. Further examples of β -diketiminato-like “naked” silyl anions were prepared from bromosilanes **58** ($R = \text{Br}$) and magnesium [75]. Reactions of anion **57** ($(D)_n = 2 \text{ THF}$) with electrophiles gave the corresponding bis(imines) **58** with tetracoordinate silicon atoms [74]. A comparable reactivity was observed for β -diketiminates **59** on several occasions.

Furthermore, lithium silanide **57** ($(D)_n = (\text{THF})_2$) was employed as starting material for the syntheses of some silyl coinage metal complexes **60**, **61a–c** (Scheme 19) [76].

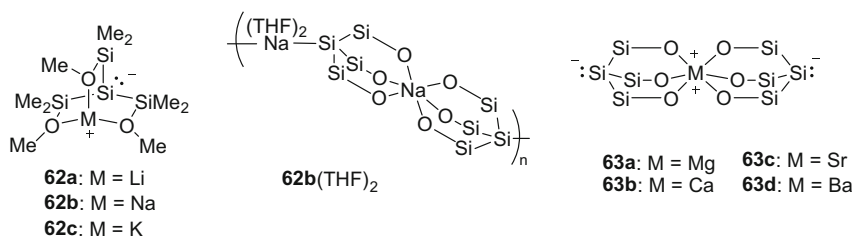
Complexes **61a–c** can be considered as being composed of the corresponding coinage metal silyl complex incorporating one equivalent of lithium iodide. Further stabilization is achieved by either coordination of anion **57** (**61a,b**) or triphenylphosphine (**61c**).



Scheme 18 Synthesis of zwitterions **57** by reaction of lithium hypersilanide, **56**, with ArCN (Ar = 2,6-Me₂C₆H₃) and conversion to silanes **58** (R = H, Cl, Br, SiMe₃, SnMe₃), β-diketiminato framework **59**



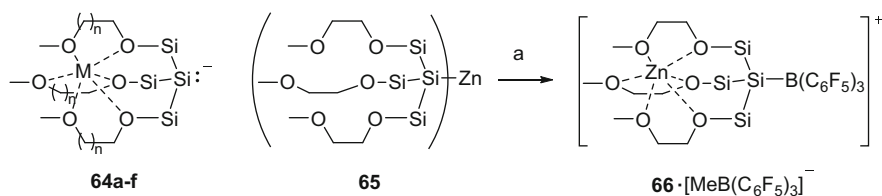
Scheme 19 Synthesis of coinage metal complexes **60**, **61a-c** from zwitterion **57**



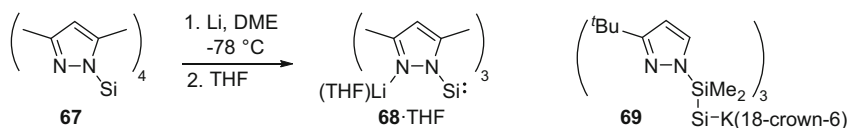
Scheme 20 Zwitterionic silyl anions **62a-c** and **63a-d**, for **62b**(THF)₂, **63a-d**: Si = Me₂Si (except bridgehead Si), O = OMe

In 2008, Krempner et al. reported zwitterionic systems with multiple ether donor groups. The initial approach employed anions of tris(methoxysilyl) ethers **62a-c** [77]. NMR studies suggest that compounds **62a-c** are monomeric in [D₈]THF solution and that the alkali metal cations are coordinated by the methoxy groups thus forming a bicyclo[2, 2, 2]octane-like core with a “naked” anionic silicon center (Scheme 20). In the solid state, however, zwitterion **62a** forms infinite one-dimensional chains through intermolecular Si-Li coordination. Sodium silanide **62b**(THF)₂ features a zigzag arrangement of monoanionic spirocyclic bicyclooctane units ([L₂Na]⁺) in the X-ray crystal structure. Na⁺(THF)₂ moieties serve as linking units for the spirocyclic cores.

The capability of two separate tris(methoxysilyl) ethers to coordinate a single metal cation was utilized for the synthesis of the first zwitterionic silanides with two “naked” anionic silicon centers **63a-d** (Scheme 20). DFT calculations on model



Scheme 21 Zwitterionic silyl anions **64a–f** ($M = \text{Li}, \text{Na}, \text{K}, n = 1, 2$) and formation of Lewis acid complex **66**·[MeB(C₆F₅)₃][−] from bis(silyl)zinc **65**. (a) + Me₂Zn, + 2 B(C₆F₅)₃



Scheme 22 Synthesis of zwitterionic silyl anion **68**·THF from tetrapyrazolylsilane **67** and lithium, tetrapyrazolylsilyl anion **69**

compounds revealed that the HOMO is located at the negatively charged Si atom in each case. Furthermore, the positive charge at the metal centers decreases from Mg to Ba while the calculated positive charges of the corresponding M(H₂O)₆ complexes increase from Mg to Ba [78].

In subsequent investigations, Krempner et al. found that self-aggregation of related alkali metal silanides is prevented by use of suitable tris(silyl) ethers with three additional donor functionalities [79]. The metal cations of silyl anions **64a–f** are coordinatively saturated (Scheme 21) and the zwitterions are monomeric in the solid state as has been evidenced by single crystal X-ray diffraction for four of the six new compounds. Some of the zwitterionic silanides were investigated with regard to their coordination behavior toward Lewis acids [79, 80].

Selected zwitterions **64** form stable complexes with B(C₆F₅)₃, AlMe₃, W(CO)₅, and ZnMe₂. The synthesis of zinc bis(silanide) **65** involves transmetalation of the corresponding potassium zwitterion with zinc chloride. Subsequent treatment with dimethylzinc and B(C₆F₅)₃ yielded the cationic Lewis acid complex **66**·[MeB(C₆F₅)₃][−].

A third example of zwitterionic silanides is closely related to previously known zwitterionic complexes with “naked,” sp³-hybridized carbon centers [81–83]. As Breher et al. demonstrated, three pyrazolyl groups efficiently establish remote coordination of the Li⁺ counter cation in silanides as well as in the corresponding carbon compounds. Tetrapyrazolylsilane **67** was converted to silanide **68** with lithium powder in DME at low temperature (Scheme 22). The primary product seems to be polymeric, presumably composed of indefinite chains with close Si–Li contacts similar to zwitterion **62a** [84]. Addition of THF allows for the isolation of THF-coordinated silyl anion **68**·THF that according to NMR spectroscopy and single crystal X-ray diffraction features a “naked” anionic silicon center both in

solution and the solid state. Reactions of silyl anion **68**·THF with silicon and tin electrophiles gave the expected coupling products with Si–Si and Si–Sn bonds.

In the case of homo-extended tris(pyrazolyl) anions, Krempner et al. obtained no clear indication concerning the coordination number of the anionic silicon center in silanide **69** [85].

2.4 α -Functionalized Silyl Anions: Silylenoids

As outlined in the previous sections, a wide variety of substituents at silicon is utilized for the generation of silyl anions. Additional functionalities at the same silicon atom (α -functionalities) that are more or less compatible with its anionic nature can either be activated at a later preparative stage or even be employed for reactions of silyl anions themselves [86]. For instance, aminosilanes can be transformed to the corresponding halosilanes quite easily and therefore aminosilyl anions are potentially versatile building blocks for organosilicon chemistry.

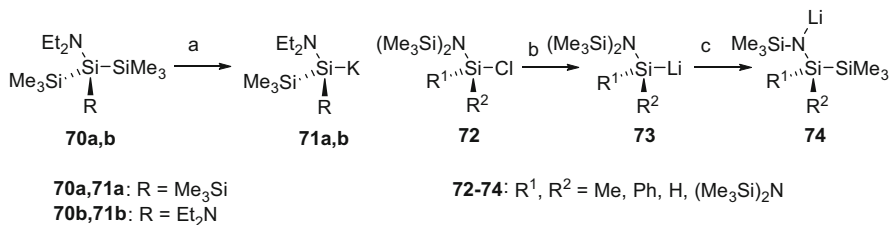
In a study by Marschner et al. diethylaminosilanes **70a,b** were converted to aminosilanides **71a,b** with potassium *tert*-butoxide at ambient temperature in good yield (Scheme 23) [87]. The N–Si bond of silyl anion **71a** remained intact after oxidation with 1,2-dibromoethane, silylation and diverse transmetalations.

Popowski et al. observed that upon warming of aminosilyl anions **73** in THF solution to ambient temperature a 1,2-silyl migration occurs to give silylamides **74** [88]. In one case ($R^1 = H$, $R^2 = Ph$) self-condensation of silanide **73** to an (aminosilyl)silyl anion supposedly by elimination of lithium hexamethyldisilazane was found. Neither compounds **73**, **74** nor the condensation products were isolated, but quenched with chlorodimethylsilane instead and analyzed as the corresponding disilanes and trisilanes, respectively.

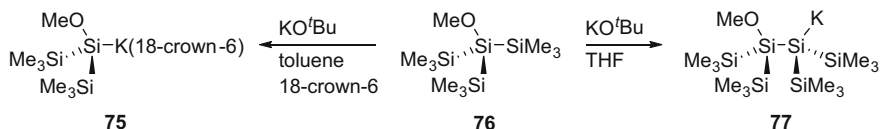
It had been shown previously that complexation of the metal cation in α -(alkoxy) silyl anions reduces their silylenoid character and therefore their tendency for self-condensation [86]. Thus, two products were isolated from the reaction of silylether **76** with potassium *tert*-butoxide. Methoxysilyl anion **75** was the main product in toluene solution in the presence of excess 18-crown-6 [89]. In contrast, in THF solution self-condensation by elimination of potassium methoxide led to the isolation of silanide **77** (Scheme 24).

Two comprehensive studies of α -(silyloxy)silyl anions show that self-condensation is only one out of several possible reaction pathways for the decomposition of such silyl anions. Reduction of chlorosilane precursors **79** (Scheme 25) with lithium powder was performed either in THF at -78°C or in Trapp mixture at -110°C . Products and intermediates were generally quenched with chlorodimethylsilane or chlorotrimethylsilane, analyzed by GC, GC–MS, NMR spectroscopy and in some cases isolated by distillation [90, 91].

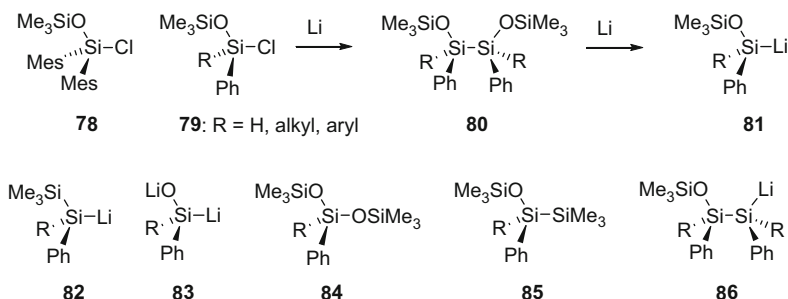
Generation of silanides **81** proceeds via initial dimerization of chlorosilanes **79** to yield disilanes **80**. In the case of dimesitylsilane **78**, the corresponding anion is formed directly probably due to steric reasons. Depending on the overall reaction



Scheme 23 Synthesis of α -aminosilyl anions **71a,b**, **73** from disilanes **70a,b**, chlorosilanes **72** and silyl migration of anions **73** to yield bis(silyl)amides **74**. (a) +KO^tBu, -Me₃SiO^tBu; (b) +2 Li, -LiCl; (c) warming to rt



Scheme 24 Solvent dependent formation of trisilane anion **75** and tetrasilane anion **77** from methoxysilane **76**

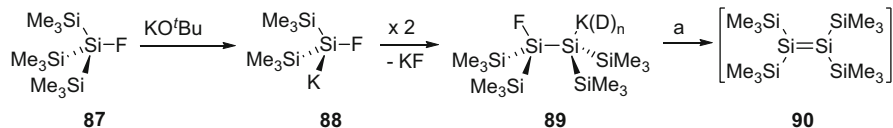


Scheme 25 Dimesitylchlorosilane **78**, synthesis of siloxysilyl anions **81** from chlorosilanes **79** via disilanes **80**, additional products **82-86** observed during syntheses of silyl anions **81**

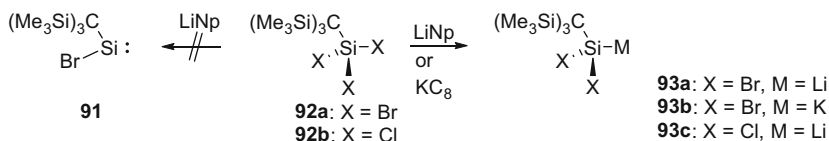
times (0.5–6 h), substrates and temperatures, different product distributions were observed. In addition to silyl anions **81**, the following compounds were identified: silyl anions **82**, dianions **83**, bis(silyloxy)silanes **84**, disilanes **85**, and disilanyl anions **86**. Sterically more demanding substituents give rise to slower conversion of disilane **80** and disfavor formation of disilanide **86** by self-condensation. Structures and reactivities of lithium α -(*tert*-butoxy)silanides were also studied theoretically [92, 93].

The stable β -fluorosilyl anion **89** is accessible from fluorosilane **87** and potassium *tert*-butoxide (Scheme 26) presumably via intermediate silylenoid **88** [94, 95].

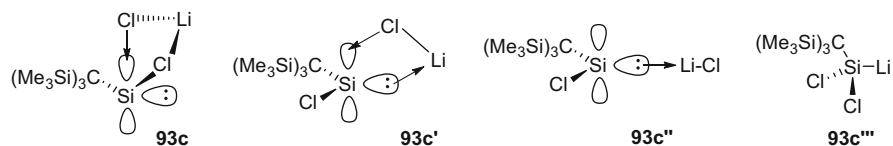
The X-ray single crystal structure analysis of anion **89** ($D = 18$ -crown-6) revealed surprisingly short Si–Si and Si–F distances while the K⁺(18-crown-6)



Scheme 26 Reaction of fluorosilane **87** with KO^tBu to yield potassium tetrasilanide **89** via silylenoid **88** and formation of disilene **90**. (a) $-\text{KF}$, $-n \text{ D}$



Scheme 27 Synthesis of stable silylenoids **93a-c** from trihalosilanes **92a,b**, bromosilylene **91**



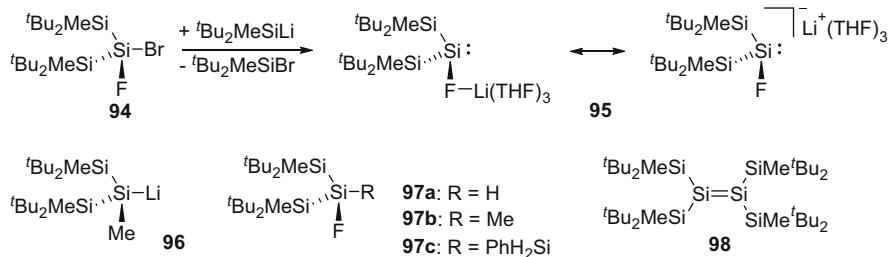
Scheme 28 Structures of calculated minima for silylenoid **93c**

moiety is far remote. Attempted transmetalations with, e.g., LiCl or MgBr_2 caused the otherwise slow formation of unstable disilene **90**, that was trapped with naphthalene and 2,3-dimethyl-1,3-butadiene.

Silylenoids with halogen leaving groups have been the focus of many experimental and theoretical studies. The first example of this class of compounds that was stable at ambient temperature had initially been assigned the structure of bromosilylene **91** by Lee et al. (Scheme 27) [96]. As transpired later on, reaction of trihalosilanes **92a,b** with lithium naphthalenide ($\text{X} = \text{Cl}$, Br) or potassium graphite ($\text{X} = \text{Br}$) at -78°C in fact resulted in THF solutions of silylenoids **93a-c** that were stable even at ambient temperature [97, 98].

Since experimental data on the structure of silylenoids of type **93** was not forthcoming, conceivable gas phase structures of several α -(halo)silylenoids [99–101] including compound **93c** [102] were analyzed by theoretical methods.

The calculated structure with the lowest energy **93c** exhibits a dative interaction of one chloride anion with the formally empty p_z -orbital at silicon (Scheme 28). The lithium cation occupies a bridging position between the two chlorine atoms (p-complex, silylenoid-like structure, sometimes named 4-membered ring structure, related to well-known inverted structures). In structure **93c'** one chloride anion again features a dative interaction with the empty p-orbital at silicon. The lithium cation, however, is coordinated by the silicon lone pair in this case (silylenoid-like



Scheme 29 Synthesis of stable silylenoid **95** from bromofluorosilane **94** and derivatives **96–98** of the former

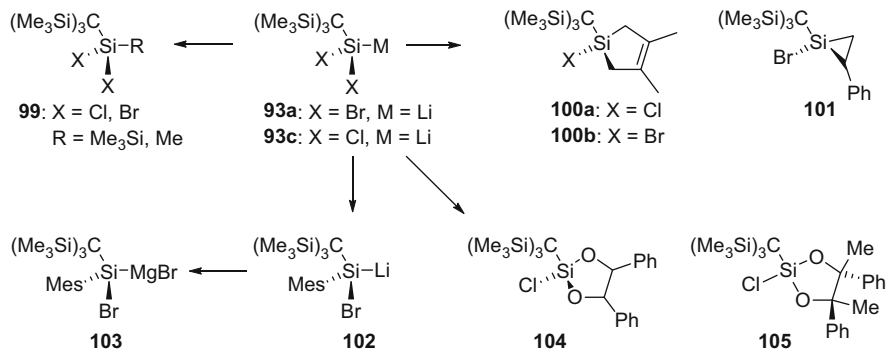
complex, sometimes called three-membered ring structure). The third structure **93c''** has a quasi-linear alignment of the Si–Li–Cl axis due to σ -coordination of the silicon lone pair to the lithium cation (also referred to as σ -complex). The fourth structure **93c'''** – the one with the highest energy – exhibits a classical tetrahedral arrangement. It is important to note that another study with different model compounds came to quite similar results [103]. If dimethyl ether was included in computations for coordination of the lithium cation, though, only structures analogous to **93c''** and **93c'''** are still minima and the energetic preference between these two depends on the substituents at silicon.

The first and to date only solid state structure of an α -(halo)silylenoid was published by Apeloig et al. in 2006 [104, 105]. Bromofluorosilane **94** was converted to α -(fluoro)silylenoid **95** by metal-halogen exchange with a lithium di-*tert*-butylmethylsilanide (Scheme 29).

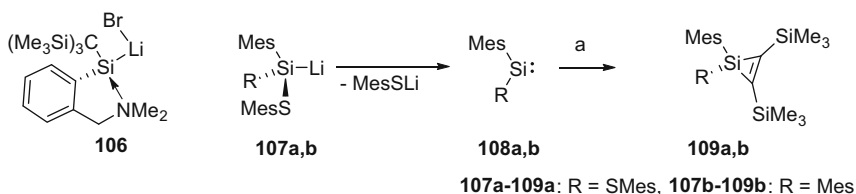
The lithium cation in **95** exhibits no close contact to the silicon lone pair but is coordinated by the fluoride group and three molecules of THF in the solid state instead, which is in good agreement with the predicted structures of silylenoids coordinated by dimethyl ether [103]. Supported by results from computations, compound **95** is best described as a fluoride adduct of the corresponding silylene and has an amphiphilic character. It reacts as an electrophile toward methylolithium to silyl anion **96** and as a nucleophile in the formation of fluorosilanes **97a–c**. Furthermore, silylenoid **95** can be converted thermally or photochemically to the known disilene **98** previously reported by Sekiguchi et al. [106].

The reactivity of dihalosilylenoids has been the topic of several theoretical [107–109] and experimental studies. As in the case of compound **95** (Scheme 29), reactions of silylenoids **93a,c** with electrophiles yielded methyl- and silyldihalosilanes **99** (Scheme 30) [98]. Similar to silylenes, silylenoids can react with alkenes and 1,3-dienes by [1+2] [98] and [1+4] cycloaddition [98]. Silacyclopentenes **100a,b** were synthesized from the corresponding silylenoids **93a,c** and 2,3-dimethyl-1,3-butadiene; silacyclopropane **101** is accessible from **93a** and styrene [110].

Reaction of **93a** with mesityl lithium in THF solution afforded the new silylenoid **102** upon warming to -10°C , however, slow decomposition occurs at



Scheme 30 Conversion of silylenoids **93a,b** to dihalosilanes **99**, silacyclopentenes **100a,b**, silacyclopropane **101** and 1,3,2-dioxasilolanes **104**, **105**; synthesis of silylenoid **102** and its transmetalation to magnesium compound **103**



Scheme 31 Donor-stabilized silylenoid **106**, lithium mesitylenethiolate elimination from silyl anions **107a,b** to give silylenes **108a,b** and [1+2]cycloaddition to yield silacyclopropenes **109a,b**. (a) + bis(trimethylsilyl)acetylene

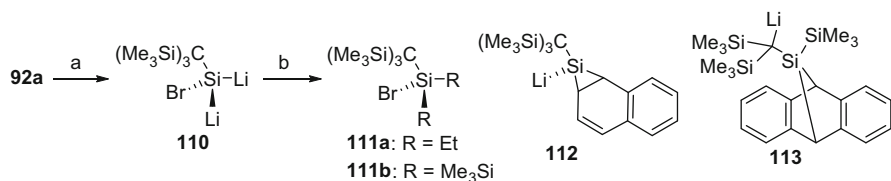
this temperature. The silylenoid **102** was transformed into the first stable magnesium silylenoid **103** after thermal elimination of lithium bromide at 45°C [111]. 1,3,2-Dioxasilolanes **104**, **105** were, among others, synthesized from compound **93c** and two equivalents of the appropriate aldehyde [112] or ketone [113], respectively.

The synthesis of silylenoid **106** with a pendant donor substituent that is stable in solution up to 110°C was accomplished by Lee et al. (Scheme 31) and a structure with a N–Si dative bond was suggested based on DFT calculations and NMR spectroscopic data [114].

Sulfur-substituted lithium silanides **107a,b** do not only react as nucleophiles but also degrade in solution to silylenes **108a,b** by elimination of lithium mesitylenethiolate and show a reactivity typical for silylenes (Scheme 31) [115].

For example, silacyclopropenes **109a,b** were synthesized from bis(trimethylsilyl)ethyne and solutions containing lithium mesitylenethiolate and silylenes **108a,b**.

According to Lee et al., reaction of tribromosilane **92a** with four equivalents of lithium naphthalenide or lithium anthracenide afforded dilithium silandiide **110**.



Scheme 32 Synthesis of dilithio silanide **110** and its alkyl and silyl derivatives **111a,b**, products of formal lithiosilylene addition to naphthalene and anthracene **112**, **113**. (a) +NpLi, (b) +EtBr/+Me₃SiBr

The latter was successfully derivatized with bromoethane and bromotrimethylsilane to yield bromosilanes **111a,b** (Scheme 32) [116].

Dilithiosilane **110** adds to naphthalene and anthracene via formal [1+2] and [1+4] cycloaddition, respectively, to yield lithiosilanes **112**, **113** [117]. Trapping experiments suggest that the first step of these reactions is a 1,2-addition and accordingly a 9,10-addition of a Li–Si bond followed by lithium bromide elimination. The formation of tris(silyl)carbanion **113** apparently involves an additional trimethylsilyl migration.

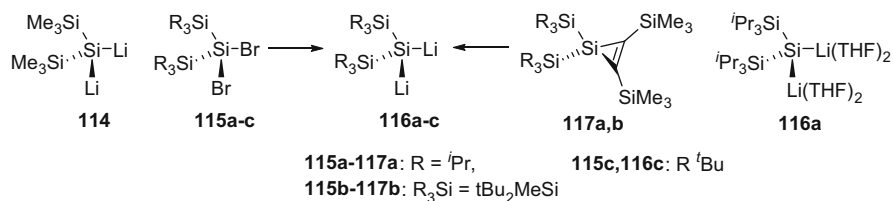
3 Silyl Dianions

3.1 Geminal Silyl Dianions

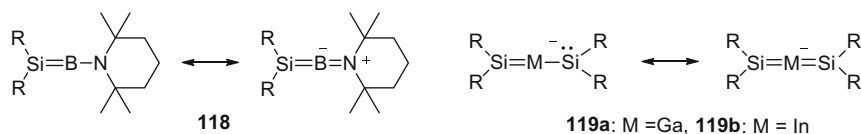
Dilithio silane **110** (Sect. 2.4, Scheme 32) occupies a linking position between silylenoids and geminal silyl dianions. The latter are very attractive synthetic targets inter alia due to their high synthetic potential.

The first geminal organodilithiosilane **114** is accessible by pyrolysis of supersilyl lithium in low yield as reported in 1990 by Lagow et al. (Scheme 33) [118]. Related dianions **116a–c** were later isolated by the Sekiguchi group either directly from the corresponding dibromosilanes **115a–c** or by reaction of silacyclopropanes **117a,b** with lithium metal in THF [119, 120].

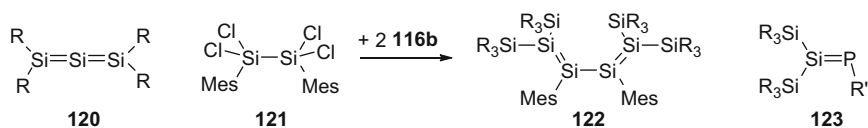
Dilithiosilane **116a** exhibits a monomeric structure in THF solution and in the solid state with two additional molecules of THF coordinating each lithium cation (Scheme 33) and a Si–Li bond length that is about 10 pm shorter than those in comparable THF-solvated lithium tris(silyl)silanes [121, 122]. Especially dianion **116b** turned out to be an excellent starting material for the syntheses of hitherto unknown low-valent main group compounds. Reactions with TMP–BCl₂ (TMP = 2,2,6,6-tetramethylpiperidino) and group 13 trichlorides MCl₃ (M = Ga, In) afforded the first silaborene with a dicoordinate boron center **118** and 1,3-disila-2-gallataallen/1,3-disila-2-indataallen anions **119a,b** (Scheme 34) [29, 123, 124].



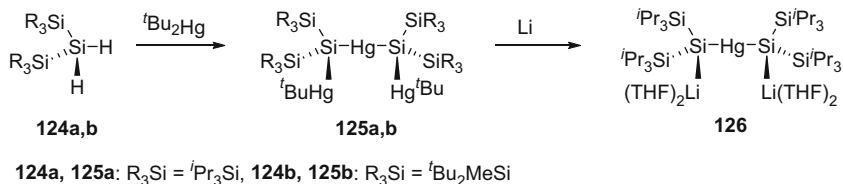
Scheme 33 Dilithiosilanes **114**, **116a** and synthesis of dilithiosilanes **116a-c** from dibromosilanes **115a-c** and silacyclopropenes **117a,b**



Scheme 34 Canonical forms of silaborene **118**, gallataallene **119a**, and indatallene **119b**



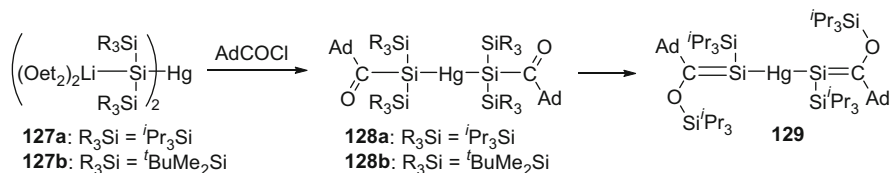
Scheme 35 Trisilaallene **120**, phosphasilene **123** and synthesis of tetrasilabutadiene **122** from tetrachlorodisilane **121** and dilithiosilane **116b**, R = ^tBu₂MeSi, R₃Si = ^tBu₂MeSi, R' = 2,4,6-^tBu₃C₆H₂



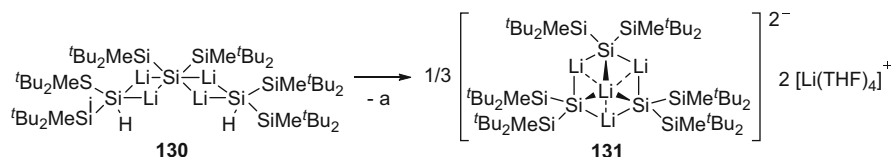
Scheme 36 Reaction of silanes **124a,b** with ^tBu₂Hg and synthesis of silyl dianion **126** by transmetalation of silanide **125a**

The same strategy involving α,α -dilithiosilanes in combination with α,α -dihalo electrophiles was applied for the preparation of trisilaallene **120** [125], tetrasila-1,3-butadiene **122** from 1,1,2,2-tetrachlorodisilane **121** [126] and phosphasilene **123** (Scheme 35) [127].

Starting in 2002, Apeloig et al. developed a different approach for the syntheses of geminal silyl dianions. Trisilanes **124a,b** were converted to mercury silanides **125a,b** by reaction with di-*tert*-butylmercury in moderate to good yields (Scheme 36) [128–131].



Scheme 37 Synthesis of acylsilanes **128a,b** and bis(silenide) mercury **129** from silyl dianions **127a,b** and 1-adamantanecarboxylic acid



Scheme 38 Dilithio silane aggregates **130** and **131**

The well-known transmetalation of silylmercury compounds with excess lithium metal [132, 133] was then employed for the synthesis of silyl dianion **126** in THF solution, the first compound with a silicon center connected to lithium and mercury at the same time. Furthermore, a complete exchange of mercury in **125a** for lithium was achieved in hexane solution to yield an aggregate with a novel Li₆-motif, [(ⁱPr₃Si)₂SiLi₂]₂[*tert*-BuLi]₂. The latter was converted thermally to the first donor-free, polymeric dilithio silane [(ⁱPr₃Si)₂SiLi₂]_n.

Reaction of silyl dianions **127a,b** with two equivalents of 1-adamantanecarboxylic acid chloride was investigated experimentally and theoretically (Scheme 37) [134].

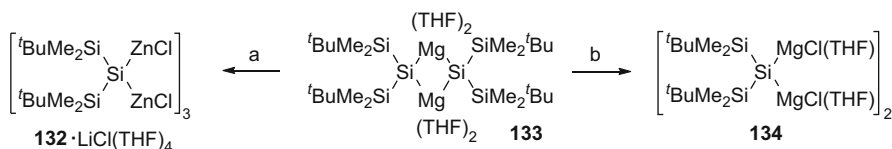
The initial product, mercury bis(acylsilane) **128a**, was not detected in case of silyl dianion **127a** but double Brook rearrangement allowed for the isolation of mercury bis(silenide) **129**, the first metal-substituted silene. Mercury bis(acylsilane) **128b**, however, is perfectly stable up to at least 200°C.

Starting from trisilane **124b** two additional dilithio silane aggregates **130**, **131** were isolated and structurally characterized in the Apeloig group (Scheme 38).

The central anionic silicon center of aggregate **130** is hexacoordinate and linked to four lithium atoms. It can be described as a co-aggregate of two equivalents of lithium silanide (*tert*-Bu₂MeSi)₂SiHLi with geminal dilithiosilane (*tert*-Bu₂MeSi)₂SiLi₂. Dissolution of compound **130** in THF causes a break-up of the co-aggregate and the very unusual trimeric geminal dianion **131**·[Li(THF)₄]₂ was isolated and characterized by single crystal X-ray diffraction [135].

Consecutive transmetalation of dilithiosilane (*tert*-BuMe₂Si)₂SiLi₂ allowed for the syntheses of the first dimagnesium and dizinc silane derivatives **132**·LiCl(THF)₄, **133**, **134** (Scheme 39) [136].

All three of the above silyl dianions **132**·LiCl(THF)₄, **133**, **134** were characterized by single crystal X-ray diffraction.



Scheme 39 Conversion of magnesium silanide **133** to trimeric zinc silanide **132**·LiCl(THF)₄ and magnesium silanide **134**. (a) +ZnCl₂, (b) +^tBuMgCl(MgCl₂)₂

3.2 Silole Monoanions and Dianions

Silole monoanion and dianion **135**, **136** [137–139] and related indene and fluorene systems **137–139** [140–144] have been studied extensively both experimentally and theoretically (Scheme 40) [11, 145, 146]. They are usually prepared by reaction of the corresponding dihalosilanes with alkali metals in polar solvents. All structurally characterized silole dianion derivatives known to date exhibit one η^5 -coordinated and one η^1 -coordinated alkali metal cation.

The reactions of silole dianion **136**[Li⁺]₂ with an α,α -bifunctional electrophile, a ketone, and 1,3-dienes have been investigated in recent years. Reaction of dianion **136**[Li⁺]₂ with a dichlorocyclopropene yielded disilapentalene **141** via *trans,trans*-diradical **140**. The latter was detected by ESR spectroscopy and the preferential formation of the suggested isomer is supported by DFT calculations (Scheme 41) [147].

Depending on reaction conditions silole **136**[Li⁺]₂ reacts with one or two equivalents of 2-adamantanone (Scheme 42) [148].

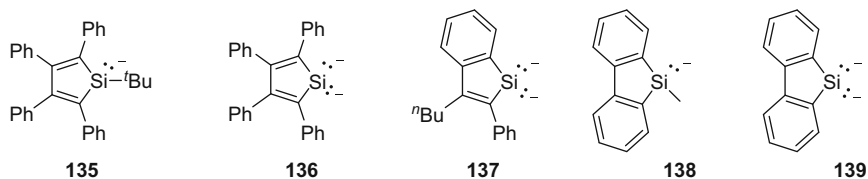
Silenes have previously been prepared through sila Peterson-type olefination by Kira and co-workers [149]. The formation of a silene **142** by direct coupling of a ketone with a silyl dianion and elimination of alkali metal oxide, however, remains a spectacular exception. In the reaction of **136**[Li⁺]₂ with two equivalents of 2-adamantone, diol **143** was obtained as expected after protonation of the corresponding bis(alkoxide), the primary double addition product.

Silole dianion **136**[Li⁺]₂ reacts with different 1,3-dienes via formal two-electron oxidation/[1+4]cycloaddition. Amazingly, silaspiroalkene **144** and lithium metal were obtained from the reaction with 2,3-dimethyl-1,3-butadiene (Scheme 43) [150].

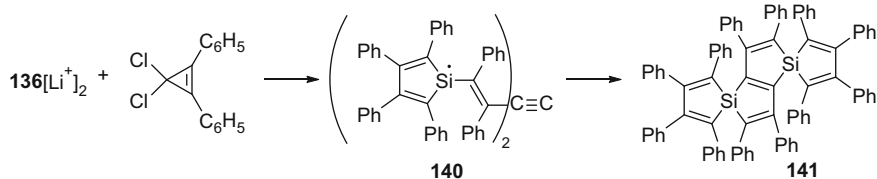
The formation of siladiazaspiroalkene **145** was accompanied by two-electron reduction of a second equivalent of diimine to give enamide **146** as byproduct [151]. The mechanisms for the above reactions were also investigated by computations.

4 Unsaturated Systems, Small Rings, and Clusters

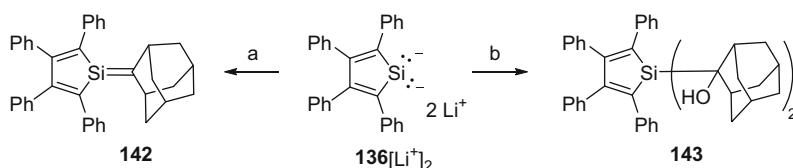
The isolation and characterization of the first disilene **147** [152], disilynes **148a,b** [153, 154], tetrasilabutadiene **149** [155], and tetrasilatetrahedrane **25** [37] are undoubtedly milestones of modern inorganic chemistry (Scheme 44).



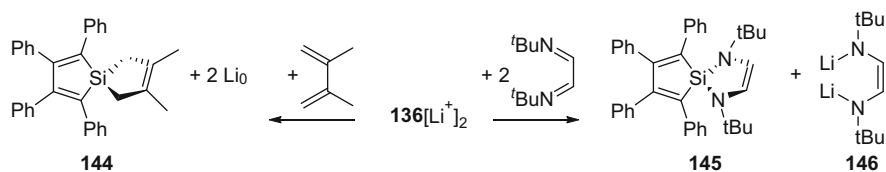
Scheme 40 Silole monoanion **135**, dianion **136**, silaindene dianion **137**, silafluorene anion **138**, and dianion **139**



Scheme 41 Reaction of silole dianion **136**[Li⁺]₂ with a dichlorocyclopropene to yield disilapentalene **141** via stable diradical **140**

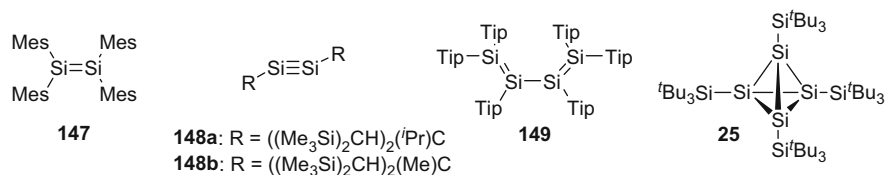


Scheme 42 Conversion of silole dianion **136**[Li⁺]₂ to silene **142** and diadamantylsilane **143**. (a) +2-adamantanone, -Li₂O; (b) +2 2-adamantanone, +2 H⁺

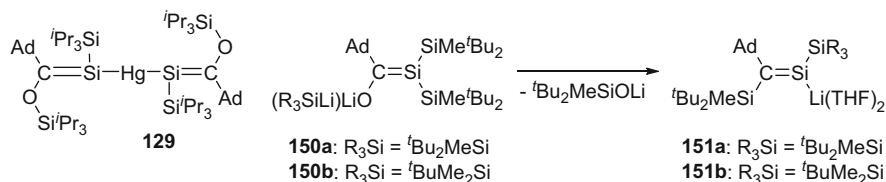


Scheme 43 Reaction of silole dianion **136**[Li⁺]₂ with 2,3-dimethyl-1,3-butadiene and di-*tert*-butylethanedimine to yield spirosilanes **144**, **145**, lithium and bis(enamide) **146**

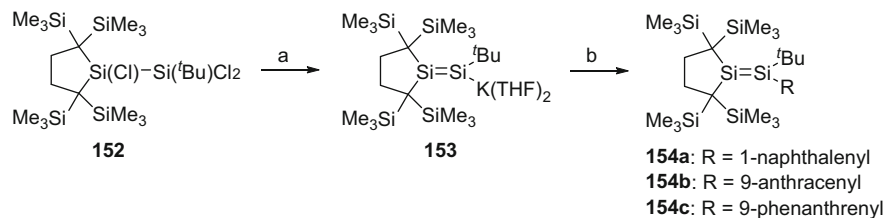
In recent years, numerous compounds with unsaturated silicon centers have been isolated and their reactivity studied. Especially functionalized derivatives such as mercury silenide **129** [134] or lithium silenides **151a,b** [156] possess a high degree of synthetic potential (Scheme 45). The latter are accessible from lithium silanide-silenolate aggregates **150a,b**. Supported by DFT calculations silynes and silylidenes are likely intermediates during their formation.



Scheme 44 Known silicon analogs of an alkene **147**, alkynes **148a,b**, butadiene **149**, and tetrasilatetrahedrane **25**



Scheme 45 Mercury bis(silenide) **129** and elimination of ^tBu₂MeSiLi from silenes **150a,b** to yield lithium silenides **151a,b**

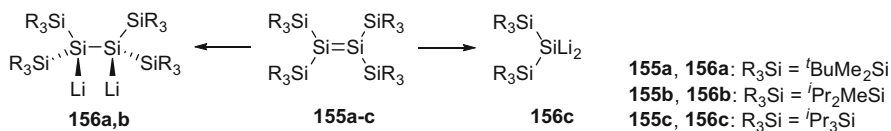


Scheme 46 Synthesis of potassium disilenide **153** by reductive dehalogenation of trichlorodisilane **152**, reaction of anion **153** with aryl bromides to yield aryltrialkyldisilenes **154a-c**. (a) Excess K⁺C₈, (b) +RBr

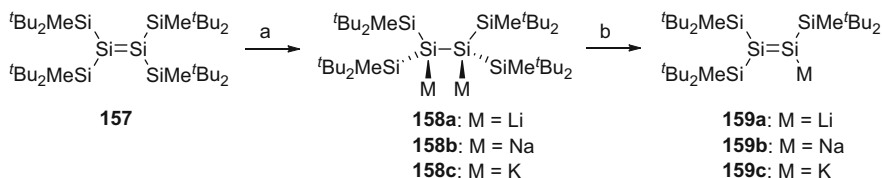
The utilization of disilenes, first suggested by Weidenbruch as an intermediates during the synthesis of tetrasilabutadiene **149** (Scheme 44) [155], allowed for a straightforward access to many otherwise inaccessible compounds and has previously been reviewed [14, 15]. Several examples and synthetic methods for the preparation of alkaline metal disilenes have been described to date. Most recently, the first trialkyl derivative, isolable potassium disilenide **153**, was synthesized by direct reductive dehalogenation of trichlorodisilane **152** and converted to arylsilenes **154a-c** that exhibit intramolecular [$\pi(\text{Si}=\text{Si}) \rightarrow \pi^*(\text{aryl})$] charge transfer interactions (Scheme 46) [157].

Reaction of disilenes **155a-c** with lithium in THF solution was already reported in 2001 to yield 2,3-dilithiotetrasilanes **156a,b** and 2,2-dilithiotrisilane **156c** (Scheme 47) [158].

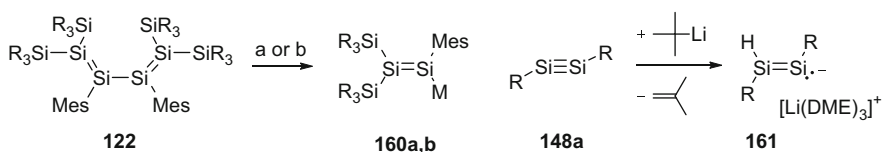
THF solutions of dianions **158a-c** were obtained by reduction of disilene **157** with stoichiometric amounts of alkaline metal naphthalenides. The presence of



Scheme 47 Synthesis of 2,3-dilithiotetrasilanes **156a,b** and 2,2-dilithiosilane **156c** from disilenes **155a-c** with lithium powder in THF



Scheme 48 Conversion of disilene **157** to 2,3-dimetallatetrasilanes **158a-c** and elimination of M-SiMe^tBu₂ to yield trisilyldisilenes **159a-c**. (a) +2 Naph-M, (b) -M-SiMe^tBu₂



Scheme 49 Cleavage of tetrasilabutadiene **122** to yield disilenes **160a,b** and formal addition of LiH to silyne **148a** to give disilene **161**, R₃Si = ^tBu₂MeSi, R = ((Me₃Si)₂CH)₂(ⁱPr)Si. (a) +2 ^tBuLi, -2 ^tBu; (b) +KC₈

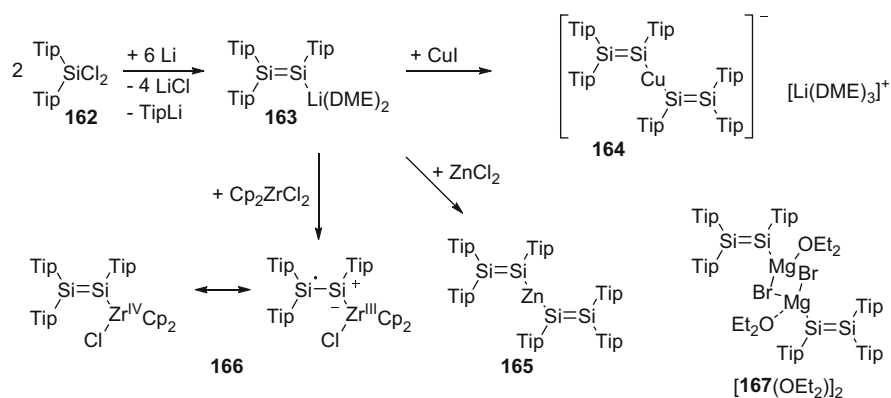
dianion **158a** was confirmed by ²⁹Si NMR spectroscopy and by isolation of the corresponding protonation product (Scheme 48) [159].

Exchange of the solvent for nonpolar benzene prompted the generation of disilenes **159a-c** by elimination of M-SiMe^tBu₂ (M = Li, Na, K). The structure of disilene **159a**(THF)₂ was investigated by single crystal X-ray diffraction.

Sekiguchi et al. also reported the syntheses of three other disilenes by four different methods between 2004 and 2010. The central Si-Si bond of tetrasilabutadiene **122** can be cleaved with *tert*-butyllithium as reducing agent to yield the mixed silyl/aryl disilene **160a** (Scheme 49) [126]. Cleavage of the same bond is also possible with potassium graphite to furnish potassium disilene **160b** [160].

A formal transfer of lithium hydride from *tert*-butyllithium to disilyne **148a** [153] eventually allowed for the isolation of lithium hydrodisilene **161** [161]. The initial product of this reaction in THF solution did not exhibit coordinating solvent molecules and was converted to the solvent separated ion pair **161** by crystallization from a solvent mixture containing DME. 1,2-Addition of methylithium to disilyne **148a** yielded the corresponding methyl-substituted disilene which is unstable at ambient temperature [162].

The first isolated and possibly most thoroughly studied disilene **163** was obtained in one step from dichlorosilane **162** upon reaction with lithium powder



Scheme 50 One-step synthesis of disilenide **163** from dichlorosilane **162**, transition metal and magnesium disilenides **164–167**

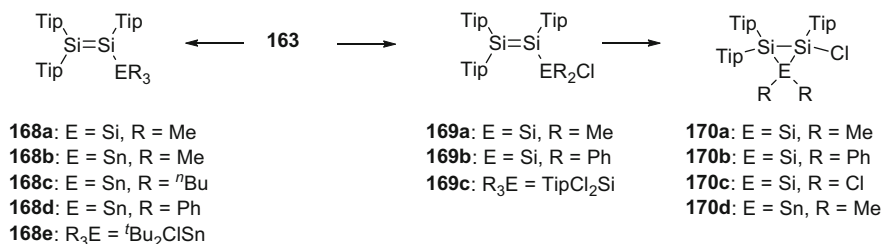
in DME (Scheme 50) [163]. Transmetalation with Cp_2ZrCl_2 [164], ZnCl_2 and CuI [165] gave access to η^1 -disilenide transition metal complexes **164–166** (Scheme 50).

Zirconium disilenide **166** was the first η^1 -disilenide transition metal complex to be reported in the literature. A high wavelength UV absorption, low-field ^{29}Si NMR signals, and distinctive Si–Si and Si–Zr bond lengths point to a significant contribution of the silylene– Zr^{III} canonical form for complex **166**. An undeniable drawback of organolithium and silyl lithium compounds is their high reduction potential that might cause side reactions or even prevent product formation completely. As in the case of their carbon counterparts bis(disilylene) cuprate **164** and zinc bis(disilylene) **165** are expected to be comparatively mild disilenide transfer agent with a high synthetic potential. An analog of a vinyl Grignard reagent, disilylenyl-magnesium bromide **167**, was obtained by transmetalation of disilenide **163** with magnesium bromide (Scheme 50) [165]. Compound **167** was crystallized as a dimer with two bridging bromide anions and two equivalents of diethyl ether coordinating the magnesium centers.

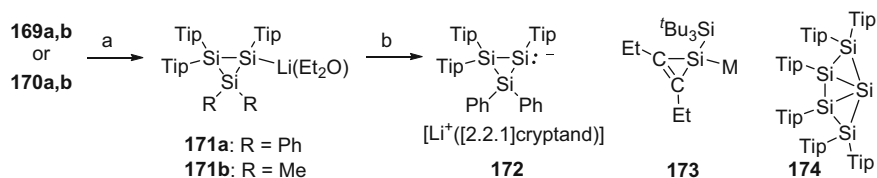
Trimethylsilyl derivatives of main group compounds have been used as mild transfer agents on many occasions and triorganostannyl substituted alkenes and alkynes are widely known for their role in Stille Coupling. In this context, silyl substituted disilenes **168a**, **169a–c** [163, 166, 167] and especially stannyl substituted disilenes **168b–e** [168] have been synthesized although their synthetic potential remains unexplored to date (Scheme 51).

In case of trisilyl chlorides **169a,b** a ring closure can be induced by means of solvent exchange to yield three-membered rings **170a,b** [166]. However, no analogous intermediates were observed during the formation of trisilylirane **170c** [169] and disilastannirane **170d** [168].

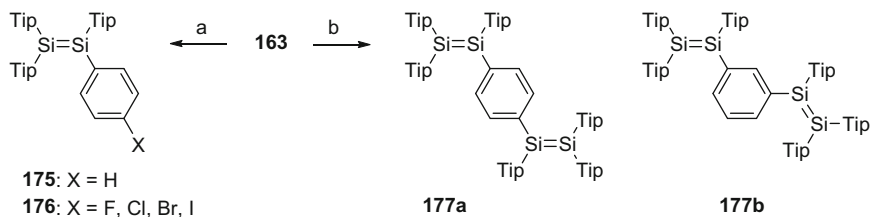
Cyclotrisilanes **170a,b** and trisilanes **169a,b** were successfully converted to the corresponding lithium cyclotrisilanides **171a,b** and two single crystal X-ray structures of the latter could be established, contact ion pair **171a** and solvent



Scheme 51 Silyl and stannyldisilenes **168a–e**, **169a–c** and three-membered rings **170a–d**



Scheme 52 Syntheses of trisilacyclopropanides **171a,b**, **172**, alkali metal silacyclopropenide **173**, and silicon cluster **174**, M = Li, Na, K. (a) Li/Et₂O, (b) **171a** + [2.2.1]cryptand



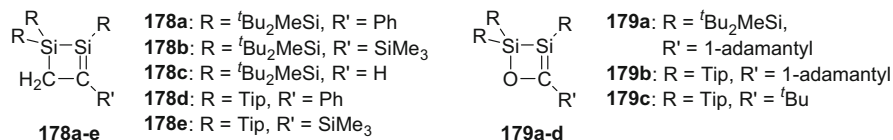
Scheme 53 Synthesis of tetraaryl disilenes **175**, **176** and *para/meta*-phenylene bridged disilenes **177a,b**. (a) **175**: +I/Br–C₆H₅, **176**: +*para*-I–C₆H₄–X; (b) **177a**: +*para*-I₂C₆H₄, **177b**: +*meta*-I₂C₆H₄

separated ion pair **172** (Scheme 52) [166]. Three examples of alkali metal silacyclopropenides **173** have also been published recently [170, 171].

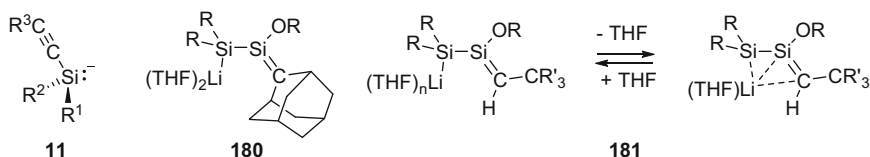
Reaction of disilene **163** with silicon tetrachloride also afforded the molecular silicon cluster **174** in one step [172].

In addition to the syntheses of phosphino and iodo substituted disilenes [173] much effort has been made to obtain aryl substituted and phenylene bridged disilenes due to their very promising optical properties. Disilene **163** readily reacts with phenyl bromide and iodide to yield tetraaryl disilene **175** (Scheme 53), whereas phenyl chloride and fluoride do not react under the same conditions [174, 175].

This synthetic pathway was also applied for the preparation of *para*-substituted tetraaryl disilenes **176** and the direct production of *para/meta*-phenylene bridged disilenes **177a,b**.



Scheme 54 1,4-dihydro-1,2-disilenes **178a–e** and 2*H*-1,2,3-oxadisilenes **179a–c**



Scheme 55 Ethynylsilyl anion **11**, silenylsilyl anion **180** and interconversion between η^1 and η^3 coordination in silenylsilyl anion **181**, R = ^tBu₂MeSi, R' = 3,5-^tBu₂C₆H₃

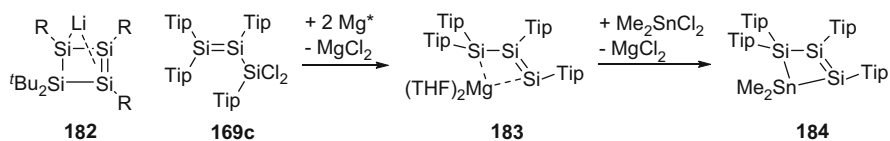
Disilenides **159a** (Scheme 48) and **163** exhibit identical reactivities toward acyl chlorides and vinyl bromides. No intermediate 1,2-disilabutadienes were observed during the reaction with vinyl bromides but 1,4-dihydro-1,2-disilenes **178a–e** (Scheme 54) were isolated in good to high yields, resulting from formal intramolecular [2+2] cycloaddition [176].

Likewise, 2*H*-1,2,3-oxadisilenes **179a–c** were synthesized from disilenides **159a**, **163** and the corresponding acyl chloride [177], again without any detectable intermediates.

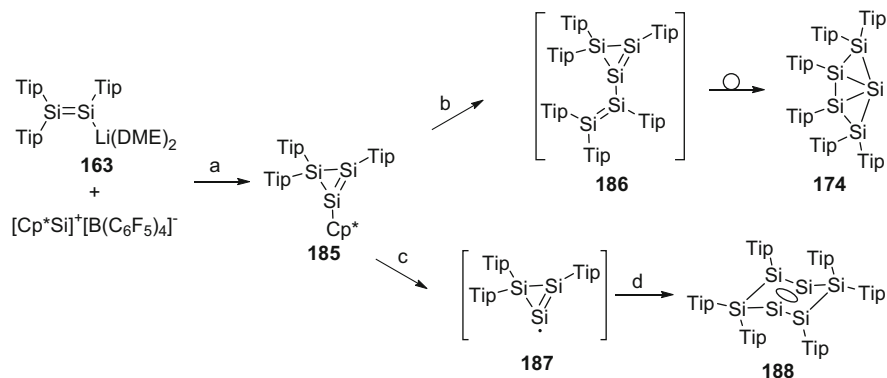
As has been shown before, ethynylsilyl anions **11** (Schemes 4 and 54) exhibit only little π -conjugation between the C–C triple bond and the anionic silicon center [27]. Reaction of disilenide **159a** (Scheme 48) with 2-adamantanone gave access to silenylsilyl anion **180** (Scheme 55) [178]. As in the case of anion **11**, combined single crystal X-ray data, NMR investigations, UV/Vis measurements, and theoretical calculations support the description as an isomer with a Si-localized negative charge and little to no π -electron delocalization.

An interesting behavior was observed for lithium silanide **181** [179]. Even though compound **181** is also best described as a silenylsilyl anion based on experimental data, an interconversion between η^1 -silenylsilyl and η^3 -allyl like counter anion coordination could be induced through the choice of solvents (Scheme 55).

Tetrasilacyclobutenide **182** is related to silenylsilyl anion **181** with η^3 -coordination of the lithium cation by means of η^1 -coordination to the anionic silicon center plus η^2 -coordination to the endocyclic Si–Si double bond [180]. The first α,ω -dianionic unsaturated oligosilane **183** was synthesized from silyldisilene **169c** and excess activated magnesium (Mg^{*}) in THF solution (Scheme 56) [167]. Like in the cases of ethynylsilyl anion **11** and silenylsilyl anions **180**, **181**, the negative charges of trisilapropene-1,3-diide **183** are essentially localized at the respective vinylic and allylic silicon center.



Scheme 56 Tetrasilacyclobutenide **182** and synthesis of magnesium trisilapropene-1,3-diide **183** from silyldisilene **169c** and conversion to trisilastannete **184**, R = ^tBu₂MeSi

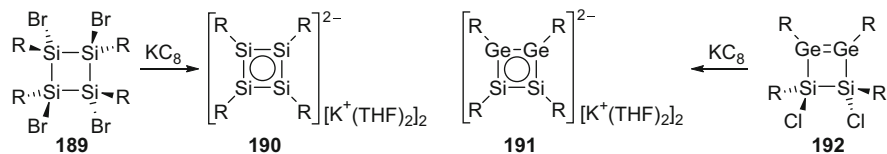


Scheme 57 Synthesis of trisilacyclopropene **185** from disilenide **163** and [Cp*Si]⁺[B(C₆F₅)₄]⁻ and subsequent enlargement of the silicon framework to yield siliconoids **174**, **188** via proposed intermediates **186**, **187**. (a) -Li[B(C₆F₅)₄], (b) +**163**, -Cp*Li, (c) +**163**, -0.5 (Tip₃Si₂)₂ or +Li naphthalenide, -Cp*Li, (d) x2

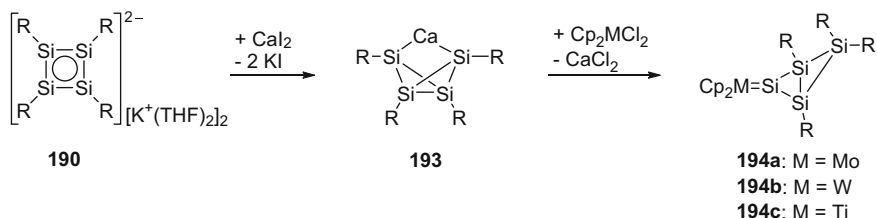
1,4-Dihydro-1,2,3,4-trisilastannete **184** was prepared from dianion **183** and dimethyltin dichloride on small scale and characterized by multinuclear NMR spectroscopy.

The Cp*Si⁺ cation [181] has been utilized as a stoichiometric source of silicon in reactions with disilenide **163** [182]. Initially, the 1:1 reaction of Cp*Si⁺ with **163** gave access to the first trisilacyclopropene without silyl substituents **185** (Scheme 57) [183].

In a subsequent step, a second equivalent of disilenide **163** can act as either a reducing agent or a nucleophile toward the Cp*Si moiety, thus following the characteristic reaction pathways of main group Cp* compounds [184]. Substitution of the Cp* substituent of **185** with the disilynyl anion yielded the previously reported Si₅-cluster **174** [172] via a proposed tetrasilabutadiene intermediate **186**. The preferred reaction pathway, a SET from disilenide **163** to cyclotrisilene **185**, ultimately turned out to be an alternative for the synthesis of recently discovered hexasilabenzene isomer **188** [169]. Trisilacyclopropenyl radical **187** was suggested as an intermediate in this reaction and the direct generation of **187** by reaction of



Scheme 58 Heavier cyclobutadiene dianion analogs **190**, **191** synthesized from halosilanes **189**, **192**, R = ^tBu₂MeSi



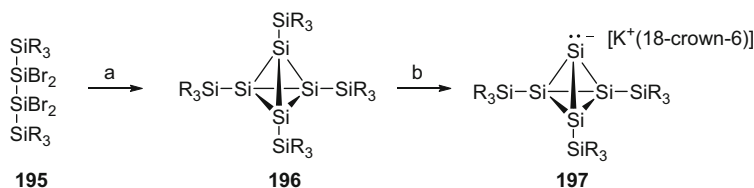
Scheme 59 Synthesis of bicyclobutane dianion **193** from dianion **190** and silylene-transition metal complexes **194a–c**, R = ^tBu₂MeSi

cyclotrisilene **185** with one equivalent of lithium naphthalenide did indeed yield silicon cluster **188** selectively.

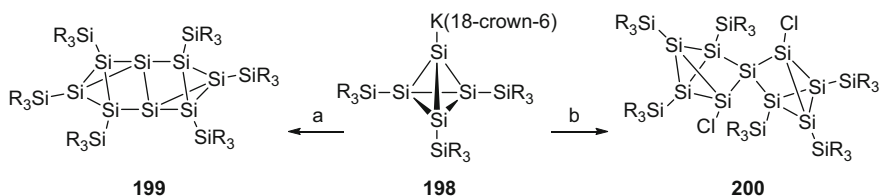
Heavier group 14 analogs of cyclobutadiene dianions and isomeric bicyclobutandiides have been synthesized and thoroughly characterized by Sekiguchi et al. in recent years. Tetrasilacyclobutadiene dianion **190** and digermadisilacyclobutadiene dianion **191** were prepared from the corresponding halogenated precursors **189**, **192** by reduction with KC₈ (Scheme 58) [185].

Even though the [R₄E₄]²⁻ cores of dianions **190**, **191** are depicted in Scheme 58 as aromatic planar systems with six delocalized π-electrons, experimental and theoretical results reveal that this description is insufficient. The silicon and germanium centers of the crystallographically isomorphous dianions **190**, **191** are strongly pyramidalized and the four-membered rings thus deviate significantly from planarity [185, 186]. NICS values [187] of model compounds indicate that diides **190**, **191** exhibit little to no aromaticity depending on the substituents and counter cations [188]. The selective methylation of digerma dianion **191** at the germanium centers with dimethyl sulfate shows that the negative charges are indeed mainly localized at these positions. Several transition metal complexes derived from dianions **190**, **191**⁺ and a germatrisilacyclobutadiene dianion exhibiting η⁴-(R₄E₄)M (M = Co, Fe, Ru) cores have been described to date [189–192].

Calcium bicyclobutandiide **193** is accessible from tetrasilabutadiene dianion **190** by transmetalation with calcium iodide (Scheme 59) [193]. Related disiladiger-mabicyclo[1.1.0]butandiides were also reported [194].



Scheme 60 Synthesis of tetrasilatetrahedrane **196** and tetrasilatetrahedrane anion **197**, $R_3Si = ((Me_3Si)_2CH)_2MeSi$, (a) $+2 \text{ }^tBu_3SiNa$, -2 ^tBu_3SiBr , $-2 NaBr$; (b) KC_8/Et_2O



Scheme 61 Synthesis of siliconoid **199** and spirocyclic **200** from potassium tetrasilatetrahedranide **198**, $R_3Si = \text{ }^tBu_3Si$, (a) $+ICl$, (b) $+SiCl_4$

Two donor-free (**194a,b**) and one donor-stabilized silylene-transition metal complex **194c** (donor = THF, PMe_3 , NHC) were synthesized from dianion **193** involving the migration of one substituent R [193, 195].

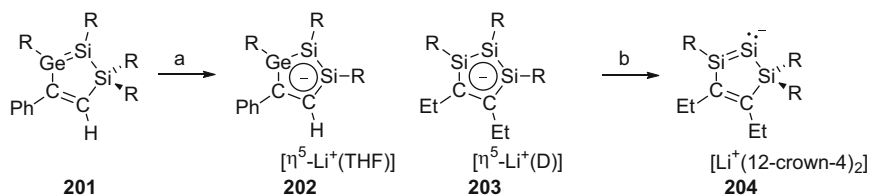
Tetrasilatetrahedrane **196**, accessible from tetrasilane **195** and two equivalents ^tBu_3SiNa , was converted to solvent separated ion pair **197** with KC_8 in diethyl ether (Scheme 60) [196].

The tetrasilatetrahedrane core of anion **197** exhibits a characteristic elongation of a Si–Si skeletal bond and one silicon center with an inverted tetrahedral geometry that is responsible for a close distance between the anionic silicon center and one silicon atom of a substituent. Only one signal for the skeletal silicon atoms was observed in ^{29}Si NMR even at 200 K, presumably due to a fast exchange of the substituents on the NMR time-scale. A related pentasilatricyclo[2.1.0.0^{2,5}]pentane and its anion were synthesized from calcium bicyclobutandiide **193** [197].

A second tetrasilatetrahedranide **198** was prepared in a similar fashion and utilized for the syntheses of siliconoid **199**, as well as spirocyclic **200** (Scheme 61) [198, 199].

Potassium tetrasilatetrahedranide **198** was crystallized as a contact ion pair and does not show the rather unusual geometry of compound **197** in the solid state but two sets of about equal skeletal Si–Si bond length and unsuspecting Si–Si–Si angles.

No significant π -electron delocalization and thus aromaticity was observed for the anionic silicon compounds discussed in this subsection so far. The same, however, is not true for heavier cyclopentadienyl analogs **202** and **203**. Reductive cleavage of one Si–R bond in heterocyclopentadiene **201** allowed for the synthesis



Scheme 62 Synthesis of germadisilacyclopentadienide **202** from germadisilacyclopentadiene **201**, conversion of trisilacyclopentadienide **203** to cyclic disilenide **204**, R = ^tBu₂MeSi, D = ^tBu₂CO, (a) +2 K⁺C₈H₁₈⁻; (b) 12-crown-4

of 1-germa-2,3-disilacyclopentadienide **202** (Scheme 62) [200]. A comparison of the X-ray crystal structures of cyclopentadiene **201** and cyclopentadienide **202** evidence an elongation of the former double bonds and a shortening of the former single bonds. Together with the overall planar structure of anion **202** and the η⁵-coordination of the lithium counter cation and also cationic [CpFe]⁺ [201], [Rh(CO)₂]⁺ and [Cp^{*}Ru]⁺ fragments [202] a cyclic π-delocalization and aromaticity can be assumed which is further supported by theoretical calculations.

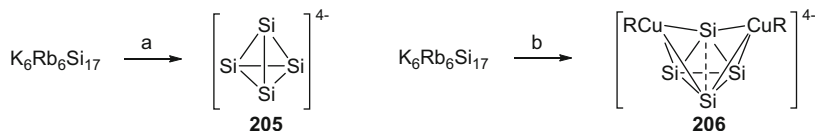
Trisilacyclopentadienide **203**, a trisila analog of anion **202**, was prepared in a similar way and converted to cyclic disilenide **204** upon addition of 12-crown-4 [203].

5 Soluble Zintl Anions

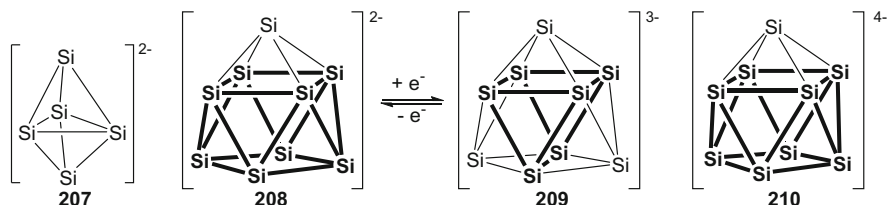
Zintl phases and Zintl anions of group 14 have been a domain of solid state chemistry for a long time and numerous examples are known in the literature [204–207]. Several molecular silicon cage compounds and small clusters **196–200** in which the number of substituents is equal or similar to the number of skeletal atoms are discussed in the previous section. Since very recently, a few virtually unsubstituted, negatively charged clusters of silicon and other group 14 elements that can be handled or prepared in solution have appeared in the literature in the last 10 years [206, 208].

The smallest cluster possible, [Si₄]⁴⁻ **205** (Scheme 63), was recently detected by ²⁹Si NMR spectroscopy in liquid ammonia solution in the presence of [2.2.2] cryptand [209]. Dissolution of a ²⁹Si-enriched (20% ²⁹Si) silicide with the nominal composition K₆Rb₆Si₁₇ that contains both [Si₄]⁴⁻ and [Si₉]⁴⁻ polyanions in the solid state yielded stable solutions which can be stored at 195 K for months with only little decomposition. The ²⁹Si NMR signal of **205** in solution (δ = 323 ppm) exhibits only a marginal downfield shift if compared to MAS-NMR data of **205** in K₆Rb₆Si₁₇ (δ = 311 ppm).

Dissolution of K₆Rb₆Si₁₇ in liquid ammonia in the presence of 18-crown-6 and mesitylcopper allowed for the isolation and characterization of copper-stabilized



Scheme 63 Tetrasilicide tetraanion **205** and copper-stabilized tetraanion **206** (cations: $[\text{Rb}^+(18\text{-crown-6})]_2\text{Rb}^{+1.54}\text{K}^{+0.46}$, $\text{R} = \text{Mes}$, (a) $\text{NH}_3(\text{l})$, [2.2.2]cryptand; (b) $\text{NH}_3(\text{l})$, 18-crown-6, MesCu)



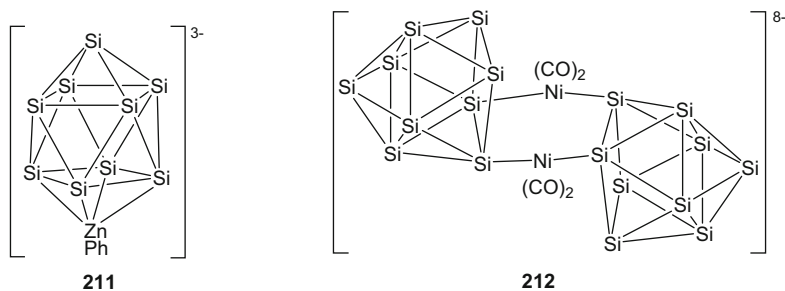
Scheme 64 Pentasilicide dianion **207**, reversible redox couple nonasilicides **208** and **209**, nonasilicide tetraanion **210** (counterions: **207**: $[\text{Rb}^+[2.2.2]\text{cryptand}]_2$, **208**: $[\text{K}(18\text{-crown-6})]_2$, **209**: $[\text{K}^+/\text{Rb}^+[2.2.2]\text{cryptand}]_3$, **210**: $[\text{Rb}^+[2.2.2]\text{cryptand}][\text{Rb}^+]_3$ or $[\text{Rb}^+]_4$)

tetrasilicide tetraanion $[(\text{MesCu})_2(\eta^3\text{-Si}_4)]^{4-}$ **206**. All Si–Si bonds in **206** are comparable to those found in $[\text{Si}_4]^{4-}$ tetraanions in binary phases except for the Si–Si bond between the two η^3 -coordinated Si_3 faces, which is significantly longer (depicted as a dashed line in Scheme 63).

The five atom cluster $[\text{Si}_5]^{2-}$ **207** was obtained in low yield from an ammonia solution of $\text{Rb}_{12}\text{Si}_{17}$ in the presence of [2.2.2]cryptand after addition of PMe_3 (Scheme 64) [210]. Pentasilicide dianion **207** exhibits a trigonal bipyramidal structure, in agreement with its *closo* electron count of $(n + 1)$ cluster electron pairs.

Soluble nine-vertex silicon clusters **208–210** with two, three, and four negative charges were isolated to date. Their structures are surprisingly similar and are best described as either tricapped trigonal prism (**209**) or monocapped square antiprisms (**208**, **210**). Nonasilicite trianion $[\text{Si}_9]^{3-}$ **209** was obtained as the major product during the synthesis of pentasilicide **207** or alternatively from $\text{K}_{12}\text{Si}_{17}$ under similar conditions but without PMe_3 [210]. Dianion $[\text{Si}_9]^{2-}$ **209** is accessible by oxidation of ammonia solutions of trianion **208** with Ph_3GeCl , Me_3SnCl , or *tert*-BuCl [211]. The $[\text{Si}_9]^{2-}/[\text{Si}_9]^{3-}$ single electron redox couple was investigated by cyclic voltammetry in DMF and pyridine and shown to be quasi reversible. Binary and ternary solid state phases $\text{M}_{12}\text{Si}_{17}$ ($\text{M} = \text{K}, \text{Rb}$) are known to contain $[\text{Si}_4]^{4-}$ and $[\text{Si}_9]^{4-}$ tetraanions. The isolation of nonasilicide tetraanion $[\text{Si}_9]^{4-}$ **210** from solution was achieved by dissolution of $\text{K}_6\text{Rb}_6\text{Si}_{17}$ in ammonia in the presence of 18-crown-6 and subsequent slow crystallization [212].

Nonasilicide tetraanion **210** was already employed as a ligand for transition metal complexes prior to its isolation in substance. Crystalline material containing



Scheme 65 *closo*-[Si₉ZnPh]³⁻ Trianion **211** and octaanionic [Ni(CO)₂]₂ complex **212**, (counterions: **211**: [K⁺[2.2.2]cryptand]₃, **212**: [Rb⁺(18-crown-6)]₂[K⁺(18-crown-6)]₂[Rb⁺]₄)

the [Si₉ZnPh]³⁻ trianion was obtained from a pyridine solution of K₁₂Si₁₇, ZnPh₂, and [2.2.2]cryptand (Scheme 65) [213]. The transition metal fragment [ZnPh]⁺ takes part fully in cluster bonding and tetraanion **211** is therefore best described as a bicapped square antiprismatic *closo*-[Si₉ZnPh]³⁻ cluster, in agreement with the Wade rules.

It has been found that [Si₉]⁴⁻ tetraanion **210** can also coordinate to a transition metal center in a σ -like fashion [214]. The octaanionic complex **212** was isolated from an ammonia solution of K₆Rb₆Si₁₇ in the presence of 18-crown-6 and (Ph₃P)₂Ni(CO)₂. The reaction can be considered as a simple ligand exchange of nonasilicide **210** with triphenylphosphine. IR spectroscopic investigations show that the donor–acceptor properties of Ph₃P and μ -[Si₉]⁴⁻ toward the Ni(CO)₂ fragment are comparable.

6 Conclusion

This chapter summarizes contribution to the field of silyl anion research of the approximately last 10 years. In addition to important publications focusing on synthetic and structural aspects of silyl anions themselves, several other areas have seen remarkable progress. The now well-established synthesis of sophisticated organosilicon precursors for materials chemistry is expected to be increasingly important in the near future and the somewhat difficult handling of functionalized silyl anions, e.g., silylenoids and chiral silanides, should not be an obstacle for further progress anymore. Some only recently discovered low-valent anionic silicon species and small clusters have been established as versatile building blocks for the synthesis of numerous hitherto unknown main group compounds in a very short period of time and many more exciting results can be expected. Last but not least soluble, the functionalization of multiple charged Zintl anions offers new and rather unexpected possibilities in the future.

References

1. Müller R (1965) One hundred years of organosilicon chemistry. *J Chem Edu* 42:41
2. Kraus CA, Eatough H (1933) Triphenylsilyl ethylamine ($C_6H_5)_3Si-C_2H_5NH_2$. *J Am Chem Soc* 55:5008
3. Kraus CA, Nelson WK (1934) The chemistry of the triethylsilyl group. *J Am Chem Soc* 56:195
4. Kipping FS (1937) The Bakerian lecture: organic derivatives of silicon. *Proc R Soc Lond A* 159:139
5. Gilman H, Wu TC (1951) Cleavage of the Silicon–Silicon Bond in hexaphenyldisilane. *J Am Chem Soc* 73:4031
6. Benkeser RA, Severson RG (1951) The preparation and reactions of triphenylsilyl potassium. *J Am Chem Soc* 73:1424
7. Lee VY, Sekiguchi A (2010) Heavy analogs of carbanions: Si-, Ge-, Sn- and Pb-centered anions. In: Lee VY, Sekiguchi A (eds) *Organometallic compounds of low-coordinate Si, Ge, Sn, and Pb*. Wiley, Chichester
8. Marschner C (2006) Preparation and reactions of polysilyl anions and dianions. *Organometallics* 25:2110
9. Lee VY, Sekiguchi A (2007) Aromaticity of group 14 organometallics: experimental aspects. *Angew Chem Int Ed* 46:6596
10. Lerner HW (2005) Silicon derivatives of group 1, 2, 11 and 12 elements. *Coord Chem Rev* 249:781
11. Saito M, Yoshioka M (2005) The anions and dianions of group 14 metalloids. *Coord Chem Rev* 249:765
12. Lee VY, Sekiguchi A (2008) Cyclic polyenes of heavy group 14 elements: new generation ligands for transition-metal complexes. *Chem Soc Rev* 37:1652
13. Sekiguchi A, Lee VY, Nanjo M (2000) Lithiosilanes and their application to the synthesis of polysilane dendrimers. *Coord Chem Rev* 210:11
14. Scheschkewitz D (2011) The versatile chemistry of disilenes: disila analogues of vinyl anions as synthons in low-valent silicon chemistry. *Chem Lett* 40:2
15. Scheschkewitz D (2009) Anionic reagents with silicon-containing double bonds. *Chem Eur J* 15:2476
16. Sakurai H, Okada A, Kira M, Yonezawa K (1971) Trimethylsilylsodium. A new preparation and some reactions involving a facile electron transfer from trimethylsilyl anion to naphthalene. *Tetrahedron Lett* 19:1511
17. Sakurai H, Kondo F (1975) Chemistry of organosilicon compounds LXXX. Useful modifications in the preparation of trimethylsilylsodium and trimethylsilyl potassium. *J Organomet Chem* 92:C46
18. Fischer R, Konopa T, Ullrich S, Baumgartner J, Marschner C (2003) Route Si_6 revisited. *J Organomet Chem* 685:79
19. Zirmgast M, Baumgartner J, Marschner C (2008) Synthesis of cyclic and bicyclic polysilanes of variable ring sizes. *Organometallics* 27:6472
20. Wallner A, Hlina J, Konopa T, Wagner H, Baumgartner J, Marschner C (2010) Cyclic and bicyclic methylpolysilanes and some oligosilanylene-bridged derivatives. *Organometallics* 29:2660
21. Wagner H, Baumgartner J, Marschner C (2007) 1,1'-Oligosilanylferrrocene compounds. *Organometallics* 26:1762
22. Hassler K, Dzambaski A, Baumgartner J (2008) Dihaloheptasilanes $X_2Si[SiMe(SiMe_3)_2]_2$ as potential precursors for silylenes, disilenes and cyclotrisilanes. *Silicon Chem* 3:271
23. Stueger H, Mitterfellner T, Fischer R, Walkner C, Patz M, Wieber S (2012) Selective synthesis and derivatization of alkali metal silanides $MSi(SiH_3)_3$. *Chem Eur J* 18:7662

24. Brefort JL, Corriu R, Guerin C, Henner B (1989) Hypervalent silicon hydrides: evidence of their intermediacy in the reaction of optically active 1NpPhMeH(D) with hydrides. *J Organomet Chem* 370:9
25. Iwamoto T, Okita J, Kabuto C, Kira M (2002) Sila-metalation route to hydrido(trialkylsilyl)silyllithiums. *J Am Chem Soc* 124:11604
26. Iwamoto T, Okita J, Kabuto C, Kira M (2003) Synthesis, structure and isomerization of $A_2Si=SiB_2$ -type tetrakis(trialkylsilyl)disilenes. *J Organomet Chem* 686:105
27. Kira M, Kadowaki T, Yin D, Sakamoto K, Iwamoto T, Kabuto C (2007) Synthesis and structure of ethynylsilyllithiums. *Organometallics* 26:4890
28. Kajiwara T, Takeda N, Sasamori T, Tokitoh N (2008) Synthesis of alkali metal salts of borylsilyl anions utilizing highly crowded silylboranes and their properties. *Organometallics* 27:880
29. Nakata N, Sekiguchi A (2006) A stable silaborene: synthesis and characterization. *J Am Chem Soc* 128:422
30. Ichinohe M, Kinjo R, Sekiguchi A (2003) The first methyl-substituted disilene: synthesis, crystal structure, and regioselective MeLi addition. *Organometallics* 22:4621
31. Allred AL, Smart RT, Van Beek DA (1992) Cleavage of Carbon–Silicon bonds in the presence of Silicon–Silicon bonds by electron-transfer reagents. *Organometallics* 11:4225
32. Strohmann C, Schildbach D, Auer D (2005) Selective Si–C bond cleavage as synthetic entry to a functionalized lithiosilane. *J Am Chem Soc* 127:7968
33. Strohmann C, Däschlein C, Kellert M, Auer D (2007) A highly enantiomerically enriched lithiosilane by selective cleavage of a Silicon–Phenyl bond with lithium. *Angew Chem Int Ed* 46:4780
34. Däschlein C, Strohmann C (2010) The competition between Si–Si and Si–C cleavage in functionalised oligosilanes: their reactivity with elemental lithium. *Dalton Trans* 39:2062
35. Strohmann C, Däschlein C (2008) Bent phenyl groups in lithiosilanes – crystal structures and interpretation of this unanticipated feature. *Chem Commun* 2791
36. Arp H, Marschner C, Baumgartner J (2010) The quest for silylhydroboranes: $(Me_3Si)_3SiBH_2$. *Dalton Trans* 39:9270
37. Wiberg N, Finger C, Polborn K (1993) Tetrakis(tri-*tert*-butylsilyl)-*tetrahedro*-tetrasilane (tBu_3Si)₄Si₄: the first molecular silicon compound with a Si₄ tetrahedron. *Angew Chem Int Ed Engl* 32:1054
38. Meyer-Wegner F, Scholz S, Sängler I, Schödel F, Bolte M, Wagner M, Lerner HW (2009) Synthesis of Wiberg's tetrasilatetrahedrane (tBu_3Si)₄Si₄ by a one-pot procedure. *Organometallics* 28:6835
39. Scheer M, Balázs G, Seitz A (2010) P₄ activation by main group elements and compounds. *Chem Rev* 110:4236
40. Lerner HW, Wagner M, Bolte M (2003) A novel type of phosphide: synthesis and X-ray crystal structure analysis of (tBu_3Si)₃P₄Li₃. *Chem Commun* 990
41. Wiberg N, Wörner A, Lerner HW, Karaghiosoff K, Fenske D, Baum G, Dransfeld A, von Ragué Schleyer P (1998) The triphosphide (tBu_3Si)₂P₃Na: formation, X-ray and Ab initio structure analyses, protonation and oxidation to triphosphane (tBu_3Si)₂P₃H and hexaphosphanes (tBu_3Si)₄P₆. *Eur J Inorg Chem* 833
42. Lerner HW, Sängler I, Schödel F, Lorbach A, Bolte M, Wagner M (2008) Isoelectronic caesium compounds: the triphosphenide Cs[$tBu_3SiPPPSi$ / tBu_3] and the enolate Cs [OCH=CH₂]. *Dalton Trans* 37:787
43. Lorbach A, Nadj A, Tüllmann S, Dornhaus F, Schödel F, Sängler I, Margraf G, Bats JW, Bolte M, Holthausen MC, Wagner M, Lerner HW (2009) Supersilylated tetraphosphene derivatives M₂[t -Bu₃SiPPPSi- t -Bu₃] (M = Li, Na, Rb, Cs) and Ba[t -Bu₃SiPPPSi- t -Bu₃]: reactivity and *cis*-*trans* isomerization. *Inorg Chem* 48:1005
44. Lorbach A, Breitung S, Sängler I, Schödel F, Bolte M, Wagner M, Lerner HW (2011) The difference regarding the reactivity of the silanides Na[Si/ t -Bu₃] and Na[SiPh/ t -Bu₂] towards white phosphorus. *Inorg Chim Acta* 378:1

45. Nanjo M, Nanjo E, Mochida K (2004) Tris(trimethylsilyl)-substituted heavy group 14-element-centered anions: unsolvated trimeric germyllithium and solvated dimeric silyl- and stannylithiums. *Eur J Inorg Chem* 2961
46. Kyushin S, Kawai H, Matsumoto H (2004) (*trans*-1,2,2,3,4,4-Hexa-*tert*-butyl-1,3-cyclotetrasilanediyldipotassium: supramolecular structure of the silylpotassium–benzene complex. *Organometallics* 23:311
47. Lerner HW, Scholz S, Bolte M, Wagner M (2004) Alkali metal di-*tert*-butylphenylsilylanides – *t*Bu₂PhSiM (M = Li, Na, K) – syntheses, structures, and reactivity. *Z Anorg Allg Chem* 630:443
48. Teng W, Englich U, Ruhlandt-Senge K (2003) Syntheses and structures of barium silanides: contact and separated ions. *Angew Chem Int Ed* 42:3661
49. Lerner HW, Scholz S, Bolte M, Wiberg N, Nöth H, Krossing I (2003) Synthesis and structures of Alkaline–Earth metal supersilanides: *t*Bu₃SiMX and *t*Bu₃Si–M–Si*t*Bu₃ (M = Be, Mg; X = Cl, Br). *Eur J Inorg Chem* 666
50. Saulys DA, Powell DR (2003) Synthesis, experimental/theoretical characterization, and thermolysis chemistry of CpBe(SiMe₃), a molecule containing an unprecedented Beryllium–Silicon bond. *Organometallics* 22:407
51. Teng W, Ruhlandt-Senge K (2004) Syntheses and structures of the first heavy alkaline earth metal bis(tris(trimethylsilyl)silanides). *Organometallics* 23:2694
52. Gaderbauer W, Zirngast M, Baumgartner J, Marschner C (2006) Synthesis of polysilylanyl-magnesium compounds. *Organometallics* 25:2599
53. Wiberg E, Stecher O, Andrascheck HJ, Kreuzbichler L, Staude E (1963) Recent developments in the chemistry of metal silyls of the type M(SiR₃)_n. *Angew Chem Int Ed Engl* 2:507
54. Arnold J, Tilley TD, Rheingold AL, Geib SJ (1987) Preparation and characterization of tris(trimethylsilyl)silyl derivatives of zinc, cadmium, and mercury. X-ray crystal structure of Zn[Si(SiMe₃)₃]₂. *Inorg Chem* 26:2106
55. Wiberg N, Amelunxen K, Lerner HW, Nöth H, Appel A, Knizek J, Polborn K (1997) Disupersilylmetals (^tBu₃Si)₂M and supersilylmetal halides ^tBu₃SiMX with M = Zn, Cd, Hg: syntheses, properties, structures. *Z Anorg Allg Chem* 623:1861
56. Wiberg N, Niedermayer W, Lerner HW, Bolte M (2001) Disupersilylsilanides M(SiHR*₂)₂ of metals of the zinc group (M = Zn, Cd, Hg; R* = Si*t*Bu₃): syntheses, characterization, and structures. *Z Allg Anorg Chem* 627:1043
57. Gaderbauer W, Balatoni I, Wagner H, Baumgartner J, Marschner C (2010) Synthesis and structural diversity of oligosilylanylzinc compounds. *Dalton Trans* 39:1598
58. Dobrovetsky R, Kratish Y, Tumanskii B, Botoshansky M, Bravo-Zhivotovskii D, Apeloig Y (2012) Radical activation of Si–H bonds by organozinc and silylzinc reagents: synthesis of geminal dizincosilanes and zinciolithiosilanes. *Angew Chem Int Ed* 51:4671
59. Nanjo M, Oda T, Mochida K (2003) Preparation and structural characterization of trimethylsilyl-substituted germylzinc halides, (Me₃Si)₃GeZnX (X = Cl, Br, and I) and silylzinc chloride, R(Me₃Si)₂SiZnCl (R = SiMe₃, and Ph). *J Organomet Chem* 672:100
60. Woods JB, Yu X, Chen T, Xue ZL (2004) A trisilyl zincate containing bidentate [(Me₃Si)₂Si(CH₂)₂Si(SiMe₃)₂]²⁻. *Organometallics* 23:5910
61. Sommer LH, Frye CL, Parker GA, Michael KW (1964) Stereochemistry of asymmetric silicon. I. Relative and absolute configurations of optically active α-naphthylphenylsilylanes. *J Am Chem Soc* 86:3271
62. Colomer E, Corriu R (1976) Optically active silylanions. Evidence for the formation of analogues of silyl Grignard reagents. *J Chem Soc Chem Commun* 176
63. Omote M, Tokita T, Shimizu Y, Imae I, Shirakawa E, Kawakami Y (2000) Stereospecific formation of optically active trialkylsilyllithiums and their configurational stability. *J Organomet Chem* 611:20
64. Oh HS, Imae I, Kawakami Y, Ray S, Yamane T (2003) Synthesis, stereochemistry and chiroptical properties of naphthylphenyl-substituted optically active oligosilanes with α, ω-chiral silicon centers. *J Organomet Chem* 685:35

65. Strohmann C, Hörnig J, Auer D (2002) Synthesis of a highly enantiomerically enriched silyllithium compound. *Chem Commun* 766
66. Däschlein C, Gessner VH, Strohmann C (2008) (*S*)-1,2-Dimethyl-1,1,2-triphenyl-2-(4-piperidinomethyl)disilane chloride. *Acta Cryst E* 64:1950
67. Strohmann C, Däschlein C (2008) Synthesis of a highly enantiomerically enriched silagermane and selective cleavage of the Si–Ge bond with lithium. *Organometallics* 27:2499
68. Oestreich M, Auer G, Keller M (2005) On the mechanism of the reductive metallation of asymmetrically substituted silyl chlorides. *Eur J Org Chem* 184
69. Strohmann C, Bindl M, Fraaß VC, Hörnig J (2004) Enantiodivergence in the reactions of a highly enantiomerically enriched silyllithium compound with benzyl halides: control of inversion and retention by selection of halide. *Angew Chem Int Ed* 43:1011
70. Däschlein C, Bauer SO, Strohmann C (2011) Mechanistic insights into the reaction of enantiomerically pure lithiosilanes and electrophiles: understanding the difference between aryl and alkyl halides. *Eur J Inorg Chem* 1454
71. Strohmann C, Däschlein C, Auer D (2006) Crystal structures of the chiral lithiosilanes [(*Lis*)-PhMe₂SiLi·THF·(-)-Sparteine] and [Ph₂(NEt₂)SiLi·(-)-Sparteine]. *J Am Chem Soc* 128:704
72. Däschlein C, Strohmann C (2009) Structural studies on (-)-sparteine-coordinated lithiosilanes. *Eur J Inorg Chem* 43
73. Hitchcock PB, Lappert MF, Layh M (1998) Novel lithium 3-sila and 3-germa-β-diketiminates. *Chem Commun* 2179
74. Farwell JD, Fernandes MA, Hitchcock PB, Lappert MF, Layh M, Omondi B (2003) Synthesis, crystal structures and reactions of sila- and germa-β-diketiminates. *Dalton Trans* 1719
75. Farwell JD, Hitchcock PB, Lappert MF, Protchenko AV (2005) Synthesis and structures of a 3-sila-β-diketiminatomagnesium bromide, ketenimide and triflate. *Chem Commun* 2271
76. Farwell JD, Hitchcock PB, Lappert MF, Protchenko AV (2007) Synthesis and structures of 3-sila-β-diketiminato complexes of the coinage metals. *J Organomet Chem* 692:4953
77. Krempner C, Chisholm MH, Galluci J (2008) The multidentate ligand [MeOMe₂Si]₃Si⁻: unusual coordination modes in alkali metal silanides. *Angew Chem Int Ed* 47:410
78. Carlson B, Aquino A, Hope-Weeks LJ, Whittlesey B, McNerney B, Hase WL, Krempner C (2011) Homoleptic tris(methoxydimethylsilyl)silanides of the alkaline earth metals: first zwitterionic silanides with two naked silyl anions. *Chem Commun* 47:11089
79. Li H, Hope-Weeks LJ, Krempner C (2011) A supramolecular approach to zwitterionic alkaline metal silanides and formation of heterobimetallic silanides. *Chem Commun* 47:4117
80. Li H, Hung-Low F, Krempner C (2012) Synthesis and structure of zwitterionic silylborates and silylzincates with pendant polydonor arms. *Organometallics* 31:7117
81. Lawrence SC, Skinner M, Green C, Mountford P (2001) A structurally characterized, naked sp³-hybridised carbanion in the zwitterionic imido complex [Ti(NBu¹){C(Me₂pz)₃}Cl(THF)] (HMe₂pz = 3,5-dimethylpyrazole). *Chem Commun* 705
82. Breher F, Gruenberg J, Lawrence SC, Mountford P, Rügger H (2004) A monomeric organolithium compound containing a free pyramidal carbanion in solution and in the solid state. *Angew Chem Int Ed* 43:2521
83. Kratzert D, Leusser D, Stern D, Meyer J, Breher F, Stalke D (2011) Experimental charge density distribution of non-coordinating sp³ carbanions in [Mg{(pz*)₃C}₂]. *Chem Commun* 47:2931
84. Armbruster F, Fernandez I, Breher F (2009) Syntheses, structures, and reactivity of poly(pyrazolyl)silanes, -disilanes, and the ambidentate κ¹Si/κ³N-coordinating tris(3,5-dimethylpyrazolyl)silanide ligand [Si(3,5-Me₂pz)₃]⁻ (^{Me}Tpsd). *Dalton Trans* 5612
85. McNerney B, Whittlesey B, Krempner C (2011) Synthesis and reactivity of new pyrazolyl-functionalized potassium silanides. *Eur J Inorg Chem* 1699
86. Tamao K, Kawachi A (1995) The chemistry of silylenoids: preparation reactivity of (Alkoxysilyl)lithium compounds. *Angew Chem Int Ed Engl* 34:818
87. Zirngast M, Baumgartner J, Marschner C (2008) Preparation, structure and reactivity of Et₂N(Me₃Si)₂SiK. *Eur J Inorg Chem* 1078
88. Popowski E, Rietz I, Fischer C, Erben S, Harloff J, Reinke H (2012) Reactions of bis(trimethylsilyl)aminochlorosilanes with lithium – N, Si-migration of trimethylsilyl groups

- or self-condensation of bis(trimethylsilyl)aminosilyllithium compounds. *Z Anorg Allg Chem* 638:1187
89. Likhar PR, Zirngast M, Baumgartner J, Marschner C (2004) Preparation and structural characterisation of methoxybis(trimethylsilyl)silyl potassium and its condensation product. *Chem Commun* 1764
 90. Harloff J, Popowsk E, Reinke H (2007) Substituted lithiumtrimethylsiloxysilanides $\text{LiSiRR}'(\text{OSiMe}_3)$ – investigations of their synthesis, stability and reactivity. *J Organomet Chem* 692:1421
 91. Harloff J, Popowski E (2008) Reactions of trimethylsiloxychlorosilanes with lithium metal – on the mechanism of the formation of trimethylsiloxysilyllithium compounds $\text{LiSiRR}'(\text{OSiMe}_3)$. *J Organomet Chem* 693:1283
 92. Feng D, Xie J, Feng S (2004) Theoretical study on the structures and isomerization of silylenoid [(*tert*-butoxy)diphenylsilyl]lithium. *Chem Phys Lett* 396:245
 93. Xie J, Feng D, He M, Feng S (2005) Insertion reactions of silylenoid $\text{Ph}_2\text{SiLi}(\text{O}i\text{Bu}-t)$ into X–H Bonds (X = F, OH, and NH_2). *J Phys Chem A* 109:10563
 94. Fischer R, Baumgartner J, Kickelbick G, Marschner C (2003) The first stable β -fluorosilylanion. *J Am Chem Soc* 125:3414
 95. Zirngast M, Flock M, Baumgartner J, Marschner C (2008) Formation of formal disilene fluoride adducts. *J Am Chem Soc* 130:17460
 96. Lee ME, Cho HM, Ryu MS, Kim CH, Ando W (2001) A stable halosilylene at room temperature in THF solution. *J Am Chem Soc* 123:7732
 97. Flock M, Dransfeld A (2003) The solution structure of $(\text{Me}_3\text{Si})_3\text{CSiBr}$ – an Ab initio/NMR study. *Chem Eur J* 9:3320
 98. Lee ME, Cho HM, Lim YM, Choi JK, Park CH, Jeong SE, Lee U (2004) Syntheses and reactivities of stable halosilylenoids, $(\text{Tsi})\text{X}_2\text{SiLi}$ (Tsi = $\text{C}(\text{SiMe}_3)_3$, X = Br, Cl). *Chem Eur J* 10:377
 99. Feng S, Lai G, Zhou Y, Feng D (2005) An ab initio study on structures and isomerization of magnesium chlorosilylenoid $\text{H}_2\text{SiClMgCl}$. *Chem Phys Lett* 415:327
 100. Xie J, Feng D, Feng S, Zhang J (2005) Theoretical study on insertion of silylenoid H_2SiLiF into X–H bonds (X = CH_3 , SiH_3 , NH_2 , PH_2 , OH, SH and F). *J Mol Struct THEOCHEM* 755:55
 101. Zhang Y, Li M, Lai G, Feng D, Feng S (2008) *Ab initio* study on structures and isomerization of magnesium fluorosilylenoid H_2SiFMgF . *Chin J Chem Phys* 21:541
 102. Xie J, Feng D, Feng S (2006) Theoretical study on the isomeric structures and the stability of silylenoid $(\text{Tsi})\text{Cl}_2\text{SiLi}$ (Tsi = $\text{C}(\text{SiMe}_3)_3$). *J Comp Chem* 27:933
 103. Flock M, Marschner C (2005) Silyl anions or silylenoids? – a DFT study of silyllithium compounds with π -donating substituents. *Chem Eur J* 11:4635
 104. Molev G, Bravo-Zhivotovskii D, Karni M, Tumanskii B, Botoshansky M, Apeloig Y (2006) Synthesis, molecular structure, and reactivity of the isolable silylenoid with a tricoordinate silicon. *J Am Chem Soc* 128:2784
 105. Weidenbruch M (2006) A stable silylenoid and a donor-stabilized chlorosilylene: low-coordinate silicon compounds – a never-ending story? *Angew Chem Int Ed* 45:4241
 106. Sekiguchi A, Inoue S, Ichinohe M, Arai Y (2004) Isolable anion radical of blue disilene ($^t\text{Bu}_2\text{MeSi}$) $_2\text{Si} = \text{Si}(\text{Si}^t\text{Bu}_2\text{Me})_2$ formed upon one-electron reduction: synthesis and characterization. *J Am Chem Soc* 129:9626
 107. Xie J, Feng D, Feng S (2007) Theoretical study on the substitution reactions of silylenoid H_2SiLiF with CH_4 , NH_3 , H_2O , HF, SiH_4 , PH_3 , H_2S , and HCl. *J Phys Chem A* 111:8475
 108. Qi Y, Feng D, Feng S (2008) Theoretical study on the addition reactions of silylenoids H_2SiLiX (X = F, Cl) to formaldehyde. *J Mol Struct THEOCHEM* 856:96
 109. Qi Y, Geng B, Che Z (2012) The insertion reactions of the p-complex silylenoid H_2SiLiF with Si–X (X = F, Cl, Br, O, N) bonds. *J Mol Model* 18:1015
 110. Cho HM, Bok K, Park SH, Lim YM, Lee ME, Choi MG, Lee KM (2012) A new synthetic route for silacyclopropanes: reactions of a bromosilylenoid with olefins. *Organometallics* 31:5227

111. Lim YM, Cho HM, Lee ME, Baek KK (2006) A stable magnesium bromosilylenoid: transmetalation of a lithium bromosilylenoid by magnesium bromide. *Organometallics* 25:4960
112. Lim YM, Park CH, Yoon SJ, Cho HM, Lee ME, Baek KK (2010) New synthetic routes for silaheterocycles: reactions of a chlorosilylenoid with aldehydes. *Organometallics* 29:1355
113. Cho HM, Lim YM, Lee ME (2010) Reactivities of chlorotrisilylsilylenoid with ketones. *Dalton Trans* 39:9232
114. Cho HM, Lim YM, Lee BW, Park SJ, Lee ME (2011) Synthesis and reactivity of stable tris(aminomethylphenyl)silylenoid. *J Organomet Chem* 696:2665
115. Kawachi A, Oishi Y, Kataoka T, Tamao K (2004) Preparation of sulfur-substituted silyllithiums and their thermal degradation to silylenes. *Organometallics* 23:2949
116. Lee ME, Lim YM, Son JY, Seo WG (2008) Stable halodilithiosilanes: synthesis and reactivity of TsiXSiLi₂ (X = Br, and Cl). *Chem Lett* 37:680
117. Lim YM, Lee ME, Lee J, Do Y (2008) Reactivity of bromodilithiosilane to naphthalene and anthracene. *Organometallics* 27:6375
118. Mehrotra SK, Kawa H, Baran JR, Ludvig MM, Lagow RJ (1990) Synthesis of the first organodilithiosilane by thermal rearrangement. *J Am Chem Soc* 112:9003
119. Sekiguchi A, Ichinohe M, Yamaguchi S (1999) An unexpected reaction of silacyclopentene to form an organodilithiosilane: isolation and characterization of a 1,1-dilithiosilane derivative. *J Am Chem Soc* 121:10231
120. Ichinohe M, Arai Y, Sekiguchi (2001) A new approach to the synthesis of unsymmetrical disilenes and germasilenes: unusual ²⁹Si NMR chemical shifts and regioselective methanol addition. *Organometallics* 20:4141
121. Dias H, Olmstead MM, Ruhlandt-Senge K, Power PP (1993) The X-ray crystal structures of the mononuclear silyllithium species Li(THF)₃SiPh₃ and Li(THF)₃Si(SiMe₃)₃. *J Organomet Chem* 462:1
122. Heine A, Herbst-Irmer R, Sheldrick GM, Stalke D (1993) Structural characterization of two modifications of tris(tetrahydrofuran)tris(trimethylsilyl)silyl)lithium: a compound with a ²⁹Si-⁷Li NMR coupling. *Inorg Chem* 32:2694
123. Nakata N, Izumi R, Lee VY, Ichinohe M, Sekiguchi A (2004) 1,3-Disila-2-gallata- and indatallaenic anions [$\text{>SiMSi<}^- \cdot \text{Li}^+$] (M = Ga, In): compounds featuring double bonds between elements of group 13 and 14. *J Am Chem Soc* 126:5058
124. Nakata N, Izumi R, Lee VY, Ichinohe M, Sekiguchi A (2005) Reaction of dilithiosilane R₂SiLi₂ and dilithiogermane R₂GeLi₂ (R = SiMe^tBu₂) with MesBCl₂ (Mes = 2,4,6-trimethylphenyl): evidence for the formation of silaborene R₂Si=BMes and germaborene R₂GeBMes. *Chem Lett* 34:582
125. Tanaka H, Inoue S, Ichinohe M, Driess M, Sekiguchi A (2011) Synthesis and striking reactivity of an isolable tetrasilyl-substituted trisilaallene. *Organometallics* 30:3475
126. Ichinohe M, Sanuki K, Inoue S, Sekiguchi A (2004) Disilynyllithium from tetrasila-1,3-butadiene: a silicon analogue of a vinylolithium. *Organometallics* 23:3088
127. Lee VY, Kawai M, Sekiguchi A, Ranaivonjatovo H, Escudé J (2009) A "Push-Pull" phosphasilene and phosphagermene and their anion-radicals. *Organometallics* 28:4262
128. Bravo-Zhivotovskii D, Yuzefovich M, Sigal N, Korogodsky G, Klinkhammer K, Tumanskii B, Shames A, Apeloig Y (2002) The synthesis of the first compound with Li-Si-Hg bonding: [$\text{Li}(i\text{Pr}_3\text{Si})_2\text{Si}_2\text{Hg}$] – a source for the [$\text{Li}(i\text{Pr}_3\text{Si})_2\text{Si}$] radical. *Angew Chem Int Ed* 41:649
129. Bravo-Zhivotovskii D, Ruderfer I, Melamed S, Botoshansky M, Tumanskii B, Apeloig Y (2005) Nonsolvated, aggregated 1,1-dilithiosilane and the derived silyl radicals. *Angew Chem Int Ed* 44:739
130. Bravo-Zhivotovskii D, Ruderfer I, Yuzefovich M, Kosa M, Botoshansky M, Tumanskii B, Apeloig Y (2005) Mercury-substituted silyl radical intermediates in formation and fragmentation of geminal dimercury silyl compounds. *Organometallics* 24:2698
131. Bravo-Zhivotovskii D, Molev G, Kravchenko V, Botoshansky M, Schmidt A, Apeloig Y (2006) Novel aggregation motif of *gem*-dilithiosilanes: coaggregation of two R₂SiLi₂ molecules with two RLi molecules. *Organometallics* 25:4719

132. Biffar W, Nöth H, Schwerthöffer R (1981) Contributions to the chemistry of boron. Synthesis and reactivity of trimethylsilylboranes. *Liebigs Ann Chem* 122:2067
133. Nanjo M, Sekiguchi A, Sakurai H (1999) Crystal structure of unsolvated lithiosilanes with Si–Si bonds. *Bull Chem Soc Jpn* 72:1387
134. Bravo-Zhivotovskii D, Dobrovetsky R, Nemirovsky D, Molev V, Bendikov M, Molev G, Botoshansky M, Apeloig Y (2008) The synthesis and isolation of a metal-substituted bis-silene. *Angew Chem Int Ed* 47:4343
135. Bravo-Zhivotovskii D, Ruderfer I, Melamed S, Botoshansky M, Schmidt A, Apeloig Y (2006) $[(t\text{Bu}_2\text{Me})_2\text{Si}]_3\text{Li}_4^{2-}$: an aggregated dianion of a 1,1-dilithiosilane with a unique structural motif. *Angew Chem Int Ed* 45:4157
136. Dobrovetsky R, Bravo-Zhivotovskii D, Tumanskii B, Botoshansky M, Apeloig Y (2010) Synthesis, isolation, and characterization of 1,1-diGrignard and 1,1-dizinc silanes. *Angew Chem Int Ed* 49:7086
137. Hong JH, Boudjouk P (1993) A stable aromatic species containing silicon. Synthesis and characterization of the 1-*tert*-Butyl-2,3,4,5-tetraphenyl-1-silacyclopentadienide anion. *J Am Chem Soc* 115:5883
138. Joo WC, Hong JH, Choi SB, Son HE, Kim CH (1990) Synthesis and reactivity of 1,1-disodio-2,3,4,5-tetraphenyl-1-silacyclopentadiene. *J Organomet Chem* 391:27
139. Bankwitz U, Sohn H, Powell DR, West R (1995) Synthesis, solid-state structure, and reduction of 1,1-dichloro-2,3,4,5-tetramethylsilole. *J Organomet Chem* 499:C7
140. Choi SB, Boudjouk P, Wei P (1998) Aromatic benzannulated silole dianions. The dilithio and disodio salts of a silaindenyl dianion. *J Am Chem Soc* 120:5814
141. Choi SB, Boudjouk P (2000) Synthesis and characterization of dibenzannulated silole dianions. The 1,1-dilithiosilafluorene and 1,1'-dilithiobis(silafluorene) dianion. *Tetrahedron Lett* 41:6685
142. Liu Y, Ballweg D, West R (2001) Reductive coupling of carbonyl compounds using silole and germole dianions. *Organometallics* 20:5769
143. Liu Y, Ballweg D, Müller T, Guzei IA, Clark RW, West R (2002) Chemistry of the aromatic 9-germafluorenyl dianion and some related silicon and carbon species. *J Am Chem Soc* 124:12174
144. Liu Y, Stringfellow TC, Ballweg D, Guzei IA, West R (2002) Structure and chemistry of 1-silafluorenyl dianion, its derivatives, and an organosilicon diradical dianion. *J Am Chem Soc* 124:49
145. Hong JH (2011) Synthesis and NMR-study of the 2,3,4,5-tetraethylsilole dianion $[\text{SiC}_4\text{Et}_4]^{2-} \cdot 2[\text{Li}]^+$. *Molecules* 16:8033
146. Hong JH (2011) Dissociation of the disilatricyclic diallylic dianion $[(\text{C}_4\text{Ph}_4\text{SiMe})_2]^{2-}$ to the silole anion $[\text{MeSiC}_4\text{Ph}_4]^-$ by halide ion coordination or halide ion nucleophilic substitution at the silicon atom. *Molecules* 16:8451
147. Touloukhouva IS, Stringfellow TC, Ivanov SA, Masunov A, West R (2003) A disilapentalene and a stable diradical from the reaction of a dilithiosilole with a dichlorocyclopropene. *J Am Chem Soc* 125:5767
148. Touloukhouva IS, Guzei IA, West R (2004) Synthesis of a silene from 1,1-dilithiosilole and 2-adamantanone. *J Am Chem Soc* 126:5336
149. Sakamoto K, Ogasawara J, Sakurai H, Kira M (1997) The first silatriafulvene derivative: generation, unusually low reactivity towards alcohols, and isomerization to silacyclobutadiene. *J Am Chem Soc* 119:3405
150. Touloukhouva IS, Friedrichsen DR, Hill NJ, Müller T, West R (2006) Unusual reaction of 1,1-dilithio-2,3,4,5-tetraphenylsilole with 1,3-dienes yielding spirosilanes and elemental lithium. *Angew Chem Int Ed* 45:2578
151. Touloukhouva IS, Timokhin VI, Bunck DN, Guzei I, West R, Müller T (2008) Silylene and germylene intermediates in the reactions of silole and germole dianions with *N,N'*-di-*tert*-butylethylenediimine. *Eur J Inorg Chem* 2344

152. West R, Fink MJ, Michl J (1981) Tetramesityldisilene, a stable compound containing a silicon-silicon double bond. *Science* 214:1343
153. Wiberg N, Vasisht SK, Fischer G, Mayer P (2004) Disilynes. III a relatively stable disilyne $\text{RSi}\equiv\text{SiR}$ ($\text{R} = \text{SiMe}(\text{Si}t\text{Bu}_3)_2$). *Z Anorg Allg Chem* 630:1823
154. Sekiguchi A, Kinjo R, Ichinohe M (2004) A stable compound containing a Silicon-Silicon triple bond. *Science* 305:1755
155. Weidenbruch M, Willms S, Saak W, Henkel G (1997) Hexaaryltetrasilabuta-1,3-diene: a molecule with conjugated Si-Si double bonds. *Angew Chem Int Ed* 36:2503
156. Zborovsky L, Dobrovetsky BM, Bravo-Zhivotovskii D, Apeloig Y (2012) Synthesis of silynyllithiums $\text{Li}(\text{R}_3\text{Si})\text{Si}=\text{C}(\text{SiR}_3)(1\text{-Ad})$ via transient silyne-silylidene intermediates. *J Am Chem Soc* 134:18229
157. Iwamoto T, Kobayashi M, Uchiyama K, Sasaki S, Nagendran S, Isobe H, Kira M (2009) Anthryl-substituted trialkyldisilene showing distinct intramolecular charge-transfer transition. *J Am Chem Soc* 131:3156
158. Kira M, Iwamoto T, Yin D, Maruyama T, Sakurai H (2001) Novel 1,2-dilithiosilanes derived from reduction of stable tetrakis(trialkylsilyl)disilenes with lithium metal. *Chem Lett* 30:910
159. Inoue S, Ichinohe M, Sekiguchi A (2005) Disilynyl anions derived from reduction of tetrakis(di-*tert*-butylmethylsilyl)disilene with metal naphthalenide through disilene dianion intermediate: synthesis and characterization. *Chem Lett* 34:1564
160. Ichinohe M, Sanuki K, Inoue S, Sekiguchi A (2007) Tetrasil-1,3-butadiene and its transformation to disilynyl anions. *Silicon Chem* 3:111
161. Kinjo R, Ichinohe M, Sekiguchi A (2007) An isolable disilyne anion radical and a new route to the disilenide ion upon reduction of a disilyne. *J Am Chem Soc* 129:26
162. Yamaguchi T, Ichinohe M, Sekiguchi A (2010) Addition of methyllithium to disilyne $\text{RSi}\equiv\text{SiR}$ ($\text{R} = \text{Si}i\text{Pr}[\text{CH}(\text{SiMe}_3)_2]$), giving a disilynyllithium, and its unexpected isomerization to a disilacyclopropylsilyllithium. *New J Chem* 34:1544
163. Scheschkewitz D (2004) A silicon analogue of vinylolithium: structural characterization of a disilenide. *Angew Chem Int Ed* 43:2965
164. Nguyen TI, Scheschkewitz D (2005) Activation of a Si=Si bond by η^1 -coordination to a transition metal. *J Am Chem Soc* 127:10174
165. Cowley MJ, Abersfelder K, White A, Majumdar M, Scheschkewitz D (2012) Transmetalation reactions of a lithium disilenide. *Chem Commun* 48:6595
166. Abersfelder K, Scheschkewitz D (2008) Syntheses of trisila analogues of allyl chlorides and their transformations to chlorocyclotrisilanes, cyclotrisilanides, and a trisilaindane. *J Am Chem Soc* 130:4114
167. Abersfelder K, Güclü D, Scheschkewitz D (2006) An unsaturated α, ω -dianionic oligosilane. *Angew Chem Int Ed* 45:1643
168. Abersfelder K, Nguyen TI, Scheschkewitz D (2009) Stannyl-substituted disilenes and a disilastannirane. *Z Anorg Allg Chem* 635:2093
169. Abersfelder K, White A, Rzepa HS, Scheschkewitz D (2010) A tricyclic aromatic isomer of hexasilabenzene. *Science* 327:564
170. Tanaka T, Ichinohe M, Sekiguchi A (2004) Photochemical generation of halo(silyl)silylene: spectroscopic observation and reactivity. *Chem Lett* 33:1420
171. Sekiguchi A, Tanaka T, Ichinohe M, Akiyama K, Gaspar PP (2008) Tri-*tert*-butylsilylenes with alkali metal substituents ($\text{Bu}_3\text{Si})\text{SiM}$ ($\text{M} = \text{Li}, \text{K}$): electronically and sterically accessible triplet ground states. *J Am Chem Soc* 130:426
172. Scheschkewitz D (2005) A molecular silicon cluster with a “Naked” vertex atom. *Angew Chem Int Ed* 44:2954
173. Hartmann M, Haji-Abdi A, Abersfelder K, Haycock PR, White A, Scheschkewitz D (2010) Synthesis, characterization and complexation of phosphino disilenes. *Dalton Trans* 39:9288
174. Bejan I, Scheschkewitz D (2007) Two Si-Si double bonds connected by a phenylene bridge. *Angew Chem Int Ed* 46:5783

175. Jeck J, Bejan I, White A, Nied D, Breher F, Scheschkewitz D (2010) Transfer of a disilyl moiety to aromatic substrates and lateral functional group transformation in aryl disilenes. *J Am Chem Soc* 132:17306
176. Bejan I, Inoue S, Ichinohe M, Sekiguchi A, Scheschkewitz D (2008) 1,2-Disilacyclobut-2-enes: donor-free four-membered cyclic silenes from reaction of disilenides with vinylbromides. *Chem Eur J* 14:7119
177. Bejan I, Güclü D, Inoue S, Ichinohe M, Sekiguchi A, Scheschkewitz D (2007) Stable cyclic silylenes from reaction of disilenides with carboxylic acid chlorides. *Angew Chem Int Ed* 46:3349
178. Inoue S, Ichinohe M, Sekiguchi A (2007) Conversion of a disilene into a silene: silyl-anion-substituted silene by a sila-peterson-type reaction from an sp^2 -type silyl anion. *Angew Chem Int Ed* 46:3346
179. Tanaka H, Inoue S, Ichinohe M, Sekiguchi A (2009) An $(\eta^3\text{-disilaallyl})\text{lithium}$ derivative: interconversion of π -allyl-type bonding and η^1 coordination to a silyllithium fragment. *Organometallics* 28:6625
180. Matsuno T, Ichinohe M, Sekiguchi A (2002) Cyclotetrasilene ion: a reversible redox system of cyclotetrasilanyl cation, radical, and anion. *Angew Chem Int Ed* 41:1575
181. Jutzi P, Mix A, Rummel B, Schoeller WW, Neumann B, Stammeler HG (2004) The $(\text{Me}_5\text{C}_5)\text{Si}^+$ cation: a stable derivative of HSi^+ . *Science* 305:849
182. Leszczyńska K, Abersfelder K, Majumdar M, Neumann B, Stammeler HG, Rzepa HS, Jutzi P, Scheschkewitz D (2012) The Cp^*Si^+ cation as a stoichiometric source of silicon. *Chem Commun* 48:7820
183. Leszczyńska K, Abersfelder K, Mix A, Neumann B, Stammeler HG, Cowley MJ, Jutzi P, Scheschkewitz D (2012) Reversible base coordination to a disilene. *Angew Chem Int Ed* 51:6785
184. Jutzi P, Reumann G (2000) Cp^* Chemistry of main-group elements. *J Chem Soc Dalton Trans* 2237
185. Lee VY, Takanashi K, Matsuno T, Ichinohe M, Sekiguchi A (2004) Cyclobutadiene dianions consisting of heavier group 14 elements: synthesis and characterization. *J Am Chem Soc* 126:4758
186. Lee VY, Takanashi K, Kato R, Matsuno T, Ichinohe M, Sekiguchi A (2007) Heavy analogues of the 6p-electron anionic ring systems: cyclopentadienide ion and cyclobutadiene dianion. *J Organomet Chem* 692:2800
187. von Ragué Schleyer P, Maerker C, Dransfeld A, Jiao H, van Eikema Hommes N (1996) Nucleus-independent chemical shifts: a simple and efficient aromaticity probe. *J Am Chem Soc* 118:6317
188. Kim S, Wang S, Schaefer HF (2011) Structure, energetics, and aromaticities of the tetrasilacyclobutadiene dianion and related compounds: $(\text{Si}_4\text{H}_4)^{2-}$, $(\text{Si}_4\text{H}_4)^{2-}\cdot 2\text{Li}^+$, $[\text{Si}_4(\text{SiH}_3)_4]^{2-}\cdot 2\text{Li}^+$, $[\text{Si}_4(\text{SiH}_3)_4]^{2-}\cdot 2\text{Na}^+$, $[\text{Si}_4(\text{SiH}_3)_4]^{2-}\cdot 2\text{K}^+$. *J Phys Chem A* 115:5478
189. Takanashi K, Lee VY, Matsuno T, Ichinohe M, Sekiguchi A (2005) Tetrasilacyclobutadiene $(\text{tBu}_2\text{MeSi})_4\text{Si}_4$: a new ligand for transition-metal complexes. *J Am Chem Soc* 127:5768
190. Takanashi K, Lee VY, Ichinohe M, Sekiguchi A (2006) A (Tetrasilacyclobutadiene) tricarbonyliron complex $[(\eta^4\text{-}(\text{tBu}_2\text{MeSi})_4\text{Si}_4)\text{Fe}(\text{CO})_3]$: the silicon cousin of Pettit's (Cyclobutadiene)tricarbonyliron complex $[(\eta^4\text{-H}_4\text{C}_4)\text{Fe}(\text{CO})_3]$. *Angew Chem Int Ed* 45:3269
191. Takanashi K, Lee VY, Ichinohe M, Sekiguchi A (2007) $(\eta^5\text{-Cyclopentadienyl})(\eta^4\text{-tetrasilacyclobutadiene})\text{cobalt}$: sandwich complexes featuring heavy cyclobutadiene ligands. *Eur J Inorg Chem* 5471
192. Takanashi K, Lee VY, Sekiguchi A (2009) Tetrasilacyclobutadiene and cyclobutadiene tricarbonylruthenium complexes: $[\eta^4\text{-}(\text{tBu}_2\text{MeSi})_4\text{Si}_4]\text{Ru}(\text{CO})_3$ and $[\eta^4\text{-}(\text{Me}_3\text{Si})_4\text{C}_4]\text{Ru}(\text{CO})_3$. *Organometallics* 28:1248
193. Takanashi K, Lee VY, Yokoyama T, Sekiguchi A (2009) Base-free molybdenum and tungsten bicyclic silylene complexes stabilized by a homoaromatic contribution. *J Am Chem Soc* 131:916

194. Lee VY, Takanashi K, Ichinohe M, Sekigucji A (2004) The first bicyclo[1.1.0]butane dianion of heavier group 14 elements. *Angew Chem Int Ed* 43:6703
195. Lee VY, Aoki S, Yokoyama T, Horiguchi S, Sekiguchi A, Gornitzka H, Guo JD, Nagase S (2013) Towards a silicon version of metathesis: from schrock-type titanium silylidenes to silatitanacyclobutenes. *J Am Chem Soc* 135:2987
196. Ichinohe M, Toyoshima M, Kinjo R, Sekiguchi A (2003) Tetrasilatetrahedranide: a silicon cage anion. *J Am Chem Soc* 125:13328
197. Lee VY, Yokoyama, Takanashi K, Sekiguchi A (2009) Pentasilatricyclo[2.1.0.0^{2,5}]pentane and its anion. *Chem Eur J* 15:8401
198. Klapötke TM, Vasisht SK, Fischer G, Mayer P (2010) A reactive Si₄ cage: K(Si⁻Bu₃)₃Si₄. *J Organomet Chem* 695:667
199. Klapötke TM, Vasisht SK, Mayer P (2010) Spirocycle (Si⁻Bu₃)₆Si₉Cl₂: the first of its kind among group 14 elements. *Eur J Inorg Chem* 3256
200. Lee VY, Kato R, Ichinohe M, Sekiguchi A (2005) The heavy analogue of CpLi: lithium 1,2-disila-3-germacyclopentadienide, a 6π-electron aromatic system. *J Am Chem Soc* 127:13142
201. Lee VY, Kato R, Sekiguchi A, Krapp A, Frenking G (2007) Heavy ferrocene: a sandwich complex containing Si and Ge atoms. *J Am Chem Soc* 129:10340
202. Yasuda H, Lee VY, Sekiguchi A (2009) η⁵-1,2,3-Trisilacyclopentadienyl – a ligand for transition metal complexes: rhodium half-sandwich and ruthenium sandwich. *J Am Chem Soc* 131:9902
203. Yasuda H, Lee VY, Sekiguchi A (2009) Si₃C₂-rings: from a nonconjugated trisilacyclopentadienide and cyclic disilenide. *J Am Chem Soc* 131:6352
204. Schäfer H, Eisenmann B, Müller W (1973) Zintl phases: transition between metallic and ionic bonding. *Angew Chem Int Ed Engl* 12:694
205. Fässler TF (Editor) (2011) Zintl phases. Principles and recent development. In: Mingos DMP (Series editor) *Struct bond* 139. Springer, Berlin Heidelberg
206. Fässler TF (ed) (2011) Zintl Ions. Principles and recent development. In: Mingos DMP (Series editor), *Struct bond* 140. Springer, Berlin Heidelberg, Germany
207. Scharfe S, Kraus F, Stegmaier S, Schier A, Fässler TF (2011) Zintl ions, cage compounds, and intermetaloid clusters of group 14 and group 15 elements. *Angew Chem Int Ed* 50:3630
208. Sevov SC, Goicoechea JM (2006) Chemistry of deltahedral zintl ions. *Organometallics* 25:5678
209. Neumeier M, Fendt F, Gärtner S, Koch C, Gärtner T, Korber N, Gschwind RM (2013) Detection of the elusive highly charged zintl ions Si₄⁴⁻ and Sn₄⁴⁻ in liquid ammonia by NMR spectroscopy. *Angew Chem Int Ed* 52:4483
210. Goicoechea JM, Sevov SC (2004) Naked deltahedral silicon clusters in solution: synthesis and characterization of Si₉³⁻ and Si₅²⁻. *J Am Chem Soc* 126:6860
211. Goicoechea JM, Sevov SC (2005) Ligand-free deltahedral clusters of silicon in solution: synthesis, structure, and electrochemistry of Si₉²⁻. *Inorg Chem* 44:2654
212. Joseph S, Suchentrunk C, Kraus F, Korber N (2009) Si₉⁴⁻ Anions in solution – structures of the solvates Rb₄Si₉·4.75NH₃ and [Rb(18-crown-6)]Rb₃Si₉·4NH₃, and chemical bonding in Si₉⁴⁻. *Eur J Inorg Chem* 4641
213. Goicoechea JM, Sevov SC (2006) Organozinc derivatives of deltahedral zintl ions: synthesis and characterization of *closo*-[E₉Zn(C₆H₅)]³⁻ (E = Si, Ge, Sn, Pb). *Organometallics* 25:4530
214. Joseph S, Hamberger M, Mutzbauer F, Härtl O, Meier M, Korber N (2009) Chemistry with bare silicon clusters in solution: a transition-metal complex of a polysilicide anion. *Angew Chem Int Ed* 48:8770

Substituted Polyhedral Silicon and Germanium Clusters

Masafumi Unno

Abstract Chemistry of polyhedral silicon and germanium clusters is summarized. Historical background, synthesis, structure, physical properties, and reactions are described in detail.

Keywords Hexasilaprismane · Octasilacubane · Polysilane · Steric protection · Strained molecules · Tetrasilatetrahedrane

Contents

| | | |
|-----|--|----|
| 1 | Introduction | 51 |
| 2 | Synthesis, Structures, and Properties | 51 |
| 2.1 | Octasilacubanes and Octagermacubanes | 51 |
| 2.2 | Hexasilaprismanes and Hexagermaprismanes | 58 |
| 2.3 | Tetrasilatetrahedranes and Tetragermatetrahedranes | 59 |
| 3 | Reactions | 61 |
| 3.1 | From Octasilacubanes and Octagermacubanes | 61 |
| 3.2 | From Hexasilaprismane and Hexagermaprismane | 68 |
| 3.3 | From Tetrahedranes | 69 |
| 4 | Other Polyhedral Clusters | 72 |
| 4.1 | Strained Cage Molecules | 72 |
| 4.2 | Polysilicon and Polygermane Cage Molecules | 78 |
| 5 | Summary, Conclusions, Outlook | 81 |
| | References | 82 |

M. Unno (✉)

Department of Chemistry and Chemical Biology, International Education and Research Center for Silicon Science, Faculty of Science and Technology, Gunma University, 1-5-1 Tenjin-cho, Kiryu 376-8515, Japan
e-mail: unno@gunma-u.ac.jp

Abbreviations

| | |
|----------------|------------------------------------|
| <i>t</i> -Bu | <i>Tert</i> -Butyl |
| 18-Cr-6 | 18-Crown-6 |
| cat | Catalyst |
| d | Day(s) |
| DEP | 2,6-Diethyphenyl |
| DME | 1,2-Dimethoxyethane |
| DMF | Dimethylformamide |
| DMSO | Dimethyl sulfoxide |
| equiv | Equivalent(s) |
| e.g. | For example |
| Et | Ethyl |
| exc. | Excess |
| h | Hour(s) |
| HMPA | Hexamethylphosphoric triamide |
| LiNapht | Lithium naphthalenide |
| <i>m</i> -CPBA | <i>m</i> -Chloroperoxybenzoic acid |
| Me | Methyl |
| Mes | Mesityl, 2,4,6-trimethylphenyl |
| MS | Mass spectrometry |
| min | Minute(s) |
| mol | Mole(s) |
| NBS | <i>N</i> -Bromosuccinimide |
| NCS | <i>N</i> -Chlorosuccinimide |
| Nu | Nucleophile |
| Ph | Phenyl |
| Pr | Propyl |
| <i>i</i> -Pr | Isopropyl |
| py | Pyridine |
| rt | Room temperature |
| s | Second(s) |
| SCE | Saturated calomel electrode |
| TBAF | Tetrabutylammonium fluoride |
| TBDMS | <i>Tert</i> -butyldimethylsilyl |
| TBDPS | <i>Tert</i> -butyldiphenylsilyl |
| Tf | Trifluoromethanesulfonyl (triflyl) |
| TFA | Trifluoroacetic acid |
| TGA | Thermogravimetric |
| thexyl | 1,1,2-Trimethylpropyl |
| THF | Tetrahydrofuran |
| TEP | 2,4,6-Triethylphenyl |
| TIP | 2,4,6-Triisopropylphenyl |
| TIPS | Triisopropylsilyl |

| | |
|--------|---|
| TMEDA | <i>N,N,N',N'</i> -tetramethyl-1,2-ethylenediamine |
| TMS | Trimethylsilyl |
| Tol | 4-Methylphenyl |
| trityl | Triphenylmethyl |

1 Introduction

Synthesis of organic compounds that possess platonic solid geometries allured many chemists because of their aesthetic appeal and synthetic challenge. Before the middle of the 1980s, except for icosahedral and octahedral molecules that could not be accessed in the case of carbon, tetrahedrane, cubane, and dodecahedrane were prepared by multistep synthesis, which are globally referred to as platonic hydrocarbons [1, 2].

With the development of the higher group-14 element chemistry, heavier platonic hydrocarbon counterparts were the next logical synthetic targets. Unlike platonic hydrocarbons that are basically stable in the air, polyhedral silicon and germanium compounds are inherently unstable towards oxidation. This prohibited the successful synthesis of cage compounds of silicon and germanium until 1988, about quarter century later than the synthesis of cubane, when octasilacubane was first isolated [3]. The kinetic instability was overcome by the use of sterically shielding substituents; many other examples of the family have been prepared since then. This review will therefore focus on cage compounds with substituents and does not aim to include the rather extensive chemistry of polyhedral Zintl anions in the solid state and – since recently – also in solution, which are covered elsewhere in this volume. In addition to the platonic compounds, other substituted silicon or germanium clusters were prepared. In Table 1, platonic hydrocarbons and heavier group 14 element congeners are summarized.

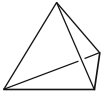
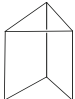
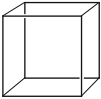
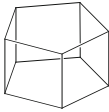
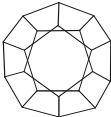
Compared to carbon clusters, silicon and germanium clusters show quite different physical properties and reactivities, due to the σ -conjugation that makes low ionization potentials [4]. In this review, synthesis, structure, properties, and reactivities of silicon and germanium clusters are described in detail.

2 Synthesis, Structures, and Properties

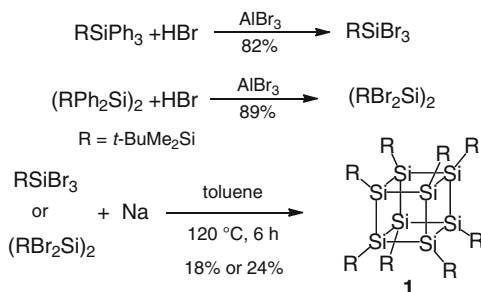
2.1 *Octasilacubanes and Octagermacubanes*

In contrast to the carbon analogs that demanded a multistep synthesis, octasilacubanes were obtained in a very facile single-step reaction. From the mid-1980s, the Matsumoto and Nagai group at Gunma University was interested in the chemistry of silyl-substituted silicon compounds. The introduction of bulky organic groups for steric protection often encounters with low reactivity or necessitates longer reaction

Table 1 List of Group-14 polyhedranes

| | Tetrahedrane | Hexaprismane | Cubane | Pentaprismane | Dodecahedrane |
|----|---|---|---|---|--|
| |  |  |  |  |  |
| C | G. Maier (1978) | T. J. Katz (1973) | P. E. Eaton (1964) | P. E. Eaton (1981) | L. A. Paquette (1982) |
| Si | N. Wiberg (1993) | A. Sekiguchi and H. Sakurai (1993) | H. Matsumoto and Y. Nagai (1988) | | |
| Ge | N. Wiberg (1996) | A. Sekiguchi and H. Sakurai (1989) | A. Sekiguchi and H. Sakurai (1992) | | |
| Sn | | N. Wiberg (1999) | L. R. Sita and I. Kinoshita (1990) | L. R. Sita and I. Kinoshita (1990) | |

Carbon compounds listed are hydrogen substituted

**Scheme 1** Synthesis of octasilacubane **1**

times. On the other hand, silyl substituents are introduced easily by simple usage of Grignard or lithium reagents. Longer Si–Si or Si–C bond lengths compared to C–C bond are also effective for the introduction of bulky substituents. This advantage made it possible to access to the precursors of silicon clusters, and silyl-substituted octasilacubane **1**, that is the first example of a silicon polyhedral compound, was obtained in 18% from tribromomonosilane and 24% from 1,1,2,2-tetrabromodisilane [3] (Scheme 1).

Octasilacubane **1** forms yellow crystals as shown in Fig. 1. This compound is stable in a sealed tube, but gradually decomposed in air to give a white solid. The cage structure of octasilacubane **1** is responsible for the unique UV–vis absorption up to 470 nm. A cyclic voltamogram revealed the oxidation potential to be 0.40 V, and this value is much lower than the usual cyclic polysilanes.

Because of its relative instability, X-ray crystallographic analysis was not successful in 1988 because the compound gradually decomposed under exposure of X-ray

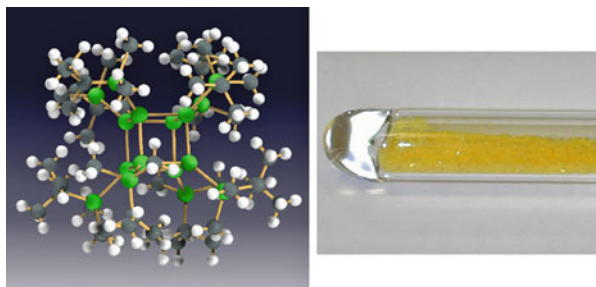
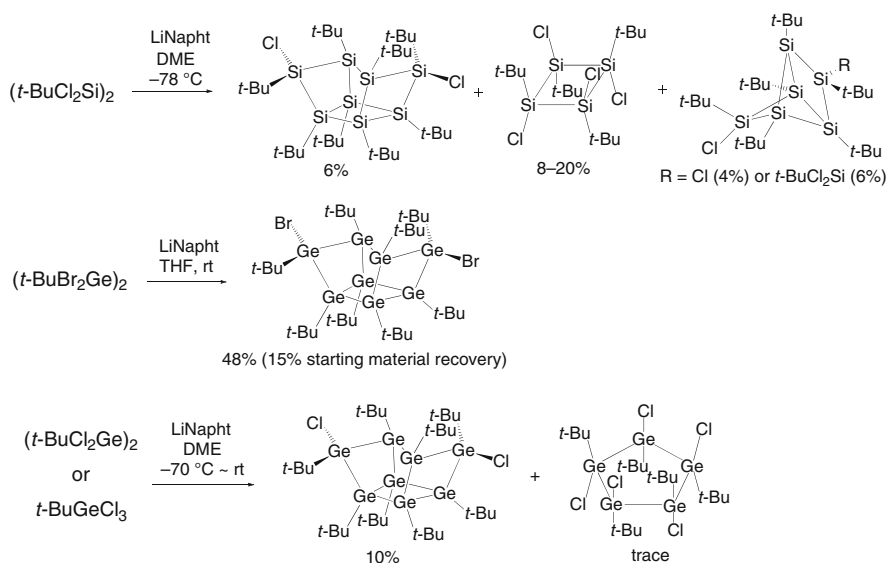


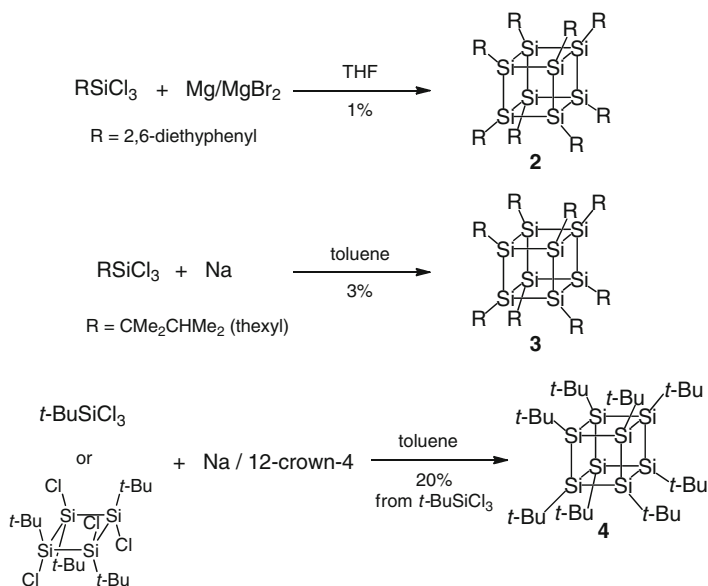
Fig. 1 Molecular structure and crystals of octasilicubane **1**



Scheme 2 Other approaches to octasilicubane and octagermacubane

even in a sealed tube. The structure analysis was possible 15 years later by rapid X-ray measurement system [5]. The structure is shown in Fig. 1. The cubic framework is well protected by bulky Si substituents to avoid oxidation. Average framework bond length was 2.412 Å and slightly longer than the usual Si–Si single bond. Framework Si–Si–Si bond angles varied from 88.0 to 91.8°, nicely approximating a cubic structure.

It is noteworthy that three independent groups published similar reactions at the same time. As shown in Scheme 2, the reactions of di(*tert*-butyl)tetrachlorodisilane and di(*tert*-butyl)tetrahalodigermane with lithium naphthalenide at low temperatures gave Si₈ and Ge₈ partial cage compounds, respectively, with two halogen atoms remaining [6–8]. Our later investigation of the reactions from octasilicubane showed that construction of strained cubic structure requires high temperatures (described below in detail).



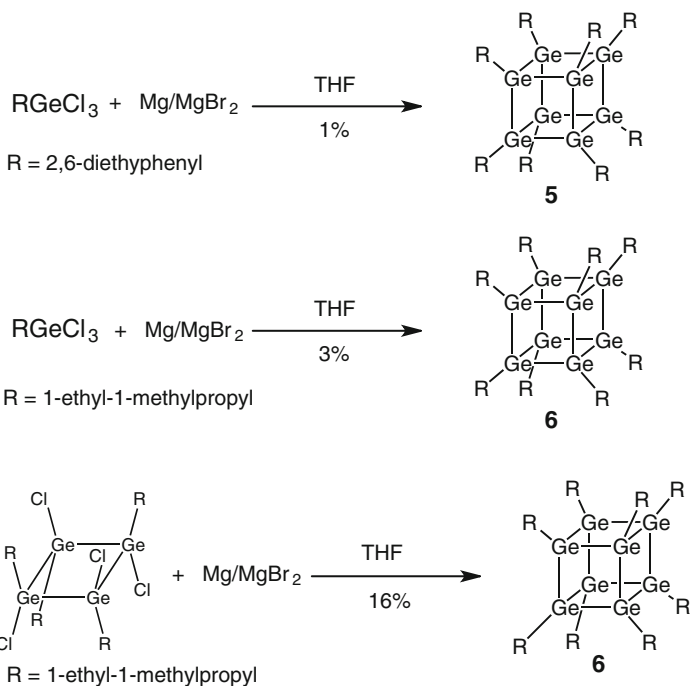
Scheme 3 Synthesis of alkyl and aryl octasilacubanes

After this work, various octasilacubanes with alkyl and aryl substituents were reported. Their syntheses are summarized in Scheme 3. Sekiguchi and Sakurai group prepared 2,6-diethylphenyl-substituted octasilacubane by the reaction with Mg/MgBr_2 [9]. The orange crystals of **2** were obtained in 1% yield. In the same year, Matsumoto group in Gunma University published the synthesis and structure of 1,1,2-trimethylpropyl (thexyl)-substituted octasilacubane **3** [10]. Independently, the synthesis of *tert*-butyl-substituted octasilacubane **4** was reported in the same year [11]. Later, the Sekiguchi and Sakurai group also reported the mesityl-substituted octasilacubane prepared in a similar manner [4]. The structures of octasilacubanes shown in Scheme 3 were determined by X-ray crystallography. Bond lengths and angles were basically independent of the substituents. Even with bulky substituents, Si–Si average bond lengths of the cubane skeleton were only slightly longer than typical Si–Si bond lengths 2.34 Å (2.412 Å for **1**, 2.399 Å for **2**, 2.421 Å for **3**, and 2.385 Å for **4**). Bond angles of the skeleton vary from 88 to 92°.

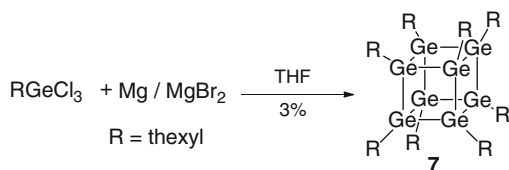
The ^{29}Si NMR chemical shift of **1** was observed at -35.03 ppm and that of aryl-substituted **2** appeared at 0.36 ppm. Alkyl-substituted **3** showed a peak at 22.24 ppm.

The reason for the successful isolation of octasilacubanes, even though the yields were poor, is their vivid color that enabled the isolation by column chromatography in a glove box. The electronic structures of octasilacubanes were intensively investigated [4] and strained polysilane systems as well as fused polycyclic structures are explained to be responsible for the unique color and reactivity.

Two octagermacubanes were introduced by Sekiguchi and Sakurai's group in 1992 [9]. The synthetic methods, similar to those of octasilacubanes, are shown in Scheme 4.



Scheme 4 Synthesis of alkyl and aryl octagermacubanes



Scheme 5 Synthesis of hexyl octagermacubane

Octagermacubane **5** with 2,6-diethyphenyl groups was obtained in 1% yield. Alkyl octagermacubane **6** was prepared by two different methods and obtained in 16% yield from cyclotetragermane or 3% from trichlorogermane.

In 2000, our group reported the synthesis, structure, and reactivity of hexyl octagermacubane. Unlike hexyl octasilacubane **3**, octagermacubane **7** was only obtained by the reaction of ThexGeCl_3 with Mg/MgBr_2 . The yield was 3.3% [12] (Scheme 5).

Aryl octagermacubane **5** was reported to be stable to atmospheric oxygen and moisture, while alkyl-substituted **7** was oxidized in solution to the corresponding dioxide in a few hours (*vide infra*). Also in a solid state, **7** decomposed slowly (half life: 5 d). This is in contrast with hexyl octasilacubane **3**, which is stable in solution. The relative stability of aryl octagermacubane **5** can be attributed to the

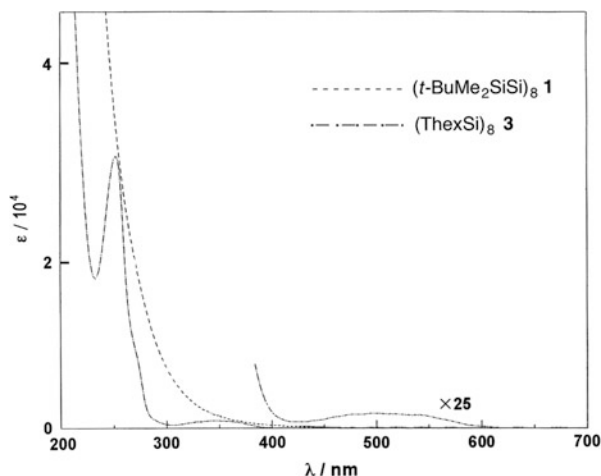


Fig. 2 UV-vis spectra of octasilacubanes **1** and **3** in hexane

electronical stabilization by aryl groups; electron is withdrawn by aryl groups from Ge_8 skeleton, diminishing the reactivity towards electrophilic reagents.

The structures of octagermacubanes are comparable to those of octasilacubane; average Ge–Ge bond lengths were 2.490 Å for **5** and 2.516 Å for **7**. Bond angles of the skeleton of **5** vary 88.9–91.1° and alkyl-substituted **7** showed wider range, 88.0–91.9°, as in the case of octasilacubanes.

All octasilacubanes are colored molecules and show absorption maxima around 500 nm in UV-vis spectra. As an example, UV-vis spectra of thexyl and silyl-substituted octasilacubane are shown in Fig. 2. The longest wavelength absorption around 500 nm for **3** was analyzed by Gaussian approximation to be a 1:5:1 mixture of 464, 508, 561 nm peaks, respectively. The absorption spectra of other octasilacubanes are summarized in the review [4, 13]. Aryl octasilacubane **2** shows much more intense absorption compared to alkyl-substituted **3**, because of the electronic perturbation by aryl groups. For example, σ – σ^* transition absorption of **2** was observed at 243 nm (ϵ 111,000), while that of **3** was detected at 252 nm (ϵ 30,800). On the other hand, the absorption at 500 nm observed for **3** was missing in the case of **2**.

Thexyl octasilacubane **3** shows thermochromism in solid state and changes its color from orange (–196°C) to bright red (200°C). The measurement of temperature-dependent UV-vis spectrum in 3-methylpentane indicated that the absorption of 561 nm decreases in intensity at lower temperature. Other peaks are basically left unchanged; therefore, slight conformational variations might be responsible for this color change. A similar feature was also observed for octagermacubane **7**, which changed its color from pale yellow (–196°C) to orange (120°C).

It is worthwhile to compare the electronic properties of octasilacubane and octagermacubane with same substituents. Figure 3 indicates the comparison of UV-vis spectra of thexyl octasilacubane **3** and octagermacubane **7**. Octagermacubane shows more intense absorption in the UV region, which tails in to the visible region around 500 nm. In contrast, aryl octasilacubane **2** and octagermacubane **5** with same

Fig. 3 UV–vis spectra of octasilacubanes **3** and octagermacubanes **7** in hexane

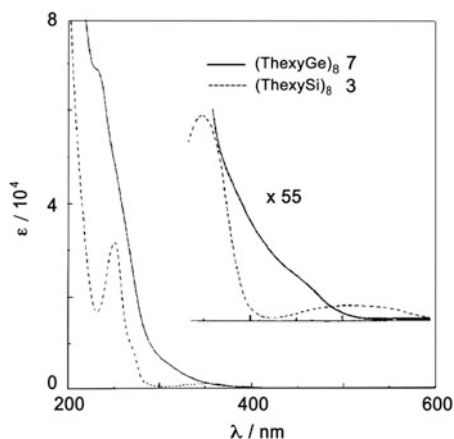
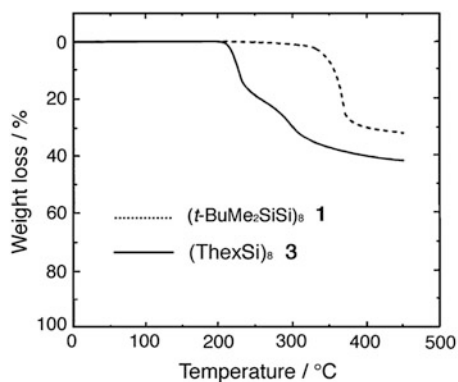


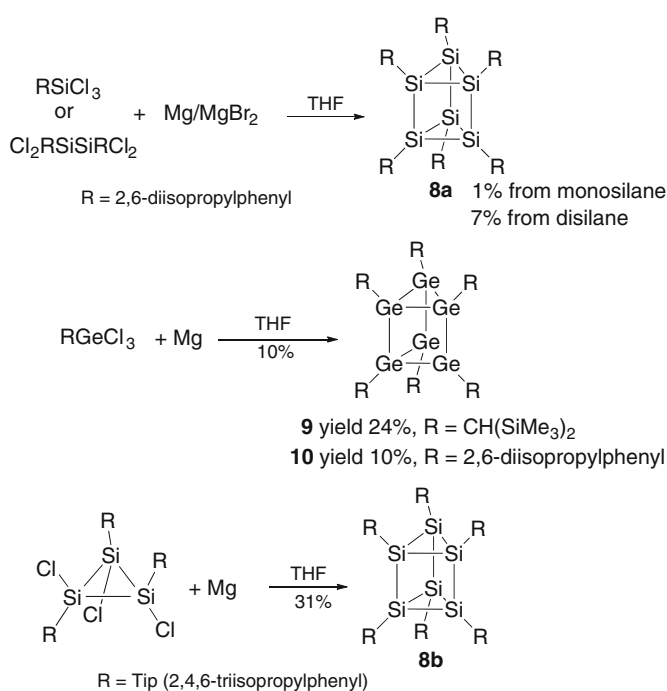
Fig. 4 TG analysis of octasilacubanes **1** and **3** in Ar atmosphere



substituents show basically similar UV–vis spectra [13]. The UV–vis spectra of alkyl octagermacubane **6** and **7** exhibit analogous features.

The high electron-donating ability of octasilacubanes is shown by the results of cyclic voltammetry. The oxidation potentials of **1** and **3** were 0.40 V and 0.43 V (in CH_2Cl_2 vs. SCE), respectively. These values are much lower than cyclic polysilanes ($i\text{-Pr}_2\text{Si}$)₄ (1.24 V, in CH_2Cl_2 vs. SCE), indicating unique electronic properties of the octasilacubane motif. Octagermacubane **7** shows even lower oxidation potential, and the value was 0.22 V (in CH_2Cl_2 vs. SCE).

The thermal properties of octasilacubane were investigated by thermogravimetric analysis (TGA). As shown in Fig. 4, silyl octasilacubane **1** shows weight decrease over 300°C, whereas thexyl-substituted **3** started to decompose from 200°C. This result was supported by the ab initio calculation indicating that silyl-substituted octasilacubane is more stable than alkyl-substituted one [14]. Octagermacubane **7** is stable up to 190°C, then starts to decompose. This temperature is slightly lower than in the case of octasilacubane **3**. The measurement of TGA-MS indicated that the weight loss is the result of the elimination of thexyl groups. The cage skeleton is thermally stable up to 500°C.



Scheme 6 Synthesis of hexaprismanes

2.2 Hexasilaprismanes and Hexagermaprismanes

A hexaprismane comprising higher group-14 element was first reported in 1989 with bis(trimethylsilyl)methyl-substituted hexagermaprismane [15]. Hexasilaprismane and hexagermaprismane with 2,6-diisopropylphenyl groups were isolated in 1993 [16] both by Sekiguchi and Sakurai group. They applied bulkier substituents to obtain smaller cages, and the essentially identical method to that employed for the preparation of octasilacubanes gave the targeted hexaprismanes. One different point is reducing reagent; Mg/MgBr₂ proved too reactive for hexagermaprismanes and Mg was used instead. For hexasilaprismane **8a**, Mg/MgBr₂ gave a good result (Scheme 6). More recently, Scheschkewitz's group reported the synthesis of hexasilaprismane **8b** by reductive coupling from trichlorocyclotrisilane [17]. Their result clearly indicates that larger prebuilt fragments afford the targeted polyhedron in much higher yields.

Theoretical calculations indicated that strain energy of hexaprismanes are higher than octasilacubanes or octagermacubanes [18]. However, hexasilaprismane **6** was oxidatively stable in the solid state. The authors described that no change was observed after a couple of months in air.

Another unique point for these compounds was hindered rotation of the aryl group of **8a** and **10**. Unlike octasilacubanes, two peaks of nonequivalent *o*-isopropyl groups

were observed in ^1H NMR. The ΔG^\ddagger values for the rotation were calculated to be 16.5 kcal/mol for hexasilaprismane **8**, and 13.1 kcal for hexagermaprismane **10**, reflecting longer Ge–Ge bond length [16].

In the solid state, hexasilaprismane **8** exhibited two peaks in ^{29}Si NMR at -22.2 and -30.8 ppm with a ratio of 2:1. The authors explained this with the distorted skeleton as shown in X-ray analysis.

The crystallographic analyses of hexaprismanes **8–10** revealed their unique structures. Thus, the average bond angles for **8a** were 2.380 \AA for the three-membered ring moiety and 2.373 nm for the four-membered ring and slightly shorter than diethyphenyl-substituted octasilacubane **2**. On the other hand, the average bond lengths of hexagermaprismane **10** were 2.503 \AA for three-membered ring and 2.468 \AA for four-membered ring. Alkyl-substituted **9** shows comparatively long bond lengths: 2.580 \AA for three-membered ring and 2.522 \AA for four-membered ring, which can readily be attributed to the bulkier alkyl groups.

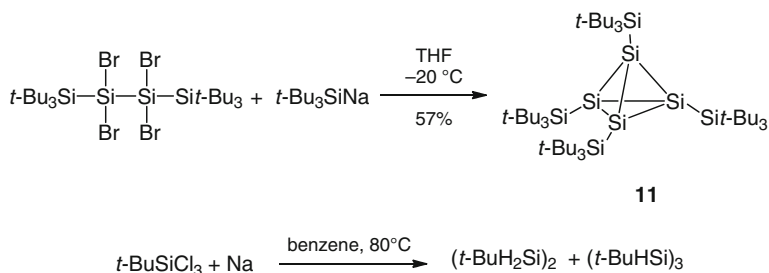
Because of the strained polysilane/polygermane structure, the polyhedral cages are all colored compounds and show UV–vis absorptions in the visible region in hexane solution. Thus, all three compounds have absorptions tailing into the visible region (500 nm). Two hexagermaprismanes **9** and **10** showed similar spectra, whereas alkyl-substituted **9** was red-shifted (280 nm, ϵ 32,200) compared to that of **10** (261 nm, ϵ 84,000). Hexasilaprismane **8** shows absorption maximum at 240 nm (ϵ 78,000) with several shoulders up to 500 nm.

2.3 Tetrasilatetrahedranes and Tetragematetrahedranes

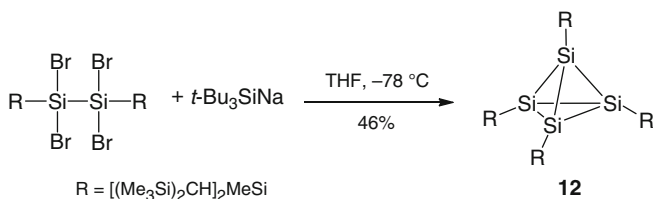
Among the polyhedral clusters, tetrahedrane is the most strained [4, 17]. The isolation of tetrasilatetrahedrane was realized in 1993, five years after the synthesis of octasilacubane. Wiberg's group applied very bulky tri-*t*-butylsilyl (*supersilyl*) groups and succeeded in the synthesis as shown in Scheme 7 [19]. Again, the choice of precursors is important; when *tert*-butyltrichlorosilane was treated with sodium, only reduced disilane and cyclotrisilane were obtained as products. In addition to using a 1,1,2,2-tetrabromodisilane precursor, *t*-Bu₃SiNa had to be employed as reducing agent instead of typical alkali metal reagents.

The tetrahedrane **11** was obtained as yellow-orange crystals and, surprisingly, stable towards water, air, and light. Because of the cage tetrasilane system, UV–vis absorptions are observed at 210 (ϵ 76,000), 235 (ϵ 71,000), 310 (ϵ 20,000), and 451 (ϵ 3,600) nm. The crystallographic analysis was possible by the co-crystallization of **1** with disilane (*t*-Bu₃Si)₂. Average skeleton Si–Si bond lengths were 2.326 \AA , and this value is slightly shorter than typical Si–Si single bond ($\sim 2.34 \text{ \AA}$). The exocyclic Si–Si bonds were longer, and average bond lengths were 2.362 \AA .

In 2003, the Sekiguchi and Ichinohe group isolated the bis(trimethylsilyl) methyl-substituted tetrasilatetrahedrane as the second example [20]. They applied



Scheme 7 Synthesis of tetrasilatetrahedrane



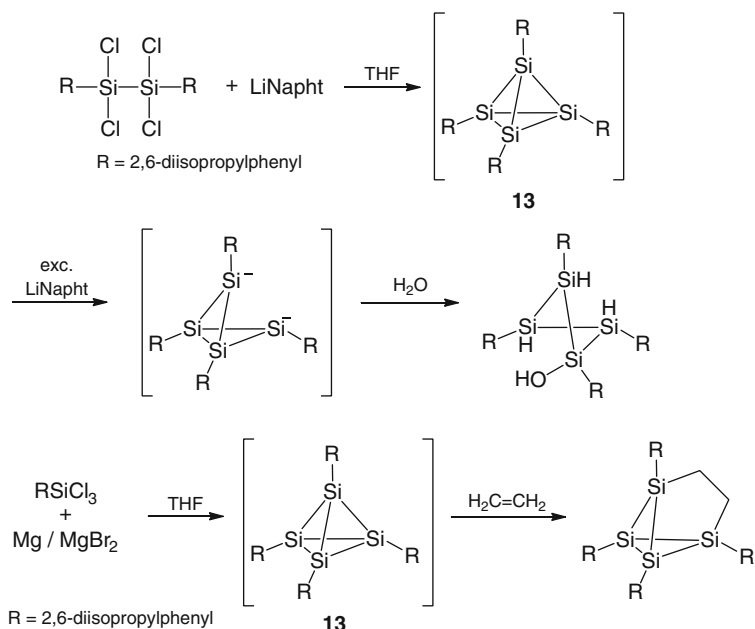
Scheme 8 Synthesis of tetrasilatetrahedrane **12**

basically identical reaction conditions and obtained the target compound in 46% yield (Scheme 8). Average Si–Si bond lengths were 2.352 Å (*endo*) and 2.409 Å (*exo*); both are slightly longer than those of **1**.

Lerner's group reported the synthesis of **12** by a one-pot procedure in 2009 [21]. Compound **12** was obtained by treatment of either HSiCl_3 , $\text{Cl}_3\text{SiSiCl}_3$, or $\text{Cl}_3\text{SiSiCl}_2\text{SiCl}_3$ with $\text{NaSi}(t\text{-Bu})_3$. In the case of HSiCl_3 and $\text{NaSi}(t\text{-Bu})_3$, the yield was 48%.

Sekiguchi's group investigated the reaction using 2,6-diisopropylphenyl groups as substituents. As shown in Scheme 9, the reaction of tetrachlorosilane with LiNaphT gave cleaved silanol after aqueous workup. When they treated substituted trichlorosilane with Mg/MgBr_2 , ethylene inserted tetrahedrane was obtained (ethylene was generated in situ by the reaction of Mg and dibromoethane) [4]. These results indicated the intermediacy of tetrahedrane **13**; isolation, however, was not possible with these aryl substituents.

The ^{29}Si NMR chemical shift of tetrahedrane **11** was reported to be 38.89 ppm, a quite different value from that of silyl-substituted octasilacubane **1** ($\delta -35.03$ ppm). ^{29}Si NMR chemical shifts are apparently drastically affected by the polyhedral cage motif. Therefore, ^{29}Si NMR seems to be a useful tool for determination of the structures of silicon polyhedranes.



Scheme 9 Attempted synthesis of tetrasilatetrahedrane **13**

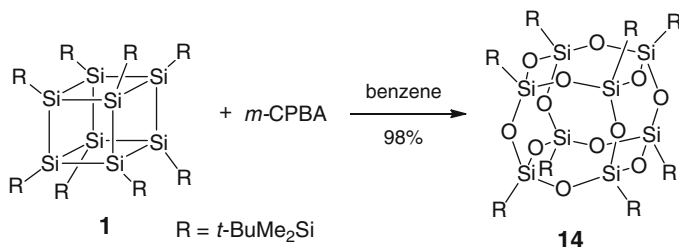
3 Reactions

3.1 From Octasilicubanes and Octagermacubanes

Although many silicon and germanium clusters were isolated, the reactions starting from them are very limited. There are several reasons:

1. With bulky steric protecting groups, reactivity of the starting compound is low.
2. Even if some reactions occurred, the stability of the products is often insufficient for separation and isolation.
3. The structure of the products are often complicated; therefore, identification by spectroscopic analyses is difficult.
4. In some cases (e.g., compounds **4** and **12**), solubility in organic solvent is too low to perform reactions.

Among all clusters listed above, thexyl-substituted octasilicubane **3** and octagermacubane **7** have unique properties. Thus, this compound can survive in the HPLC analysis with THF/MeOH eluent, and this makes it possible to isolate the products by preparative recycle-type HPLC. In addition, compounds **3** and **7** can be dissolved in many organic solvents. This is the reason why most of the known reactions are from these compounds.



Scheme 10 Oxidation of octasilacubane **1**

As mentioned in the previous chapter, octasilacubanes show low oxidation potential. Therefore reactions with electrophilic reagents can be expected. Indeed, silyl-substituted octasilacubane **1** reacted with excess amount of *m*-CPBA to give octasilsesquioxane **14** [5] (Scheme 10; the chemistry of silsesquioxanes is described in detail in a different chapter of this volume). Cage octasilsesquioxanes (T_8) are well-known compounds [22]; however, only one silyl-substituted T_8 has been known to date except **14**. In addition, if bulky substituents are applied, conventional hydrolysis-dehydration methods would not give cage products but incompletely condensed silanols. Therefore, compound **14** can be claimed to be the octasilsesquioxane with the largest substituents.

Interestingly, compound **14** exhibits relatively intense absorption in the UV region [5]. Against the fact that the silsesquioxane framework usually does not show UV-vis absorption, the lowest transition-energy absorption of **14** in cyclohexane occurs at 285 nm (ϵ 4,900) (Fig. 5). The reason of this intriguing observation is unclear as yet, however, spatial interaction of Si-Si σ bonds is most plausible because similar spectrum was obtained with trimethylsilyl- T_8 , but not with 2-trimethylsilylethyl- T_8 .

Reflecting the stability in the air, oxidation of hexyl-substituted octasilacubane **3** demanded harsher conditions. Oxidation of **3** with *m*-CPBA resulted in the mixture of $\text{Thex}_8\text{Si}_8\text{O}_n$. During the investigation of photoreaction of **3**, we found that oxidized octasilacubanes were often observed. We therefore tried the photoreaction of **3** in the presence of DMSO as an oxidant, and mono- and di-oxidized compounds were obtained in good yields (Scheme 11). Thanks to the stability of **3** as described above, all the products including residual starting material **3** were isolated by recycle-type HPLC (ODS, eluent MeOH/THF) [23].

Although many isomers for dioxide **16** are possible, only the single isomer with diagonally opposing SiOSi bridges was obtained. We also tried the oxidation of **15** in a similar manner, and again, only **16** was obtained (Scheme 11). This interesting reactivity was explained by the X-ray crystal analysis of **15**. Because of the insertion of the first oxygen atom, the hexyl groups were pushed back, and the opposing Si-Si bond was elongated (2.559 Å; other bonds were 2.423–2.463 Å). This elongation made the reactivity of this bond higher, resulted in the sole generation of **16** (Scheme 12).

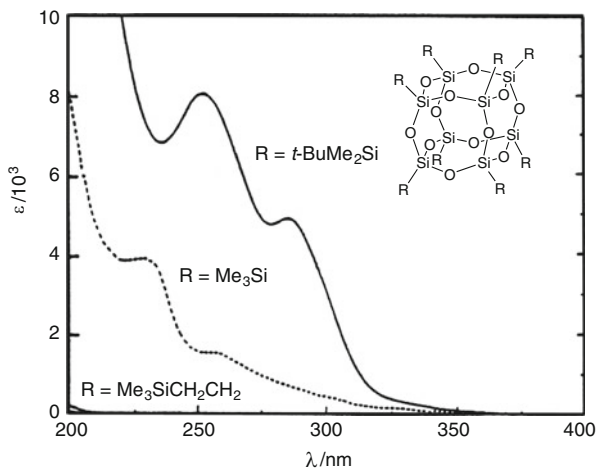
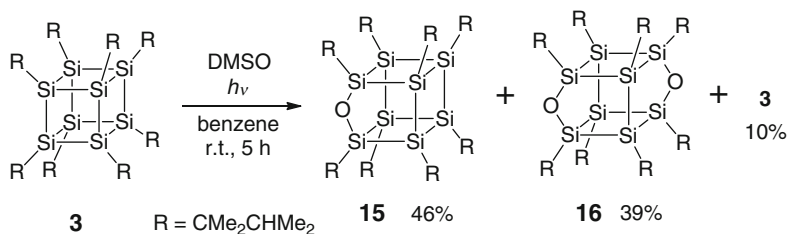
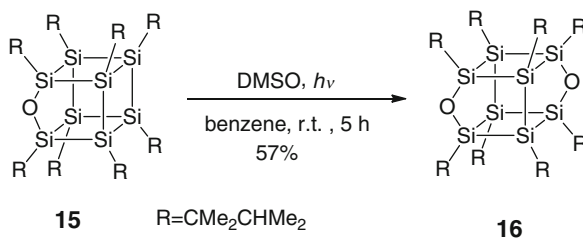


Fig. 5 UV-vis absorption of octasilsesquioxane **14** in cyclohexane

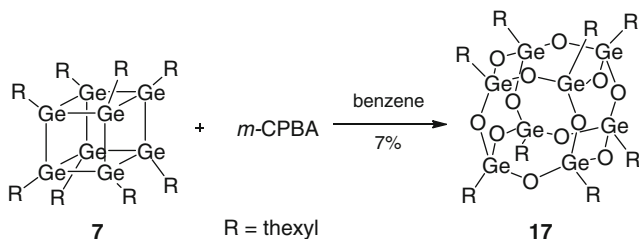


Scheme 11 Oxidation of octasilacubane **3**



Scheme 12 Oxidation of oxaoctasilacubane **15**

For octagermacubanes **7**, oxidation reaction occurred with *m*-CPBA, and octagermsesquioxane **17** was obtained in 7% yield (Scheme 13). Probably because of the longer Ge–Ge bonds, **7** is more easily oxidized compared to the silicon analog. When **7** was stirred in hexane for 12 h with oxygen, dioxide (ThexGe)₈O₂ was obtained as yellow crystals in 7% yield. The position of the two oxygens was not clear because crystallographic analysis could not be performed in this case.



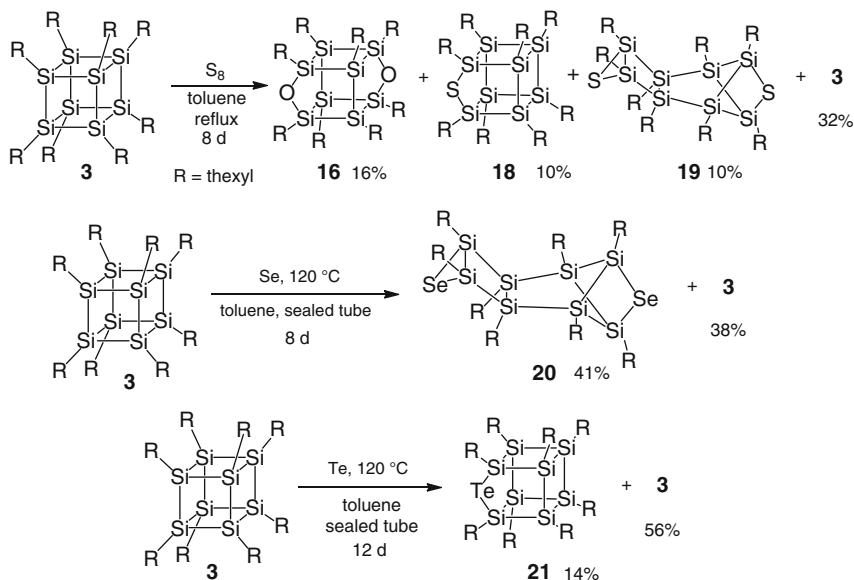
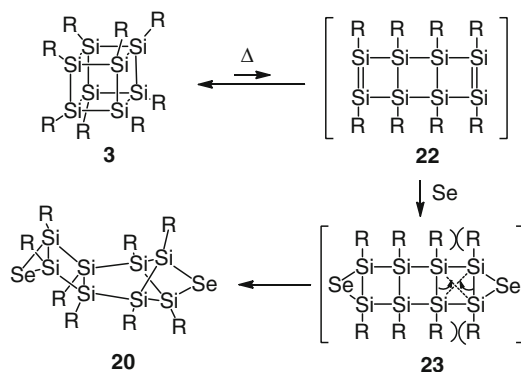
Scheme 13 Oxidation of octagermacubane **7**

The reaction of octasilacubane with sulfur, selenium, or tellurium proceeded by thermal reaction [24]. When octathexyloctasilacubane **3** was heated with sulfur under toluene reflux condition for 8 days, the HPLC chart of the reaction mixture showed the generation of three products in addition to the starting octasilacubane. Separation with recycle-type HPLC revealed that two of the products were dioxaoctasilabishomocubane **16** and monothiaoctasilabishomocubane **18**, the former probably resulting from contamination of the reaction mixture with dioxygen. Both compounds were identified by X-ray crystallographic analysis. Another product was not identified, but the reaction of **3** with selenium in a sealed tube gave a similar ring-opening compound **20** whose structure was determined crystallographically. On the basis of similar ^{29}Si NMR data, the product was determined to be **19**. In the case of tellurium, the thermal reaction of the octasilacubane resulted in the formation of a tellurium-inserted compound **21**, which decomposed in solution to give the octasilacubane and tellurium. The whole reaction is summarized in Scheme 14.

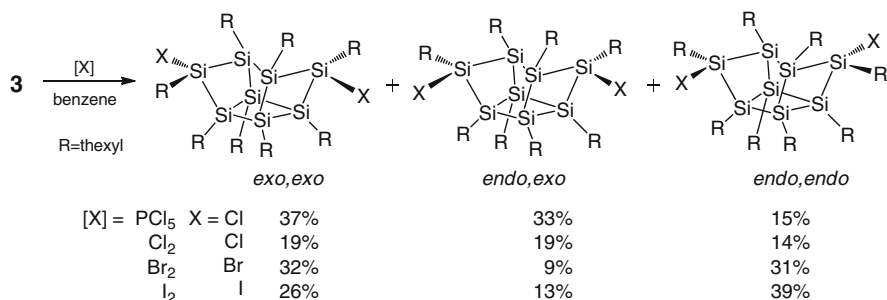
The mechanism of the formation of **19** or **20** is not clear, but it can plausibly be explained with the reaction sequence shown in Scheme 15. Usually [2,2] ring opening is thermally prohibited; however, a transiently generated ladder intermediate **22** may promptly react with selenium to give **23**. Because of the severe steric hindrance of bulky thexyl groups in **23**, skeletal rearrangement might occur to give product **20**. Similar ring-opening reaction of hexasilaprismane was also suggested by photoreaction (described below).

Octasilacubane **3** also readily reacts with halogenating reagents [25]. Simple one-bond cleaved dihalides had been anticipated, but the products obtained were all skeletal rearranged dihalides. As shown in Scheme 16, when **3** was allowed to react with halogenating reagents, three stereoisomers were obtained in good yields. All products were isolated with recycle-type HPLC (ODS, MeOH/THF), and the structures were unequivocally determined by X-ray crystallographic analyses. Usually iodosilanes are unstable to moisture; however, the diiodo compounds obtained in this reaction were stable, thanks to the steric protection by thexyl groups, and isolated without problems by HPLC.

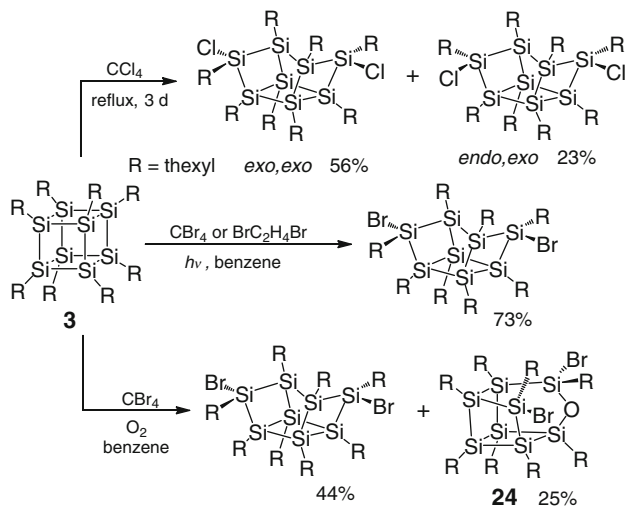
The reason of the skeletal rearrangement is explained by the release of the strain of octasilacubane. Thus, electrophilic attack by halogenating reagent resulted in the Si–Si bond cleavage and generation of silyl cation. In this stage, skeletal rearrangement occurred before the second atom attacks to give the rearranged dihalides.

**Scheme 14** Reaction of octasilacubane **3** with sulfur, selenium, and tellurium**Scheme 15** Plausible reaction mechanism for the generation of **20**

The described halogenation reaction proceeds via an ionic pathway, but radical halogenation is also possible [26]. When octasilacubane **3** was heated in CCl_4 , similar products were obtained. In this reaction, no *endo,endo*-isomer was obtained. The reaction of **3** with CBr_4 or dibromoethane demanded photo-irradiation, and the *exo,exo*-isomer was obtained as the only product. For these reactions, carefully degassed solvent was used; however, when the reaction with CBr_4 was performed in the presence of oxygen, oxahomocubane **24** in addition to the *exo,exo*-isomer were obtained. All the reactions are summarized in Scheme 17. It is noteworthy that the framework of the rearranged compounds was previously known as shown in Scheme 2.



Scheme 16 Halogenation of octasilacubane **3**

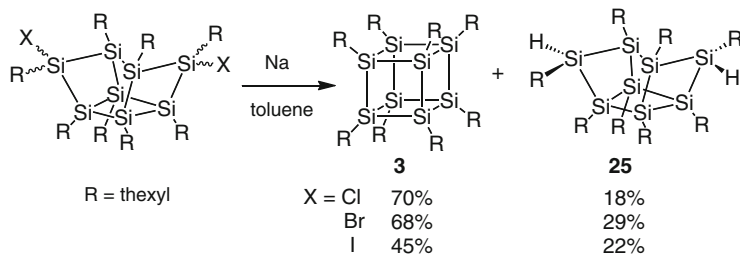
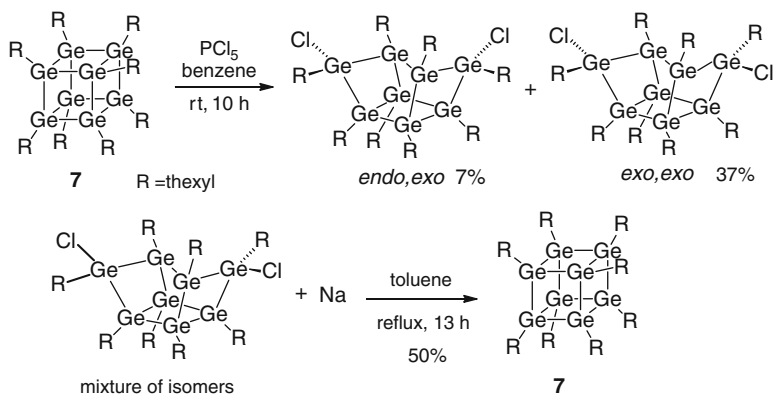


Scheme 17 Radical halogenation of octasilacubane **3**

Kabe and Masamune's group examined the further reaction of obtained *exo,exo*-dichloride with LiNapht, but dihydride **24** was the only product instead of the anticipated cage motif [6]. Considering the strained structure of octasilacubane, conversion of rearranged dihalides to octasilacubane seemed to be impossible.

Against this expectation, we succeeded in the regeneration of octasilacubane by applying similar reaction condition to the synthesis of octasilacubane [27]. As shown in Scheme 18, all isomers of dihalides could be transferred to octasilacubane by the reaction with sodium in refluxed toluene. Reduced dihydride (only *exo,exo*-isomer) was the by-product. From this result as well as the similar reaction of octagermacubanes described below, it can be concluded that generation of cubane skeleton usually requires elevated temperatures.

Similar halogenation and regeneration was also observed for octagermacubane [12]. As depicted in Scheme 19, chlorination occurred in the reaction with PCl₅, and two isomers were obtained. The identification of *exo,exo*-isomer was accomplished

**Scheme 18** Regeneration of octasilacubane **3****Scheme 19** Reaction of octagermacubane **7**

by comparing NMR spectrum with that of silicon analog of *exo,exo*-isomer. The unsymmetrical structure of *endo,exo*-isomer made it possible to identify this compound by NMR spectra. Although octagermacubane was synthesized by the reaction with Mg/MgBr₂, no reaction occurred from the rearranged dichloride. Instead, reaction with sodium in toluene gave the octagermacubane in 50% yield. Again in this reaction, the higher stability of thexyl-substituted octagermacubane is one of the reasons for the generation of octagermacubane, while the regeneration of more strained cubane skeletons demands high reaction temperature.

Photoreaction of octasilacubane **3** was investigated soon after its isolation. Irradiation of **3** at 77 K in 3-methylpentane gave intense absorptions around 450 and 700 nm in UV-vis spectrum. As shown in Fig. 6, new absorptions at 345, 471, and 714 nm increased their intensity by time. The species were stable at least for several hours at that temperature; however, starting octasilacubane was recovered when the solution was warmed to room temperature.

We first presumed that the species responsible for these absorptions include unsaturated Si-Si bonds and tried trapping experiments with diene, alcohol, or water. However, no trapped products were obtained and only octasilacubane was recovered. The absorption at 714 nm is red-shifted compared to those of most

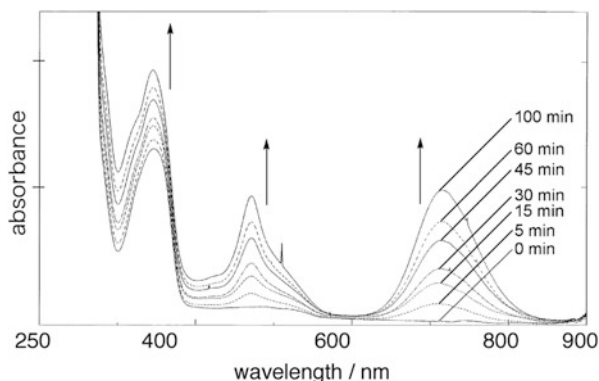
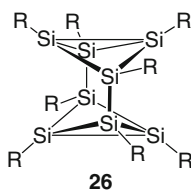


Fig. 6 UV spectra of **3** irradiated in 3-methylpentane at 77 K



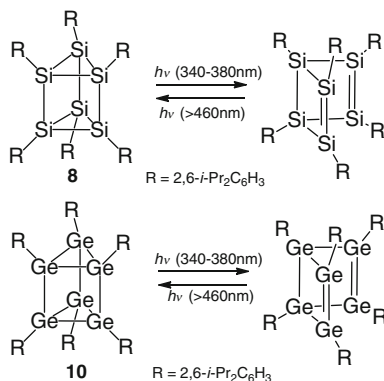
Scheme 20 Suggested intermediate of the photoreaction of octasilacubane **3**

unsaturated silicon compounds, and consequently the generation of different species had to be considered. With a collaborative work with Horiuchi and Hiratsuka photochemistry group, we could suggest the structure of the product of photoreaction [28]. From the result of INDO/S-CI calculation it was concluded that the structure of the photo-rearranged product corresponded to the saturated, but highly strained molecule **26** (Scheme 20). This compound matches well to the UV-vis spectrum as well as the inertness towards alcohol or diene. In addition, generation of the dioxaoctasilacubane **16** in the photooxidation of octasilacubane can readily be explained by the insertion of oxygen atom to top and bottom Si-Si bonds of **26**.

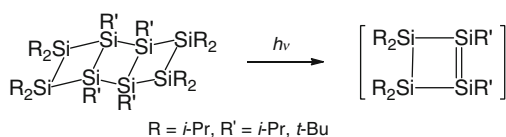
3.2 From Hexasilaprismane and Hexagermaprismane

Photoisomerization was also reported for hexasilaprismane and hexagermaprismane. The irradiation of **8** at -50°C or in a glass matrix at 77 K, new absorption bands appeared at 335, 455, and 500 nm. With a result of a HF/6-31G* level energy calculation [4], Sekiguchi and Sakurai suggested the generation of hexasila-Dewar benzene **27**. With irradiation of longer wavelength light, this species regenerated hexaprismanes (Scheme 21) [4, 13].

Similar photoreaction was observed with ladder polysilanes. In this case, generated cyclobutene was trapped by various reagents (Scheme 22) [29].



Scheme 21 Photoisomerization of hexaprismanes



Scheme 22 Photoreaction of ladder polysilane

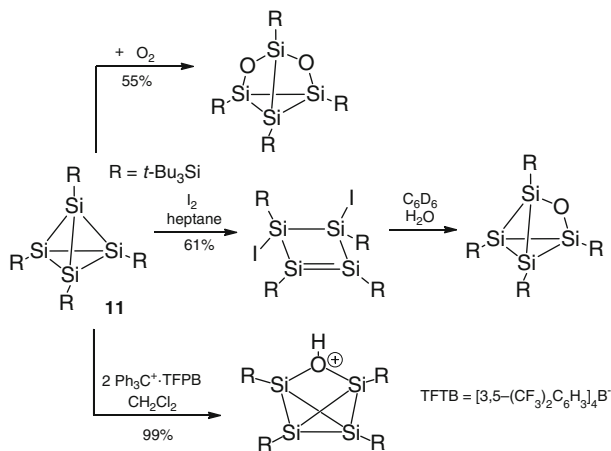
3.3 From Tetrahedranes

Tetrasilatetrahedranes are thermally of considerable stability, but a broad variety of reports on their rich reactivity have appeared up to now. Partial oxidation occurred with reaction of oxygen in solution [30]. With iodine, diido tetrasilacyclobutene is obtained [31]. When **11** was treated with trityl tetrakis[3,5-bis(trifluoromethyl)phenyl]borate protonated monoxide was obtained, probably formed under involvement of water contamination [32] (Scheme 23).

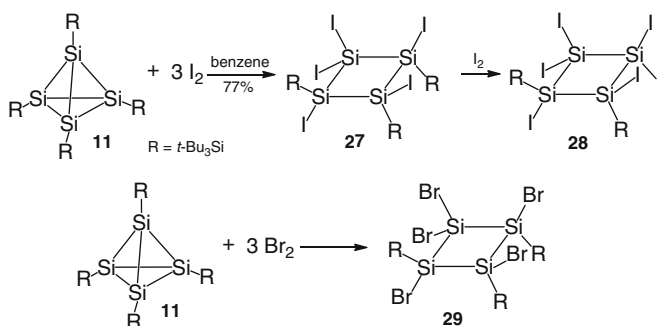
Additional halogenation reactions were also reported. With excess amount of iodine [33, 34] or bromine [35], tetrahedrane **11** underwent a substitution-addition reaction to give pentahalogenated products (Scheme 24).

From the thus obtained pentafluoride **27**, novel cage octasilane **30** was afforded by treatment with $\text{NaSi}(t\text{-Bu})_3$ (Scheme 25). The neutral cluster **30** exhibits the rare structural feature of hemispheroidally coordinated unsubstituted vertices (see Sect. 4.1).

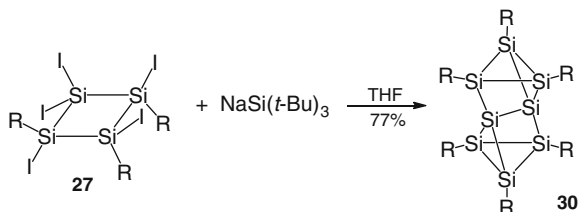
In 2003, the first silicon cage anion was reported by Ichinohe and Sekiguchi group. They reduced tetrasilatetrahedrane **12** with KC_8 in ether to obtain the anion [20]. The structure of the product was determined by X-ray crystallography. The skeletal bond lengths are similar to that of **12** (average 2.322 Å) except one bond that connected to the anionic silicon center (2.7288 Å). They also measured the ^{29}Si NMR, and single peak of tetrahedrane skeleton was observed at -153.6 ppm. Even at lower temperature (-73°C), no peak broadening or splitting manifested



Scheme 23 Reactions of tetrasilatetrahedrane with oxygen, iodine, and a trityl borate



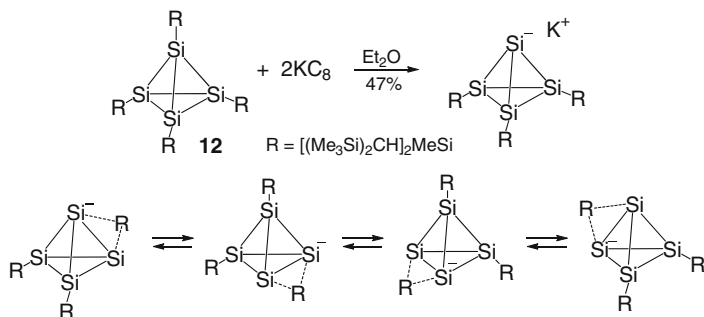
Scheme 24 Reaction of tetrasilatetrahedrane with excess iodine or bromine



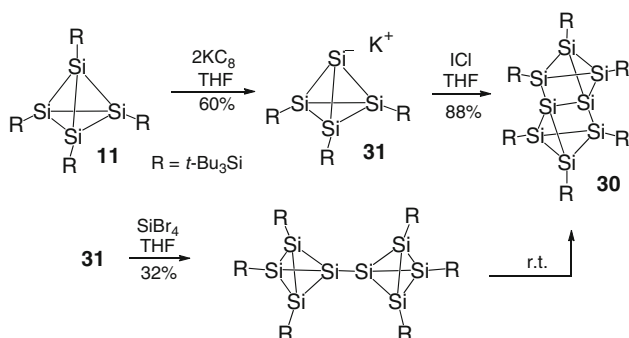
Scheme 25 Synthesis of cage octasilane

itself. The authors explained this observation with the rapid migration of the three substituents over the Si_4 skeleton (Scheme 26).

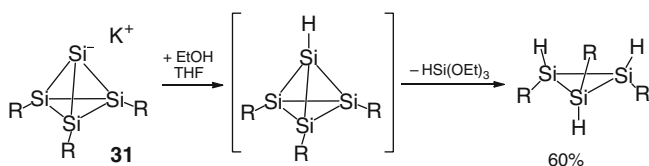
More recently, Klapötke's group in Munich reported further reactions starting from tetrahedrane **11** [36] (Scheme 27). They performed KC_8 reduction and obtained potassium salt of 3 tetrahedrane anion **31**. This anion is a stable orange



Scheme 26 Synthesis of potassium tetrasilatetrahydride and substituents migration in solution



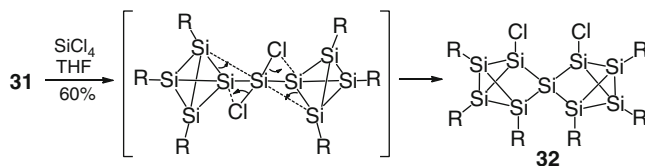
Scheme 27 Generation and reactions of potassium salt of tetrahedrane



Scheme 28 Reactions of potassium salt of tetrasilatetrahydride **31** with alcohol

red solid at rt but decomposes in solution. The reaction of **31** with SiBr_4 resulted in the formation of cage octasilane **30** via ditetrahdryl ($\text{R}_3\text{Si}_4\text{-Si}_4\text{R}_3$). Compound **30** could also be prepared in 88% yield from **31** by reaction with ICl .

When potassium salt **31** was treated with methanol or ethanol at rt, cyclotrisilane was obtained. Without bulky supersilyl groups, tetrahedrane framework could not survive to give eliminated product (Scheme 28). Although the tetrasilatetrahydride salt **31** is not stable in solution at rt, the corresponding complex with 18-crown-6 is stable in solution, which was obtained in 56% yield by simply adding 18-crown-6 to a heptane solution of **31**. It is noteworthy that the same reaction in THF gave a product in which an Si-Si bond of **31** inserted into the 18-crown-6 ring [36].



Scheme 29 Reactions of potassium salt of tetrasilatetrahedrane **31** with SiCl₄

The reaction of **31** with SiBr₄ resulted in a formation of octasilane **30** as shown above; however, reaction with SiCl₄ gave a different product. Thus, treatment of **31** with SiCl₄ in THF at -78°C after filtration and recrystallization gave a pink-red solid. The crystallographic analysis revealed that the product was the novel spiro compound, dichlorononasilane **32** [37]. The reaction mechanism is shown in Scheme 29; the release of the strain of tetrahedrane is again a driving force.

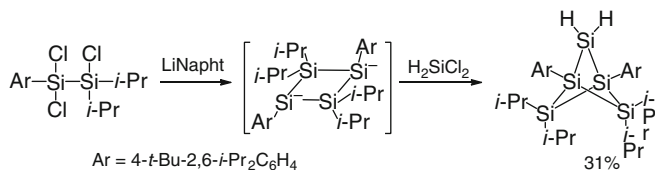
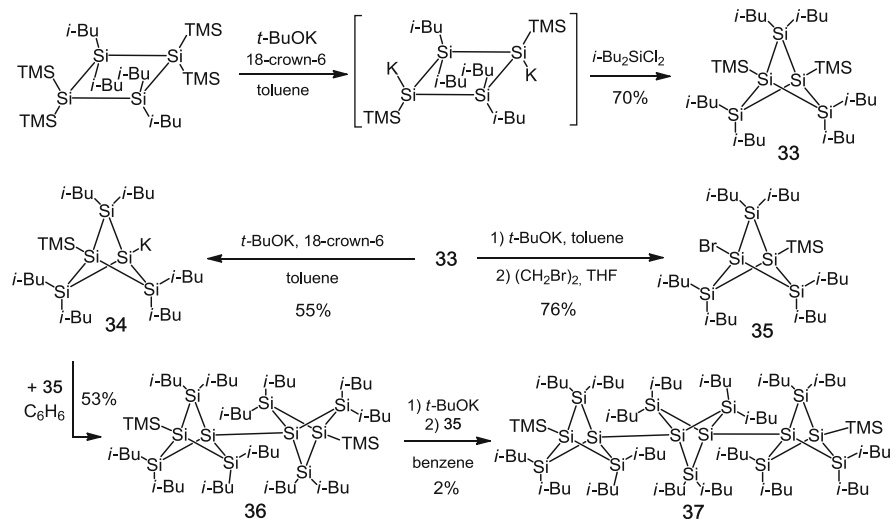
4 Other Polyhedral Clusters

As seen from the results shown above, thanks to the recent development of rapid crystallographic analysis and possible handling of unstable species in an inert atmosphere, the number of isolated strained molecules and polysilicon cage compounds drastically increased in recent years.

4.1 Strained Cage Molecules

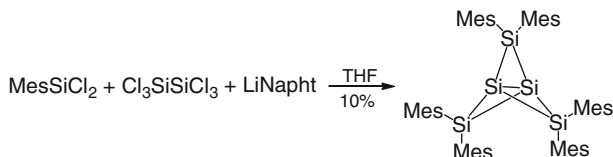
Synthesis of bicyclo[1.1.1]pentasilane was first synthesized by Kabe and Masamune's group in 1990. The reductive coupling of bulky aryl-substituted trichlorodisilane followed by treatment with dichlorosilane gave the target compound in 31% yield [38] (Scheme 30). After more than 20 years, Iwamoto's group in Sendai prepared silyl-substituted bicyclo[1.1.1]pentasilane **33** as air-stable colorless crystals. By application of a synthetic protocol (cleavage of silyl groups with KO^tBu) initially developed by Marschner et al. for oligosilanes, pentasila[*n*]staffanes **36** and **37** were obtained (catenated bicyclo[1.1.1]pentasilanes) [39] (Scheme 31).

All the compounds show very short nonbonding distances between bridgehead silicon atoms (e.g., 2.9768 Å for **33**). This value is much shorter than the sum of van der Waals radii of silicon atoms (4.20 Å). The bond lengths between bridgehead silicon atoms in **36** and **37** are similar to that of Si–TMS bond in spite of a catenated structure. Just like polysilanes, UV–vis spectra of pentasila[*n*]staffanes showed bathochromic shifts with increasing number of repeat units *n*, indicating the expansion of the σ -conjugated system. The ²⁹Si NMR peak for the bridgehead silicon atoms was observed at -99.7 ppm for **33**. This value is close to that of previously reported bicyclo[1.1.1]pentasilanes (-89.9 to -96.5 ppm) [38]. More recently, Breher's group reported the alkynyl-bridged bicyclo[1.1.1]pentane comprising silicon and tin [40].

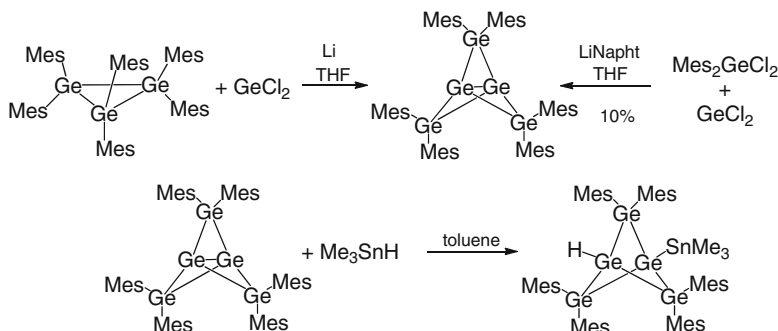
**Scheme 30** Synthesis of bicyclo[1.1.1]pentasilane**Scheme 31** Synthesis of pentasila[*n*]staffanes

Propellanes comprising heavier group 14 elements were identified as a central synthetic challenge in an article by Masamune in 1991 [41], and numerous synthetic experimental and theoretical approaches have been investigated since then. Although propellanes containing Sn were prepared by Kinoshita and Sita relatively early on [42], the syntheses of silicon or germanium homologues were only realized in 2009. Breher's group in Karlsruhe isolated first pentasila[1.1.1]propellane by the reaction of Mes₂SiCl₂ and hexachlorodisilane with LiNapht. The target compound was obtained as yellow crystals and found to be extremely sensitive to air and moisture [43]. The distance of two bridgehead silicon atoms was 2.636 Å and 13% longer than typical Si–Si single bond. On the other hand, the Si–Si bond length of *t*-Bu₃Si–Si(*t*-Bu)₃ was reported to be 2.697 Å [44]; therefore, the authors concluded that there exists a weak stretched bond between the bridgehead atoms. The ²⁹Si NMR peak of bridgehead atom was observed at –273.2 ppm and thus very high field reflecting the strained structure. Several reactions of this propellane were examined: H₂O, PhSH, PhOH, and Me₃SnH are readily added across the bridge as judged from preliminary reactions on NMR scale.

Pentagerma[1.1.1]propellane was prepared by the reaction from hexamethylcyclotrigermane with lithium and GeCl₂-dioxane [45]. Better yields were realized



Scheme 32 Synthesis and reaction of pentasila[1.1.1]propellane

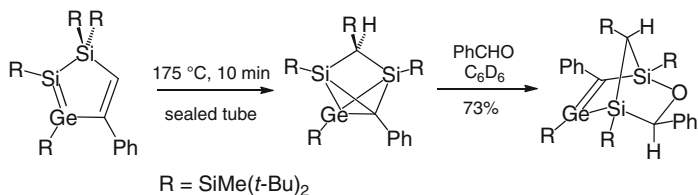
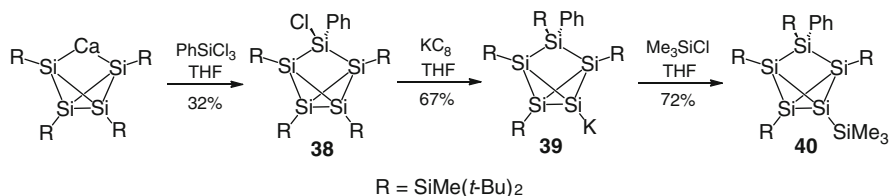
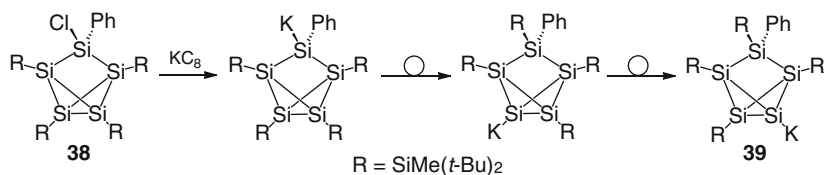


Scheme 33 Synthesis and reaction of pentagerma[1.1.1]propellane

by the reaction of $\text{Mes}_2\text{GeCl}_2$ with LiNapht in the presence of GeCl_2 -dioxane (Scheme 32). This propellane was obtained as orange crystals and sensitive to air, but stable towards degassed water. The distance of two bridgehead atoms was 2.869 Å, and that was much longer than usual Ge–Ge bond (2.40 Å). The reaction with Me_3SnH was examined, and an addition product across the bridgehead atoms was obtained (Scheme 33).

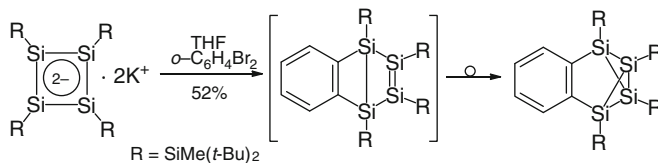
Another strained cage molecule is tricyclo[2.1.0.0^{2,5}]pentane, or “expanded tetrahedrane.” Lee and Sekiguchi group isolated the first example of such a compound with heavier group 14 elements. As shown in Scheme 34, thermal reaction starting from substituted silole homolog [46] gave 2,4-disila-1-germatricyclo[2.1.0.0^{2,5}]pentane quantitatively as air-sensitive yellow crystals. The structure of this unique “mixed cage” was established unequivocally by X-ray crystallography, and a very long Ge–C bond (2.242 Å, 15% longer than normal value) was observed. The reaction with benzaldehyde resulted in the formation of norbornene-type adduct.

Later, the same group reported simpler cases [47]. The first pentasilatricyclo[2.1.0.0^{2,5}]pentane was obtained by the reaction starting from calcium salt of tetrasilabicyclo[1.1.0]butane dianion prepared readily from tetrasilacyclobutadiene dianion [$(t\text{-Bu}_2\text{MeSi})_4\text{Si}_4$]²⁻·2K⁺. Monochloride **38** was obtained in 32% yield as yellow crystals. This monochloride served as a good precursor for the potassium salt **39**. This compound could be further transferred to silyl derivative **40** by the reaction with Me_3SiCl (Scheme 35). In the generation of potassium salt **39**, a 1,3-migration of silyl groups occurred from the anticipated anion, then further 1,2-migration afforded the final product **39** (Scheme 36). This reaction pathway

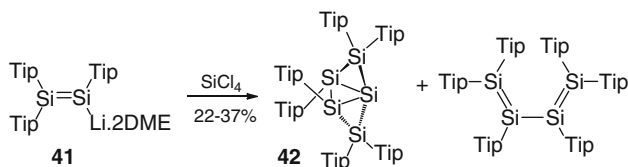
**Scheme 34** Synthesis and reaction of 2,4-disila-1-germatricyclo[2.1.0.0^{2,5}]pentane**Scheme 35** Synthesis of pentasilatricyclo[2.1.0.0^{2,5}]pentane**Scheme 36** Migration of silyl groups

was confirmed by theoretical calculations. The isomerization was thought to be driven by the tendency that anionic charge is favorably located at cage atoms with greater *s*-character. The ²⁹Si NMR peaks of bridgehead atoms were observed at -222.4 and -217.1 ppm for **38**, -253.9 ppm for **39**, and -182.3 and -178.6 ppm for **40**. The structure of **39** was determined by X-ray analysis. In the crystals, **39** exists as a contact ion pair, and the potassium cation shows interaction with the π -system of phenyl substituent. This unique structure can also explain the silyl-groups migration in the synthesis of **39**. The distance between the bridgehead atoms was determined to be 2.3801 \AA , a normal value for an Si–Si single bond.

The first synthesis of tetrasilabenzobenzvalene was reported in 2007 [48]. Starting from the same tetrasilacyclobutadiene dianion $[(t\text{-Bu}_2\text{MeSi})_4\text{Si}_4]^{2-} \cdot 2\text{K}^+$ as above, the reaction with *o*-dibromobenzene gave the target compound as air- and moisture-sensitive yellow crystals (Scheme 37). X-ray crystallographic analysis revealed that all Si–Si bond lengths are within a normal range. For instance, the bridgehead Si–Si bond length was determined to be 2.3462 \AA . The chemical shift of bridgehead silicon in ²⁹Si NMR was observed at -130.4 ppm in the expected high field region. The authors suggested the reaction mechanism as shown in Scheme 37. Thus, a transient Dewar-benzene would first be generated by [2+2] cycloaddition, then fast isomerization to give thermodynamically more stable benzvalene isomer would occur.



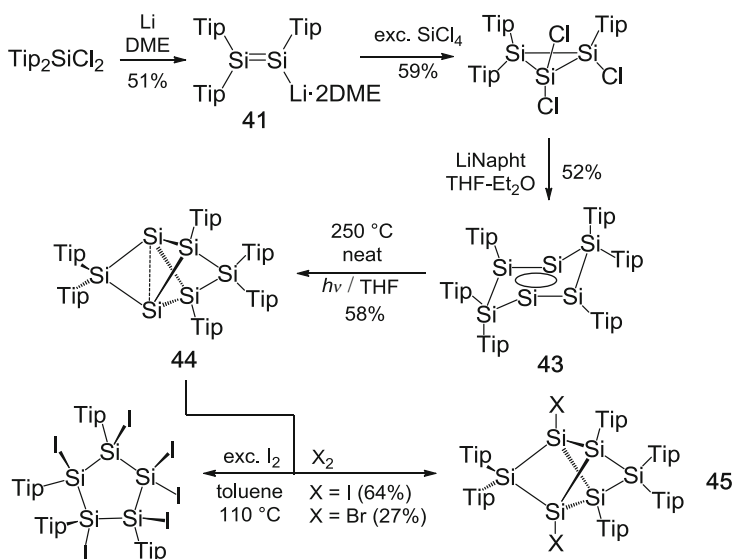
Scheme 37 Synthesis and reaction mechanism of tetrasilabenzobenzvalene



Scheme 38 Synthesis of first silicon cluster with unsubstituted vertex

In recent years, Scheschkewitz's group has reported many silicon clusters taking advantage of a reactive disilene as a starting compound. Their isolation of Tip-substituted disilene anion **41** [49], silicon analog of vinyl anion, was expected to serve as a precursor for many unusual compounds. First result appeared in 2005. As shown in Scheme 38, reaction of **41** with SiCl₄ serendipitously gave **42**, an Si₅ cluster with “naked” vertex silicon atom [50]. The yield was optimized up to 22–37%, varying because of the tedious separation from the systematically formed oxidation product of **41**. The result of ²⁹Si NMR supported that the structure of **42** was maintained in solution. Three peaks were observed at 7.4, –108.4, –124.8 ppm; non-substituted silicon's chemical shift was assigned to be –124.8 ppm by the measurement of 2D NMR spectrum. This compound forms red block crystals, and its UV–vis spectra show absorptions at 365 and 540 nm. The result of X-ray analysis indicated that the Si–Si bond between mono-tip silicon (2.306 Å) was shorter than the normal value, whereas other bonds were within normal range. The most astonishing point of this compound is that **42** represents the first example of an unsubstituted vertex silicon atom.

In 2010, Scheschkewitz's group introduced a tricyclic aromatic isomer of the elusive hexasilabenzene **43** [50]. The aromaticity of this compound was examined in detail by DFT-calculations. On the basis of the strongly negative NICS values and the pronounced stability of inversion-symmetric **43**, it was concluded that despite the presence of silicon atoms in the formal oxidation states of +II, +I and 0 compound **43** should be aromatic. The isomerism to hexasilabenzene (with a uniform formal oxidation state of +I) prompted the authors to coin the term “dimutational aromaticity.” One year later, Scheschkewitz et al. also reported the thermal isomerization of **43** to hexasilane (bridged propellane) **44** [51] (Scheme 39). From the result of X-ray crystallographic analysis of **44**, several intriguing points were observed. Thus, the distance of bridgehead atoms was 2.7076 Å, and this value is much longer than previously reported untethered propellane [43] (2.636 Å,

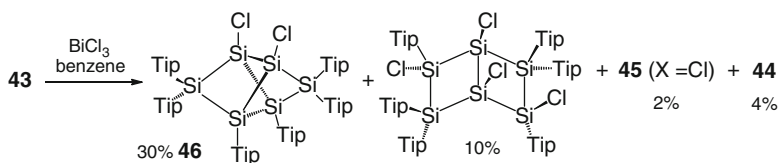


Scheme 39 Synthesis and reaction of bridged propellane

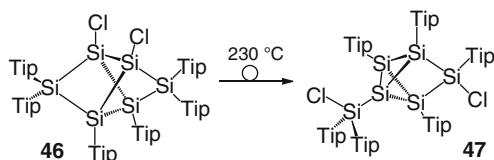
Scheme 32). All the other bond lengths are within the typical range. Because the two “propeller blades” were connected by additional silicon atom, the angle of these blades was smaller than other two angles. The ^{29}Si NMR chemical shift of bridgehead silicon was -274.2 ppm, similar to that of Mes_6Si_5 propellane. The low-field resonance at 174.6 ppm was assigned to the untethered blade silicon atom, an exceedingly unusual value for a tetracoordinate silicon atom.

Treatment of **44** with Cl_2 or Br_2 afforded dihalo compounds showing similar reactivity to Si–Si single bonds. Interestingly, the bridgehead distance was only slightly shortened; 2.6810 Å for dichloride, and 2.6547 Å for dibromide. Similarly, reaction with iodine gave diiodo compound. On the other hand, the reaction with excess iodine in refluxing toluene resulted in the quantitative formation of a hexaiodocyclopentasilane and therefore in the contraction of the silicon scaffold [17].

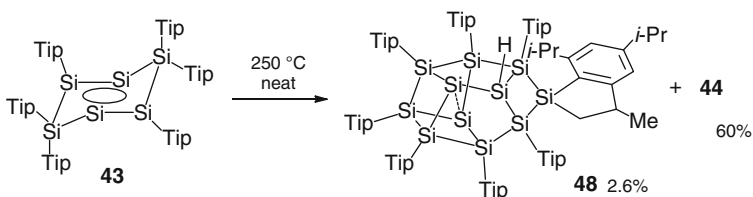
Many other reactions were reported in an article in 2012 [17]. Unlike bridged propellane **44**, compound **43** afforded complex mixture in the reaction of halogens. The authors utilized BiCl_3 as milder halogenation reagent, and a mixture of three halogenated compounds and **44** was obtained and separated. The main product **46** is the 1,2- Cl_2 -isomer of the halogenation products of **44** (30%), a ladder-type tetrachloride and **45** were obtained in 10 and 2% isolated yield, respectively (Scheme 40). The structures of all products were determined unequivocally by X-ray crystallographic analysis. The generation of tetrachloride is explained by the reaction of **46** with additional chlorine at the longest Si–Si bond although isolated **46** did not react with excess BiCl_3 .



Scheme 40 Halogenation of **43**



Scheme 41 Thermal rearrangement of **46**



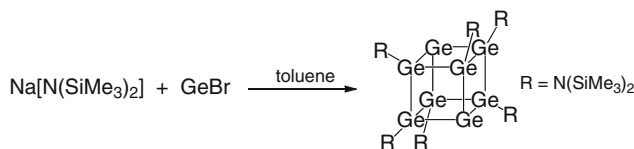
Scheme 42 Thermal reaction of **43**

Heating of dichloride **46** to $230\text{ }^\circ\text{C}$ until completely melted resulted in clean isomerization to afford **47** (Scheme 41). All these halogenated compounds should be excellent precursors of further complicated (or simple) silicon clusters.

In the thermal reaction from **43**, shown in Scheme 39, a side product was obtained in a small quantity. Isolation and structure determination revealed that the product was core-expanded Si_{11} cluster **48** (Scheme 42). Again in this case, two vertices consist of unsubstituted silicon atoms with shorter bond distance (2.4976 \AA) compared to those of **45** (2.7076 \AA) or pentasilapropellane (2.66 \AA). The reaction mechanism to form this complex compound is not clear yet.

4.2 Polysilicon and Polygermane Cage Molecules

Synthesis of polysilicon and polygermane clusters was a difficult task because separation and identification are much more difficult than smaller clusters. Nonetheless, recent development of rapid crystallographic analysis and handling unstable species made it possible to isolate a considerable number of those intriguing compounds. In this last chapter, recent reports of polysilicon and polygermane clusters are summarized.



Scheme 43 Synthesis of R_6Ge_8 cluster

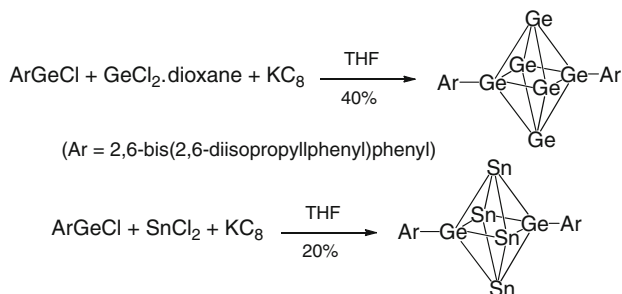
In early 2003, Schnepf and Köpfe in Karlsruhe reported Ge_8 cubic cluster with different approach [52]. They noticed that solid $\text{Ge}(\text{I})$ bromide would be a good source for the clusters, because this compound disproportionates above 90°C to produce germanium and germanium tetrabromide. Indeed, treatment of $\text{Na}[\text{N}(\text{SiMe}_3)_2]$ with GeCl afforded $\text{Ge}_8[\text{N}(\text{SiMe}_3)_2]_6$ cluster as dark red crystals. The crystallographic analysis showed that this cluster consists of a cubane skeleton with two naked germanium atoms. Two different $\text{Ge}-\text{Ge}$ bond lengths were observed; 2.67 \AA for $\text{Ge}(\text{R})-\text{Ge}(\text{R})$ and 2.50 \AA for $\text{Ge}(\text{R})-\text{Ge}$. In the crystal, two parallel toluene molecules are located above naked Ge atoms, bridging two cluster molecules in a manner (Scheme 43).

Later in the same year, Power's group in California reported the synthesis of unique octahedral clusters [53]. As shown in Scheme 44, treatment of bulky terphenyl-substituted chlorogermane and GeCl_2 -dioxane with KC_8 in THF gave hexagermaoctahedrane with only two substituents. Similar reaction with SnCl_2 also afforded Sn_4Ge_2 cluster. The unsubstituted Ge_4 or Sn_4 moieties comprise perfectly square arrays. Spectral data (^1H and ^{13}C NMR, and UV-vis spectra) showed no unusual features. The solution ^{119}Sn NMR displayed a signal at 1,583 ppm, showing a significant downfield shift.

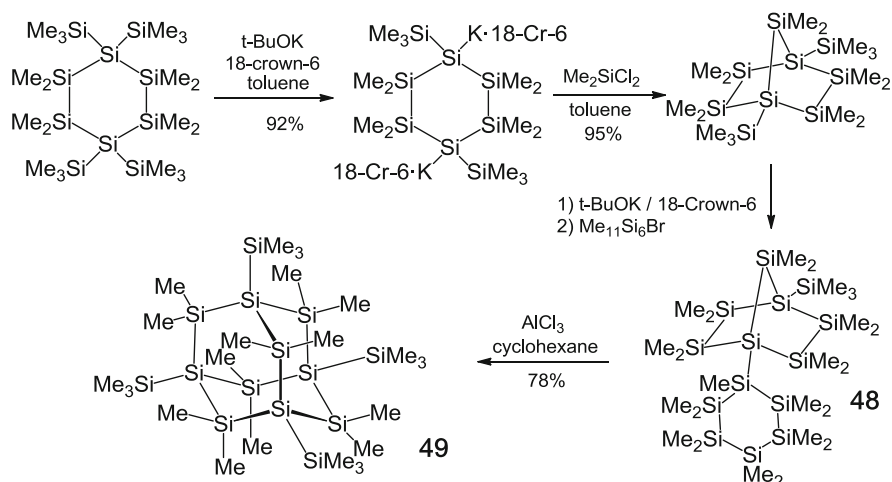
Decasilaadamantane represents a part of the bulk silicon lattice and has been a synthetic target for silicon chemists for a long time. In 2005, Marschner's group in Graz finally succeeded the synthesis [54]. They employed a rearrangement reaction with AlCl_3 , not like the previously examined step-by-step synthesis and obtained the target compound in 78% yield (Scheme 45). The synthesis began with bicyclo[2.2.1]heptasilane [55], and treatment with *t*-BuOK and following cyclohexasilanyl bromide afforded the precursor **48**. Rearrangement with catalytic AlCl_3 of **48** gave the target **49**. In solution, the ^{29}Si NMR spectrum showed three peaks at -4.8 , -26.0 , and -118.6 ppm, and these resonances were considerably downfield-shifted compared to $(\text{Me}_3\text{Si})_4\text{Si}$ or $(\text{Me}_2\text{Si})_6$. This cage polysilane showed strong absorption at 222 nm (ϵ 120,000) in UV-vis spectrum. As expected all the bond lengths and angles were within normal range.

Bicyclo[2.2.1]heptasilane, appears in Scheme 45, and bicyclo[2.2.2]octasilane are also cage compounds. Without much strain, these compounds were already prepared in 1970s [56] and have been studied since then.

In 2013, Ishida and Kyushin group in Gunma reported the synthesis of Si_{16} cluster containing octasilacubane core, an isomer of octasilacubane [57]. Reduction of tetrachlorotetra-*t*-butylcyclotetrasilane, readily available in two steps from dichlorodi-*t*-butyldiphenyldisilane, with sodium afforded the silicon cluster **50** in



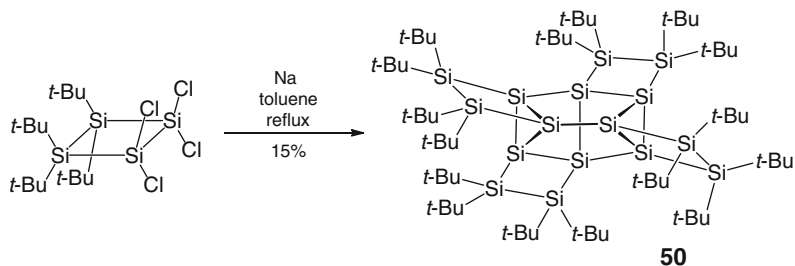
Scheme 44 Synthesis of R_2Ge_6 and $\text{R}_2\text{Sn}_4\text{Ge}_2$ cluster



Scheme 45 Synthesis of decasilaadamantane **49**

15% yield as air-sensitive orange crystals. Coincidentally, this reaction condition is exactly same as that of octasilacubanes **1** and **3**. No other isomers of **50** were observed in the reaction mixture. Apparently, only intractable polymers were generated as side products (Scheme 46).

The crystallographic analysis revealed a structure with C_2 symmetry axis. This compound contained many substructures like [3.2.1]propellane, [3.2.2]propellane, spiro[3.3]oligosilane, and spiro[4.3]oligosilane; all are previously unknown structures comprising silicon atoms. Interestingly, the bond lengths between unsubstituted bridgehead silicon atoms of [3.2.1]propellane structure were determined to be 2.384 and 2.361 Å and thus within the normal values. This feature is quite different from [1.1.1]propellane or related silicon clusters described above, all showing very long bridgehead distance. Four bridgehead atoms ([3.2.1]- and [3.2.2]propellanes) are included in this compound, and all these atoms adopted unusual trigonal monopyramidal structure. Each bridgehead silicon atom has a planar structure with



Scheme 46 Synthesis of Si_{16} cluster containing octasilacubane core

three connected silicon atoms, and the fourth bond was almost perpendicular ([3.2.2] propellane part) or about 60° angle ([3.2.1] propellane part) to these planes. The result of ^{29}Si CP-MAS NMR shows the expected eight signals. Among them, bridgehead signals were observed at -56.6 , -62.4 , and -71.8 ppm for those contained in cyclo-trisilane rings, and the resonance of the fourth one contained in cyclo-tetrasilanes ring was observed between 25.0 and 39.0 ppm (unassigned). These features clearly show the difference of this larger-ring propellanes from smaller-ring propellanes. The absorption of **50** does not show clear band above 250 nm and tails into 570 nm with several shoulders at 345 and 380 nm. With many possible oligosilyl structures, the energy levels of this molecular are probably close with a small band gap, making a broad spectrum without distinct peaks.

5 Summary, Conclusions, Outlook

In this field, most intensive research activities appears to be accumulated in 1988–1993, first 5 years from the isolation of octasilacubane. Nonetheless, just after quarter century from the beginning, it seems that we are facing a turning point with a growing numbers of new clusters.

As a matter of fact, Table 1, shown in the introduction in this article, lacks two more platonic solid compounds: octahedrane and icosahedrane. This is because those compounds comprising group-14 elements were thought to be impossible to be prepared. Obviously, Scheschkewitz's result as well as Power's octahedrane opened a gate towards octahedranes. And for icosahedranes? Yes, silicon and higher group-14 elements can adopt pentacoordinated and hexacoordinated structure!

It is noteworthy that recent approaches often adopt reactions with mixing ligands and core-atom molecules which make the syntheses simple. This development is expected to continue from now on in attempt to bridge the evident analytical gap between silicon molecules and bulk silicon.

References

1. Greenberg A, Liebman JF (1978) Strained organic molecules. Academic, New York
2. Balaban AT, Banciu M, Ciorba V (1987) Annulenes, benzo-, hetero-, homo-derivatives, and their valence isomers. CRC, Florida
3. Matsumoto H, Higuchi K, Hoshino Y, Koike H, Naoi Y, Nagai Y (1988) The first octasilacubane system: synthesis of octakis-(*t*-butyldimethylsilyl)pentacyclo[4.2.0.0^{2,5}.0^{3,8}.0^{4,7}]octasilane. J Chem Soc, Chem Commun :1083
4. Sekiguchi A, Nagase S (1998) Polyhedral silicon compounds. In: Rappoport Z, Apeloig Y (eds) The chemistry of organosilicon compounds, vol 2. Wiley, West Sussex
5. Unno M, Matsumoto T, Mochizuki K, Higuchi K, Goto M, Matsumoto H (2003) Structure and oxidation of octakis(*tert*-butyldimethylsilyl)octasilacubane. J Organomet Chem 685:156
6. Kabe Y, Kuroda M, Honda Y, Yamashita O, Kawase T, Masamune S (1988) Reductive oligomerization of 1,2-di-*tert*-butyl-1,1,2,2-tetrachlorodisilane: the tricyclo[2.2.0.0^{2,5}]hexasilane and tetracyclo[3.3.0.0^{2,7}.0^{3,6}]octasilane systems. Angew Chem Int Ed 27:1725
7. Weidenbruch M, Grimm F-T, Pohl S, Saak W (1989) A polyhedral oligogermane: 4,8-dibromoocta-*tert*-butyltetracyclo[3.3.0.0^{2,7}.0^{3,6}]octagermane. Angew Chem Int Ed 28:198
8. Sekiguchi A, Naito H, Nameki H, Ebata K, Kabuto C, Sakurai H (1989) 4,8-dichloroocta-*t*-butyltetracyclo[3.3.0.0^{2,7}.0^{3,6}]octagermane. J Organomet Chem 368:C1
9. Sekiguchi A, Yatabe T, Kamatani H, Kabuto C, Sakurai H (1992) Chemistry of organosilicon compounds. 293. Preparation, characterization, and crystal structures of octasilacubanes and octagermacubanes. J Am Chem Soc 114:6260
10. Matsumoto H, Higuchi K, Kyushin S, Goto M (1992) Octakis(1,1,2-trimethylpropyl)octasilacubane: synthesis, molecular structure, and unusual properties. Angew Chem Int Ed 31:1354
11. Furukawa K, Fujino M, Matsumoto N (1992) Cubic silicon cluster. Appl Phys Lett 60:2744
12. Unno M, Higuchi K, Furuya K, Shioyama H, Kyushin S, Goto M, Matsumoto H (2000) Synthesis, structure, and reactions of octakis(1,1,2-trimethylpropyl)octagermacubane. Bull Chem Soc Jpn 73:2093
13. Sekiguchi A, Sakurai H (1995) Cage and cluster compounds of silicon, germanium, and tin. In: Stone FGA, West R (eds) Advances in organometallic chemistry, vol 37. Academic, San Diego
14. Nagase S (1993) Theoretical study of heteroatom-containing compounds. From aromatic and polycyclic molecules to hollow cage clusters. Pure Appl Chem 65:675
15. Sekiguchi A, Kabuto C, Sakurai H (1989) [(Me₃Si)₂CHGe]₆, the first hexagermaprismane. Angew Chem Int Ed 28:55
16. Sekiguchi A, Yatabe T, Kabuto C, Sakurai H (1993) Chemistry of organosilicon compounds. 303. The missing hexasilaprismane: synthesis, x-ray analysis and photochemical reactions. J Am Chem Soc 115:5853
17. Abersfelder K, Russell A, Rzepa HS, White AJP, Peter Haycock PR, Scheschkewitz D (2012) Contraction and expansion of the silicon scaffold of stable Si₆R₆ isomers. J Am Chem Soc 134:16008
18. Nagase S (1989) Much less strained cubane analogues with Si, Ge, Sn, and Pb skeletons. Angew Chem Int Ed 28:329
19. Wiberg N, Finger CMM, Polborn K (1993) Tetrakis(tri-*tert*-butylsilyl)-tetrahedro-tetrasilane (*t*Bu₃Si)₄Si₄: the first molecular silicon compound with a Si₄ tetrahedron. Angew Chem Int Ed 32:1054
20. Ichinohe M, Toyoshima M, Kinjo R, Sekiguchi A (2003) Tetrasilatetrahedranide: a silicon cage anion. J Am Chem Soc 125:13328
21. Meyer-Wegner F, Scholz S, Sanger I, Schodel F, Bolte M, Wagner M, Lerner H-W (2009) Synthesis of Wiberg's tetrasilatetrahedrane (*t*Bu₃Si)₄Si₄ by a one-pot procedure. Organometallics 28:6835
22. Cordes DB, Lickiss PD, Rataboul F (2010) Recent developments in the chemistry of cubic polyhedral oligosilsesquioxanes. Chem Rev 110:2081

23. Unno M, Yokota T, Matsumoto H (1996) Oxaoctasilahomocubane and dioxaoctasilabishomocubane: novel silicon ring system. *J Organomet Chem* 521:409
24. Unno M, Yamashita N, Matsumoto H (2011) Thermal reaction of octasilacubane with sulfur, selenium, and tellurium: formation of novel cage systems. *Phosphorus, Sulfur, Silicon and Relat Elem* 186:1259
25. Unno M, Higuchi K, Ida M, Shioyama H, Kyushin S, Goto M, Matsumoto H (1994) Ring-opening reaction of octakis(1,1,2-trimethylpropyl)octasilacubane. *Organometallics* 13:4633
26. Unno M, Masuda H, Matsumoto H (2002) Photo-initiated bromination of octakis(1,1,2-trimethylpropyl)octasilacubane with tetrabromomethane. *Silicon Chem* 1:377
27. Unno M, Shioyama H, Ida M, Matsumoto H (1995) Reductive dehalogenation of 4,8-dihalooctakis(1,1,2-trimethylpropyl)tetracyclo-[3.3.0.0^{2,7}.0^{3,6}]octasilanes with sodium. *Organometallics* 14:4004
28. Horiuchi H, Nakano Y, Matsumoto T, Unno M, Matsumoto H, Hiratsuka H (2000) Electronic structure and photochemical reaction intermediates of octakis(1,1,2-trimethylpropyl)octasilacubane. *Chem Phys Lett* 322:33
29. Kyushin S, Meguro A, Unno M, Matsumoto H (2000) Photolysis of *anti*-dodecaalkyltricyclo [4.2.0.0^{2,5}]octasilane: generation and reactions of cyclotetrasilene. *Chem Lett* 29:494
30. Wiberg N, Auer H, Wagner S, Polborn K, Kramer G (2001) Disilene R*XS₂=SiXR* (R* = Si*t*Bu₃) mit siliciumgebundenen H- und Hal-atomen X: bildung, isomerisierung, reaktionen. *J Organomet Chem* 619:110
31. Wiberg N, Auer H, Noth H, Knizek J, Polborn K (1998) Diiodotetrasupersilylcyclotetrasilene (tBu₃Si)₄Si₄I₂ – a molecule containing an unsaturated Si₄ ring. *Angew Chem Int Ed* 37:2869
32. Ichinohe M, Takahashi N, Sekiguchi A (1999) Formation and structure of protonated tetrasilatetrahedrane-monooxide, (*tert*-Bu₃Si)₄Si₄OH. *Chem Lett* 28:553
33. Wiberg N, Auer H, Polborn K, Veith M, Huch V (2000) Products of the reaction of tetrasupersilyl-*tetrahedro*-tetrasilane (tBu₃Si)₄Si₄ with iodine. In: Auner N, Weis J (eds) *Organosilicon chemistry IV – from molecules to material*. Wiley-VCH, Weinheim
34. Fischer G, Huch V, Mayer P, Vasisht SK, Veith M, Wiberg N (2005) Si₈(Si*t*Bu₃)₆: A hitherto unknown cluster structure in silicon chemistry. *Angew Chem Int Ed* 44:7884
35. Wiberg N, Vasisht SK, Fischer G, Mayer P, Huch V, Veith M (2003) Reactivity of the unusually structured silicon cluster compound Si₈(Si*t*Bu₃)₆. *Z Anorg Allg Chem* 633:2425
36. Klapötke TM, Vasisht SK, Fischer G, Mayer P (2010) A reactive Si₄ cage: K(Si*t*Bu₃)₃Si₄. *J Organomet Chem* 695:667
37. Klapötke TM, Vasisht SK, Mayer P (2010) Spirocycle (Si*t*Bu₃)₆Si₉Cl₂: the first of its kind among group 14 elements. *Eur J Inorg Chem* :3256
38. Iwamoto T, Tsushima D, Kwon E, Ishida S, Isobe H (2012) Persilastaffanes: design, synthesis, structure, and conjugation between silicon cages. *Angew Chem Int Ed* 51:2340
39. Kabe Y, Kawase T, Okada J, Yamashita O, Goto M, Masamune S (1990) A bicyclo[1.1.1]pentasilane derivative. Synthesis, molecular structure, and comments on structural homology. *Angew Chem Int Ed* 29:794
40. Augenstein T, Oña-Burgos P, Nied D, Breher F (2012) Alkynyl-functionalised and linked bicyclo[1.1.1]pentanes of group 14. *Chem Commun* 48:6803
41. Tsumuraya T, Batcheller SA, Masamune S (1991) Strained-ring and double-bond systems consisting of the Group 14 elements Si, Ge, and Sn. *Angew Chem Int Ed* 30:902
42. Sita LR, Bickerstaff RDJ (1989) 2,2,4,4,5,5-Hexakis(2,6-diethylphenyl)pentastanna[1.1.1]propellane: characterization and molecular structure. *J Am Chem Soc* 111:6454
43. Nied D, Köppe R, Klopfer W, Schnöckel H, Breher F (2010) Synthesis of a pentasilapropellane. Exploring the nature of a stretched silicon–silicon bond in a nonclassical molecule. *J Am Chem Soc* 132:10264
44. Wiberg N, Schuster H, Simon A, Peters K (1986) Hexa-*tert*-butyldisilane—the molecule with the longest Si–Si bond. *Angew Chem Int Ed* 25:79

45. Nied D, Klopper W, Breher F (2009) Pentagerma[1.1.1]propellane: a combined experimental and quantum chemical study on the nature of the interactions between the bridgehead atoms. *Angew Chem Int Ed* 48:1411
46. Lee VA, Ichinohe M, Sekiguchi A (2002) 2,4-Disila-1-germatricyclo[2.1.0.0^{2,5}]pentane: a new type of cage compound of group 14 elements with an extremely long Ge–C bridge bond and an “umbrella”-type configuration of a Ge atom. *J Am Chem Soc* 124:9962
47. Lee VA, Yokoyama T, Takanishi K, Sekiguchi A (2009) Pentasilatricyclo[2.1.0.0^{2,5}]pentane and its anion. *Chem Eur J* 15:8401
48. Takahashi N, Lee VY, Ichinohe M, Sekiguchi A (2007) 1,2,5,6-Tetrasilabenzobenzvalene: a valence isomer of 1,2,3,4-tetrasilanaphthalene. *Chem Lett* 36:1158
49. Scheschkewitz D (2004) A silicon analogue of vinyl lithium: structural characterization of a disilenide. *Angew Chem Int Ed* 43:2965
50. Abersfelder K, White AJP, Rzepa HS, Scheschkewitz D (2010) A tricyclic aromatic isomer of hexasilabenzene. *Science* 327:564
51. Abersfelder K, White AJP, Berger RJF, Rzepa HS, Scheschkewitz D (2011) A stable derivative of the global minimum on the Si₆H₆ potential energy surface. *Angew Chem Int Ed* 50:7936
52. Schnepf A, Köppe R R (2003) Ge₈{N(SiMe₃)₂}₆: a ligand-stabilized Ge cluster compound with formally zero-valent Ge atoms. *Angew Chem Int Ed* 42:911
53. Richards AF, Hope H, Power PP (2003) Synthesis and characterization of neutral, homo and heteronuclear clusters with unsubstituted germanium or tin atoms. *Angew Chem Int Ed* 42:4071
54. Fischer J, Baumgartner J, Marschner C (2005) Synthesis and structure of sila-adamantane. *Science* 310:825
55. Fischer R, Konopa T, Ullly S, Baumgartner J, Marschner C C (2003) Route Si₆ revisited. *J Organomet Chem* 685:79
56. West R, Indriksons A (1972) Cyclic polysilanes. VI. Bicyclic and cage permethylcyclopoly-silanes. *J Am Chem Soc* 94:6110
57. Ishida S, Otsuka K, Toma Y, Kyushin S (2013) An organosilicon cluster with an octasilacuneane core: a missing silicon cage motif. *Angew Chem* 52:2507

Recent Advances in Silylene Chemistry: Small Molecule Activation En-Route Towards Metal-Free Catalysis

Burgert Blom and Matthias Driess

Abstract Previously only known as fleeting, transient laboratory curiosities in the 1960s, silylenes (species of the general type: $\text{Si}^{\text{II}}\text{R}'\text{R}''$ where R' and R'' are any σ or π -bonded substituents, homo or heteroleptic) are now one of the most rigorously investigated classes of compounds in contemporary chemistry. The breakthroughs came in 1986 when Jutzi and co-workers isolated Cp^*Si : ($\text{Cp}^* = \eta^5\text{-C}_5\text{Me}_5$), the first isolable Si(II) compound, and later in 1994 with the discovery of the first *N*-heterocyclic silylene by West and Denk, heralding the beginning of a burgeoning era in low-valent silicon chemistry. Since these and other key discoveries, massive advances have been made in understanding and elucidating the nature of these reactive compounds, and their ability, for example, to activate small molecules, or behave as ligands in transition metal complexes which can perform a variety of catalytic or stoichiometric transformations. In this chapter, recent advances in silylene chemistry will be presented, with a particular focus on developments in the last 10 years approximately. A key emphasis will rest on the reactivity of isolable silylenes, including their coordination towards metals, with respect to small molecule bond activation, and potential catalytic transformations. Although metal-coordinated silylene complexes have been shown to be catalytically useful in a variety of transformations, metal-free catalysis with silylenes is still a target.

Keywords Acyclic silylenes · Base-stabilised silylenes · Carbocyclic silylenes · Catalysis · *N*-heterocyclic silylenes · Small molecule bond activation · π -coordinated silylenes

B. Blom and M. Driess (✉)

Institute of Chemistry: Metalorganics and Inorganic Materials, Technische Universität Berlin,
Sekt. C2, Strasse des 17. Juni, 135, 10623 Berlin, Germany
e-mail: matthias.driess@tu-berlin.de

Contents

| | | |
|---|--|-----|
| 1 | Introduction | 87 |
| 2 | Free <i>N</i> -heterocyclic Silylenes (NHSis) and Their Reactivity Towards Small Molecules | 88 |
| 3 | <i>N</i> -heterocyclic Silylene (NHSi) Transition Metal Complexes and Their Reactivity | 95 |
| 4 | Base-Stabilised Silylenes of the Type: SiR ₂ ←:B | 100 |
| 5 | Carbocyclic Silylenes | 102 |
| 6 | Acyclic Silylenes Bearing Only σ-bonded Substituents | 110 |
| 7 | Silylenes Bearing π and/or σ-coordinated Ligands | 114 |
| 8 | Summary, Conclusions, Outlook | 117 |
| | References | 118 |

Abbreviations

| | |
|--------------|---|
| Ar | Aryl |
| Bu | Butyl |
| cod | Cyclooctadiene |
| concd | Concentrated |
| cot | Cyclooctatetraene |
| Cp | Cyclopentadienyl |
| Dipp | 2,6-Bis-isopropylphenyl |
| DMAP | 4-(Dimethylamino)pyridine |
| DMB | 3,4-Dimethoxybenzyl |
| DME | 1,2-dimethoxyethane |
| DMF | Dimethylformamide |
| DMPU | 1,3-Dimethyl-3,4,5,6-tetrahydro-2(1H)-pyrimidinone |
| DMSO | Dimethyl sulfoxide |
| EDTA | Ethylenediaminetetraacetic acid |
| equiv | Equivalent(s) |
| Et | Ethyl |
| h | Hour(s) |
| <i>i</i> -Pr | Isopropyl |
| KHMDS | Potassium hexamethyldisilazide potassium bis(trimethylsilyl)amide |
| LDA | Lithium diisopropylamide |
| LHMDS | Lithium hexamethyldisilazide lithium bis(trimethylsilyl)amide |
| LTMP | Lithium 2,2,6,6-tetramethylpiperidide |
| Me | Methyl |
| Mes | Mesityl 2,4,6-trimethylphenyl (not methanesulfonyl) |
| min | Minute(s) |
| mol | Mole(s) |
| Ph | Phenyl |
| Pr | Propyl |
| rt | Room temperature |
| s | Second(s) |
| <i>t</i> -Bu | <i>tert</i> -butyl |

| | |
|-------|--|
| THF | Tetrahydrofuran |
| TMEDA | <i>N,N,N',N'</i> -tetramethyl- 1,2-ethylenediamine |
| TMS | Trimethylsilyl |
| Tol | 4-Methylphenyl |
| Trip | 2,4,6-Triisopropylphenyl |

1 Introduction

In 1964, nearly 50 years ago, Skell and Goldstein first reported dimethylsilylene: SiMe_2 , as a transient intermediate, which they generated in the gas phase by reduction of dimethylchlorosilane with sodium–potassium vapour at elevated temperatures [1]. Nearly 30 years later, however, the isolation of stable divalent silicon compounds of the type: SiR_2 (R = alkyl, aryl or *N*-alkyl/*N*-aryl substituents) was still an open question despite this early report, owing to their concomitant high reactivity. This situation finally changed in 1994 with the isolation of the first stable *N*-heterocyclic silylene (NHSi) by Denk, West and co-workers [2], heralding a boost in modern silicon chemistry. In the 18 years since this groundbreaking discovery, breathtaking advances have been made in the synthesis of these previously elusive species, which can now be considered the vanguard in contemporary main group and organometallic chemistry. Silylenes now enjoy indefatigable research attention with many research groups in academia and industry world-wide feverishly pursuing their potential uses in catalysis, synthesis and stoichiometric transformations. This is not surprising, seeing as silicon is the second most abundant element in Earth's crust and is non-toxic, and given the bottleneck in metal-based resources, as well as the current energy crisis, alternative catalytic or stoichiometric transformations mediated by reactive silicon compounds represent a crucial scientific goal. The “holy grail” of silylene chemistry is metal-free catalysis, which is a target yet to be realised but given the rapid development in the field, it is likely that this goal might soon be achieved.

Existing silylenes can be essentially categorised into five distinct classes: **(I)** *N*-heterocyclic silylenes (NHSis), **(II)** base-stabilised silylenes typically stabilised by *N*-heterocyclic carbenes, **(III)** carbocyclic silylenes, **(IV)** acyclic silylenes, and **(V)** silylenes bearing π -coordinated substituents (Fig. 1)^a.

Highlights of each of these sub-classes will be addressed separately in this chapter, with a brief introduction in each case, to place the recent developments

^a Compounds featuring silicon atoms in the oxidation state + II that are *strictly* two coordinate qualify as silylenes in the formal sense. Compounds bearing silicon atoms in the oxidation state + II with π -donating ligands are perhaps better described as monomeric silicon(II) compounds. Nevertheless, given the influence such compounds have had on the development of silylene chemistry in recent years, for our purposes, we relax this definition and include compounds bearing π -coordinated substituents on silicon(II) and treat them as “silylenes.”

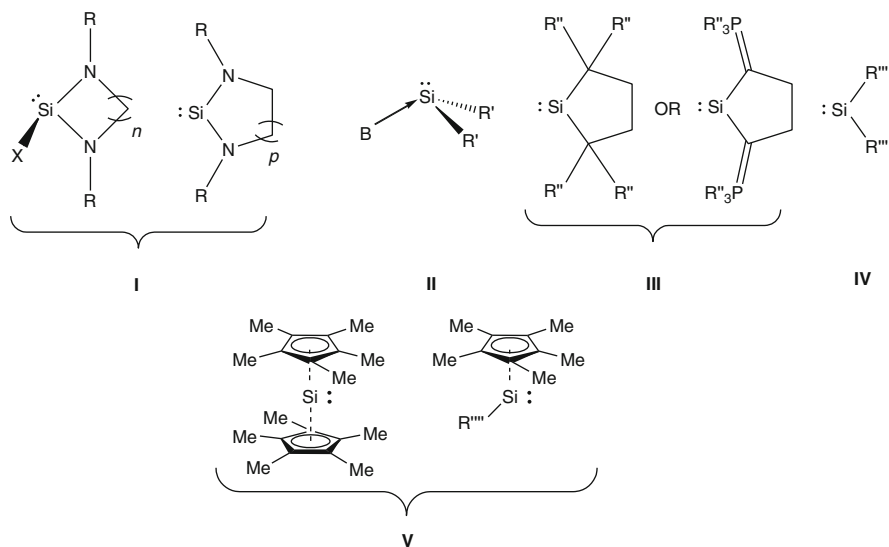


Fig. 1 Four distinct classes of silylenes: I: $n = 1-3$; $p = 1$ or 2 ; unsaturated functionalities in cyclical backbone may exist, $R =$ bulky aromatic or aliphatic groups; $X =$ halogen or some other substituent, for example *O*-*t*Bu. II: $R' =$ bulky aromatic group, alkyl chain or halogen; $B =$ Lewis base, for example *N*-heterocyclic carbene. III: $R'' = \text{Si}(\text{CH}_3)_3$ or aromatic substituent. IV: $R''' = \text{NR}_2$, SR or Boryl. V: $R''' =$ bulky aromatic or imino substituent, for example

into a historical context. A particular focus on modern developments (the last 10 years approximately) in each sub-class, with a further underlying focus on reactivity at the silicon centre will be a connecting theme throughout the discussion. The propensity of the silylenes to engage in metal complex formation and the emerging reactivity of these complexes, particularly in terms of catalytic and small molecule activation reactions will also be interwoven into the discussion where appropriate.

2 Free *N*-heterocyclic Silylenes (NHSis) and Their Reactivity Towards Small Molecules

Silylenes belonging to this class are by far the most ubiquitous. Since the pioneering work of West and Denk et al., a large number of *N*-heterocyclic silylenes (NHSis) have made their appearance in the literature (Fig. 2) [2–14]. A rich and diverse chemistry has been developed for many of these NHSis, in particular NHSis **1–8**. This is showcased by their ability to act as ligands in transition metal complexes (discussed in the next section), or in the activation of small molecules and other synthetic transformations (**3** and **4** in particular), even without coordination with a metal. The bis-NHSis **9–11** have also recently been shown to act as bidentate

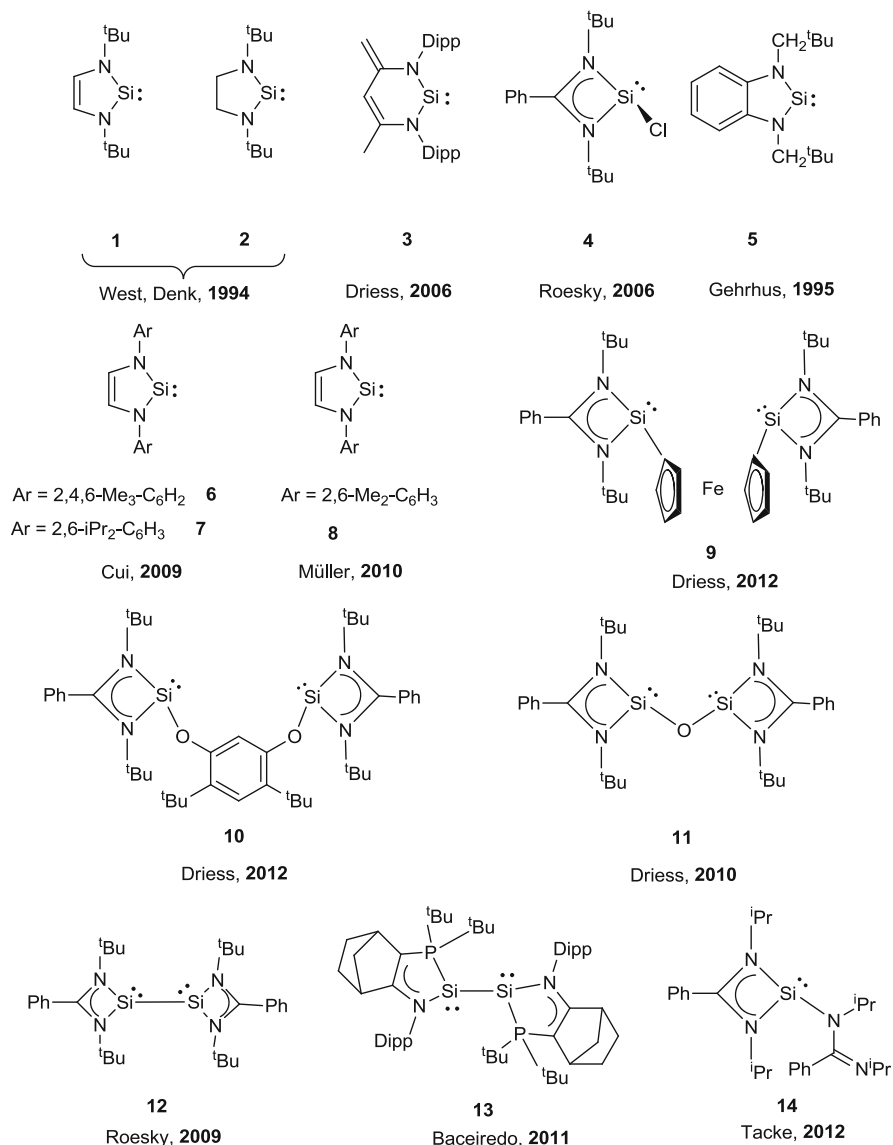
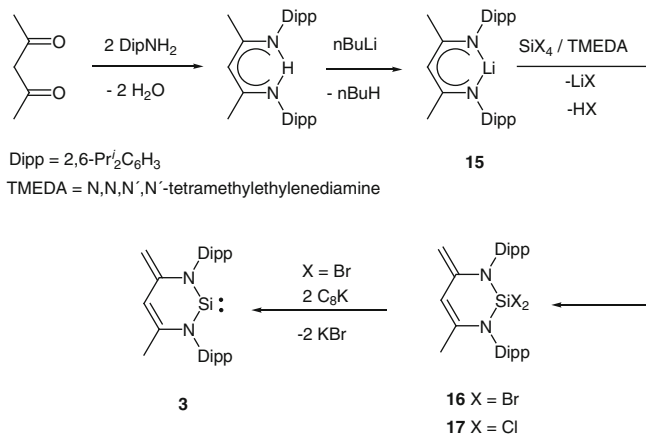


Fig. 2 A plethora of *N*-heterocyclic silylenes (NHSis). The early examples by Denk and Gehrus are included for completeness. The NHSi **13** features a P,N donor stabilisation. (Dipp = 2,6-*i*Pr₂-C₆H₃)

ligands in transition metal chemistry, opening the door to possible catalytic applications (discussed in next section), while bis-NHSis **12** and **13** are unique in that they feature two Si(I) centres, as opposed to all the other NHSis represented in Fig. 2, all bearing Si(II) centres. In this section we will discuss some recent



Scheme 1 Synthesis of the zwitterionic NHSi **3**

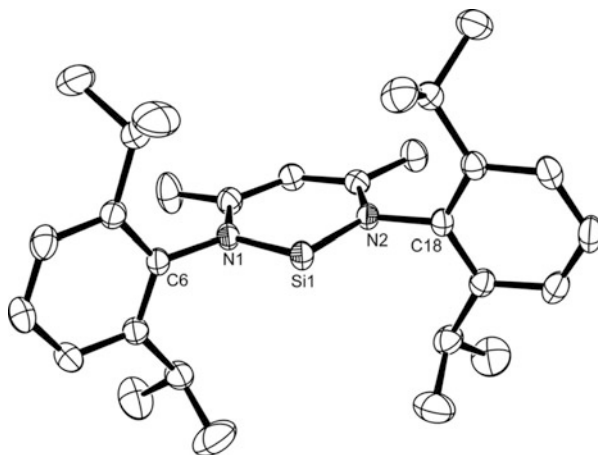
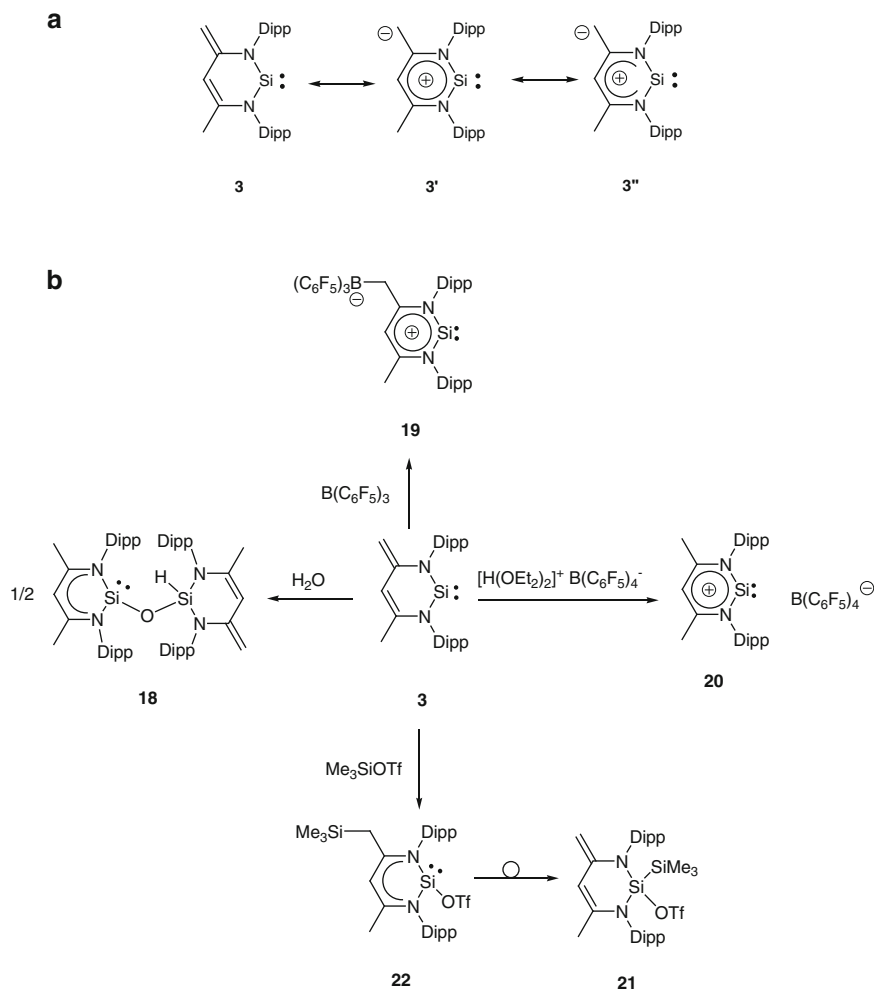


Fig. 3 Molecular structure of **3** with thermal ellipsoids drawn at 50% probability level

highlights in the synthesis and reactivity of some NHSis particularly with respect to small molecule activation.

A starting point in our discussion on NHSis is the 2006 report from Driess et al. [3], who reported the synthesis of the unique zwitterionic NHSi (**3**) following the synthetic protocol highlighted in Scheme 1. It was found necessary to use TMEDA in the synthesis, as reaction of salt **15** [15] with SiBr₄, lead to a mixture of products where LSiBr₃ was not formed.

The solid-state structure of **3** was also determined by single crystal X-ray diffraction analysis (Fig. 3). This analysis revealed that **1** consists of a planar six-membered SiN₂C₃ ring with the alternating endocyclic C–C distances of

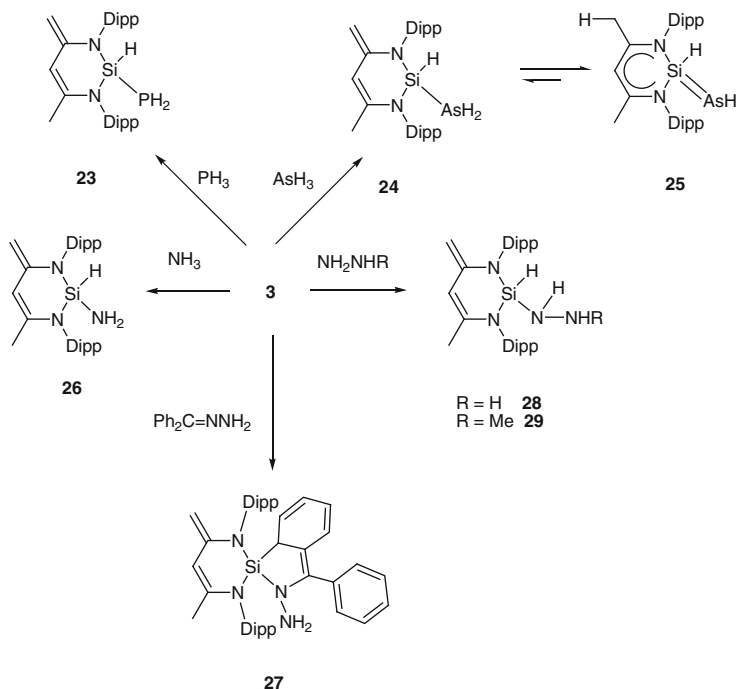


Scheme 2 (a) Mesomeric forms for the NHSi **3**. (b) Activation of various small molecules with NHSi **3**

1.402(2) (C2–C3) and 1.389(2) Å (C3–C4) and that of the exocyclic C2–C1 double bond (1.412(2) Å), respectively (Fig. 3).

Calculations point to a preference of the mesomeric form **3''** (SiN₂ allyl-like form) over **3'** (6π-heterofulvene ylide form) (Scheme 2a) as shown by the positive NICS values (NICS(O) = 3.6, NICS(1) = 1.4 ppm). The dipole moment calculation (DFT, B3LYP/6-311G) in **3** amounts to 1.8 D. Together with the theoretically calculated proton affinity of **3** (1,099 kJ mol⁻¹) due to the exocyclic methylene group, an ylide-like character was suggested for **3**.

The NHSi **3** has shown its robust and rich reactivity in a variety of small molecule activations. This is potentially a result of its zwitterionic nature with



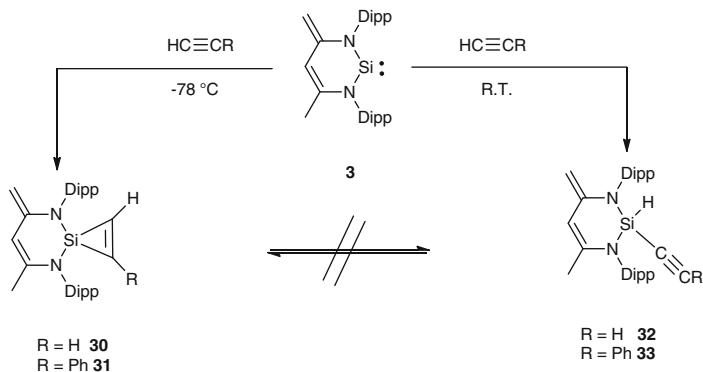
Scheme 3 Small activation reactions effected by NHSi **3**

activation of other small molecules such as ammonia, hydrazines and hydrazone [18, 19], resulting in **26–29**, respectively (Scheme 3) [20, 21].

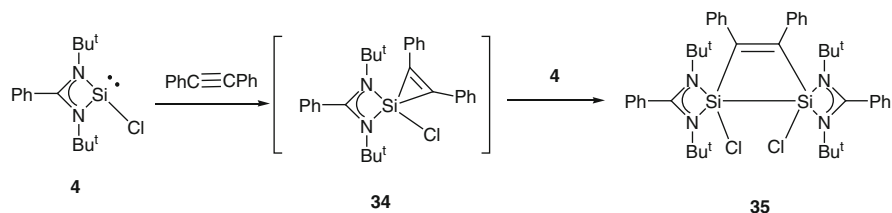
Strikingly, NHSi **3** has even been shown to activate alkynes (Scheme 4) [22, 23]. Depending on the reaction conditions, a [2 + 1] cycloaddition product can be obtained (**30** or **31**), or the expected 1,1 addition product (C–H activation over the Si centre) (**32** or **33**). Noteworthy is that **30** cannot be converted into **32**, (or **31–33**) due to kinetic reasons, which was confirmed by DFT studies.

A plethora of further investigations have been carried out with a large array of other small molecules involving **3**, including P_4 [24], C–H or C–F bond activation reactions of aromatic systems [25], activation of haloalkanes and halosilanes [26], activation of unsaturated organic groups [27, 28], coordination of NHCs [29, 30] and finally activation of CO_2 and NO_2 with species resulting from the aforementioned systems [31]. These studies provide further testimony to the exciting and rich chemistry afforded by NHSi **3**.

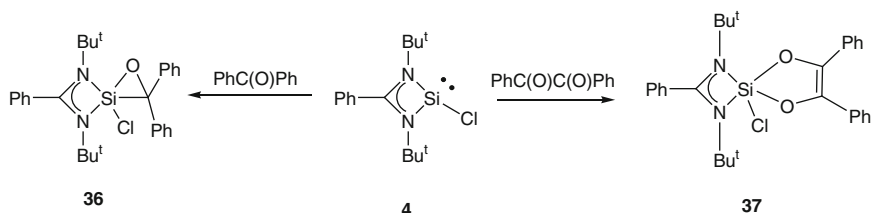
The N-donor stabilised chlorosilylene **4**, from the Roesky group, has also enjoyed substantial attention in recent years, for example with respect to the activation of small molecules. Accordingly, diphenylacetylene can be activated by **4**, resulting in the adduct **34**, which upon further reaction with **4** forms the intriguing dinuclear adduct **35** (Scheme 5).



Scheme 4 Activation of acetylene and phenyl acetylene by the zwitterionic NHCs **3**. Depending on the reaction conditions, either a [2 + 1] cycloaddition product (**30**, **31**) can result or the 1,1-addition over the Si(II) centre (**32**, **33**)



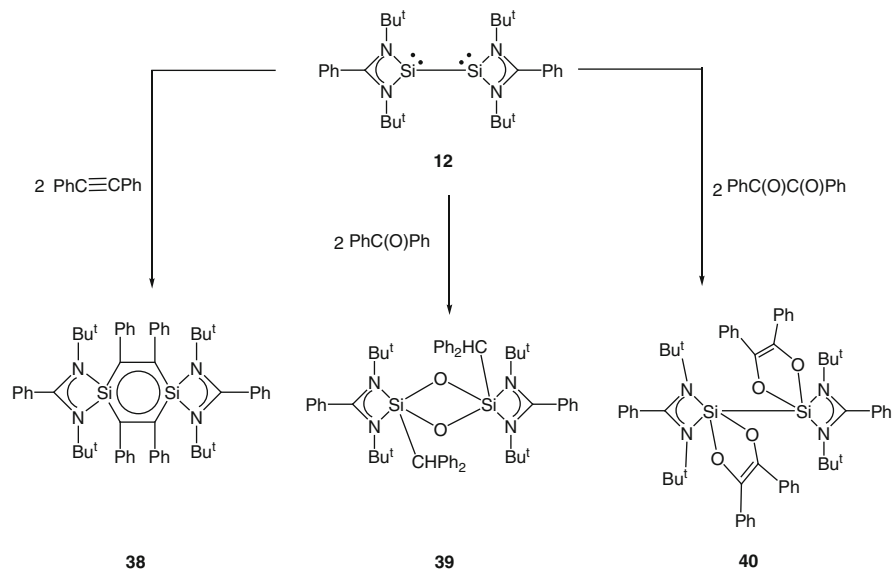
Scheme 5 Activation of diphenylacetylene by NHC **4** resulting in adduct **34**, which upon further reaction with another equivalent of **4** results in the dinuclear compound **35**



Scheme 6 Activation of benzophenone and benzil by NHC **4**

The fascinating reactivity of benzophenone and benzil towards NHC **4** has recently been reported by Roesky and co-workers [32]. Reaction of **4** with benzophenone results via [1 + 2] cycloaddition in the first example of a siloxirane **36** with a three-membered SiOC ring (Scheme 6). Moreover, the reaction with equimolar amounts of benzil led to the formation of **37** by way of a [1 + 4] cycloaddition reaction in good yield (Scheme 6).

The related Si(I) dimer (**12**) (for an excellent, detailed and up-to-date review on the reactivity of interconnected bis-silylenes such as **12**, see [33]) can also activate



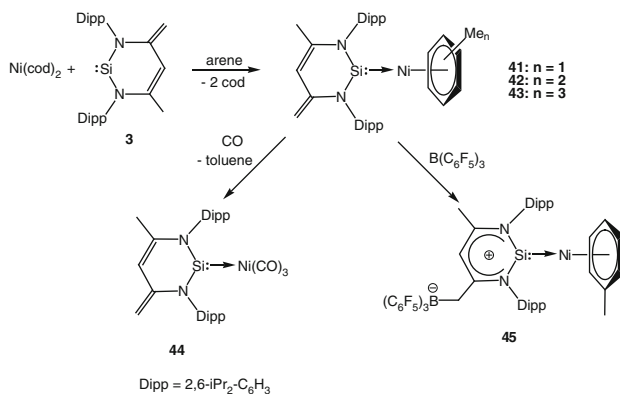
Scheme 7 Selected reactivity studies of the dinuclear Si(I) compound **12**

acetylenes as highlighted by its reaction with two molar equivalents of diphenylacetylene, resulting in a disilabenzene (**38**) [34]. The NICS value was calculated at -3.6 ppm for the ring system, presenting some indication of aromatic character. The reactions of **12** with benzophenone and benzil have also been reported, resulting in the former case in an interesting oxo-bridged dimer system (**39**) and in the latter case by way of a [1 + 4] cycloaddition reaction to give the adduct **40** (Scheme 7) [35].

3 *N*-heterocyclic Silylene (NHSi) Transition Metal Complexes and Their Reactivity^b

We have recently (2012) comprehensively reviewed all NHSi transition metal complexes, where we showed that a large array of NHSi complexes from group 4 to group 10 now exist [38, 39]. In this section we will limit the discussion to recent and representative examples of NHSi complexes that have been implicated in catalytic transformations, or interesting small molecule activation reactions over the last few years.

^b We concentrate the discussion on NHSi transition metal complexes and omit, for the sake of brevity, neutral or cationic silylene complexes of the type $\text{LnM} = \text{SiR}_2$. For excellent reviews on these complexes, see: [36, 37]



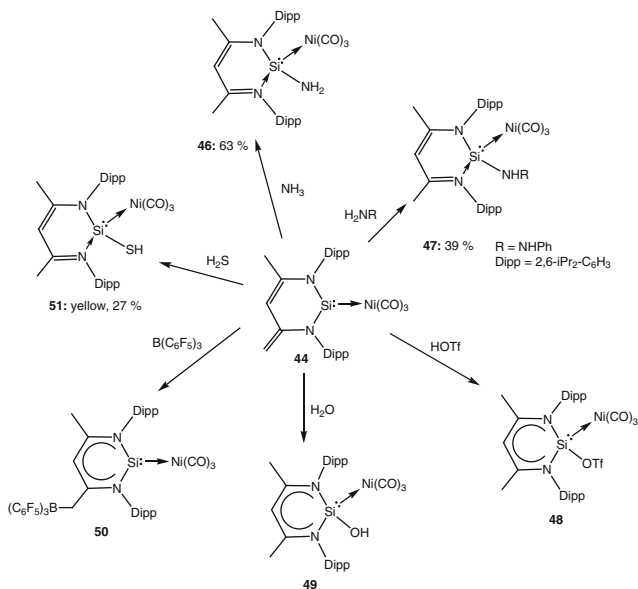
Scheme 8 NHSi-Ni(0) complexes based on the zwitterionic NHSi **3**

In 2009 the latent ability of the zwitterionic NHSi **3** to coordinate with Ni(0) upon reaction with the precursor Ni(cod)₂ in aromatic solvents, resulting in (η⁶-arene)Ni NHSi complexes **41–43** (Fig. 4b), was shown [40, 41]. These complexes have proven to readily exchange the η⁶-arene for three CO ligands upon reaction with CO, resulting in **44**. Moreover, reaction with the Lewis acidic borane B(C₆F₅)₃ resulted in **45** (Scheme 8), by attack of the Lewis acid in the 4-position of the ligand backbone, in analogy with the reaction of the same borane with silylene **3**.

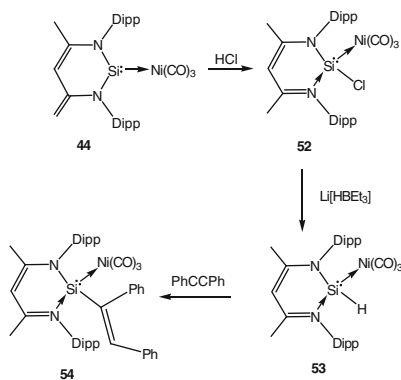
The complex **44** was found to be an excellent starting material for a wide range of further small molecule activation reactions (Scheme 9) [42, 43]. In general, owing to the presence of the protecting Ni(CO)₃ group, a 1,4-addition pattern is observed over the Si(II) centre upon reaction with substrates as exemplified by products **46–51**. This is in contrast to the reactivity of small molecules with the free silylene (*vide supra*) which can exhibit 1,1-addition chemistry (for example, the activation of NH₃). These findings emphasise the different reactivity pattern of NHSi **3** induced by coordination with a transition metal fragment.

A further highlight in the reactivity of **44** is its ability, after suitable synthetic modification, to stoichiometrically effect the hydrosilylation of alkynes (Scheme 10) [44, 45]. In this instance, reaction of **44** with HCl initially affords **52**, which by treatment with Li[HBEt₃] can be readily converted to **53**. The hydrido-NHSi complex **53** serves as an ideal starting material for the hydrosilylation of alkynes, resulting for example, in product **54**.

Some interesting NHSi complexes have also been useful in a variety of catalytic reactions, as opposed to stoichiometric transformations, outlined above. A good example is the bis-NHSi complex **55** (Fig. 5) which can be prepared by reaction of NHSi **9** with in situ generated (η⁵-cyclopentadienyl)cobalt(0). The complex **55** was shown to be catalytically active in the [2 + 2 + 2] cyclootrimerisation of substituted alkynes (Scheme 11).



Scheme 9 Activation of various small molecules using the NHSi-Ni complex **44**, showcasing its 1,4-addition reactivity pattern in contrast to the “free” NHSi, **3** which can also exhibit a 1,1-addition over the Si(II) centre



Scheme 10 Hydrosilylation with an alkyne using the hydrido-NHSi complex **53**

A further, seminal example of catalytic activity associated with NHSi complexes is that of Fürstner and co-workers, who reported a rare example of a dinuclear Pd-NHSi complex prepared by the treatment of **1** with $\text{Pd}(\text{PPh}_3)_4$ affording $[\text{Pd}_2(\mu^2\text{-1})_2(\text{PPh}_3)_2]$ (**56**) (Fig. 6) [46]. The latter was found to be effective in the Suzuki coupling of aryl boronic acids with bromoarenes (Scheme 12).

Roesky and co-workers have reported a Pd-based NHSi complex obtained by reaction of NHSi **1** with the Pd precursor, $[\text{Pd}(\eta^3\text{-C}_3\text{H}_5)\text{Cl}]_2$ affording the

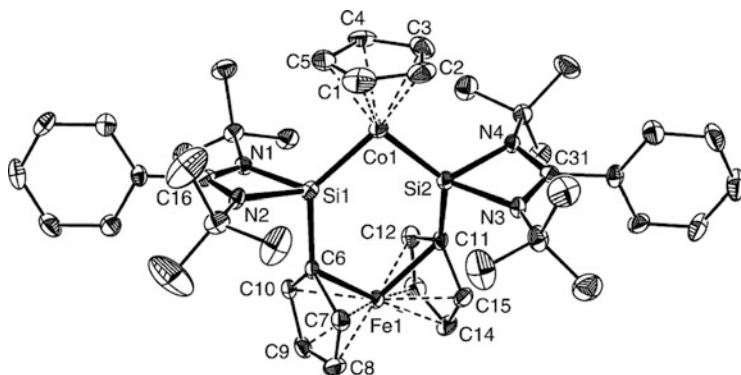
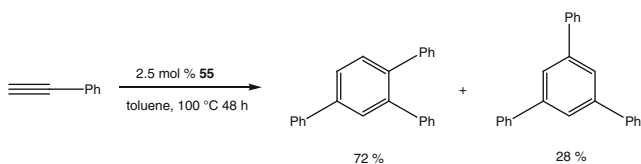


Fig. 5 ORTEP representations of the solid-state structure of complex **55**, active in the cyclotrimerisation of substituted alkynes. Thermal ellipsoids are set at 50%; H atoms have been omitted for clarity



Scheme 11 Catalytic trimerisation of substituted alkynes using the pre-catalyst **55**

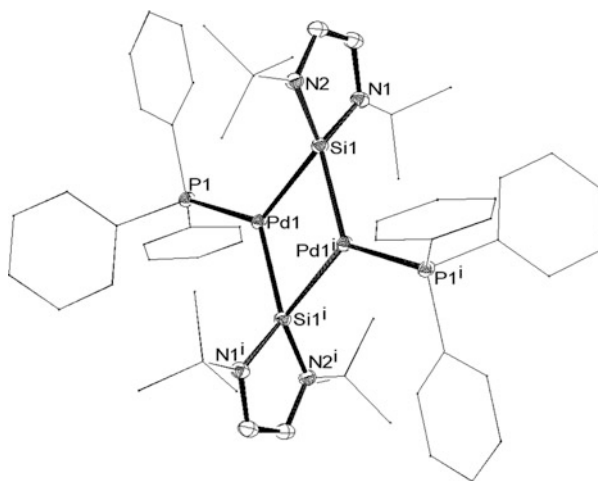
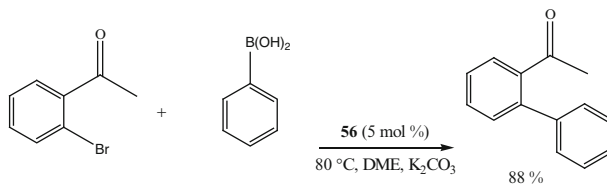
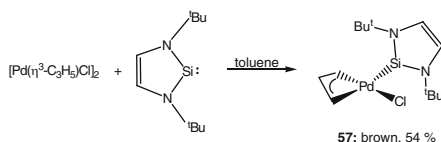


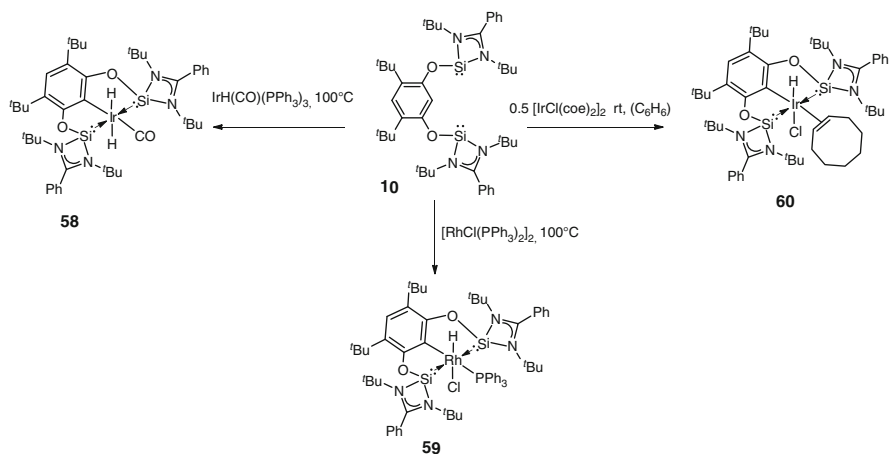
Fig. 6 ORTEP representations of the solid-state structures of the dinuclear Pd complex **56**. Thermal ellipsoids are set at 50%; H atoms have been omitted for clarity; *t*Bu and phenyl groups are represented by wire-frame



Scheme 12 Catalytic activity of Pd complex **56** by Fürstner and co-workers



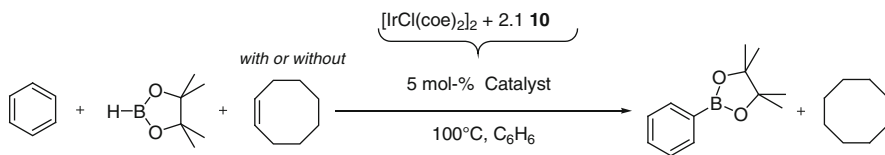
Scheme 13 Synthesis of square-planar NHSi-Pd complex **57** which is suitable for Heck coupling of styrene and bromoacetophenone



Scheme 14 Synthesis of novel pincer-type Si(II) or Ge(II) ligand systems and their reactivity toward Ir and Rh precursors

mononuclear complex $[\text{PdCl}(\eta^3\text{-C}_3\text{H}_5)(\mathbf{1})]$ (**57**), found to be effective in the Heck coupling of styrene and bromoacetophenone, further showcasing the potential of these complexes [47] (Scheme 13).

Finally, very recently we reported the use of the pincer ligand system **10** which upon reaction with various group 10 precursors result in Ir- and Rh-based NHSi complexes (Scheme 14), which are catalytically active. These complexes catalytically affect the C–H borylation of arenes with pinacolborane (Scheme 15) [48, 49]. The main aspect of this work is a comparison to analogous and established



Scheme 15 Catalytic C–H hydroborylation of arenes with pinacolborane with in situ generated **60** as pre-catalyst

P(III) donor systems, where it can readily be shown that the novel Si(II) and Ge(II) pincer systems are much better σ donor ligands, thereby tuning catalytic activity.

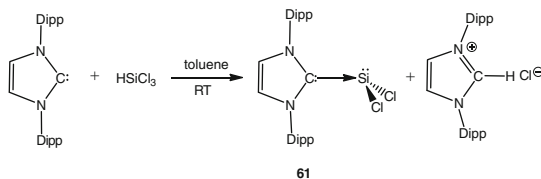
4 Base-Stabilised Silylenes of the Type: $\text{SiR}_2\leftarrow\text{:B}$

Silylenes of this type are reviewed in detail elsewhere in this book. This serves only as a brief summary to put these developments into context with respect to other silylenes. The independent and simultaneous reports of Filippou and co-workers [50] and Roesky's group [51] in 2009 showed that facile entry to such silylenes are indeed possible. The $\text{NHC} \rightarrow \text{SiCl}_2$ (**61**) was synthesised in a straightforward manner as shown in Scheme 16.

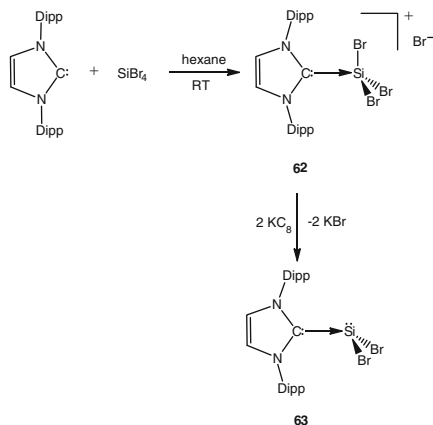
Filippou and co-workers successfully isolated the dibromo analogue of **61**, using a different and equally elegant synthetic approach. In their report, reaction of the NHC directly with SiBr_4 afforded a Si(IV) intermediate **62** which upon reduction with KC_8 afforded the desired NHC-silylene complex **63** with concomitant KBr loss (Scheme 17).

Filippou and co-workers later also showed that it is possible to stabilise silylenes of the type $\text{NHC} \rightarrow \text{Si}(\text{Cl})\text{Ar}$ (Ar = sterically demanding aryl substituent; NHC = *N*-heterocyclic carbene) [52]. In their 2010 report, Silanes of the type SiCl_2HAr (Ar = 2,6- $\text{R}_2\text{C}_6\text{H}_3$; R = Trip = 2,4,6-*i*- $\text{Pr}_3\text{C}_6\text{H}_2$ OR R = Mes = 2,4,6- $\text{Me}_3\text{C}_6\text{H}_2$) [53, 54] were reacted with the NHC (Im-Me₄) elegantly affording the desired NHC-stabilised arylsilylenes (**64** and **65**) and Im-Me₄-HCl (Scheme 18).

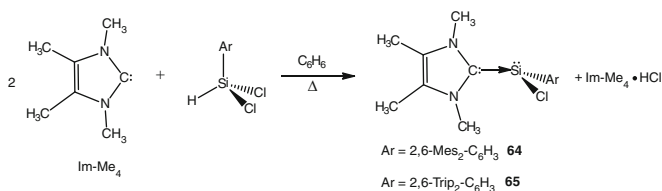
Arylchlorosilylene complex **65** paved the way for the isolation of the first neutral metal complex featuring a triple bond between a transition metal atom and silicon (Tilley and co-workers reported $[\text{CpMo}(\text{dmpe})\text{H} \equiv \text{Si-Mes}]$ (dmpe = 1,2-bis(bimethylphosphino)ethane) as a complex with “considerable silylidyne character” in 2003, but the possibility of an interaction between the H and the Si atom could not be entirely excluded. See: [55]). Although various examples of complexes featuring transition metals participating in a triple bond interaction with the heavy homologues of Ge, Sn and Pb exist (See as examples: [56–63]), no examples for Si existed until 2010. However, by using **65** as a suitable Si(II) precursor, via an NHC-stabilised intermediate **66**, Filippou and co-workers succeeded in 2010 in the isolation of the first silylyne (also called silylidyne) complex (**67**) (Scheme 19) [61, 62].



Scheme 16 Access to the first dichlorosilylene-NHC complex **61**. (Dipp = 2,6-diisopropylphenyl)



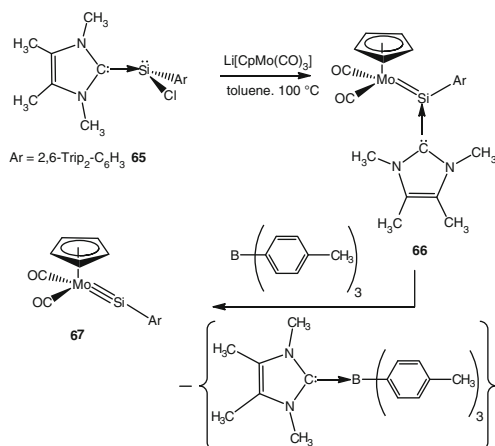
Scheme 17 Synthetic approach to the first example of a dibromosilylene stabilised by an NHC (**63**). (Dipp = 2,6-diisopropylphenyl)



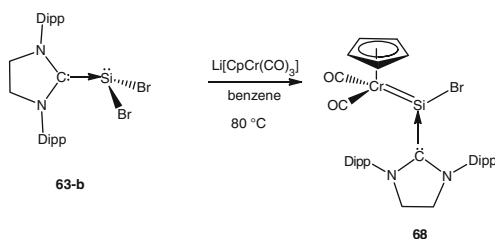
Scheme 18 Synthetic approach to the successful isolation of NHC-stabilised arylsilylene chlorides **64** and **65**

Finally an NHC-stabilised dibromosilylene, similar to **63** with the exception that the NHC is saturated in the backbone (**63-b**), has also been reported to engage in interesting chemistry with Cr precursors [64]. Accordingly, reaction of this silylene with $\text{Li}[\text{CpCr}(\text{CO})_3]$ afforded the novel halo-substituted NHC-stabilised silylene complex $[\text{Cp}(\text{CO})_2 = \{\text{SiBr}(\text{SIDipp})\}]$ (**68**) with concomitant LiBr formation (Scheme 20).

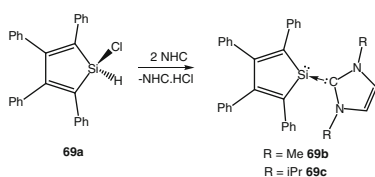
More recently, Cui and co-workers have also reported some rare examples of silylenes belonging to this class (**69b** and **69c**) in Scheme 21 [65].



Scheme 19 Successful entry to the first silylene complex of a transition metal (**67**), accessible by using the silylene precursor **65**



Scheme 20 Synthetic access to the novel halo-substituted NHC-stabilised silylene Cr complex **68** by salt metathesis with Li[CpCr(CO)₃]



Scheme 21 Dehydrohalogenation approach to novel base-stabilised silol-1-ylidenes **69b, c**, and the concomitant reactivity towards phenylacetylene-affording **69d**

5 Carbocyclic Silylenes

Silylenes belonging to this class, as with those discussed in the previous section, are far scarcer compared to NHSis. The obvious reason for this, again, is the lack of π -donation from flanking N-atoms bearing lone pairs, which can stabilise the Si(II) centre. In fact, only three examples of silylenes in this class have been reported to

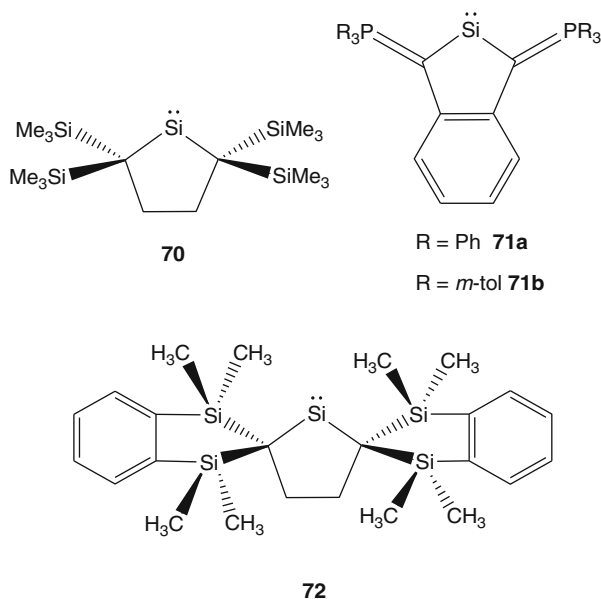


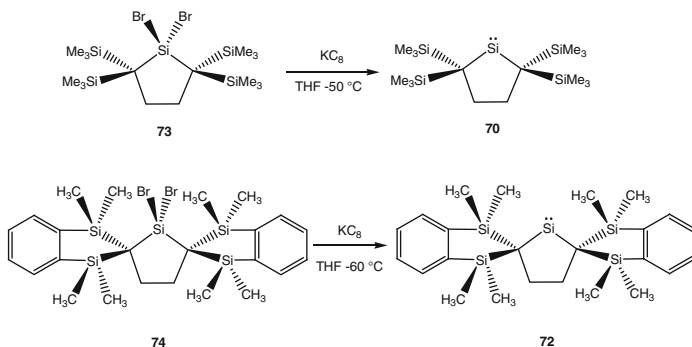
Fig. 7 Rare examples of carbocyclic silylenes reported to date

date. Kira and co-workers were the first to report a carbocyclic silylene – a dialkylsilylene 2,2,5,5-tetrakis(trimethylsilyl)silacyclopentane-1,1-diyl (**70**) as early as 1999 [66]. From our own group, we recently reported the syntheses of aromatic phosphorus ylide-stabilised carbocyclic silylenes, (**71a** and **71b**) [67], and even more recently Iwamoto and co-workers reported another rare example of a silylene in this class (**72**) [68], similar to the seminal example by Kira (Fig. 7).

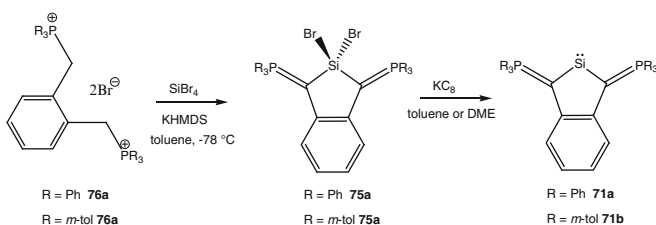
Carbocyclic silylene **70** was prepared by reduction using KC_8 as gentle reagent, starting from the corresponding dibromosilane **73** in a straightforward manner and isolated as orange crystals in 75% yield. The silylene **72** was prepared in an analogous way from dibromosilane **74** (Scheme 22). The silylenes **71a** and **71b** were also accessed by reductive KC_8 dehalogenation from the corresponding dibromosilanes **75a** and **75b**. The latter were prepared from the corresponding bisphosphonium dibromide salts **76a** and **76b** (Scheme 23).

Silylene **70** was found on the basis of a single-crystal X-ray diffraction analysis to exist in the solid state in monomeric form, while, interestingly, silylene **72** is found to exist either in monomeric form or as dimer (disilene) **77**. Recrystallisation of a sample of **72** in fact yields both products, the monomer as yellow (**72**) and the dimer (**77**) as red crystals. On the basis of NMR and UV–vis studies, it was found that in solution, an equilibrium between **72** and **77** exists (Scheme 24; Fig 8).

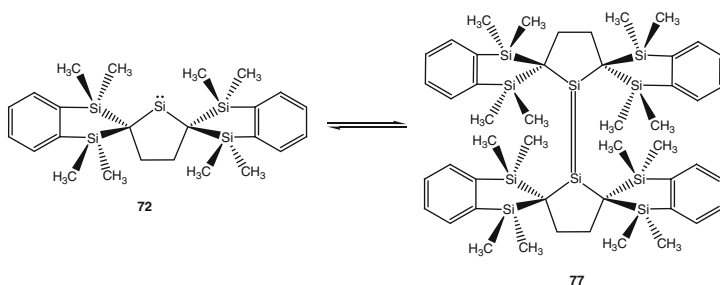
The phosphorus ylide-stabilised silylenes **71a** and **71b** were spectroscopically characterised and confirmed on the basis of trapping experiments. Reactions with 3,5-di-*t*-Bu-*o*-benzoquinone in THF in both cases resulted in the [4 + 1] respective cycloaddition adduct, which has been observed as a hallmark reactivity of



Scheme 22 Synthesis of carbocyclic silylenes **70** and **72** by reductive dehalogenation of the corresponding bromosilanes **73** and **74**, respectively



Scheme 23 Synthesis of carbocyclic silylenes **71a** and **71b**



Scheme 24 Solution equilibrium between the monomeric silylene **72** and the dimeric form (disilene) **77**

silylenes [69]. Detailed DFT investigations on **71a** were additionally carried out to further characterise the bonding situation in the molecule.

The HOMO in **71a** is comprised of ten electrons which includes the P–C ylide bonds (Fig. 9). This orbital is comparable with the HOMO of the unsaturated NHSi (**1**) by Denk [70, 71]. The [HOMO-1] orbital is also a π -bonding type orbital of the ring system, while the lone pair on the silicon atom is reflected by the [HOMO-2] orbital.

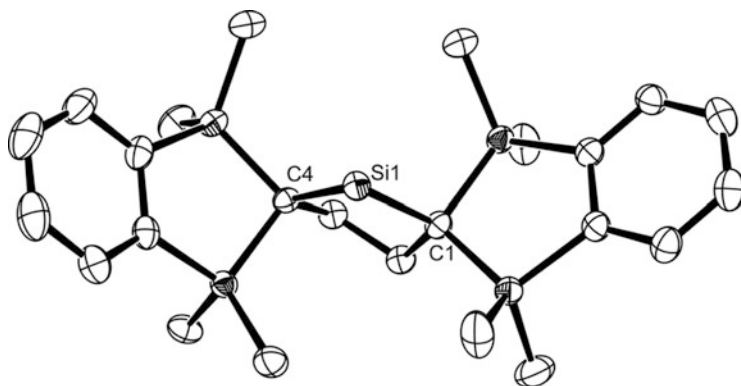


Fig. 8 ORTEP representation of carbocyclic silylene **72**. Thermal ellipsoids are set at 50% probability level; H atoms have been omitted for clarity

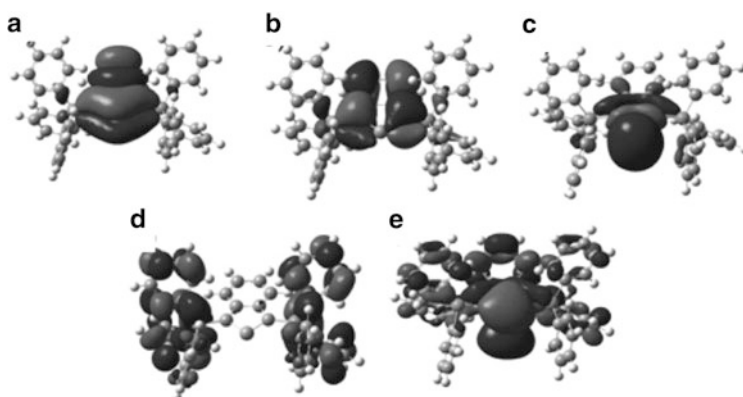
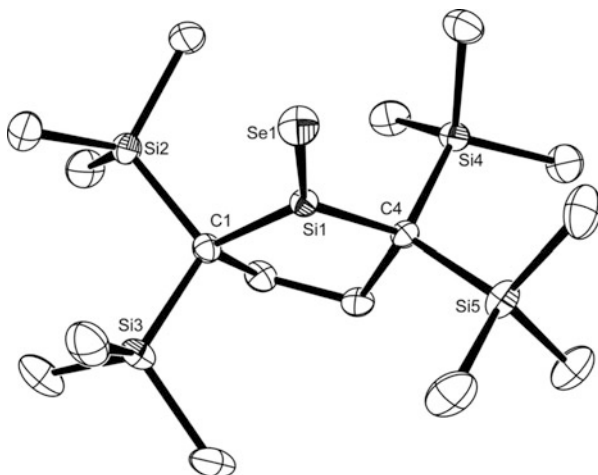


Fig. 9 Calculated molecular orbitals of silylene **71a** [HF/6-311G(d)//B3LYP/6-31G(d)]. (a) HOMO, (b) [HOMO-1], (c) [HOMO-2], (d) LUMO, (e) [LUMO + 8] (adapted from [67] with permission from the authors)

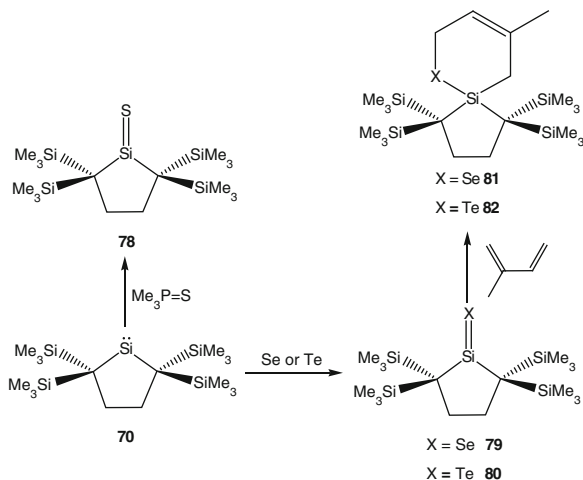
This is in contrast to NHSis which generally have this orbital as the HOMO-1, most likely due to the stabilisation of the lone pair by the π -system. Another difference is the LUMO, which for NHSis exhibit significant π character located to a large extent at the Si centre. The LUMO of **71a** is constricted to the triphenylphosphine substituents.

Although carbocyclic silylenes are rare, at least in the case of the silylene by Kira (**70**), extensive reactivity studies have been reported over the last 13 years. (For an excellent review on silylene **70** and its reactivity up until 2007, see: [72].) This has enabled vast insights into the reactivity and behaviour of silylenes of this class towards a plethora of small molecule activation reactions, or interesting

Fig. 10 ORTEP representation of the silaselone **79**, showing the non-planarity of the SiC₄ ring and the Si=Se bond. Thermal ellipsoids are set at 50% probability level; H atoms have been omitted for clarity



Scheme 25 Chalcogen activation by carbocyclic silylene **70** and emerging [2 + 4] cycloaddition behaviour of **79** and **80** towards isoprene

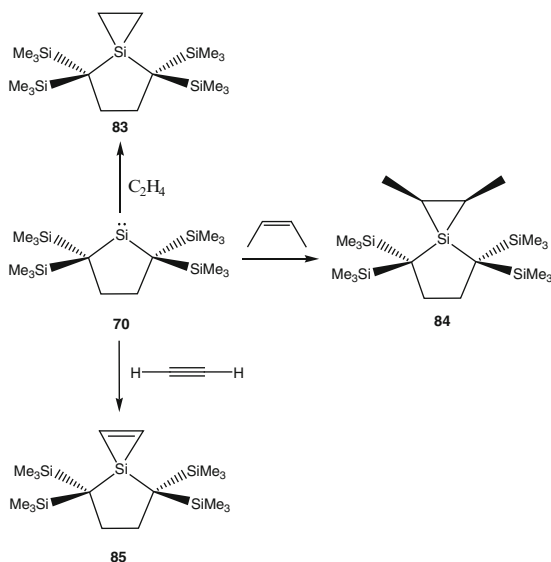


chemical transformations. We will now highlight some selected reactivity investigations of silylene **70** that have appeared in recent years.

The first examples of dialkylsubstituted silicon double bonds to chalcogen atoms (S, Se and Te) were shown to be easily accessible by reaction of **70** with $\text{Me}_3\text{P}=\text{S}$; elemental selenium or elemental tellurium, respectively [73]. These reactions lead from good to excellent yields in the silanethione $\text{L}_\text{H}\text{Si}=\text{S}$ (**78**) (72%) (L_H = ring cycle attached to Si in **70**), silaselone $\text{L}_\text{H}\text{Si}=\text{Se}$ (**79**) (92%), and finally silatellone $\text{L}_\text{H}\text{Si}=\text{Te}$ (**80**) (99%), respectively. This report is truly remarkable, since it shows the ability of the silylene **70** to activate the heavier chalcogens in their elemental form (Fig. 10).

The report also highlights the further reactivity of the emerging $\text{LSi}=\text{X}$ ($\text{X} = \text{S}, \text{Se}, \text{Te}$) compounds towards water and methanol, affording $\text{L}_\text{H}\text{Si}(\text{XH})$

Scheme 26 [1 + 2]
Cycloaddition of alkenes
and alkynes with **7**, affording
siliranes and silirenes,
respectively



(OR) R = Me or H. In addition, in the case of **79** and **80**, reaction with isoprene in toluene (100°C) affords the [2 + 4] cycloaddition adducts (**81** and **82**), respectively, in a regiospecific manner. Scheme 25 provides an overview of these reactions.

The [1 + 2] cycloaddition behaviour of **70** towards a variety of alkenes and alkynes has also been reported (Scheme 26) [74]. The reactions of **70** with ethylene, for example, afford silirane **83** in high yield. Similarly, reaction with Z-2-butene afforded silirane **84**, but due to the substantial steric hindrance in **70**, the analogous reaction with E-2-butene afforded a complex reaction mixture. In analogy, reactions with alkynes afforded silirenes as shown by the reaction of **70** with ethyne, affording silirene **85**. Other examples of alkenes and alkynes are discussed in the same report, all leading to [1 + 2] rather than [1 + 4] cycloaddition products.

The ability of **70** to activate sterically demanding organic isocyanides of the type RNC (R = Dipp or adamantyl), affording silaketenimines with strong allenic character was also reported in 2006 by Kira and co-workers [75]. Tokitoh and co-workers reported a series of silaketenimines of the type R'₂Si ← CNR'' (R' and R'' = bulky substituents) in 2003 but concluded that these are best described on the basis of their spectroscopic and theoretical work as silylene isocyanide complexes [76]. The reaction of silylene **70** with RNC (R = Dipp) afforded the allenic silaketenimines L_HSi=C=N-Dipp (**86**), in analogy with the reaction with RNC (R = adamantyl) affording L_HSi=C=N-Ad (**87**). The single-crystal X-ray data of **86** and **87** revealed C–N bond distances that were rather longer than typical C–N triple bonds, and Si–C bond lengths that were typical of silaethenes, providing evidence for the allenic structure (Fig. 11).

Moreover, their computational investigations reveal a dependence on the nature of the substituents on the N and Si atoms as to whether the emerging compound will

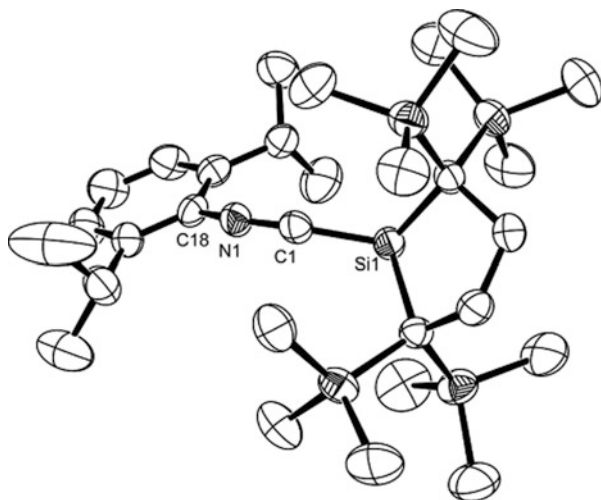


Fig. 11 ORTEP representation of **86**. Thermal ellipsoids are set at 50% probability level; H atoms have been omitted for clarity

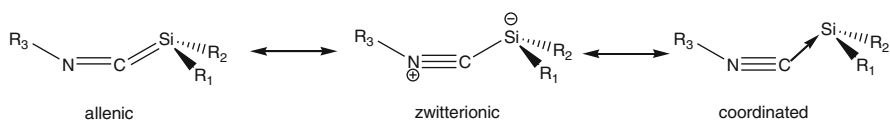
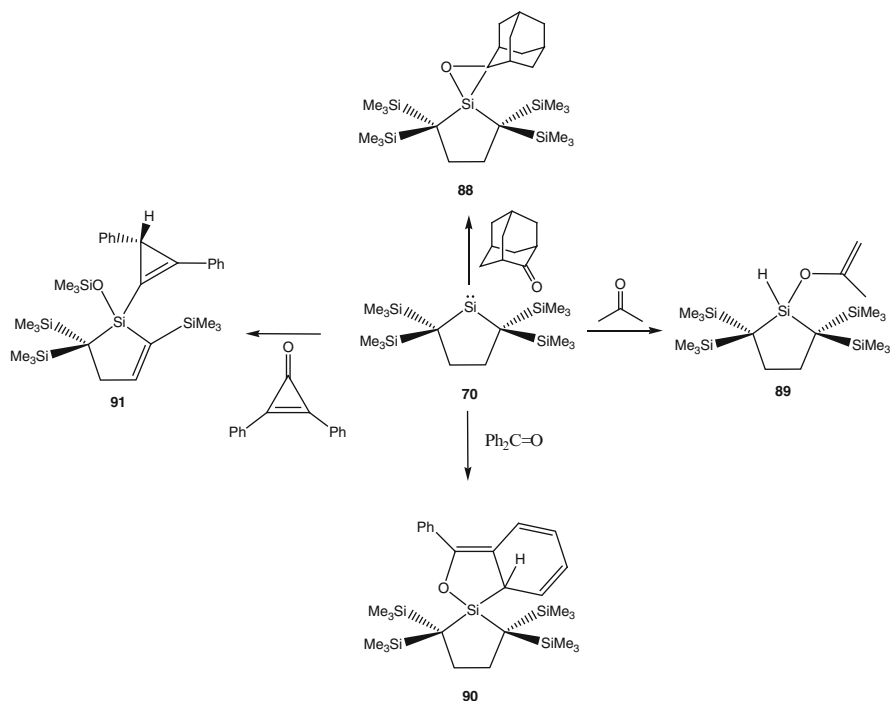


Fig. 12 Resonance forms of silaketenimines found to be dependent on the nature of the substituents (R_1 – R_3)

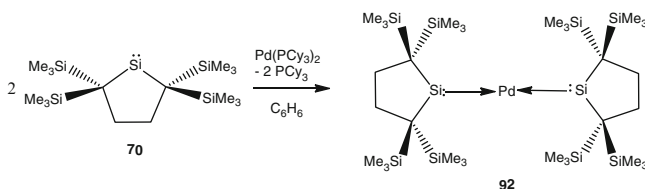
be allenic, zwitterionic or simply coordinated isocyanide, as in the case of Tokitoh's examples. In general, (*N*-aryl)diarylsilaketenimines are zwitterionic, while (*N*-alkyl)dialkylsilaketenimines are rather allenic in nature (Fig. 12).

A more recent study exploring the reactivity of carbocyclic silylene **70** with a variety of ketones was published in 2010, further showcasing its rich and diverse chemistry [77]. In this context, reaction of **70** with adamantone, acetone, benzophenone and finally cyclopropanones yielded siloxirane (**88**), silyl enol ether (**89**), 2-oxa-silacyclopentene (**90**) and cyclopropenylsilares (**91**), respectively, in each instance in a relatively selective way (Scheme 27).

The ability of silylene **70** to coordinate transition metals was first reported in 2008 [78]. In this report, it was stated that the reaction of two equivalents of **70** with $[\text{Pd}(\text{PCy}_3)_2]$ afforded the 14 electron Pd complex **92** (Scheme 28). The X-ray structure of **92** revealed a linear arrangement of the two silylene ligands with a Si1-Pd-Si2 angle of $179.28(4)^\circ$. Both silicon centres are planar, as evidenced by the sum of angles around them approximating 360° . The two silylene ligands are orientated in an orthogonal manner relative to each other, which is likely due to the steric strain associated with the SiMe_3 groups.



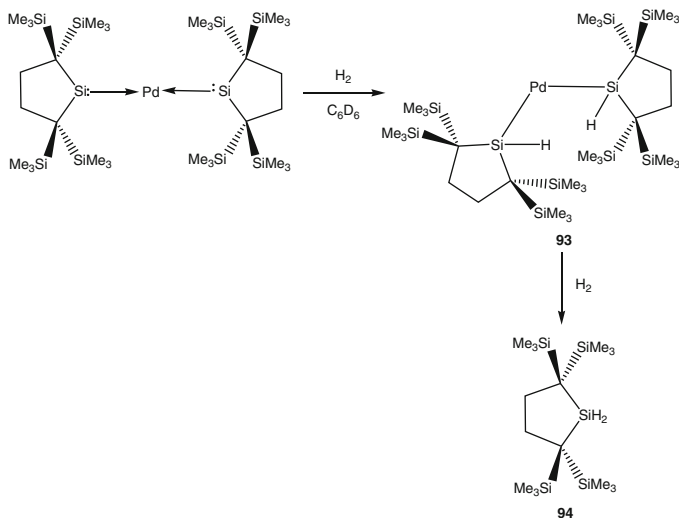
Scheme 27 Reactivity of carbocyclic silylene **70** towards various ketones, yielding an interesting array of different products, depending on the nature of the ketone employed



Scheme 28 Synthesis of the 12 valence electron Pd(0) complex **92**

Of particular interest in this report is the ability of complex **92** to activate H_2 at ambient conditions affording a bis(hydrosilyl)palladium complex (**93**) in high yield (84%) (Scheme 29). Complex **93** is remarkable in that it is the first example of a 12 valence electron Pd complex and that it exhibits a bent geometry around the Pd centre. Further reaction of **93** with H_2 results in the formation of dihydrosilane **94** in near quantitative yields (97%).

Kira and his group also more recently revealed the potential of **70** to coordinate with nickel and platinum (and other palladium) complexes, affording a further array of group 10 complexes bearing electron-rich phosphane ligands or arenes as supporting ligands [79].

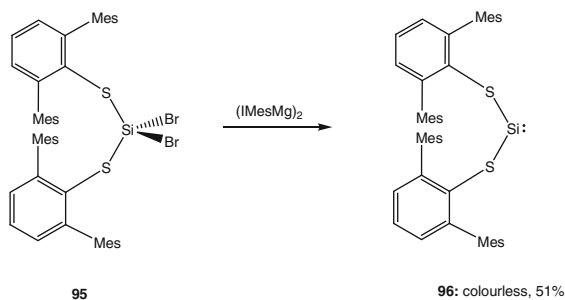


Scheme 29 H₂ activation mediated by complex **92** affording the unprecedented 12 valence electron Pd complex **93**. Further reaction of **93** with H₂ affords **94**

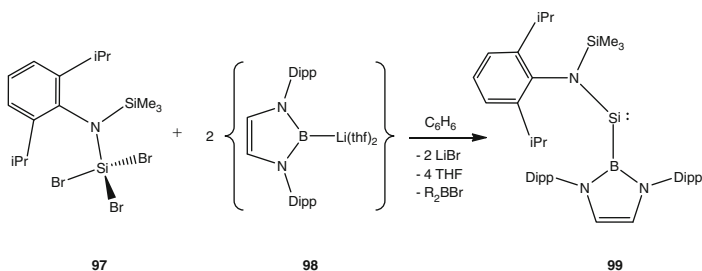
6 Acyclic Silylenes Bearing Only σ -bonded Substituents

Silylenes belonging to this class are the rarest silicon(II) compounds. In fact, until 2012 they had only been observed as transient intermediates, generally obtained under photolytic conditions and confirmed to exist on the basis of trapping experiments. Notable earlier examples include the seminal bis(*tri-tert*-butylsilyl) silylene, shown to exist as a triplet in the ground state on the basis of EPR investigations [80]; or the earlier reported singlet bis(diisopropylamino)silylene [81]. Other seminal examples include Mes₂Si: [82] and Trip₂Si: [83] which are only stable until 77 K and have been characterised by low-temperature UV–vis spectroscopy. The observation of a triplet ground state in the transient bis(*tri-tert*-butylsilyl)silylene is noteworthy, since silylenes generally exhibit a singlet ground state. This spectroscopic observation was suggestive that acyclic silylenes might feature an accessible triplet ground state, potentially increasing their reactivity, and opening up new potential to various catalytic and or small molecule activation possibilities, previously exclusively the domain of transition metal complexes. However, until very recently acyclic silylenes have remained elusive and could not be isolated as stable materials at room temperature.

The first reports of isolable silylenes belonging to this class only appeared very recently (for a recent perspective, see: [84]) and was simultaneously reported by Power and co-workers [85] and the groups of Jones, Mountford, Aldridge and Kaltsoyannis [86]. Power's approach employs reduction of the Si(IV) precursor SiBr₂(SAr^{Me}₆)₂ (Ar^{Me}₆ = 2,6-Mes₂-C₆H₃) (**95**) with the use of Jones' mild Mg(I)-Mg(I) reducing agent (IMesMg)₂ [87] affording :Si(SAr^{Me}₆)₂ **96** as a colourless



Scheme 30 Power's approach to accessing an acyclic silylene **96**. Mild reduction using Jones' Mg(I)-Mg(I) reagent for the reduction of Si(IV) precursor **95** to afford the acyclic silylene **96** in moderate yields. (IMes = [(2,4,6-trimethylphenyl)NC(CH₃)₂CH])



Scheme 31 Jones, Mountford, Aldridge and Kaltsoyannis' approach to accessing the acyclic silylene **99** upon reaction of the Si(IV) tribromo precursor **97** with lithium boranide **98**

compound in 51% yield (Scheme 30). Jones and co-workers accessed their amino boryl acyclic silylene by reacting the Si(IV) precursor $\text{SiBr}_3\{\text{N}(\text{tms})(\text{Dipp})\}$ (**97**) with two equivalents of the lithium compound $(\text{thf})_2\text{Li}[\text{B}(\text{NDippCH})_2]$ (**98**) as a nucleophilic source of a boryl group. This procedure afforded the desired silylene: $\text{Si}\{\text{N}(\text{tms})(\text{Dipp})\}[\text{B}(\text{NDippCH})_2]$ (**99**) with concomitant LiBr and $[\text{B}(\text{NDippCH})_2]$ Br formation (Scheme 31).

Even more recently, Jones, Mountford, Aldridge and Kaltsoyannis and co-workers reported a one-pot synthetic route to accessing a silyl-substituted two-coordinate acyclic silylene $:\text{Si}\{\text{N}(\text{Dipp})(\text{tms})\}\{\text{Si}(\text{SiMe}_3)_3\}$ (**100**) [88] obtained by facile reduction of the Si(IV) precursor $\text{SiBr}_3\{\text{N}(\text{Dipp})(\text{tms})\}$ (**102**) with $(\text{thf})_2\text{K}[\text{Si}(\text{SiMe}_3)_3]$ which afforded **100**. Noteworthy is that attempted reduction of **102** with the standard reducing agent KC_8 afforded the dinuclear species $\{\text{N}(\text{Dipp})(\text{tms})\}\text{SiBr}_2\text{-Br}_2\text{Si}\{\text{N}(\text{Dipp})(\text{tms})\}$ (**103**).

Single-crystal X-ray diffraction investigations of the silylenes **96**, **99** and **100** were also carried out. The most important feature of these three compounds is the observation that bonding angles formed by the central Si atom and its two substituents are rather bent (Figs. 13 and 14).

Fig. 13 ORTEP representation of **96**. Thermal ellipsoids are set at 50% probability level; H atoms have been omitted for clarity. The acute S1–Si–S2 bond angle of $90.519(19)^\circ$ is clearly visible

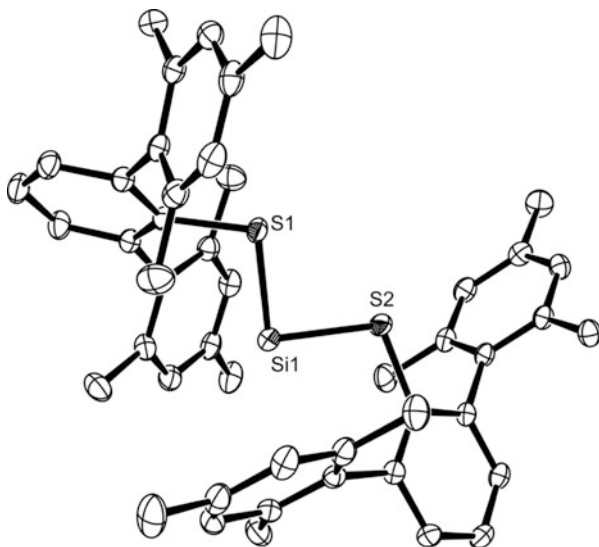
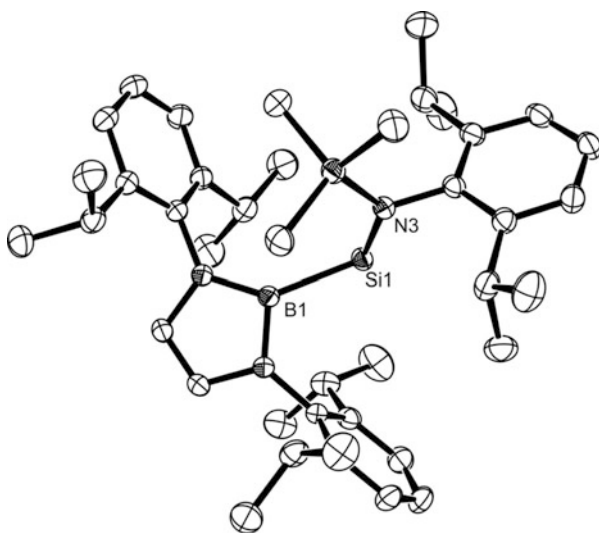


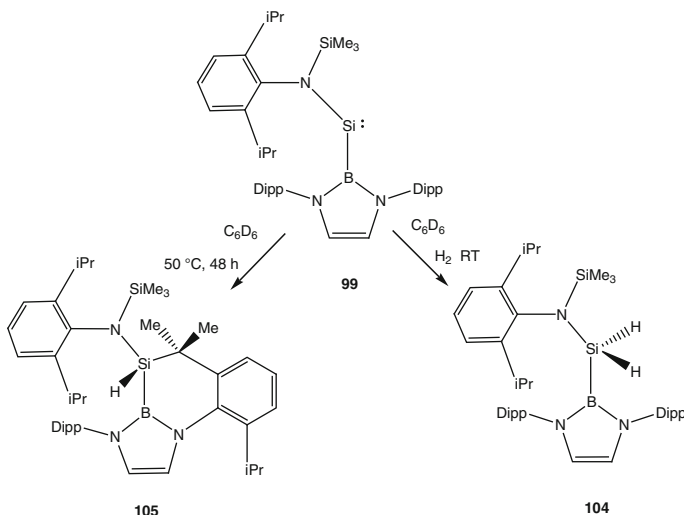
Fig. 14 ORTEP representation of **99**. Thermal ellipsoids are set at 50% probability level; H atoms have been omitted for clarity. The acute B1–Si1–N3 bond angle of $118.1(1)^\circ$ is clearly visible



An inspection of the calculated HOMO-LUMO energy gaps in silylenes **96**, **99** and **100** seems to suggest that this parameter is influenced (or dictated) by the size of the angle formed by the two substituents bound to the central silicon(II) atom. Not unexpectedly since an idealised triplet state is linear, the inspection of the experimental and computational results obtained so far reveals that the energy gap decreases as the X–Si–X angle approaches linearity. Moreover, in the case of **99** and **100** the corresponding singlet–triplet energy gaps were also computed and exhibit a rather modest separation in favour of the singlet ground state

Table 1 Summary of HOMO–LUMO values for silylenes **96**, **99** and **100**, their corresponding singlet–triplet gaps and the corresponding X–Si–X bond angles

| Silylene | DFT calculated HOMO–LUMO gap (eV) | Calculated $\Delta E_{S,T}$ (kJ mol ⁻¹) | X–Si–X angle (in the solid state) [°] |
|------------|--------------------------------------|--|--|
| 96 | –4.26 | – | 90.5 |
| 99 | –2.04 | 103.9 | 118.1 |
| 100 | –1.99 | 103.7 | 116.9 |

**Scheme 32** Facile H₂ and C–H bond activation by silylene **99**, affording the products **104** and **105**, respectively

(Early computational work by Apeloig et al. revealed that the singlet–triplet energy gap of acyclic silylenes depends essentially on electronic and steric factors. See: [89]). These results are shown in Table 1.

Strikingly, silylene **99**, as a likely consequence of the relatively small singlet–triplet energy gap, is capable of activating dihydrogen at ambient conditions, and performing activation of alkyl C–H bonds at 50°C. Accordingly, reaction of **99** with H₂ (or HD) affords the dihydrido-silane **104** (Scheme 32), while gentle heating of **99** affords, via an intramolecular C–H bond activation of the C–H bond of one of the the iPr groups of the Dipp ligand, the product **105** (Scheme 32). In close analogy, the related silyl-silylene **100** can also activate H₂ affording the adduct H₂Si{N(Dipp)(tms)}{Si(SiMe₃)₃} (**106**) under analogous reaction conditions and also undergoes an intramolecular C–H bond activation. In contrast, **96** cannot activate H₂ at ambient conditions, and this again is most likely a consequence of a somewhat higher singlet–triplet energy barrier (*vide supra*).

Although an isolable and room-temperature stable acyclic silylene that exists in a triplet ground state has yet to be isolated, the isolation of silylene **96**, **99** and **100**

represents striking milestones along the way to this target. The propensity of the latter two silylenes to activate H₂ or undergo C–H activation is indeed testimony of how tuning the singlet–triplet energy gap is of crucial importance in attaining silylene systems capable of mimicking transition metal-mediated transformations.

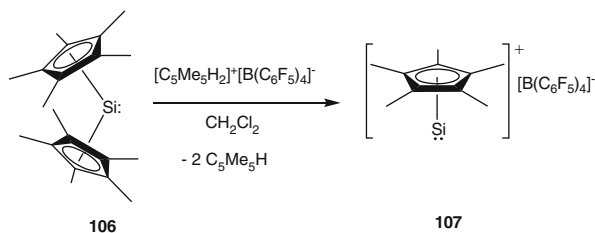
7 Silylenes Bearing π and/or σ -coordinated Ligands

The first isolable Si(II) compound, (η^5 -C₅Me₅)Si: (**106**) was reported in 1986 by Jutzi and co-workers [90, 91]. Compound **106** represents a hypercoordinate electron-rich nucleophilic silylene based on its reactivity towards a range of substrates, which has been vigorously investigated. (For a review on the rich reactivity of decamethylsilicocene up until 2003, see: [92].) Noteworthy is its ability to activate a range of small molecules, particularly electrophilic substrates such as heterocumulenes (CO₂, COS, RNCS, etc.), resulting in reactive intermediates of the type (η^5 -C₅Me₅)Si = X (X = O, X = S) which then undergo further transformations to a range of thermodynamically stable products. The isolation of **106** was indeed a significant milestone in silylene chemistry, and in this section we will discuss its synthetic use in accessing further silylenes bearing either two π -coordinated ligands (such as **106**), or a combination of one π -coordinated and one σ -coordinated substituent on the Si(II) centre.

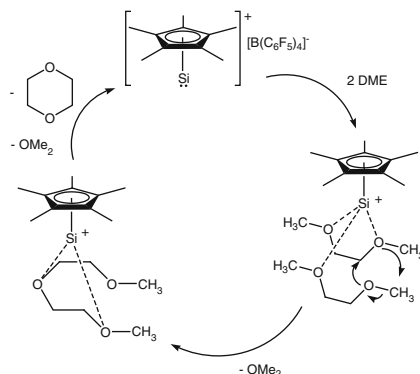
In 2004 Jutzi and co-workers reported the synthesis of the extraordinary silyliumylidene salt [$(\eta^5$ -C₅Me₅)Si:]⁺[B(C₆F₅)₄]⁻ **107** [93]. The elegant synthesis involved the reaction of **106** with the proton transfer reagent [Me₅C₅H₂]⁺[B(C₆F₅)₄]⁻ in dichloromethane which afforded the desired product **107**, with concomitant formation of the two-molar equivalents of C₅Me₅H (Scheme 33).

The synthesis of **107** was found to be anything but trivial, as it was found that the choice of proton source is crucial. The reaction of **106** with HBF₄·OEt₂, for example, afforded the short-lived silylene intermediate SiF(C₅Me₅), which then underwent self-condensation affording a polymer. Moreover, proton transfer to **106** with HBF₄ afforded by way of the dimer species {SiF(C₅Me₅)₂ the same polymer, both results suggesting the necessity of a strictly non-nucleophilic (innocent) anion.

The cation in **107** can be thought of as a stable derivative of the parent silyliumylidene SiH⁺, an extremely reactive species first observed in the 1970s by Douglas and Lutz [94] and later identified in the solar spectrum, and postulated to be an intermediate in space [95]; (For a recent example of a silyliumylidene [ClSi:]⁺ stabilised by a Bis(iminophosphorane) chelate ligand, see: [96]). This makes the isolation of **107** even more remarkable. Noteworthy in terms of applications is the ability of **107** to catalytically convert 1,2-dimethoxyethane (DME) to 1,4-dioxane and dimethyl ether, representing an extremely rare example of a “metal-free” catalytic transformation (Scheme 34) [97]. Furthermore, this process appears to be applicable for a range of oligo(ethylene glycol)diethers, in each case resulting in 1,4-dioxane and dimethyl ether.



Scheme 33 Synthesis of the silyliumylidene salt **107** from silylene **106**



Scheme 34 Proposed catalytic cycle of DME (1,2-dimethoxyethane) to 1,4-dioxane and dimethyl ether, mediated by **107**: A rare example of a “metal-free” catalytic process

Moreover, the salt **107**, upon reaction with $\text{Li}(2,6\text{-Trip}_2\text{-C}_6\text{H}_3)$ [98], results in the heteroleptic silylene: $\text{Si}(2,6\text{-Trip}_2\text{-C}_6\text{H}_3)(\eta^3\text{-C}_5\text{Me}_5)$ (**108**), bearing one π -coordinated and one σ -coordinated substituent, the first such example for silicon [99, 100]. X-ray structural investigations on **108** revealed a bent geometry about the silicon(II) atom, as expected, and metric parameters which are in accord with the Cp^* ring exhibiting a η^3 -coordination mode to the silicon atom. In fact, in comparison with the bent form of decamethylsilicocene (**106**) which features a $\text{Si}(\eta^3\text{Cp}^*)(\eta^2\text{Cp}^*)$ coordination, the η^3 Cp^* ring in **108** is more strongly coordinated with the silicon centre due to the absence of a competing second π -ligand.

Novel imino-substituted silylenes were accessed by Inoue, Jutzi and co-workers using **107** as a suitable starting material. To this end, reaction of **107** with the lithium reagent $\text{Li}[\text{NC}\{\text{N}(\text{Dipp})\text{CH}\}_2]$ [101, 102] afforded the first example of an imino-substituted silylene $:\text{Si}\{(\text{Cp}^*)[\text{NC}\{\text{N}(\text{Dipp})\text{CH}\}_2]\}$ (**109**) [103]. The researchers also showed that the emerging silylene **109** can readily coordinate with the Lewis acidic borane $\text{B}(\text{C}_6\text{F}_5)_3$ affording $(\text{C}_6\text{F}_5)_3\text{B} \leftarrow :\text{Si}\{(\text{Cp}^*)[\text{NC}\{\text{N}(\text{Dipp})\text{CH}\}_2]\}$ (**110**), a rather rare example of a silylene borane adduct, and further evidence of the potential coordination ability of **109**. The X-ray structural investigation revealed again a bent geometry on the silicon(II) centre and additionally confirmed the η^2 -coordination of the Cp^* ring, based on the bond distances (Fig. 15; Scheme 35).

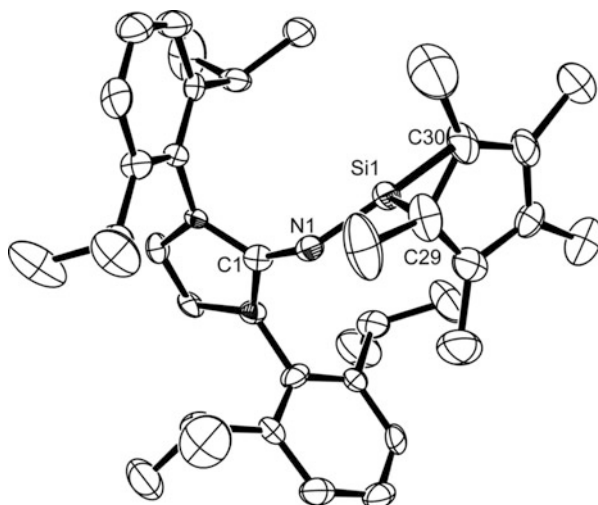
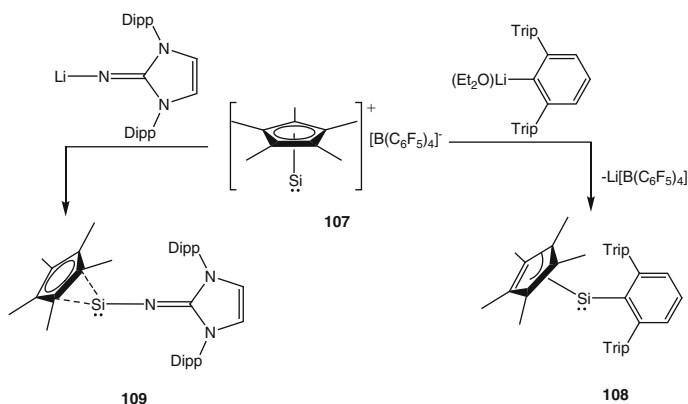


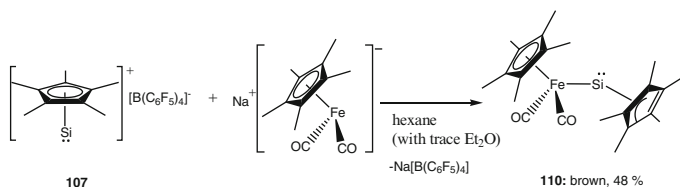
Fig. 15 ORTEP representation of **109** showing η^2 -coordination of the Cp* ring. Thermal ellipsoids are set at 50% probability level; H atoms have been omitted for clarity



Scheme 35 Synthesis of the novel silylenes **108** and **109** using the versatile salt **107** as a suitable precursor

In 2010, Jutzi and co-workers also reported facile entry to an interesting ferrio-substituted silylene using **107** as starting material [104]. Reaction of **107** with Na $[\text{Fe}(\eta^5\text{-C}_5\text{Me}_5)(\text{CO})_2]$ in hexane afforded, by salt metathesis reaction, the complex $\text{Fe}(\eta^5\text{-C}_5\text{Me}_5)(\text{CO})_2\{\text{Si}(\eta^3\text{-C}_5\text{Me}_5)\}$ (**110**) as a brown solid in 48% yield (Scheme 36).

The X-ray structural investigation of **110** revealed on the basis of bonding distances an η^3 -coordination of the Cp* ring on the silicon centre and a rather bent Fe–Si–Cg bond angle (Cg = centre of gravity of the Cp* ring bound to silicon). This bent angle is suggestive of an accumulation of electron density (a lone pair) on silicon, and hence **110** can be considered a metal (iron) substituted silylene (Fig. 16).



Scheme 36 Access to the Ferrio-substituted acyclic silylene **110**

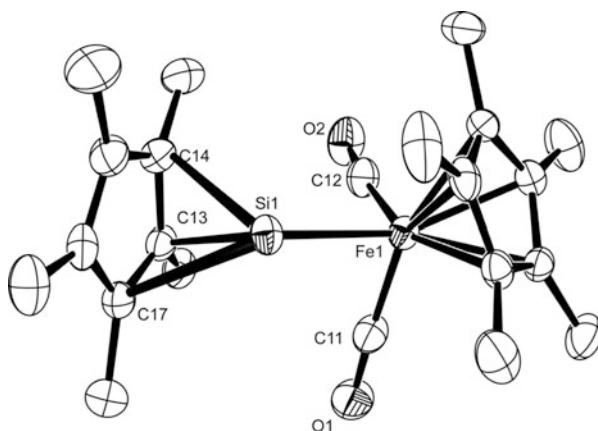


Fig. 16 Molecular structure of **110** showing η^3 -coordination of the Cp* ring with the silicon centre. Thermal ellipsoids are set at 50% probability level; H atoms have been omitted for clarity

107 has also been employed very recently in the preparation of the first cyclotrisilene with exclusively carbon-based substituents by Scheschkewitz, Jutzi and co-workers [105]. In this instance, salt metathesis of **107** with the lithium disilene $(\text{Trip})_2\text{Si} = \text{Si}(\text{Trip})(\text{Li}\{\text{dme}\}_2)$ (**111**) afforded a mixture containing 85% of the cyclotrisilene (**112**). The subsequent reaction of **112** with an NHC afforded the NHC adduct (**113**) which could additionally be characterised by X-ray diffraction analysis. Of particular interest is the observation that NHC complex formation is reversible on the basis of VT-NMR studies, with an enthalpy of dissociation at 298 K estimated at 9 kJ mol^{-1} .

8 Summary, Conclusions, Outlook

Staggering progress has been made in the last decade in the pursuits of isolating new classes of silylenes and elucidating their reactivity patterns, particularly with respect to activation of small molecules, and their ability to coordinate to transition metal centres. Of the various silylene sub-classes, *N*-heterocyclic silylenes (NHSis)

have enjoyed considerable attention and are by far the most intensively studied to date and have shown a remarkable ability to activate small molecules. Moreover, they have shown to be important ligands in transition metal chemistry, enabling a range of new and exciting catalytic and stoichiometric transformations. Carbocyclic silylenes, in contrast, are still rather rare, but the seminal example from Kira's group has shown it to be a potential "workhorse" for a wider range of transformations. Our contribution of phosphorus ylide-stabilised silylenes is a new addition to this class of silylenes, and progress in this area will certainly continue in the future. Roesky's and Filippou's important contributions with the synthesis of the first base-stabilised acyclic silylenes also represent a new sub-class of silylenes and have already highlighted their synthetic use, particularly in the isolation of novel transition metal complexes featuring formal triple bonding to silicon atoms. These fundamental discoveries pave the way for novel further transition metal-mediated transformations. Silylenes bearing π -bonded substituents, particularly pioneered by Jutzi and colleagues, have also proven to be an indispensable class of silylenes. The most recent and particularly promising new research direction is that of the recently reported isolable acyclic silylenes by Power, Jones, Aldridge and others. These indeed show promising reactivity patterns as, for example, the facile activation of dihydrogen at ambient conditions. The isolation of a room-temperature stable triplet ground state silylene is potentially very close. This discovery might open up new vistas in metal-free catalysis which remains a "holy grail" in contemporary main group chemistry. The coming years will no doubt witness further riveting advances in silylene chemistry.

Acknowledgements We are grateful to the Cluster of Excellence "Unicat" (sponsored by the Deutsche Forschungsgemeinschaft (DFG) and administered by the TU Berlin) and the Normalverfahren of the DFG (DR 17-2) for financial support. We also acknowledge Dr S. Yao and Prof Dr S. Inoue for useful material in the preparation of this chapter. We also thank L. van Hoepen for proofreading the final draft.

References

1. Skell PS, Goldstein EJ (1964) Silacyclopropanes. *J Am Chem Soc* 86:1442
2. Denk M, Lennon R, Hayashi R, West R, Belyakov AV, Verne HP, Haaland A, Wagner M, Metzler N (1994) Synthesis and structure of a stable silylene. *J Am Chem Soc* 116:2691
3. Driess M, Yao S, Brym M, van Wüllen C, Lentz D (2006) A new type of N-heterocyclic silylene with ambivalent reactivity. *J Am Chem Soc* 128:9628
4. So CW, Roesky HW, Magull J, Oswald RB (2006) Synthesis and characterization of [PhC(N*t*-Bu)₂]SiCl: a stable monomeric chlorosilylene. *Angewandte Chemie* 118:4052
5. So CW, Roesky HW, Magull J, Oswald RB (2006) Synthesis and characterization of [PhC(N*t*-Bu)₂]SiCl: a stable monomeric chlorosilylene. *Angew Chem Int Ed* 45:3948
6. Sen SS, Roesky HW, Stern D, Henn J, Stalke D (2010) High yield access to silylene RSiCl (R = PhC(N*t*-Bu)₂) and its reactivity toward alkyne: synthesis of stable disilacyclobutene. *J Am Chem Soc* 132:1123

7. Wang W, Inoue S, Irran E, Driess M (2012) Synthesis and unexpected coordination of a silicon(II)-based SiCSi pincerlike arene to palladium. *Angewandte Chemie* 124:3751; *Angewandte Chemie International Edition* 51:3691
8. Wang W, Inoue S, Yao S, Driess M (2012) An isolable bis-silylene oxide ("Disilylenoxane") and its metal coordination. *J Am Chem Soc* 132:15890
9. Wang W, Inoue S, Enthaler S, Driess M (2012) Bis(silylenyl)- and bis(germylenyl)-substituted ferrocenes: synthesis, structure, and catalytic applications of bidentate silicon (II)-cobalt complexes. *Angew Chem Int Ed* 51:6167
10. Kong L, Zhang J, Song H, Cui C (2009) N-aryl substituted heterocyclic silylenes. *Dalton Trans* 28:5444
11. Zark P, Schäfer A, Mitra A, Haase D, Saak W, West R, Müller T (2010) Synthesis and reactivity of N-aryl substituted N-heterocyclic silylenes. *J Organomet Chem* 695:398
12. Sen S, Jana A, Roesky HW, Schulzke C (2009) A remarkable base-stabilized bis(silylene) with a silicon(I)-silicon(I) bond. *Angew Chem Int Ed* 48:8536-8538
13. Gau D, Rodriguez R, Kato T, Affon-Merceron CA, Cossío FP, Baceiredo A (2011) A synthesis of a stable disilyne bisphosphine adduct and its non-metal-mediated CO₂ reduction to CO. *Angew Chem Int Ed* 50:1092
14. Junold K, Baus JA, Burschka C, Tacke R (2012) Bis[N, N'-diisopropylbenzamidinato(-)] silicon(II): A Silicon(II) compound with both a bidentate and a monodentate amidinato ligand. *Angewandte Chemie* 124:7126
15. Ding Y, Roesky HW, Noltemeyer M, Schmidt HG, Power PP (2001) Synthesis and structures of monomeric divalent germanium and tin compounds containing a bulky diketiminato ligand. *Organometallics* 20:1190
16. Driess M, Yao S, Brym M, van Wuelen C (2006) Low-valent silicon cations with two-coordinate silicon and aromatic character. *Angew Chem Int Ed* 45:6730
17. Wang RH, Su MD (2008) Theoretical investigations of the reactivities of cationic six-membered carbene analogues of group 14 elements. *J Phys Chem A* 112:7689
18. Jana A, Schulzke C, Roesky HW (2009) Oxidative addition of ammonia at a silicon(II) center and an unprecedented hydrogenation reaction of compounds with low-valent group 14 elements using ammonia borane. *J Am Chem Soc* 131:4600
19. Jana A, Roesky HW, Schulzke C, Samuel PP (2009) Insertion reaction of a silylene into a N-H bond of hydrazine and a [1+4] cycloaddition with diphenyl hydrazone. *Organometallics* 28:6574
20. Präsang C, Stoelzel M, Inoue S, Meltzer A, Driess M (2010) Metallfreie aktivierung von EH₃ (E = P, As) durch ein ylid-artiges silylen und bildung eines donorstabilisierten arasilens mit einer HSi = AsH-untereinheit. *Angewandte Chemie* 122:10199
21. Präsang C, Stoelzel M, Inoue S, Meltzer A, Driess M (2010) Metal-free activation of EH₃ (E = P, As) by an ylide-like silylene and formation of a donor-stabilized arasilene with a HSi-AsH subunit. *Angew Chem Int Ed* 49:10002
22. Yao S, van Wüellen C, Sun XY, Driess M (2008) Dichotome reaktivität eines stabilen silylens gegenüber terminalen alkinen: C-H-insertion oder autokatalytische bildung von silacycloprop-3-en. *Angewandte Chemie* 120:3294
23. Yao S, van Wüellen C, Sun XY, Driess M (2008) Dichotomic reactivity of a stable silylene toward terminal alkynes: facile C-H bond insertion versus autocatalytic formation of silacycloprop-3-ene. *Angew Chem Int Ed* 47:3250
24. Xiong Y, Yao S, Brym M, Driess M (2007) Consecutive insertion of a silylene into the P₄ tetrahedron: facile access to strained SiP₄ and Si₂P₄ cage compounds. *Angew Chem Int Ed* 46:4511
25. Jana A, Samuel PP, Tavčar G, Roesky HW, Schulzke C (2010) Selective aromatic C-F and C-H bond activation with silylenes of different coordinate silicon. *J Am Chem Soc* 132:10164
26. Xiong Y, Yao S, Driess M (2009) Reactivity of a zwitterionic stable silylene toward halosilanes and haloalkanes. *Organometallics* 28:1927

27. Xiong Y, Yao S, Driess M (2010) Unusual [3 + 1] cycloaddition of a stable silylene with a 2,3-diazabuta-1,3-diene versus [4 + 1] cycloaddition toward a buta-1,3-diene. *Organometallics* 29:987–990
28. Xiong Y, Yao S, Driess M (2009) Versatile reactivity of a zwitterionic isolable silylene toward ketones: silicon-mediated, regio- and stereoselective C–H activation. *Chemistry* 15:5545
29. Xiong Y, Yao S, Driess M (2009) An isolable NHC-supported silanone. *J Am Chem Soc* 131:7562–7563
30. Xiong Y, Yao S, Driess M (2010) Synthesis and rearrangement of stable NHC → silylene adducts and their unique reactivity towards cyclohexylisocyanide. *Chemistry* 5:322
31. Yao S, Xiong Y, Driess M (2010) N-heterocyclic carbene (NHC)-stabilized silanechalcohenones: NHC→Si(R₂)E (E = O, S, Se, Te). *Chemistry* 16:1281
32. Ghadwal RS, Sen SS, Roesky HW, Granitzka M, Kratzert D, Merkel S, Stalke D (2010) Convenient access to monosilicon epoxides with pentacoordinate silicon. *Angew Chem Int Ed* 49:3952
33. Sen SS, Khan S, Nagendran S, Roesky HW (2012) Interconnected bis-silylenes: a new dimension in organosilicon chemistry. *Acc Chem Res* 45:578
34. Sen SS, Roesky HW, Meindl K, Stern D, Henn J, Stückl AC, Stalke D (2010) Synthesis, structure, and theoretical investigation of amidinatosupported 1,4-disilabenzene. *Chem Commun* 46:5873
35. Sen SS, Tavcar G, Roesky HW, Kratzert D, Hey J, Stalke D (2010) Synthesis of a stable four-membered Si₂O₂ ring and a dimer with two four-membered Si₂O₂ rings bridged by two oxygen atoms, with five-coordinate silicon atoms in both ring systems. *Organometallics* 29:2343
36. Lickiss PD (1992) Transition metal complexes of silylenes, silenes, disilenes and related species. *Chem Soc Rev* 21:271
37. Waterman R, Hayes PG, Tilley TD (2007) Synthetic development and chemical reactivity of transition-metal silylene complexes. *Acc Chem Res* 40:712
38. Blom B, Stoelzel M, Driess M (2013) New vistas in N-heterocyclic silylene (NHSi) transition-metal coordination chemistry: syntheses, structures and reactivity towards activation of small molecules. *Chemistry* 19:1
39. Blom B, Stoelzel M, Driess M (2013) New vistas in N-heterocyclic silylene (NHSi) transition-metal coordination chemistry: syntheses, structures and reactivity towards activation of small molecules. *Chemistry* 19:40
40. Meltzer A, Präsang C, Milsmann C, Driess M (2009) Bemerkenswerte stabilisierung von Ni(η⁶-Aren)-komplexen durch einen ylid-artigen silylenliganden. *Angewandte Chemie* 121:3216
41. Meltzer A, Präsang C, Milsmann C, Driess M (2009) The striking stabilization of Ni(η⁶-Arene) complexes by an ylide-like silylene ligand. *Angew Chem Int Ed* 48:3170
42. Meltzer A, Präsang C, Driess M (2009) Diketiminat silicon(II) and related NHSi ligands generated in the coordination sphere of nickel(0). *J Am Chem Soc* 131:7232
43. Meltzer A, Inoue S, Präsang C, Driess M (2010) Steering S – H and N – H bond activation by a stable N-heterocyclic silylene: different addition of H₂S, NH₃, and organoamines on a silicon(II) ligand versus its Si(II) → Ni(CO)₃ complex. *J Am Chem Soc* 132:3038
44. Stoelzel M, Präsang C, Inoue S, Enthaler S, Driess M (2012) Hydrosilylierung von alkinen mit einem Ni(CO)₃-stabilisierten silicium(II)-hydrid. *Angewandte Chemie* 124:411
45. Stoelzel M, Präsang C, Inoue S, Enthaler S, Driess M (2012) Hydrosilylation of alkynes by Ni(CO)₃-stabilized silicon(II) hydrid. *Angew Chem Int Ed* 51:399
46. Fürstner A, Krause H, Lehmann CW (2001) Preparation, structure and catalytic properties of a binuclear Pd(0) complex with bridging silylene ligands. *Chem Commun* 2001:2372
47. Zhang M, Liu X, Shi C, Ren C, Ding Y, Roesky HW (2008) The synthesis of (η³-C₃H₅)Pd{Si[N(tBu)CH]₂}Cl and the catalytic property for Heck reaction. *Zeitschrift für anorganische und allgemeine Chemie (Journal of Inorganic and General Chemistry)* 634:1755

48. Brück A, Gallego D, Wang W, Irran E, Driess M, Hartwig JF (2012) Forcieren der σ -donorstärke in iridium-pinzettenkomplexen: bis(silylen)- und bis(germylen)-liganden sind stärkere donoren als bis[phosphor(III)]-liganden. *Angewandte Chemie* 124:11645
49. Brück A, Gallego D, Wang W, Irran E, Driess M, Hartwig JF (2012) Pushing the σ -donor strength in iridium pincer complexes: bis(silylene) and bis(germylene) ligands are stronger donors than bis(phosphorus(III)) ligands. *Angew Chem Int Ed* 51:11478
50. Filippou AC, Chernov O, Schnakenburg G (2009) SiBr₂(Idipp): a stable N-heterocyclic carbene adduct of dibromosilylene. *Angewandte Chemie* 121:5797
51. Ghadwal RS, Roesky HW, Merkel S, Henn J, Stalke D (2009) Lewis base stabilized dichlorosilylene. *Angewandte Chemie* 121:5793
52. Filippou AC, Chernov O, Blom B, Stumpf KW, Schnakenburg G (2010) Stable N-heterocyclic carbene adducts of arylchlorosilylenes and their germanium homologues. *Chemistry* 16:2866
53. Simons RS, Haubrich ST, Mork BV, Niemeyer M, Power PP (1998) The syntheses and characterization of the bulky terphenyl silanes and chlorosilanes 2,6-Mes₂C₆H₃SiCl₃, 2,6-Trip₂C₆H₃SiCl₃, 2,6-Mes₂C₆H₃SiHCl₂, 2,6-Trip₂C₆H₃SiHCl₂, 2,6-Mes₂C₆H₃SiH₃, 2,6-Trip₂C₆H₃SiH₃ and 2,6-Mes₂C₆H₃SiCl₂SiCl₃. *Main Group Chem* 2:275
54. Weidemann N, Schnakenburg G, Filippou AC (2009) Neuartige silane mit sterisch anspruchsvollen aryl-substituenten. *Zeitschrift für anorganische und allgemeine Chemie (Journal of Inorganic and General Chemistry)* 635:253
55. Mork BV, Tilley TD (2003) Multiple bonding between silicon and molybdenum: a transition-metal complex with considerable silylyne character. *Angewandte Chemie* 115:371
56. Filippou AC, Portius P, Philippopoulos AI, Rohde H (2003) Dreifachbindung zu zinn: synthese und charakterisierung des stannylidinkomplexes *trans*-[Cl(PMe₃)₄W≡Sn-C₆H₃-2,6-Mes₂]. *Angewandte Chemie* 115:461
57. Filippou AC, Portius P, Philippopoulos AI, Rohde H (2003) Triple bonding to tin: synthesis and characterization of the stannylyne complex *trans*-[Cl(PMe₃)₄W≡Sn-C₆H₃-2,6-Mes₂]. *Angew Chem Int Ed* 42:445
58. Filippou AC, Philippopoulos AI, Schnakenburg G (2003) Triple bonding to tin: synthesis and characterization of the square-pyramidal stannylyne complex cation [(dppe)₂WSn-C₆H₃-2,6-Mes₂] + (dppe=Ph₂PCH₂CH₂PPh₂, Mes=C₆H₂-2,4,6-Me₃). *Organometallics* 22:3339
59. Filippou AC, Rohde H, Schnakenburg G (2004) Triple bond to lead: synthesis and characterization of the plumbilydyne complex *trans*-[Br(PMe₃)₄MoPbC₆H₃-2,6-Trip]. *Angewandte Chemie* 116:2293
60. Filippou AC, Weidemann N, Schnakenburg G, Rohde H, Philippopoulos AI (2004) Tungsten-lead triple bonds: syntheses, structures, and coordination chemistry of the plumbilydyne complexes *trans*-[X(PMe₃)₄WPb(2,6-Trip₂C₆H₃)]. *Angewandte Chemie* 116:6676
61. Filippou AC, Chernov O, Stumpf KW, Schnakenburg G (2010) Metall-silicium-dreifachbindungen: synthese und charakterisierung des silylidin-komplexes [Cp(CO)₂Mo ≡ Si-R]. *Angewandte Chemie* 122:3368
62. Filippou AC, Chernov O, Stumpf KW, Schnakenburg G (2010) Metal-silicon triple bonds: the molybdenum silylydyne complex [Cp(CO)₂Mo ≡ Si-R]. *Angew Chem Int Ed* 49:3296
63. Blom B (2011) Reactivity of ylens at late transition metal centres. Doctoral Dissertation. University of Bonn (Published as a book, Cuvillier Verlag, Göttingen, 2011, ISBN-10: 3869559071)
64. Filippou AC, Chernov O, Schnakenburg G (2011) Chromium Silicon multiple bonds: the chemistry of terminal N-heterocyclic-carbene-stabilized halosilylydyne ligands. *Chemistry* 17:13574
65. Gao Y, Zhang J, Hu H, Cui C (2010) Base-stabilized 1-silacyclopenta-2,4-dienylidenes. *Organometallics* 29:3063
66. Kira M, Ishida S, Iwamoto T, Kabuto C (1999) The first isolable dialkylsilylene. *J Am Chem Soc* 121:9722

67. Asay M, Inoue S, Driess M (2011) Aromatic ylide-stabilized carbocyclic silylene. *Angew Chem Int Ed* 50:9589
68. Abe T, Tanaka R, Ishida S, Kira M, Iwamoto T (2012) New isolable dialkylsilylene and its isolable dimer that equilibrate in solution. *J Am Chem Soc* 134:20029
69. See reference 20 in 67
70. Schleyer PR, Maerker C, Dransfeld A, Jiao H, Hommes NJRE (1996) Nucleus-independent chemical shifts: a simple and efficient aromaticity probe. *J Am Chem Soc* 118:6317
71. Chen Z, Wannere CS, Corminboeuf C, Puchta R, Pvr S (2005) Nucleus-independent chemical shifts (NICS) as an aromaticity criterion. *Chem Rev* 105:3842
72. Kira M, Iwamoto T, Ishida S (2007) A helmeted dialkylsilylene. *Bull Chem Soc Jpn* 80:258
73. Iwamoto T, Sato K, Ishida S, Kabuto C, Kira M (2006) Synthesis, properties, and reactions of a series of stable dialkyl-substituted silicon–chalcogen doubly bonded compounds. *J Am Chem Soc* 128:16914
74. Ishida S, Iwamoto T, Kira M (2011) Addition of a stable dialkylsilylene to carbon–carbon unsaturated bonds. *Heteroatom Chem* 22:432
75. Abe T, Iwamoto T, Kabuto C, Kira M (2006) Synthesis, structure, and bonding of stable dialkylsilylketenimines. *J Am Chem Soc* 128:4228
76. Takeda N, Kajiwara T, Suzuki H, Okazaki R, Tokitoh N (2003) Synthesis and properties of the first stable silylene–isocyanide complexes. *Chemistry* 9:3530
77. Ishida S, Iwamoto T, Kira M (2010) Reactions of an isolable dialkylsilylene with ketones. *Organometallics* 29:5526
78. Watanabe C, Iwamoto T, Kabuto C, Kira M (2008) Fourteen-electron bis(dialkylsilylene) palladium and twelve-electron bis(dialkylsilyl)palladium complexes. *Angew Chem Int Ed* 47:5386
79. Watanabe C, Inagawa Y, Iwamoto T, Kira M (2010) Synthesis and structures of (dialkylsilylene)bis(phosphine)-nickel, palladium, and platinum complexes and (η^6 -arene) (dialkylsilylene)nickel complexes. *Dalton Trans* 39:9414
80. Sekiguchi A, Tanaka T, Ichinohe M, Akiyama K, Tero-Kubota S (2003) Bis(tri-tert-butylsilyl)silylene: triplet ground state silylene. *J Am Chem Soc* 125:4962
81. Tsutsui S, Sakamoto K, Kira M (1998) Bis(diisopropylamino)silylene and its dimer. *J Am Chem Soc* 120:9955
82. West R, Fink MJ, Michl J (1981) Tetramesityldisilene, a stable compound containing a silicon–silicon double bond. *Science* 214:1343
83. Ando W, Fujita M, Yoshida H, Sekiguchi A (1988) Stereochemistry of the addition of diarylsilylenes to cis- and trans-2-butenes. *J Am Chem Soc* 110:3310
84. Driess M (2012) Main group chemistry: breaking the limits with silylenes. *Nat Chem* 4:525
85. Recken BD, Brown TM, Fettinger JC, Tuononen HM, Power PP (2012) Isolation of a stable, acyclic, two-coordinate silylene. *J Am Chem Soc* 134:6504
86. Protchenko AV, Birjkumar K, Dange D, Schwarz AD, Vidovic D, Jones C, Kaltsoyannis N, Mountford P, Aldridge S (2012) A stable two-coordinate acyclic silylene. *J Am Chem Soc* 134:6500
87. Green SP, Jones C, Stasch A (2007) Stable magnesium(I) compounds with Mg–Mg bonds. *Science* 318:1754
88. Protchenko AV, Schwarz AD, Blake MP, Jones C, Kaltsoyannis N, Mountford P, Aldridge S (2013) A generic one-pot route to acyclic two-coordinate silylenes from silicon(IV) precursors: synthesis and structural characterization of a silylsilylene. *Angew Chem Int Ed* 52:568
89. Holthausen MC, Koch W, Apeloig Y (1999) Theory predicts triplet ground-state organic silylenes. *J Am Chem Soc* 121:2623
90. Jutzi P, Kanne D, Krüger C (1986) Decamethylsilicocen – synthese und struktur. *Angewandte Chemie* 98:163
91. Jutzi P, Kanne D, Krüger C (1986) Decamethylsilicocene – synthesis and structure. *Angew Chem Int Ed* 25:164

92. Kühler T, Jutzi P (2003) Decamethylsilicocene: synthesis, structure, bonding and chemistry. *Adv Organometallic Chem* 49:1
93. Jutzi P, Mix A, Rummel B, Schoeller WW, Neumann B, Stammler HG (2004) The $(\text{Me}_5\text{C}_5)\text{Si}^+$ cation: a stable derivative of HSi^+ . *Science* 305:849
94. Douglas AE, Lutz BL (1970) Spectroscopic identification of the SiH^+ molecule: The $\text{A}1\Pi-\text{X}1\Sigma^+$ system. *Can J Phys* 48:247
95. Singh PD, Vanlandingham FG (1978) Line positions and oscillator strengths of rotation-vibration bands of possible interstellar SiH and SiH^+ . *Astronomy Astrophys* 66:87
96. Xiong Y, Yao S, Inoue S, Irran E, Driess M (2012) The elusive silyliumylidene $[\text{ClSi:}]^+$ and silathionium $[\text{ClSiS}]^+$ cations stabilized by bis(iminophosphorane) chelate ligand. *Angew Chem Int Ed* 51:10074
97. Leszczyńska K, Mix A, Berger RJF, Rummel B, Neumann B, Stammler HG, Jutzi P (2011) The pentamethylcyclopentadienylsilicon(II) cation as a catalyst for the specific degradation of oligo(ethyleneglycol) diethers. *Angew Chem Int Ed* 50:6843
98. Schiemenz B, Power PP (1996) Synthesis of sterically encumbered terphenyls and characterization of their metal derivatives $\text{Et}_2\text{OLiC}_6\text{H}_3\text{-2,6-Trip}_2$ and $\text{Me}_2\text{SCuC}_6\text{H}_3\text{-2,6-Trip}_2$ ($\text{Trip} = 2,4,6\text{-i-Pr}_3\text{C}_6\text{H}_2^-$). *Organometallics* 15:958
99. Jutzi P, Leszczyńska K, Neumann B, Schoeller WW, Stammler HG (2009) $[\text{2,6-(Trip)}_2\text{H}_3\text{C}_6](\text{Cp}^*)\text{Si}$, eine stabile monomere arylsilicium(II)-verbindung. *Angewandte Chemie* 121:2634
100. Jutzi P, Leszczyńska K, Neumann B, Schoeller WW, Stammler HG (2009) $[\text{2,6-(Trip)}_2\text{H}_3\text{C}_6](\text{Cp}^*)\text{Si}$: a stable monomeric arylsilicon(II) compound. *Angew Chem Int Ed* 48:2596
101. Tamm M, Petrovic D, Randoll S, Beer S, Bannenberg T, Jones PG, Grunenberg J (2007) Structural and theoretical investigation of 2-iminoimidazolines – carbene analogues of iminophosphoranes. *Org Biomol Chem* 5:523
102. Beer S, Brandhorst K, Hrib CG, Wu X, Haberlag B, Grunenberg J, Jones PG, Tamm M (2009) Experimental and theoretical investigations of catalytic alkyne cross-metathesis with imidazolin-2-iminato tungsten alkylidyne complexes. *Organometallics* 28:1534
103. Inoue S, Leszczyńska K (2012) An acyclic imino-substituted silylene: synthesis, isolation, and its facile conversion into a zwitterionic silaimine. *Angew Chem Int Ed* 51:8589
104. Jutzi P, Leszczyńska K, Mix A, Neumann B, Rummel B, Schoeller W, Stammler HG (2010) Synthesis and characterization of the ferrio-substituted silicon(II) compound $\text{Me}_5\text{C}_5(\text{CO})_2\text{FeSiC}_5\text{Me}_5$. *Organometallics* 29:4759
105. Leszczyńska K, Abersfelder K, Mix A, Neumann B, Stammler HG, Cowley MJ, Jutzi P, Scheschkewitz D (2012) Reversible base coordination to a disilene. *Angew Chem Int Ed* 51:6785

Multiple Bonds with Silicon: Recent Advances in Synthesis, Structure, and Functions of Stable Disilenes

Takeaki Iwamoto and Shintaro Ishida

Abstract In the present chapter, the recent progress in the chemistry of disilenes ($R_2Si=SiR_2$) with functional groups in the last decade will be reviewed. Especially, novel synthetic routes to disilenes via functionalized disilenes and disilynes, as well as structures, properties, and selected new reactivity of disilenes, reported mainly in the last decade will be discussed. Fundamental structural and spectroscopic data of new disilenes reported after 2004 are tabulated at the end of the chapter.

Keywords Disilene · Disilenide · Disilyne · Functional group · Multiple bond · Reactions · Silicon · Structure

Contents

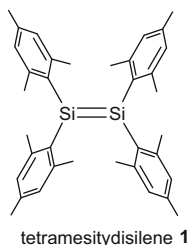
| | | |
|-----|---|-----|
| 1 | Introduction | 127 |
| 2 | Synthesis, Molecular Structure, and Physical Properties | 129 |
| 2.1 | Synthetic Routes to Stable Disilenes | 129 |
| 2.2 | Metal-Substituted Disilenes | 130 |
| 2.3 | Heteroatom-Substituted Disilenes | 133 |
| 2.4 | Disilenes with Functional Organic π -Electron Systems | 141 |
| 2.5 | Conjugated Disilenes | 147 |
| 2.6 | Miscellaneous | 152 |
| 2.7 | Stable Disilynes | 159 |
| 3 | Reactivity | 159 |
| 3.1 | Unimolecular Reactions | 160 |
| 3.2 | Bimolecular Reactions | 165 |
| 4 | Outlook | 172 |
| | References | 197 |

Abbreviations

| | |
|--------------|---|
| 12-crown-4 | 1,4,7,10-Tetraoxacyclododecane |
| 3-MP | 3-Methylpentane |
| Ad | Adamantyl |
| Ar | Aryl |
| Bbp | 2,6-bis[bis(trimethylsilyl)methyl]phenyl |
| Bbt | 2,6-bis[bis(trimethylsilyl)methyl]-4-[tris(trimethylsilyl)methyl]phenyl |
| Bu | Butyl |
| Cp | Cyclopentadienyl |
| Cp* | Pentamethylcyclopentadienyl |
| CV | Cyclic voltammetry |
| Cy | Cyclohexyl |
| d | Day(s) |
| DMAP | 4-(Dimethylamino)pyridine |
| DME | 1,2-Dimethoxyethane |
| Dsi | bis(trimethylsilyl)methyl |
| equiv | Equivalent(s) |
| Et | Ethyl |
| h | Hour(s) |
| HOMO | Highest occupied molecular orbital |
| <i>i</i> -Pr | Isopropyl |
| LDA | Lithium diisopropylamide |
| LUMO | Lowest unoccupied molecular orbital |
| Me | Methyl |
| Mes | Mesityl, 2,4,6-trimethylphenyl |
| min | Minute(s) |
| mol | Mole(s) |
| Naph | Naphthalenide |
| NBS | <i>N</i> -bromosuccinimide |
| NICS | Nucleus-independent chemical shift |
| Np | Neopentyl |
| Nu | Nucleophile |
| Ph | Phenyl |
| py | Pyridine |
| rt | Room temperature |
| <i>s</i> -Bu | <i>sec</i> -Butyl |
| SOMO | Singly occupied molecular orbital |
| Tbt | 2,4,6-Tris{bis(trimethylsilyl)methyl}phenyl |
| <i>t</i> -Bu | <i>tert</i> -Butyl |
| Tf | Trifluoromethanesulfonyl (triflyl) |
| THF | Tetrahydrofuran |
| Tip | 2,4,6-Triisopropylphenyl |
| Tol | 4-Methylphenyl |
| Tsi | Tris(trimethylsilyl)methyl |

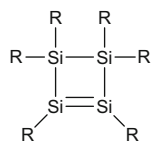
1 Introduction

Since the synthesis of tetramesityldisilene **1** as the first isolable silicon–silicon doubly bonded compound (disilene) was reported as one of the most striking events in the silicon chemistry by West, Fink, and Michl in 1981 [1], the chemistry of stable disilenes ($R_2Si=SiR_2$) as well as silene ($R_2Si=CR_2$) and related multiply bonded silicon compounds represents a thriving field over now more than three decades [2–7].



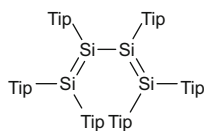
In the first 15 years after 1981, several stable silicon analogs of ethylenes bearing an isolated $Si=Si$ double bond have been synthesized by introduction of bulky groups such as aryl, alkyl, and silyl groups to protect the $Si=Si$ double bond. Fundamentals of molecular structure and bonding, reactivity, and physical properties of the silicon–silicon double bond have been investigated extensively. These studies have shown that typical silicon–silicon double bonds have a nonplanar geometry (normally *trans*-bent), a weak π bond energy ($60\text{--}100\text{ kJ mol}^{-1}$) that is less than those of alkenes ($>200\text{ kJ mol}^{-1}$), and a small $\pi\text{--}\pi^*$ gap ($\sim 3\text{ eV}$) compared with those of the corresponding alkenes ($\sim 6\text{ eV}$) (for instance, $\lambda_{\max}(\pi \rightarrow \pi^*) = 344\text{ nm}$ for $Me_2Si=SiMe_2$ in argon matrix [8], 165 nm for $H_2C=CH_2$). These differences manifest in a considerably higher reactivity toward various small organic and inorganic reagents.

Since the middle of 1990s, the types of compounds with $Si=Si$ double bond gradually increased. Silicon analogs of cyclic alkenes [9], conjugated dienes [10], *spiro*-conjugated dienes [11], and cumulated dienes [12] have been synthesized, taking advantage of the kinetic stabilization provided by bulky substituents. These studies have indicated that silicon–silicon double bond can be involved in the various skeletal structures and suggested that the chemistry of disilenes can be both comparable and complementary to the chemistry of alkenes.



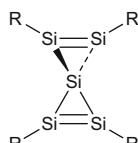
$R = t\text{-BuMe}_2\text{Si}$

cyclic disilene



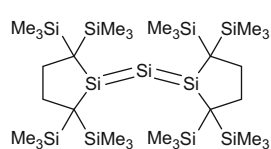
$Tip = 2,4,6\text{-}(i\text{-Pr})_3\text{C}_6\text{H}_2$

conjugated disilene



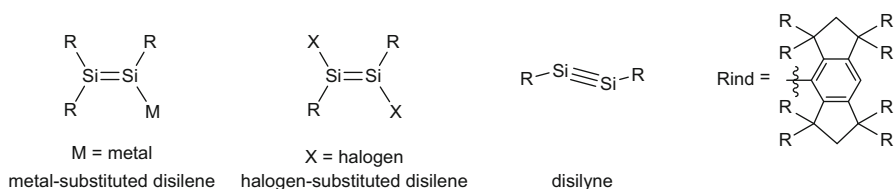
$R = (t\text{-BuMe}_2\text{Si})_3\text{Si}$

spiroconjugated disilene



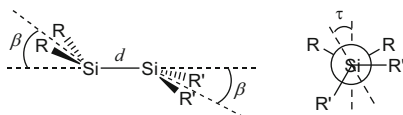
cumulated disilene

In the last decades, the chemistry of disilenes has made further progress. Study of stable multiply bonded compounds with silicon have focused not only on the synthesis of stable multiply bonded compounds with new skeletal structures but also on the exploration of functionalized multiply bonded compounds as “silicon π -electron systems.” The isolable disilenes with functional groups such as alkali metals, transition metals, heteroatom groups, and functional aromatic groups at the unsaturated silicon atoms have been reported. Especially, important contribution to the evolution of the chemistry of disilenes have been made by the successful synthesis and isolation of disilenides as nucleophilic disilenes [13], halodisilenes as electrophilic disilenes [14], and silicon–silicon triply bonded compounds (disilynes) bearing formally two reactive Si=Si double bonds [14–16]. In addition, novel well-designed protecting groups such as Rind groups have become available [17], which enable to synthesis of various functional disilenes.



Although several excellent reviews on stable disilenes involving topics of functionalized disilenes [18] have been already available, in the present chapter, the recent progress in the chemistry of disilenes with functional groups in the last decade will be comprehensively addressed. Especially, new synthetic routes to disilenes by using functionalized disilenes and disilynes, structures, properties, and some new reactivity of the resulting disilenes will be discussed. Although several outstanding reviews on disilynes are also available [5, 19–24], some stable disilynes will also be mentioned as important and useful precursors for functional disilenes.

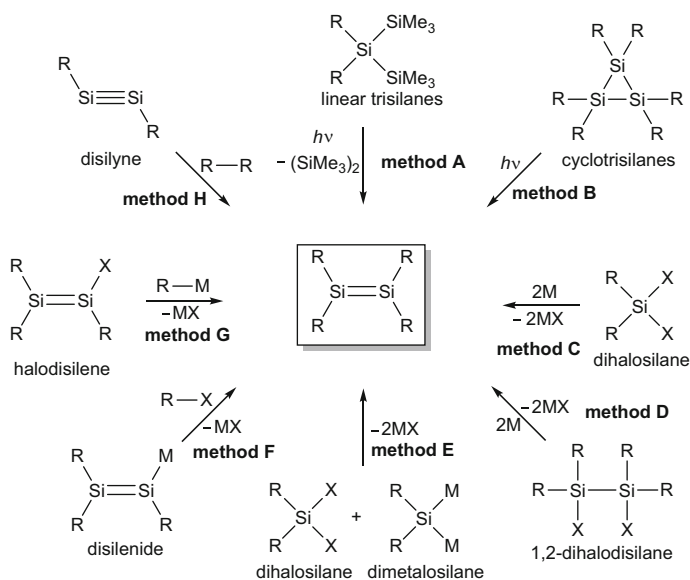
Fundamental structural and spectroscopic data for new disilenes reported up to 2004 were summarized in two comprehensive reviews in *Adv. Organomet. Chem.* series by Okazaki and West in 1996 [2] and Kira and Iwamoto in 2006 [4]. The data of new disilenes reported after 2004 including some which are not mentioned in the main text of this chapter are tabulated at the end of this review (Tables 1–4). This is to complement the data on the Si=Si bond distance (d), bent angle (β) (the angle between the axis through the Si=Si bond and R–Si(sp^2)–R plane), twist angle (τ) (the angle between the two axes that bisect the R–Si(sp^2)–R angles as viewed along the Si=Si axis), absorption maxima, and CCDC numbers (if available).



2 Synthesis, Molecular Structure, and Physical Properties

2.1 Synthetic Routes to Stable Disilenes

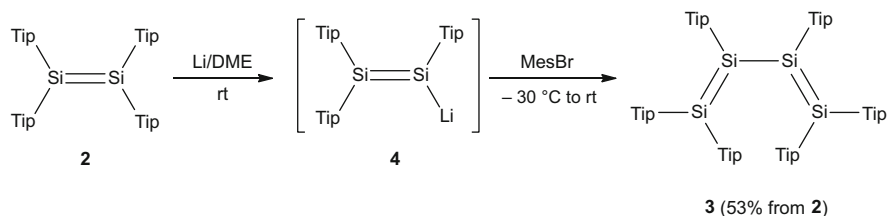
Typical synthetic methods for disilenes are summarized in Scheme 1. Stable disilenes have been synthesized by photolysis of the appropriate linear trisilane (method A), photolysis of the corresponding cyclotrisilane (method B), reductive dehalogenation of dihalosilane (method C), reductive dehalogenation of 1,2-dihalodisilane (method D), and metathesis of 1,1-dihalosilane and 1,1-dimetallated silane (method E). Since 2004, reagents with silicon–silicon multiple bonds such as silicon analogs of vinyl anions (disilenides) and acetylenes (disilynes) have been available and applied for various functionalized disilenes. In addition to the traditional routes to disilenes, substitution at the sp^2 silicon atoms involving reactions of disilenide with electrophiles (method F), reactions of halogen-substituted disilenes with nucleophiles (method G), and 1,2-addition across the silicon–silicon triply bonded compounds (disilynes) (method H) have appeared as useful and versatile ways to disilenes with functional groups. In the following sections, synthesis, molecular structure, and properties of new disilenes with functional groups are summarized.



Scheme 1 Typical synthetic routes to stable disilenes

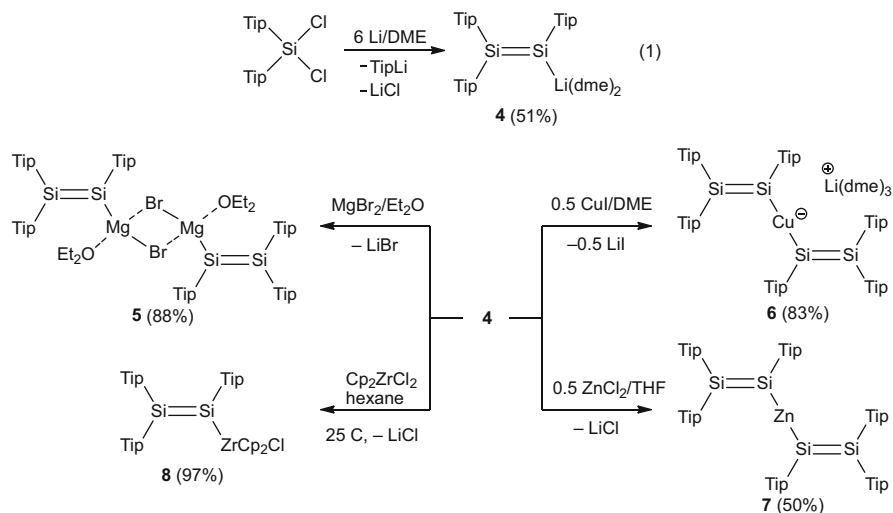
2.2 Metal-Substituted Disilenes

Metal-substituted disilenes (metal disilenides) have been first proposed as a possible intermediate in the reduction of $\text{Tip}_2\text{Si}=\text{SiTip}_2$ **2** with excess lithium giving tetrasila-1,3-diene **3** by Weidenbruch as shown in Scheme 2 [10].



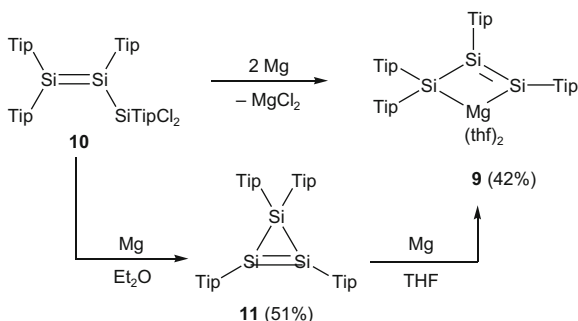
Scheme 2

In 2004, Scheschkewitz obtained the triaryldisilenide **4** as orange crystals of $\text{Tip}_2\text{Si}=\text{SiTipLi}(\text{dme})_2$ in 51% yield by the reduction of $\text{Tip}_2\text{SiCl}_2$ with excess lithium in DME as shown in Eq. (1) [13]. Lithium disilene **4** works as a good precursor for other metal disilenides. For instance, transmetallation gave the corresponding magnesium, copper, and zinc disilenides **5–7** in excellent to moderate yields (Scheme 3) [25]. Metathesis of **4** with Cp_2ZrCl_2 gave the corresponding zirconium disilenide **8** [26]. Chemical shifts of unsaturated ^{29}Si nuclei of $\text{Tip}_2\text{Si}^{\text{A}}=\text{Si}^{\text{B}}(\text{Tip})\text{M}$ type disilenides depend on the metals. The ^{29}Si nuclei bound to metal (Si^{B}) resonate at lower field compared to that to Si^{A} . ($\delta\text{Si}^{\text{A}}$, $\delta\text{Si}^{\text{B}}$ in ppm): (94.5, 100.5) for **4**, (11.3, 59.5) for **5**, (91.8, 93.6) for **6**, (57.48, 107.05) for **7**, and (116.8, 152.5) for **8**.



Scheme 3

As a related species, magnesium trisilene-1,3-diide **9** was synthesized by the reaction of TipCl_2Si -substituted disilene **10**, which was prepared by the reaction of **4** with TipSiCl_3 , with magnesium metal [27]. After detailed investigations, neutral tetrakis(2,4,6-triisopropylphenyl)cyclotrisilene **11** could also be isolated and was proposed as an intermediate during the synthesis of **9** (Scheme 4) [28].

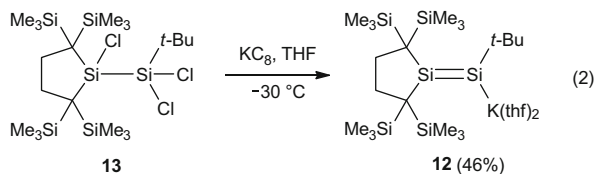


Scheme 4

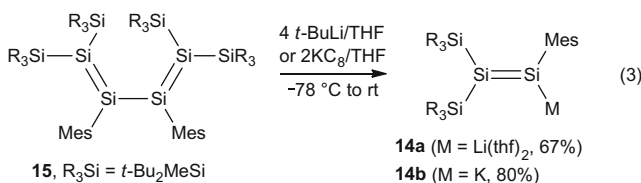
Silicon–silicon double-bond lengths ($d(\text{Si}=\text{Si})$) of Tip-substituted disilenes are 2.1824(5) Å for **5**, 2.1721(12) and 2.1696(11) Å for **6**, 2.198(1) Å for **7**, and 2.1920(6) Å for **4**, which are slightly longer than that of $\text{Tip}_2\text{Si}=\text{SiTip}_2$ **2** (2.144 Å) [29] but within the range of typical double-bond lengths (2.14–2.29 Å) [2, 4]. The $\text{Si}=\text{Si}$ bond length of **8** is significantly longer [2.2144(7) Å] than that in the lithium disilene **4** [2.1920(6) Å], which can be attributed to the electron-deficient 16e zirconium center. The $\text{Si}=\text{Si}$ bond of **8** is considerably twisted with the twist angle (τ) of 20.24°, while both silicon atoms are virtually planar; the sum of angles around silicon atoms are 359.68 (Zr side) and 359.51 (Tip_2Si side).

In UV–vis spectra in hexane, the longest absorption bands of **6** and **7** are observed at 462 and 468 nm, being red-shifted compared to the lithium and magnesium disilenes **4** (417 nm) and **5** (425 nm). These results can be explained by intramolecular orbital interaction between disilene units and the transition metal centers. Zirconium disilene **8** in hexane solution shows a considerable red-shifted absorption band at 715 nm due to ligand (disilene) to metal (zirconium) charge transfer [26].

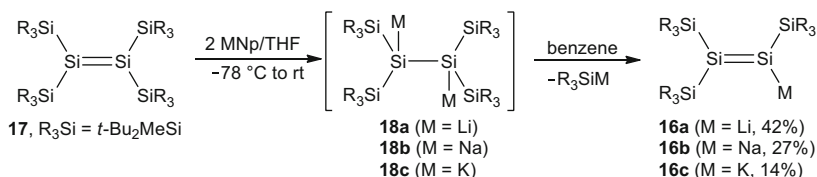
Using a similar reductive dehalogenation, potassium trialkyldisilene **12** was synthesized by the reduction of the corresponding 1,1,2-trichlorodisilane **13** with excess potassium graphite (Eq. 2) [30].



Sekiguchi et al. have reported that lithium disilyaryldisilenide **14a** was synthesized as red crystals in 67% yield together with isobutene by the reaction of the corresponding tetrasilyldiaryltetrasilene-1,3-diene **15** with *t*-BuLi in THF (Eq. 3) [31]. Possible mechanism for formation of **14a** involves single electron transfer giving anion radical of **14a** and *t*-butyl radical followed by the cleavage of the central Si–Si bond. Treatment of **15** with KC_8 gave the corresponding potassium disilenide **14b** in 80% yield [32]. Interestingly, potassium disilenide **14b** has a typical Si=Si double-bond length [2.2114(10) Å] but an unusually large Si=Si–K angle [171.44(4)°] probably due to intramolecular π -coordination of Mes group to the potassium atom.

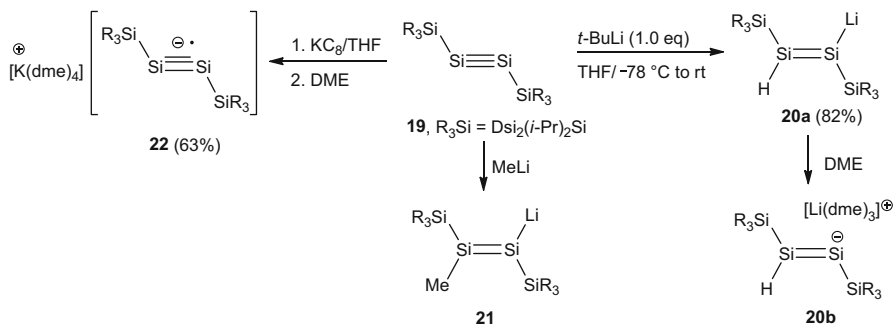


In a more straightforward manner, tris(di-*t*-butylmethylsilyl)disilenides **16a–16c** can also be synthesized as lithium, sodium, and potassium salts by the reduction of tetrakis(di-*t*-butylmethylsilyl)disilene **17** with the corresponding alkali metal naphthalenide in THF followed by exchanging the solvent from THF to benzene (Scheme 5) [33]. Although initial reduction in THF gave the corresponding 1,2-dimetallodisilanes **18a–18c**, which were confirmed by NMR spectroscopy and product analysis after hydrolysis, similarly to the reduction of other tetrasilyldisilenes [34], exchange of the solvent from THF to benzene prompted elimination of *t*-Bu₂MeSiLi to give **16a–16c**. In the ²⁹SiNMR spectra, two signals are observed for the unsaturated ²⁹Si atoms. The chemical shifts of the unsaturated ²⁹Si nuclei are the following: 77.6 and 328.4 ppm for **16a**, 79.5 and 325.6 ppm for **16b**, and 81.7 and 323.1 ppm for **16c**. Low-field shifted signals around 320–330 ppm are assignable to silicon nuclei bonded to M (M = Li, Na, K).



Scheme 5

Sekiguchi and coworkers show that 1,2-addition of metal reagents across the silicon–silicon triple bond in disilyne can also be a good route to metal-substituted disilenes (Scheme 6). For instance, hydrometalation of disilyne **19** with *t*-BuLi in THF gave the corresponding lithium hydridodisilenide **20a** in 82% yield [35]. Disilenide **20a** was isolated as a solvent-separated ion pair form (**20b**) after addition



Scheme 6

of DME. Reaction of **19** with methyllithium gave the corresponding carbometallation product **21** [36]. As a related species, disilyne anion radical **22** was formed by the reduction of disilyne **19** with potassium graphite in 63% yield [35].

In the ^1H NMR spectrum of **20a**, the H(-Si(sp²)) signal is observed at 7.10 ppm with the coupling constant ($^1J_{\text{SiH}}$) of 155 Hz (see also Sect. 2.3.6). In the ^{29}Si NMR spectrum in C₆D₆, the two peaks of **20a** at 124.7 and 165.0 ppm are assignable to the H-substituted Si(sp²) atom and the Li-substituted Si(sp²) atom, respectively. A similar ^{29}Si NMR signals of disilene moiety of **21** in THF-*d*₈ are observed at 114.1 (SiMe) and 143.4 (SiLi) ppm.

ESR spectrum of the radical anion **22** shows a triplet signal (g -factor = 1.99962) with satellites due to two methine ^1H nuclei on *i*-Pr groups, two unsaturated ^{29}Si nuclei ($^{29}\text{Si}^\alpha$), and two ^{29}Si nuclei on Dsi₂(*i*-Pr)Si groups ($^{29}\text{Si}^\beta$). The hyperfine coupling constants (hfcc) are as follows: $a(^1\text{H}) = 0.23$ mT, $a(^{29}\text{Si}^\alpha) = 3.92$ mT, and $a(^{29}\text{Si}^\beta) = 2.24$ mT. These three hfccs indicate that an unpaired electron delocalizes over the R-SiSi-R moiety. The molecular structure of **22** obtained by X-ray crystallography presents (1) a *trans*-bent structure with the Si-Si-R angles of 112.84(6) and 113.97(6)° which are smaller than that of neutral disilyne **19** [137.44(4)°] and (2) a central Si-Si bond length of 2.1728(14) Å, which is longer than that of **19** [2.0622(9) Å], confirming the antibonding nature of the SOMO.

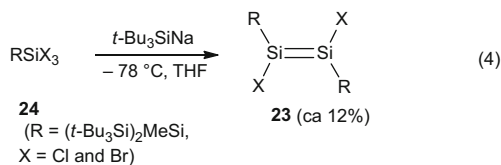
A cyclic disilenide was obtained from the reduction of a trisilacyclopentadiene (See, Sect. 2.5.4) [37].

2.3 Heteroatom-Substituted Disilenes

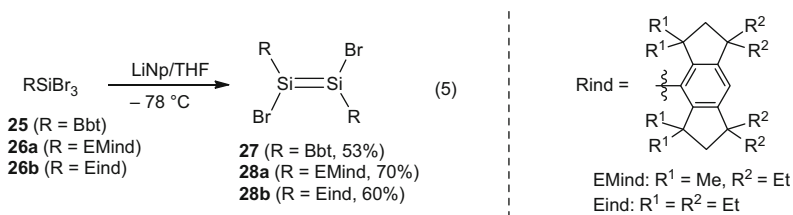
Various stable disilenes with functional heteroatom substituents such as stannyl, phosphinyl, halogeno, and hydrido substituents have been synthesized mainly through reductive dehalogenation of dihalosilane (method C), nucleophilic substitution of disilenide (method F), and 1,2-addition across the silicon-silicon triply bonded compounds (disilynes) (method G).

2.3.1 Halogen (Group 17 Element) and Pseudohalogen-Substituted Disilenes

First halogenated disilenes **23** were synthesized by Wiberg et al. via the reductive dehalogenation of RSiClBrX **24** ($\text{R} = (t\text{-Bu}_3\text{Si})_2\text{MeSi}$, $\text{X} = \text{Cl}, \text{Br}$) with $t\text{-Bu}_3\text{SiNa}$ in THF in ca. 12% yield (Eq. 4) [14].

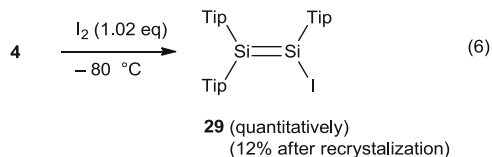


Similarly, reductive dehalogenation of tribromosilane with very bulky aryl substituents such as Bbt and Rind (Eind, EMind) (**25** and **26**) gave the corresponding 1,2-diaryl-1,2-dibromodisilenes **27** and **28** (Eq. 5) [38, 39].



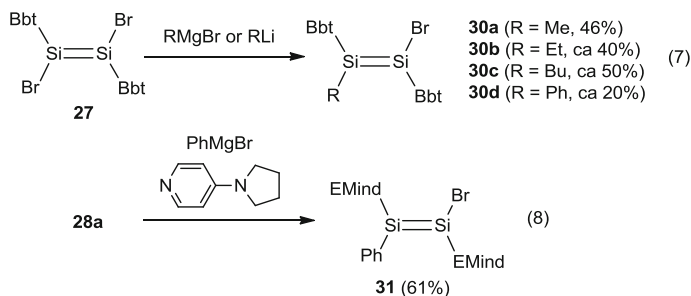
Molecular structures of stable 1,2-dibromodisilenes **27** and **28b** determined by X-ray structural analysis are highly *trans*-bent structure with bent angles $\beta = 32.4^\circ$ and 39.8° for **27** and $\beta = 29.0^\circ$ for **28b**. The large *trans*-bent angles β of halogen-substituted disilenes are consistent with the CGMT model predicting that electronegative substituents on the $\text{Si}=\text{Si}$ double bond lead to increased *trans*-bending [40–42]. Although the $\text{Si}=\text{Si}$ bond length of **27** [2.2264(8) Å] is longer than that of **28b** [2.1795(9) Å], both values are within the range of typical disilenes (2.14–2.29 Å) [2, 4]. In the ^{29}Si NMR spectra, the characteristic signal of $\text{Si}=\text{Si}$ was observed at 79.4 ppm for **27**, 74.6 ppm for **28a**, and 73.2 ppm for **28b**.

Mono-halogenated disilene **29** was synthesized by simple metal-halogen exchange reaction of lithium disilene **4** with I_2 (Eq. 6) [43].



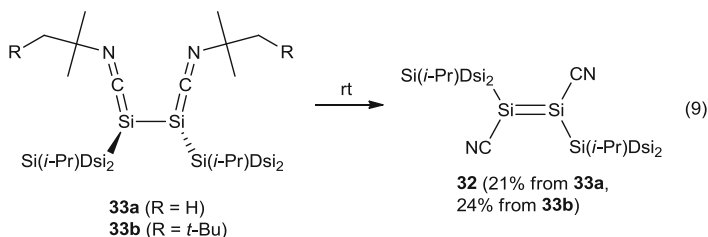
Mono-halogen-substituted disilenes **30a–d** and **31** were obtained by partial alkylation and arylation of 1,2-dihalodisilenes via formal substitution reaction on

the sp^2 -silicon atoms (Eqs. 7 and 8) [38, 39]. Notably, the reaction of **28a** with PhMgBr does not proceed in the absence of piperidylpyridine (PPy). Mechanism of the substitution reactions on the sp^2 -silicon atoms will be discussed in Sect. 3.2.2. When excess phenyllithium was used as a nucleophile for the reaction of **28a** and **31**, 1,2-diphenyldisilene (EMind)PhSi=Si(EMind)Ph was obtained (see compound **192** in Table 1).



The ^{29}Si NMR signals of sp^2 -silicon on monobromo-disilenes **30a-d** and **31** appear 67.5–86.6 ppm as listed in Table 1. Structural parameters of disilene **30c** obtained by X-ray diffraction study are as follows: $d(Si=Si) = 2.2019(12)$ Å, $\beta = 25.1^\circ$ for SiBbt(Bu) and 26.2° for SiBbt(Br), and $\tau = 2.6^\circ$.

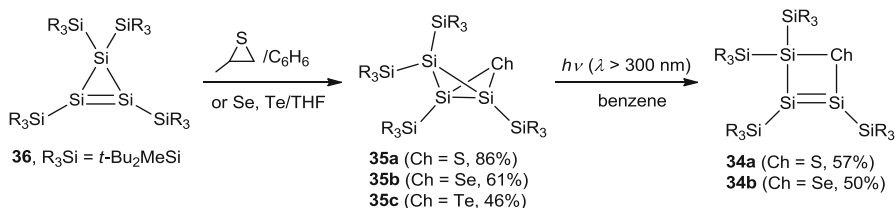
Cyano-substituted disilene **32** was synthesized by thermal decomposition of disilyne–isocyanide adduct, **33a** and **33b** (Eq. 9). Radical intermediate resulting from homolytic cleavage of $N(sp^2) - CMe_2(CH_2R)$ is proposed for formation of **32** [44].



Only X-ray structure and UV–vis spectrum of 1,2-dicyanodisilene **32** are available because of its low solubility. The π -accepting cyano groups do not affect the molecular structure of **66**. In compound **32**, the Si=Si bond length is 2.213(2) Å and the unsaturated three-coordinate silicon is slightly pyramidalized ($\beta = 16.9^\circ$) but not twisted ($\tau = 0^\circ$). The UV–vis spectrum of **32** in THF showed that $\pi(Si=Si) \rightarrow \pi^*(Si=Si)$ (HOMO–LUMO) transition band at 414 nm similarly to those of typical stable disilenes [2, 4]. Theoretical studies suggest that the electron-withdrawing cyano groups stabilize both energy levels of HOMO and LUMO.

2.3.2 Chalcogen (Group 16 Element)-Substituted Disilenes

Stable disilenes with group 16 element substituents are still quite rare. Sulfur- and selenium-substituted cyclic disilenes **34a** and **34b** were obtained as orange-red crystals by photochemical valence isomerization of the corresponding chalcogenatrisilabicyclo[1.1.0]butanes **35a** and **35b** derived from the reaction of cyclotrisilene **36** with propylene sulfide in benzene and elemental selenium in THF, respectively (Scheme 7) [45].

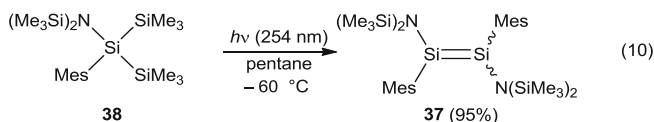


Scheme 7

The ^{29}Si NMR resonances of the sp^2 -silicon nuclei bonded to the chalcogen atoms are low-field shifted (195.0 and 192.1 ppm) in comparison to those of the remaining sp^2 -silicon nuclei (95.1 and 100.8 ppm) in **34a** and **34b**. In the UV–vis spectra, the longest wavelength absorption bands assignable to the $\pi(\text{Si}=\text{Si}) \rightarrow \pi^*(\text{Si}=\text{Si})$ transitions of **34a** and **34b** are observed at 454 and 463 nm, respectively. In the solid state, the four-membered ring and the geometry around silicon atoms in **34b** are almost planar. The $\text{Si}=\text{Si}$ bond length of 2.1706(12) Å is typical for cyclic disilenes [2, 4]. No notable interactions between lone pair on chalcogen atom and the $\text{Si}=\text{Si}$ was found in the molecular structure.

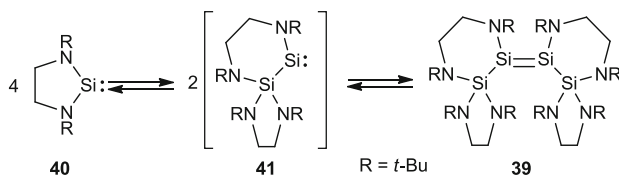
2.3.3 Amino- and Phosphino-Substituted Disilenes

Amino-substituted disilenes have been synthesized via various ways. First amino-substituted disilene **37** was synthesized by photolysis of the corresponding trisilane **38** (method A) (Eq. 10) [46].



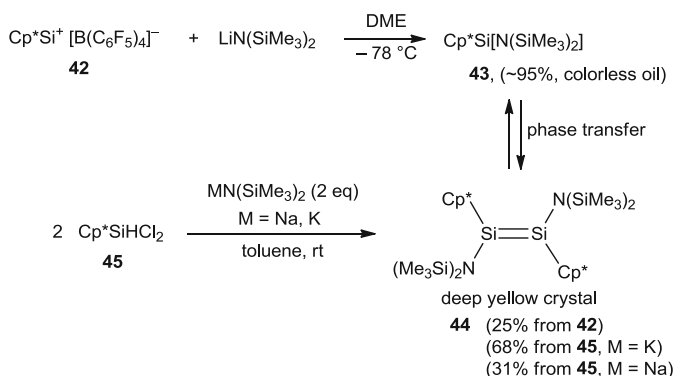
Unique route to amino-substituted disilene **39** was reported by West as shown in Scheme 6. Upon recrystallization of isolable diaminosilylene **40**, insertion of $\text{Si}-\text{N}$ bond of silylene moiety of **40** followed by dimerization of the resulting

aminosilyldisilylene **41** gave **39**. In solution, reverse reaction occurs to give **40** (Scheme 8) [47].



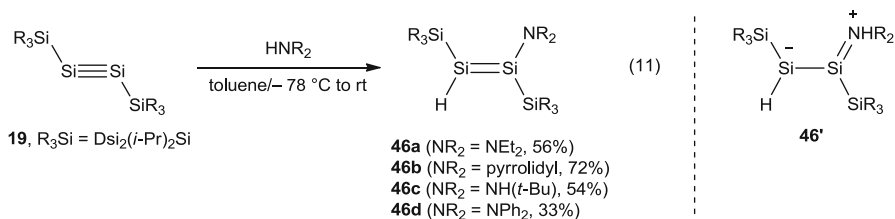
Scheme 8

Jutzi and coworkers have shown that reaction of silyliumylidene borate $\text{Cp}^*\text{Si}^+[\text{B}(\text{C}_6\text{F}_5)_4]^-$ (**42**) with $\text{LiN}(\text{SiMe}_3)_2$ gave aminosilylene $\text{Cp}^*[(\text{Me}_3\text{Si})_2\text{N}]\text{Si}:$ (**43**), which undergoes dimerization giving diaminodisilene $\text{Cp}^*[(\text{Me}_3\text{Si})_2\text{N}]\text{Si}=\text{Si}[\text{N}(\text{SiMe}_3)_2]\text{Cp}^*$ (**44**) upon crystallization (Scheme 9) [48, 49]. Alternatively **44** was obtained by the reaction of **45** with 2 equiv of metal amides, which act as both nucleophile and base [50].



Scheme 9

H-substituted aminodisilenes are easily obtained by the hydroamination of disilyne **19** (Eq. 11) [51, 52].



The $\pi \rightarrow \pi^*$ electronic transition of amino-substituted disilenes **46a–d** are red-shifted (438, 433, 411, and 440 nm, respectively) compared to that of structurally

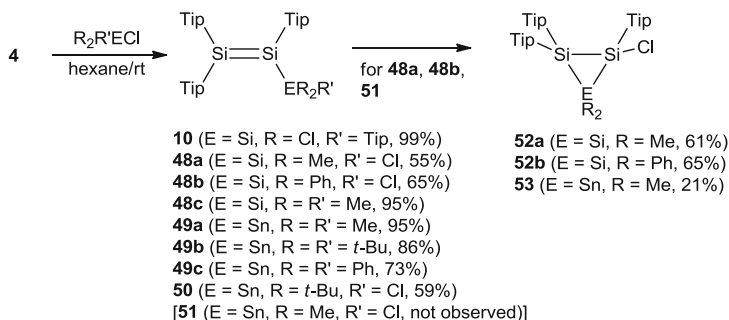
similar $R_3Si(H)Si=Si(Li)SiR_3$ **20a** (390 nm), owing to the significant π -conjugation between $\pi(Si=Si)$ orbital and lone pair orbital on nitrogen atom. The δ_H values of the protons on unsaturated silicon of 1-amino-1,2-disilyldisilenes **46a–d** varied between 2.80 (**46c**) and 4.54 ppm (**46d**).

In the ^{29}Si NMR spectra, two characteristic signals of the disilene moiety appear at 39.3 and 170.5 ppm for **46a**, 34.1 and 159.0 ppm for **46b**, 47.2 and 136.5 ppm for **46c**, and 66.6 and 136.4 ppm for **46d**. The signals due to ^{29}Si nuclei bound to hydrogen atom appear at higher field (around 30–60 ppm), which can be attributed to the anionic charge on the H-substituted silicon atom from the contribution of a zwitterionic structure **46'**. In disilenes **46a–d**, the Si=Si double-bond lengths $d(Si=Si)$ would depend on the size of amino groups; $d(Si=Si) = 2.1647(2)$, $2.1596(17)$, $2.1949(7)$, and $2.1790(14)$ Å for **46a**, **46b**, **46c**, and **46d**, respectively. Nitrogen atoms in **46a–d** are trigonal planar geometry. Bulky amino groups cause large torsion angles between $\pi(Si=Si)$ plane and $n(NR_2)$ plane (Si=Si–N–C) of 7, 12, 29, and 67° for **46a–d**.

Metathesis of disilenide **4** with chlorophosphines gave phosphino-substituted disilenes $Tip_2Si=SiTip(PR_2)$ (R = Ph (**47a**, 46%), *i*-Pr (**47b**), cyclohexyl (**47c**, 23%), and *t*-Bu (**47d**)) [43]. Disilene **47a** was also obtained by reaction of iododisilene **29** with Ph_2PLi . The ^{29}Si resonances appear at 52.5–54.4 ppm ($Si(Tip)PR_2$) and 95.4–99.8 ppm ($SiTip_2$). The ^{31}P chemical shifts depend on the substituents on the phosphorus: –45.7, –21.9, –36.3, and +8.9 for **47a–d**. The $^1J(^{29}Si-^{31}P)$ couplings increase with increasing the steric demand of the substituent on the phosphorus, 116, 118, ca. 115, and 133 Hz for **47a–d**, respectively. The longest wavelength absorption maxima assignable to $\pi \rightarrow \pi^*$ transition of **47a** and **47c** are 423 and 416 nm, respectively, which are typical of those of triaryldisilenes. The Si=Si distance of **47c** determined by X-ray analysis is 2.1542(11) Å, which is at the shorter end of the typical Si=Si distance (2.14–2.29 Å) [2, 4]. The P–Si distance of 2.2367(12) Å is relatively short compared with that of HC($SiMe_3$)₂($SiMe_2PPh_2$) (2.295 Å), which may indicate a significant allylic delocalization. The geometry around the Si=Si double bond in **47c** are considerably flat with the bent angle β of 7.7° ($SiTip(PCy_2)$) and 8.9° ($SiTip_2$) and the twist angle τ of 3.5(1)°. The phosphino-substituted disilenes **47a** and **47b** are applied for the ligands for transition metal complexes **47** [$Pd(PCy_3)$], in which the Si=Si double bond η^2 -coordinate to the palladium metal center in preference to the phosphorus atom of the phosphino group.

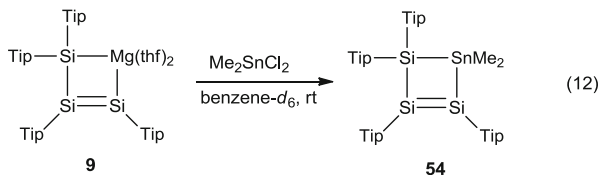
2.3.4 Heavy Group 14 Element-Substituted Disilenes

Disilenes with substituents of heavy group 14 elements such as silyl and stannyl are very common, most of which have been synthesized by reductive dehalogenation of the corresponding dihalosilanes (method C). Metathesis of disilenides and halosilanes and halostannanes are also simple route to these disilenes (Scheme 10) [13, 27, 53, 54]. Similarly, cyclic stannyl disilene **54** was obtained by the reaction of trisilene-1,3-diide **9** with Me_2SnCl_2 (Eq. 12). Interestingly, when less bulky



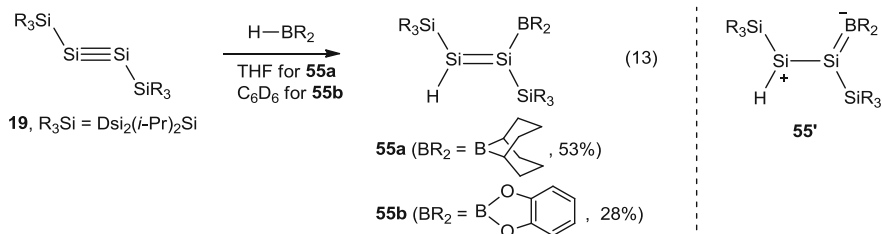
Scheme 10

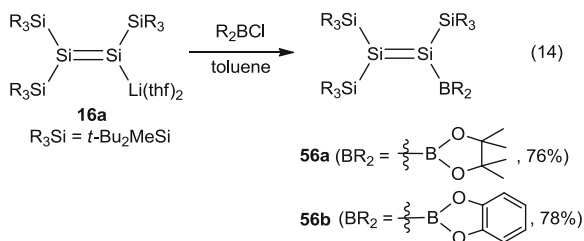
dihalosilanes were used for the reaction of **4**, the resulting silylated disilenes **48a** and **48b** undergo further cyclization, giving the corresponding three-membered ring compounds **52a** and **52b**. Isomerization to cyclotrisilane **52a** and **52b** was explained by 1,2-migration of chlorosilyl group over the Si=Si double bond, giving a disilylndisilene followed by Si–Cl insertion reaction of the resulting silylene (for details, see Sect. 3.1.2). In the case of Me₂SnCl₂, disilastannacyclopropane **53** was formed without observation of the corresponding stannyl disilene **51**.



2.3.5 Boryl-Substituted Disilenes

Electron-deficient boryl groups can be introduced on the Si=Si double bond via hydroborylation reactions of disilynes [**51**, **55**] and reactions of disilenide with haloboranes (Eqs. 13 and 14) [**56**].

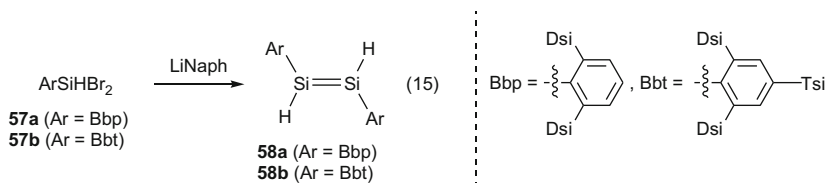




The ^{29}Si NMR signals of sp^2 -silicons among boryl-substituted disilenes $[\text{Dsi}_2(i\text{-Pr})\text{Si}]\text{SiHSi}^{\text{A}}=\text{Si}^{\text{B}}[\text{Si}(i\text{-Pr})\text{Dsi}_2](\text{BR}_2)$ are as follows: 150.5 ppm (Si^{A}) and 121.7 ppm (Si^{B}) for **55a** and 123.4 (Si^{A}) and 84.3 ppm (Si^{B}) for **55b**. The low-field shifted $\delta(\text{Si}^{\text{A}})$ of **55a** and **55b** compared with those of structurally similar amino-substituted disilenes $[\text{Dsi}_2(i\text{-Pr})\text{Si}]\text{SiHSi}^{\text{A}}=\text{Si}^{\text{B}}[\text{Si}(i\text{-Pr})\text{Dsi}_2](\text{NR}_2)$ **46a–d** ($\delta(\text{Si}^{\text{A}}) = 30\text{--}60$ ppm) are indicative of the contribution of a zwitterionic resonance structure **55'**. The $\pi \rightarrow \pi^*$ transition energy of the boryl-substituted disilenes are significantly affected by substituents on the boron atom. The $\pi \rightarrow \pi^*$ transition band of **55b** having dialkylboryl group was observed at 469 nm, which red-shifts by 58 nm to that of structurally similar **55a** having dialkoxyboryl group (411 nm) and by ca. 75 nm to those of dialkoxyboryl-substituted disilenes **56a** and **56b** (393 and 395 nm). Available low-lying vacant 2p orbital on boron atom in **55a** is responsible for the observed considerable red-shift. The Si=Si double-bond lengths of **55a** and **55b** determined by X-ray analysis are 2.1838(12) and 2.1634(12) Å, respectively. The dihedral angle of Si=Si–B–C of **55a** is 18° , allowing for π -conjugation between the Si=Si bond and the boryl group. In contrast, **55b** has a twisted arrangement with a dihedral angle of Si=Si–B–O torsion of 52° , indicative of less effective π -conjugation.

2.3.6 Hydrogen-Substituted Disilenes

Hydrogen-substituted disilenes had previously been obtained from the hydroborylation and hydroamination of disilynes. The reductive coupling of bulky aryl-substituted hydridodibromosilanes **57a** and **57b** provides access to the corresponding 1,2-dihydridodisilenes **58a** and **58b** (Eq. 15) [57].



The ^{29}Si resonances due to three-coordinate silicon nuclei in **58a** and **58b** were observed at 63.3 and 61.8 ppm, being typical $\text{A}_2\text{Si}=\text{SiA}_2$ tetraaryldisilenes (53–66 ppm). In the ^1H NMR spectra of 1,2-diaryldisilenes **58a** and **58b** in C_6D_6 , the signal due to proton nuclei on the $\text{Si}(\text{sp}^2)$ atom (δ_{H}) appears at 6.04 and 6.11 ppm, respectively. Both values are low-field shifted compared to the δ_{H} of a structurally similar 1,2-diaryldisilane, $\text{BbpSiH}_2-\text{SiH}_2\text{Bbp}$ (4.83 ppm in C_6D_6) because of the magnetic anisotropic effect of $\pi(\text{Si}=\text{Si})$ unit. The observed $^1J_{\text{SiH}}$ values in **58a** (216 Hz) and **58b** (210 Hz) are larger than that in $\text{BbpSiH}_2-\text{SiH}_2\text{Bbp}$ (188 Hz) due to the increased *s*-character of the $\text{Si}-\text{H}$ bonds (formally from sp^3 to sp^2). 1,2-Diaryldisilenes **58a** and **58b** exhibited much larger $^1J_{\text{SiH}}$ values compared to those of 1-lithio-1,2-bissilyldisilene ($^1J_{\text{SiH}} = 155$ Hz for **20a**) and 1,2-bissilyldisilene ($^1J_{\text{SiH}} = 149.8$ Hz for $\{(t\text{-Bu}_3\text{Si})_2\text{MeSi}\}\text{SiH}=\text{SiH}\{\text{SiMe}(\text{Si}t\text{-Bu}_3)_2\}$) [58] due to the higher *s*-character of the $\text{Si}-\text{H}$ bond increased by more electronegative carbon substituents compared to silicon and lithium substituents.

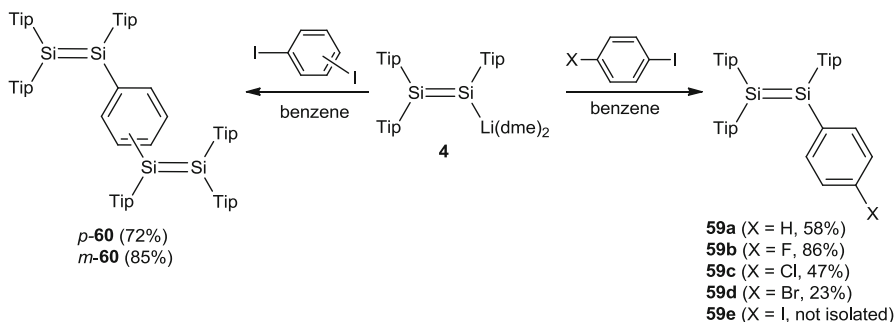
2.4 Disilenes with Functional Organic π -Electron Systems

Since the first isolation of tetramesityldisilene **1**, a lot of stable disilenes have been synthesized by taking advantage of bulky aryl groups as “spectator” substituents. Recently, several disilenes with functional and organic π -electron systems such as substituted phenyl group, polycyclic aromatic substituents, and metallocenyl groups.

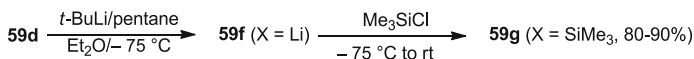
2.4.1 Disilenes with Substituted Phenyl Groups

Metathesis of disilenide and aryl halides is a convenient route to disilenes with functional aryl substituents (Scheme 11). Triaryldisilenide **4** reacted with various *p*-substituted iodobenzene derivatives to give **59a–59e** [59, 60]. Plausible mechanisms for the metathesis involve $\text{S}_{\text{N}}2$ -type reactions. Halogen–lithium exchange reaction successfully occurred for **59d** to give the corresponding 4-lithiophenyl disilene **59g**, which reacted with Me_3SiCl to afford 4-(trimethylsilyl)phenyldisilene **59g** (Scheme 12). When 1,4-diiodo- and 1,3-diiodobenzene were used for the reaction of **4**, the corresponding *p*-phenylenetetrasiladiene *p*-**60** and *m*-phenylenetetrasiladiene *m*-**60** were obtained in good yields (Scheme 11) [59, 60].

The ^{29}Si NMR resonances of **59a–e** are observed around 55 ppm (Tip₂Si side) and 70 ppm (*p*- $\text{XC}_6\text{H}_4\text{Si}$ side). In the UV–vis spectra of **59a–d** in hexane, absorption bands due to $\pi(\text{Si}=\text{Si}) \rightarrow \pi^*(\text{Si}=\text{Si})$ transition are slightly redshifted on going from $\text{X} = \text{F}$ ($\lambda_{\text{max}} = 437$ nm) to $\text{X} = \text{Br}$ ($\lambda_{\text{max}} = 447$ nm). A linear relationship between λ_{max} and the modified Hammett parameter σ_{P}^+ [61] was pointed out.



Scheme 11



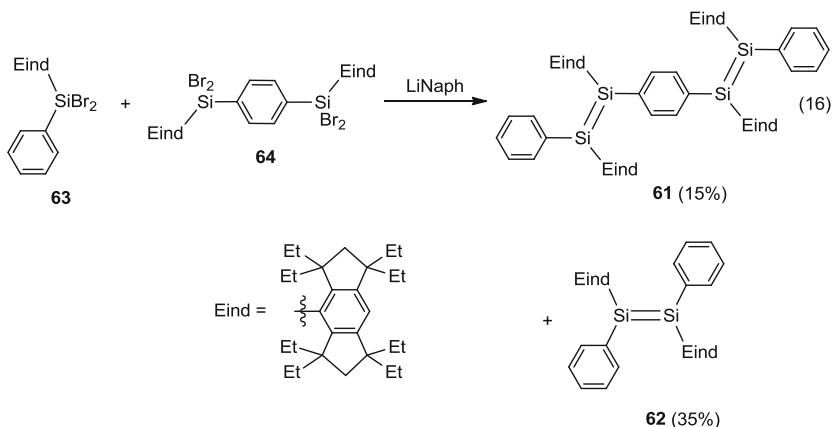
Scheme 12

The Si=Si double-bond lengths in *m*-**60** are 2.1914(9) and 2.1861(9) Å, which are considerably longer than the Si=Si bond in *p*-**60** [2.1674(8) Å]. Dihedral angles of the Si=Si units and the central phenylene ring of *m*-**60** [44.0(2)° and 47.6(2)°] are slightly larger than those in *p*-**60** [41.0(2)°]. Compound *m*-**60** has larger *trans*-bent angles (20.3–26.7°) than those in *p*-**60** (16.5 and 19.3°). The increased steric strain between the two disilynyl units in *m*-**60** compared to that in *p*-**60** would be responsible for the structural features found in *m*-**60**.

The different properties of *m*-**60** and *p*-**60** are owing to effective conjugation in *p*-**60**. Both *m*-**60** and *p*-**60** display irreversible oxidation processes at $E_p = -0.14$ V for *m*-**60** and $E_p = -0.35$ V for *p*-**60** in THF. In contrast to the reported oxidation behavior of Tip₂Si=SiTip₂ **2** ($E_{1/2}^{\text{ox}} = +0.56$ and $+1.32$ V), *m*-**60** and *p*-**60** show only one oxidation wave with low oxidation potentials. Although **2** exhibits only one reduction wave ($E_{1/2} = -2.66$ V), two well-separated quasi-reversible reduction waves centered at $E_{1/2}^{\text{red}} = -2.70$ and -3.30 V for *m*-**60** and $E_{1/2}^{\text{red}} = -2.70$ and -3.02 V for *p*-**60** were observed. In the UV-vis spectrum, $\pi(\text{Si}=\text{Si}) \rightarrow \pi^*(\text{Si}=\text{Si})$ transition of *p*-**60** is observed at 508 nm, which is red-shifted to that of *m*-**60** (450 nm) due to effective conjugation.

The radical anion of *m*-**60** in THF frozen solution at 100 K shows anisotropic EPR spectra with approximately axial symmetry with two different satellites due to two hyperfine coupling (hfc) of ²⁹Si nuclei. The *g*-factors and estimated hfc tensors of *m*-**60** are $g_{\parallel} = 2.0064$, $g_{\perp} = 2.0057$, $a_{\parallel}({}^{29}\text{Si}^{\text{a}}) = 1.55$ mT, $a_{\perp}({}^{29}\text{Si}^{\text{a}}) = 0.69$ mT, $a_{\parallel}({}^{29}\text{Si}^{\text{b}}) = 1.45$ mT, and $a_{\perp}({}^{29}\text{Si}^{\text{b}}) = 0.65$ mT, while those for *p*-**60** are $g_{\parallel} = 2.0062$, $g_{\perp} = 2.0058$, $a_{\parallel}({}^{29}\text{Si}^{\text{a}}) = 0.90$ mT, $a_{\perp}({}^{29}\text{Si}^{\text{a}}) = 0.38$ mT, $a_{\parallel}({}^{29}\text{Si}^{\text{b}}) = 0.72$ mT, and $a_{\perp}({}^{29}\text{Si}^{\text{b}}) = 0.32$ mT. The larger hfc tensors of [*m*-**60**]^{•-} compared to those of [*p*-**60**]^{•-} suggest an increased *s*-orbital contribution in the Si=Si bond in [*m*-**60**]^{•-} due to *trans*-bending upon one-electron reduction.

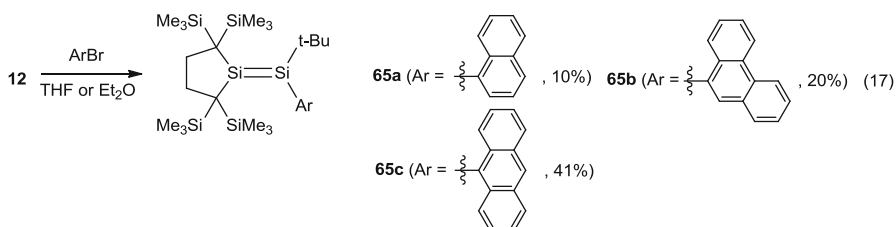
Another example of a *p*-phenylenetetrasiladiene was obtained with **61** alongside disilene **62** by reductive dehalogenation of the corresponding halosilanes **63** and **64** (Eq. 16) [17].



The crystal structure of **61** shows the following two features (1) coplanar tetrasiladienylbenzene skeleton with the dihedral angle between the central and terminal benzene rings of 9.0° and (2) planar geometry around the Si=Si bonds with the twist angles of 0.3 and 3.8° and with small *trans*-bent angles of 0.7 and 2.7° . Disilastilbene **62** has also planar geometry. The absorption maxima of **62** and **61** corresponding to the $\pi(\text{Si}=\text{Si}) \rightarrow \pi^*(\text{Si}=\text{Si})$ transition appear at 461 and 543 nm, respectively, indicating remarkable extension of the π -conjugation through the phenylene moiety in **61**. The absorption maximum of **61** is also red-shifted by 35 nm relative to that of Tip derivative *p*-**60** (508 nm). Substituents on the unsaturated silicon atoms can control the planarity around the Si=Si double bond to affect their electronic characteristics.

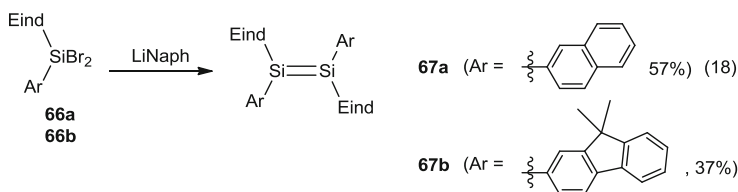
2.4.2 Disilenes with Polycyclic Aromatic Groups

Disilenes with polycyclic aromatic substituents were synthesized by metathesis of trialkyldisilene **12** with the corresponding aryl bromides (method F) (Eq. 17) [30].



X-ray analysis shows that the Si=Si bond lengths of 2.1943(14) Å for **65a**, 2.209(2) Å for **65b**, and 2.1754(12) Å for **65c** are in the standard region of the Si=Si double bonds. Disilene $\pi(\pi\text{Si})$ and aromatic $\pi(\pi\text{C})$ systems are almost perpendicular to each other with a dihedral angle of 83°, 80°, and 88° for **65a–c**, indicating very little conjugative interaction between $\pi(\pi\text{Si})$ and aromatic $\pi(\pi\text{C})$. Notably, 9-anthryl disilene **65c** shows a broad and distinct intramolecular charge transfer (ICT) absorption band at 525 nm in 3-methylpentane in addition to the usual absorption bands owing to $\pi \rightarrow \pi^*$ transitions (around 370–380 nm) of anthracene and disilene moieties. The ICT band red-shifts to 535 nm in more polar 1,2-dichlorobenzene. Theoretical calculations revealed that the Si–Si π orbital bond and the anthracene ligand's π^* orbital of **65c** function as donor and acceptor of that ICT, respectively.

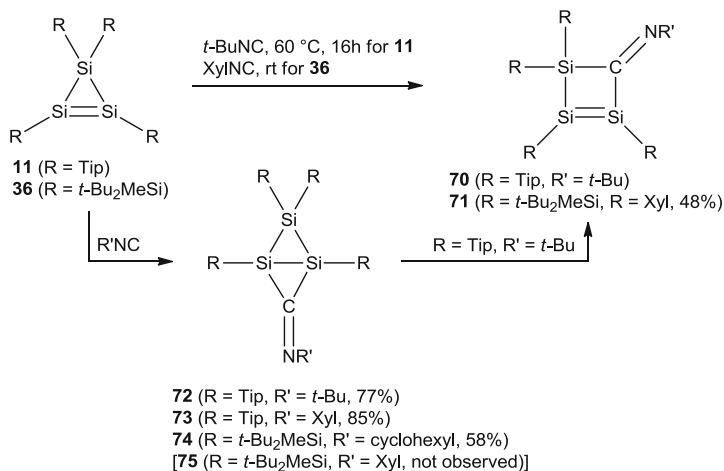
Disilenes with polycyclic aromatic substituents were also synthesized by reductive dehalogenation of the corresponding dihalosilanes with polycyclic aromatic substituents (method C) (Eq. 18) [62, 63].



Compound **61** in hexane exhibits fluorescence at 612 nm with $\Phi_f = 0.10$. Although disilenes **67a** and **67b** show very weak fluorescence in THF ($\lambda_{\text{FL}} = 586$ nm, $\Phi_f = 0.01$ for **67a**, $\lambda_{\text{FL}} = 575$ nm, $\Phi_f = 0.01$ for **67b**), the intensity of the fluorescence observed for these disilenes in the solid state increased with significant red-shifts ($\lambda_{\text{FL}} = 619$ nm, $\Phi_f = 0.23$ for **67a**, $\lambda_{\text{FL}} = 600$ nm, $\Phi_f = 0.20$ for **67b**) [17, 62]. Disilene **67a** was applied for an emissive material in organic light-emitting diode (OLED) [64]. A fabricated multilayer OLED device using a mixture of disilene **67a** and polyfluorene derivative as a light-emitting layer and a hole-transporting layer displayed an electroluminescence with the maximum brightness L_{max} of 119 cd cm⁻¹ at the driving voltage of 8.5 V. The emission maximum of this OLED device is 588 nm, which corresponds to the fluorescence of **67a** in THF (586 nm) probably due to homogeneous mixture of **67a** and polyfluorene.

2.4.3 Disilenes with Various Functional Organic π -Electron Systems

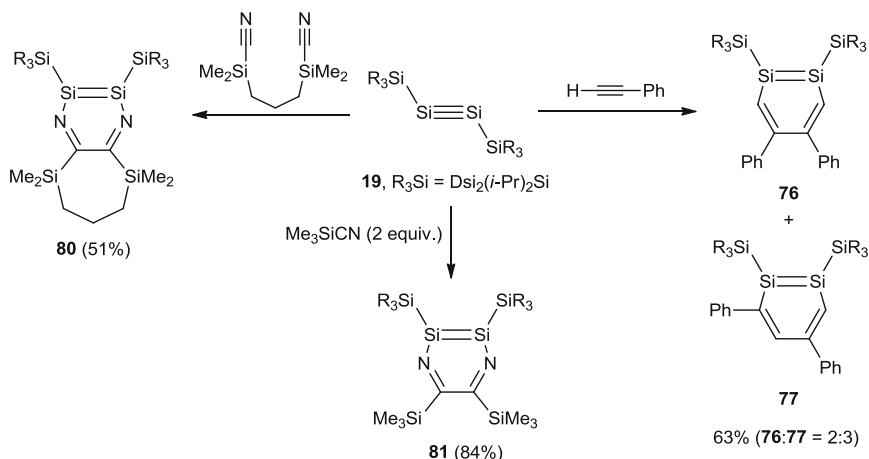
Metallocenyl-substituted disilenes **68a** and **68b** [65, 66] and alkynyldisilenes **69a** and **69b** [67] have been synthesized by the corresponding dibromosilanes with bulky aromatic substituents as protecting groups (Eq. 19).



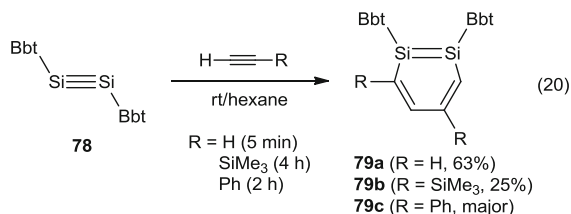
Scheme 13

2.4.4 Disilabenzenes and Related Compounds

Cycloaddition of disilyne with unsaturated organic compounds gave several disilaaromatic compounds. Disilyne **19** undergoes formal [2+2+2] cycloaddition with phenylacetylene to give a regioisomeric mixture of 1,2-disilabenzene derivatives **76** and **77** (Scheme 14) [69]. Similar reactions occur for aryl-substituted disilyne **78** to afford **79a–c** (Eq. 20) [70]. Reactions of **19** with nitriles gave the corresponding 2,3-disilapyrazines **80** or **81** [71, 72].



Scheme 14

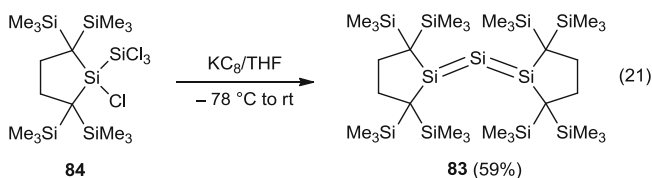


The ²⁹Si nuclei of 1,2-disilyl-1,2-disilabenzene **76** resonate at 99.2 ppm for **76** and 99.4 and 96.8 ppm for **77**, which are low-field shifted compared to those of 1,2-diaryl-1,2-disilabenzene (57.1 ppm for **79a**, 55.0 and 61.7 ppm for **79b**, 64.1 and 65.0 ppm for **79c**). X-ray structural study of **76** and **79a** showed that the 1,2-disilabenzene ring is almost planar. The large torsion angle of C(Bbt)–Si–Si–C (Bbt) (45.6°) is found in **79a** due to the *trans*-bent character of the Si=Si bond (*trans*-bent angles $\beta = 12.1^\circ, 13.7^\circ$). Such feature is in sharp contrast to that of 1,2-bis(silyl)-1,2-disilabenzene **76**, having planar geometries around the two skeletal Si atoms [Si–Si=Si–Si = $13.1(2)^\circ$]. The length of the endocyclic Si–Si bond in **76** is $2.2018(18)$ Å. The Si–Si bond distance [$2.2334(7)$ Å] in **79a** is slightly longer than structurally similar cyclic disilene **82** [$2.213(3)$ Å] having Bbt in *cis* geometry [see Sect. 2.6.1, Eq. (30)] [73]. The longest wavelength absorption maxima of **76** and **79a** in hexane were observed at 427 and 378 nm, respectively, which are redshifted compared to the value of 1-Tbt-silabenzene (331 nm) [74]. The NICS calculations of model compounds confirm the aromaticity of both 1,2-bis(silyl)- and 1,2-bis(aryl)-1,2-disilabenzene as 6π electron system.

2.5 Conjugated Disilenes

2.5.1 Trisiladiene (Trisilaallene)

Tetraalkyltrisilaallene **83** was synthesized as the first trisilaallene by the reductive dehalogenation of dialkyltetrachlorodisilane **84** (Eq. 21) [12].



Silyl-substituted trisilaallene **85** was synthesized by the reaction of 1,1-dilithiosilane **86** with a NHC complex of SiCl₂ **87** (Eq. 22) [75]. Electronic character of trisilaallenes is significantly affected by their substituents. Terminal and central ²⁹Si resonances of compound **85** were observed at 44.6 and 418.5 ppm, respectively, which contrasts with the ²⁹Si NMR chemical shifts of **83** (central Si, 157.0 ppm; terminal Si, 196.9 ppm).



The optimized structure of **85** (**85**_{opt}) calculated at the B3LYP/6-31G(d) level has considerably wider central bond angle of 164.3° versus that of **83** (136°) obtained by X-ray structural analysis. The Si=Si bond lengths of **85**_{opt} are 2.1792 Å and 2.1742 Å. The two planes of terminal R₂Si groups are almost perpendicular (86.6° for **85**_{opt}). In contrast to **83** having nondegenerate and delocalized on Si=Si=Si unit, two $\pi(\text{Si}=\text{Si})$ and two $\pi^*(\text{Si}=\text{Si})$ orbitals of **85**_{opt} are almost degenerate similarly to the case of all-carbon allenes.

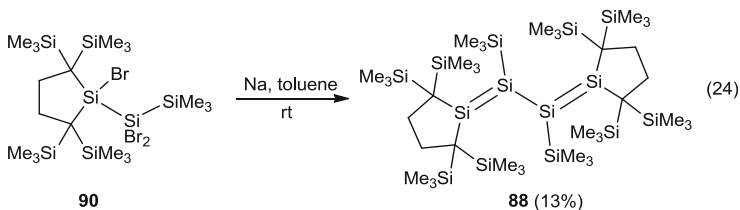
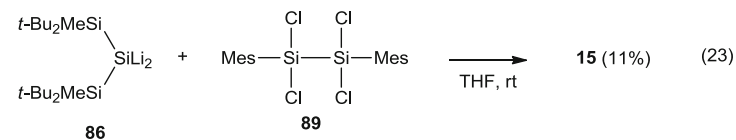
The regioselectivity of the nucleophilic addition of ROH (R = H, Me) of **85** is different from those of **83**. This will be detailed in Schemes 32 and 33 in Sect. 3.2.5.

2.5.2 Tetrasiladienes

The first tetrasiladiene **3** was synthesized by Weidenbruch et al. (Scheme 2) [10].

The redox properties of disilene Tip₂Si=SiTip₂ **2** and tetrasiladiene Tip₂Si=Si(Tip)–Si(Tip)=SiTip₂ **3** have been investigated by CV [76]. In *o*-dichlorobenzene and [Me₃PhN]⁺[B(C₆F₅)₄][–] used as an electrolyte, disilene **2** exhibited reversible redox couples in both oxidation ($E_{1/2}^{\text{ox}} = +0.56$ V) and reduction processes ($E_{1/2}^{\text{red}} = -0.50$ V). In the same condition, tetrasiladiene **3** showed a reversible oxidation process ($E_{1/2}^{\text{ox}} = +0.07$ V) but an irreversible wave ($E_p^{\text{red}} = -0.65$ V) during reduction. As expected, conjugated tetrasiladiene **3** has lower oxidation potentials than that of disilene **2**. Irreversible reduction wave of **3** may be attributed to reductive Si–Si bond cleavage to afford disilenides (see Sect. 2.2).

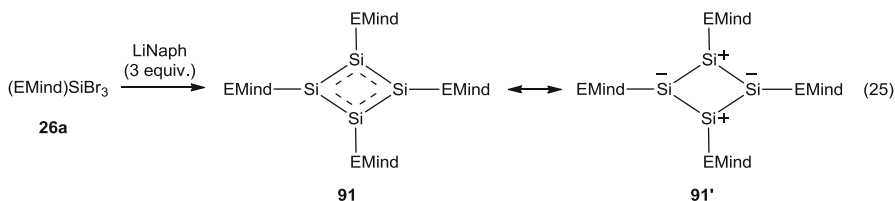
Tetrasiladienes **15** and **88** were obtained by the reaction of tetrachlorodisilane **89** with 1,1-dilithiosilane **86** in THF (Eq 23) [31] and reductive dehalogenation of tribromodisilane **90** with sodium in toluene (Eq. 24) [77].



In the solid state of **88**, the tetrasiladiene skeleton is not planar but highly twisted with the dihedral angle between the Si=Si double bonds of $122.56(7)^\circ$. The large dihedral angle of **88** shows an anticlinal conformation in contrast to **3** and **15** having a synclinal conformation ($\delta = 51^\circ$ and 72° , respectively). The Si=Si double-bond lengths of **88** are 2.1980(16) and 2.2168(16) Å. The ^{29}Si resonances of central and terminal unsaturated Si nuclei of **88** are observed at 9.3 and 210.2 ppm. The UV–vis spectrum of **88** shows the longest wavelength absorption maximum at 510 nm at 77 K in a 3-MP glass matrix assignable to a $\pi(\text{Si}=\text{Si}) \rightarrow \pi^*(\text{Si}=\text{Si})$ transition band. The maximum is comparable to those of **3** (518 nm) [10] and **15** (531 nm) [32], suggesting conjugation between the two $\pi(\text{Si}=\text{Si})$ systems.

2.5.3 Cyclotetrasiladiene Derivatives

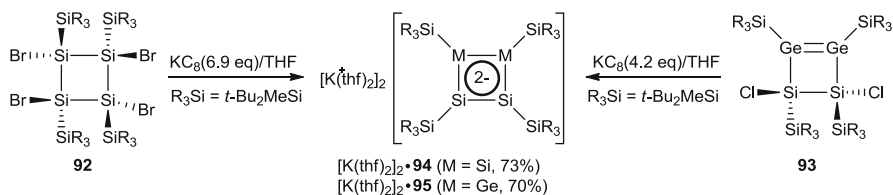
Recently, cyclic neutral tetrasiladiene derivative **91** was synthesized by reductive dehalogenation of tribromosilane with bulky Rind group (Eq. 25) [78].



Detailed investigations revealed that the significant contribution of charge-separated structure **91'** in the molecular structure of **91** by polar Jahn–Teller effect to avoid antiaromaticity. X-ray analysis showed that the Si₄ ring in compound **91** has a planar rhombic structure and rather long Si–Si bonds with small bond alternation [Si–Si bond lengths; 2.2671(8), 2.2846(8), 2.2877(8), and 2.2924(8) Å]. Pyramidalized silicons (the sums of the angles of 338.8° and 335.1°) and planar silicons (the sum of the angles of 360.0°) are positioned alternately at the four-membered ring. In the solid-state CP/MAS ^{29}Si NMR spectrum of **91**, two sets of two resonances are found in the higher-field region (-52 and -50 ppm) and in the lower-field region (300 and 308 ppm). The former are assignable to the negatively charged pyramidalized silicon atoms and the latter are positively charged planar silicon atoms.

Reduction of tetrabromocyclotetrasilane **92** and dichlorodisiladigermetane **93** with potassium graphite gave the corresponding dianions of tetrasilacyclobutadiene and digermadisilacyclobutadiene, **94** and **95** as $[\text{K}(\text{thf})_2]_2$ salts being isomorphous (Scheme 15) [79]. In the solid state, the four-membered silicon ring of **94** is not planar with the folded angle of 34° and potassium cations are located above and below the silicon ring being coordinated at 1,3 and 2,4 positions. The ring Si–Si distances are not equal with distances of 2.2989(8), 2.3300(8), 2.3576(8), and 2.3301(8) Å and the geometries around three-coordinate silicon atoms are pyramidalized with the sum of the bond angles of 341° and 326° . This

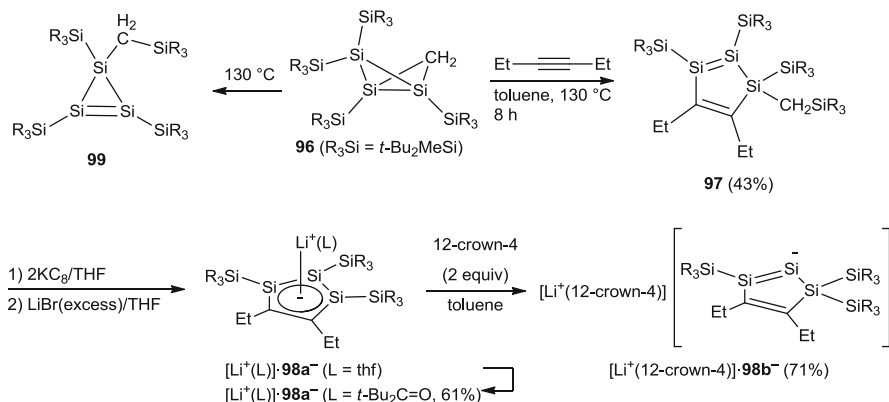
structural feature indicates that **94** and **95** are nonaromatic in the solid state, which is supported by the NICS values of model compounds **94** and **95** where silyl groups are replaced by Me₃Si groups (+4.3 and +6.1 ppm). In solution **94** and **95** show different behavior. The ²⁹Si resonances due to three-coordinate silicon nuclei (δ_{Si}) are observed at 113.7 ppm for **95** being suggestive of double-bond character between Si atoms and localization of the negative charge on the more electronegative germanium atoms. On the other hand, the δ_{Si} for **94** observed at 17.0 ppm are considerably upfield shifted compared to those for the typical Si=Si double bond and that of **95**, which was interpreted as a sign of significant delocalization of the negative charges due to the symmetric skeletal ring.



Scheme 15

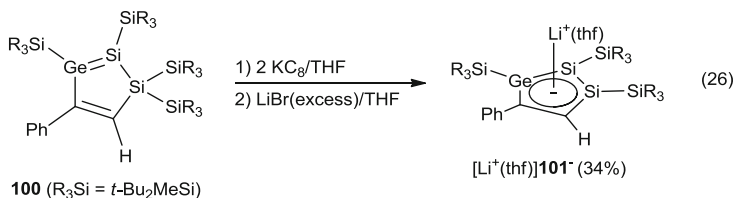
2.5.4 Disilacyclopentadienes

Reaction of trisilabicyclo[1.1.0]butane **96** with 3-hexyne gives trisilacyclopentadiene **97** (Scheme 16) [37]. The ²⁹Si resonances due to the three-coordinate silicon nuclei appears at 95.6 ppm for Si=Si-C=C and 166.4 ppm for Si-Si-C=C. In the solid state the five-membered ring in **97** is planar with the sum of the interior bond angles of 539.9° and the Si=Si distance is 2.1808(5) Å. The $\pi \rightarrow \pi^*$ absorption bands of **97** was observed at 493 nm. Reduction of **97** with potassium graphite followed by addition of LiBr gave $[\text{Li}^+(\text{thf})]\mathbf{98a}^-$. The THF ligand on the lithium cation can be exchanged by a *t*-Bu₂C=O ligand. X-ray analysis of $[\text{Li}^+(\textit{t}\text{-Bu}_2\text{C=O})]\mathbf{98a}^-$ shows the Li⁺ cation coordinates to trisilacyclopentadienide in an η^5 -fashion and the five-membered ring retained its planarity with the sum of bond angle of 538.5°. Upon reduction, the Si=Si and C=C distances in the five-membered ring are elongated and all single bonds are shortened, indicating the aromaticity of compound **98a**⁻. The ²⁹Si chemical shifts for the unsaturated silicon nuclei are 22.0 and 22.9 for $[\text{Li}^+(\text{thf})]\mathbf{98a}^-$ and 22.4 and 28.3 ppm for $[\text{Li}^+(\textit{t}\text{-Bu}_2\text{C=O})]\mathbf{98a}^-$. The ⁷Li NMR signal appears at the high-field region; -5.8 and -5.0 for $[\text{Li}^+(\text{thf})]\mathbf{98a}^-$ and $[\text{Li}^+(\textit{t}\text{-Bu}_2\text{C=O})]\mathbf{98a}^-$, respectively, which is indicative of the aromatic ring current effects inside the five-membered ring of **98a**⁻. Addition of 12-crown-4 to $[\text{Li}^+(\text{thf})]\mathbf{98a}^-$ in toluene gave cyclic disilenide **98b**⁻ as a result of 1,2-silyl migration. $[\text{Li}^+(\text{12-crown-4})]\mathbf{98b}^-$ exists as solvent-separated ion pair in the solid state. The skeletal bond angle around the Si=Si-Si is reduced on going from neutral **97** to anionic **98b**⁻, which can be attributed to the higher s-character of the anionic orbital of **98b**⁻. Thermolysis of **96** at 130°C in toluene gave cyclotrisilene **99** [80].



Scheme 16

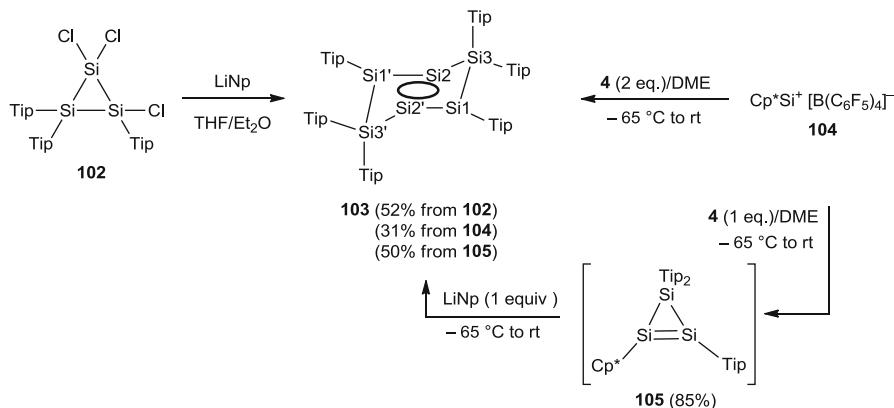
A similar reaction of germa-disilacyclopentadiene **100** giving the corresponding germa-disilacyclopentasilanide **101⁻** was reported (Eq. 26) [79].



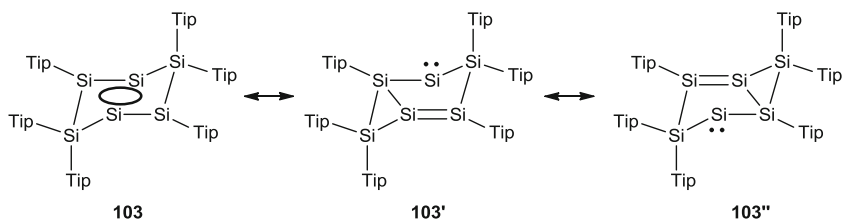
2.5.5 Isomers of Hexasilabenzenes

Reductive dechlorination of 1,1,2-triaryltrichlorocyclotrisilane **102** with lithium naphthalenide gave an isomer of hexasilabenzene **103** as green crystals (Scheme 17) [81]. Alternatively, **103** was obtained by reaction of Cp^{*}Si⁺[B(C₆F₅)₄]⁻ (**104**) with 2 equiv of disilene **4** or 1 equiv of **4** giving cyclotrisilene **105** followed by 1 equiv of lithium naphthalenide [82].

The molecular structure of **103** shows a chair-shaped conformation with a rhomboid central Si₄ ring and with a dihedral angle between the central Si₄ ring and terminal Si₃ ring of 66.80(2)°. The formal oxidation states of the silicon atoms in **103** are 0 for Si without Tip substituent (Si²), +1 for SiTip (Si¹), and +2 for SiTip₂ (Si³), and their ²⁹Si NMR signals are observed at -89.3, +124.6, and -84.8 ppm, respectively. The UV-vis spectrum of **103** showed the longest wavelength absorption band at 623 nm. The Si1-Si2' distance and the distance between Si1 and Si2 atoms connecting Si3 atom are 2.3034(5) and 2.3275(5) Å, respectively, which are shorter than typical Si-Si single-bond distance. The diagonal distance between Si2 atoms is 2.7287(7) Å. On the basis of the structural data and detailed theoretical investigations, a resonance hybrid



Scheme 17



Scheme 18

between **103'** and **103''** by delocalization of six electrons from nonbonding electron pair, $\pi(\text{Si}=\text{Si})$ bond and $\pi(\text{Si}-\text{Si})$ bond, is suggested to describe the electronic structure of **103** (Scheme 18). Interestingly, calculated NICS(0) values of model compound of -23.8 ppm being larger than that of benzene (~ -10 ppm) suggest that **103** exhibits significant aromatic character. Rzepa and Scheschkewitz propose the term “dismutational aromaticity” for this type of hitherto unknown aromatic delocalization found in **103**.

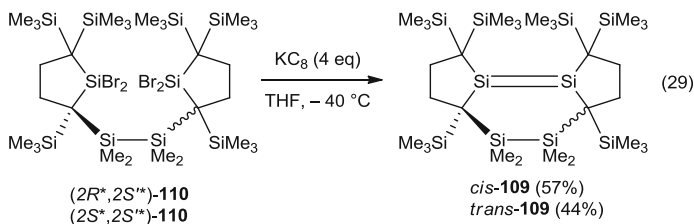
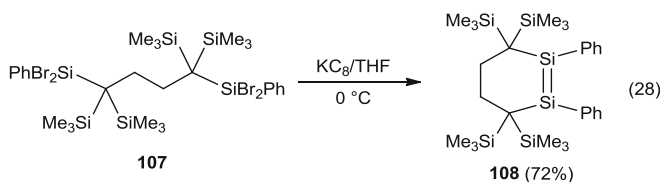
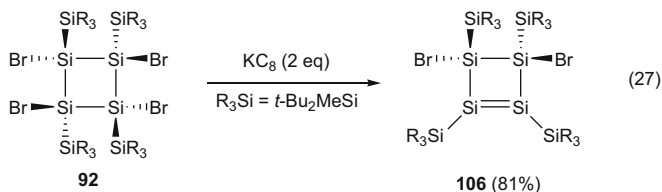
2.6 Miscellaneous

2.6.1 New Routes to Cyclic Disilenes

Typical cyclic disilenes such as cyclotrisilenes and cyclotetrasilenes have been synthesized mainly by simple reductive dehalogenation of the corresponding halosilanes. Recently several alternative routes to cyclic disilenes have been reported.

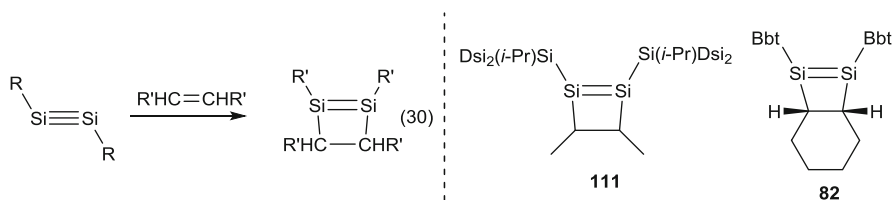
Partial reductive debromination of 1,2,3,4-tetrabromocyclotetrasilane **92** gave 3,4-dibromocyclotetrasilene **106** (Eq. 27) [83]. Reductive dehalogenation of a

precursor tethering two dihalosilane moieties (**107**) gave the corresponding cyclic disilene **108** (Eq. 28) [84]. In a similar manner, fused tricyclic disilenes *cis*-**109** and *trans*-**109** were obtained from **110** (Eq. 29) [85].

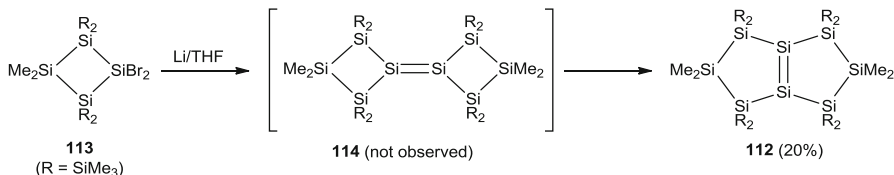


The $\pi \rightarrow \pi^*$ absorption bands are found to be considerably affected by the geometrical change around double bond in *cis/trans*-**109**, two isomeric tetraalkyl-disilenes. Disilene *trans*-**109** has a markedly long Si=Si double bond [2.2687(7) Å], large *trans*-bent angles ($\beta = 30.9$ and 32.9°), and twist angle ($\tau = 42.5^\circ$) owing to strained fused tricyclic structure. On the other hand, *cis*-**109** has a normal structural parameters of disilene; $d(\text{Si}=\text{Si}) = 2.1767(6)$ Å, $\beta = 3.9$ and 12.4° , and $\tau = 3.9^\circ$. As a consequence, *trans*-**109** showed $\pi \rightarrow \pi^*$ transition at 517 nm, which is remarkably red-shifted from that of less distorted *cis*-**109** ($\lambda_{\text{max}} = 433$ nm). The small $\pi \rightarrow \pi^*$ transition energy of *trans*-**109** is explained by poor π -bonding as a result of the elongated, *trans*-bent, and twisted Si=Si bond.

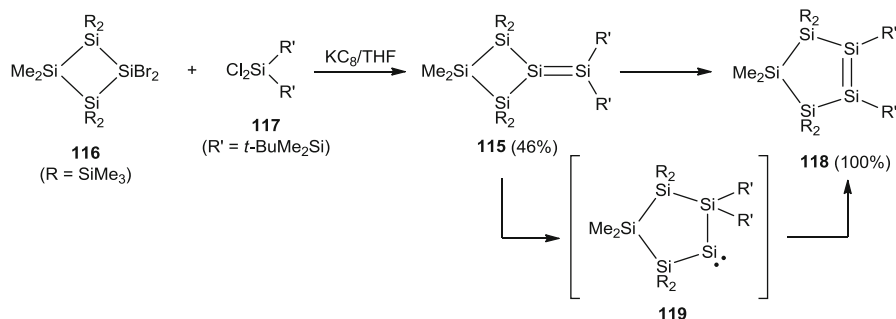
Cycloaddition of disilynes with alkenes is a simple route to cyclic disilenes (Eq. 30). 1,2-Disilacyclobutenes **111** and **82** were synthesized by [2+2] cycloaddition of the corresponding disilyne with alkenes using this method [15, 69, 73].



A fused bicyclic disilene bicyclo[3.3.0.0^{1,5}]octasil-1(5)-ene **112** was synthesized unexpectedly by reaction of 1,1-dichlorocycloctetrasilane **113** with lithium in THF in 20% yield (Scheme 19) [86]. A possible mechanism for formation of **112** involves formation of exocyclic disilene **114**, which was not observed, followed by double 1,2-silyl migration. The following reaction supports this mechanism: silylenecycloctetrasilane **115** obtained from selective reductive coupling of **116** and **117** undergoes 1,2-silyl migration accompanied by ring expansion to give cyclopentasilene **118** (Scheme 20) [87]. DFT calculation predicts that this reaction proceeds through cyclic silylene **119** via stepwise 1,2-silyl migration.



Scheme 19

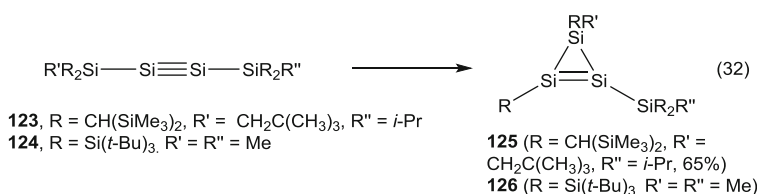
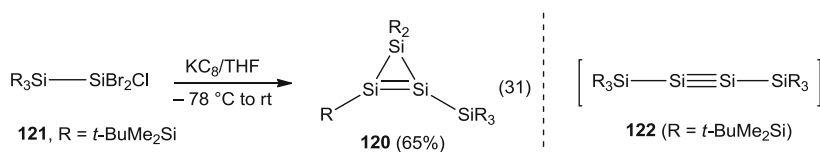


Scheme 20

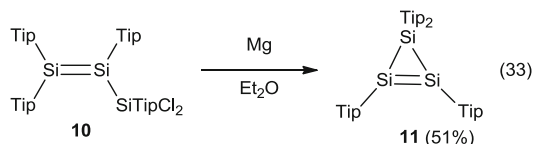
The structure of tetrasilyldisilene **112** is topologically similar to a partial structure of the Si(001) surface up to the third layer. In the solid state, the Si=Si bond distance of **112** is 2.180(3) Å. The Si=Si double bond of **112** adopts a slightly *cis*-bent geometry with the bent angle β of 1.6°, where the angle β is defined as an angle between the Si(sp³)-Si(sp²)-Si(sp³) plane and the Si(sp²)-Si(sp²) bond. The ²⁹Si NMR resonance for the unsaturated silicon nuclei in **112** appears at 167.4 ppm. Disilene **112** showed an intense absorption band at 468 nm

due to $\pi(\text{Si}=\text{Si}) \rightarrow \pi^*(\text{Si}=\text{Si})$ transition. The absorption maximum of **112** is remarkably red-shifted by about 50 nm relative to those for typical silyl-substituted disilenes (412–425 nm) [2, 4]. The redshift suggests significant σ – π interaction between the $\text{Si}=\text{Si}$ π -bonding orbital and σ -type orbitals from eight trimethylsilyl groups.

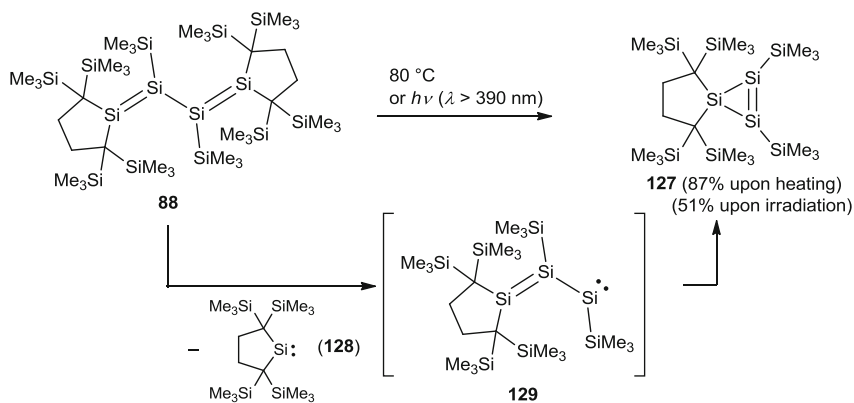
Stable cyclotrisilenes have been synthesized through various methods. Cyclotrisilene **120** was synthesized as the first stable cyclotrisilene by the reduction of dibromochlorosilane with tris(*t*-butyldimethylsilyl)silyl group **121** (Eq. 31) [88]. Proposed mechanism for formation of **120** involves generation of disilyne **122** and its rearrangement accompanied by silyl migration. Recently, similar rearrangement reactions of disilynes **123** and **124** to cyclotrisilenes **125** and **126**, respectively, were reported (Eq. 32) [15, 89].



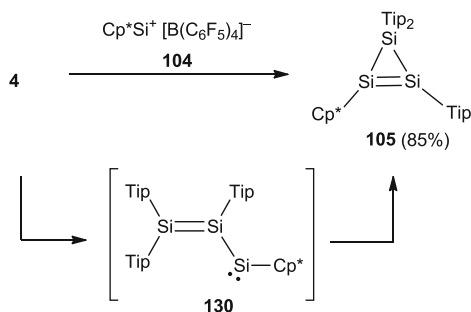
Thermolysis or photolysis of tetrasiladiene **88** gave cyclotrisilene **127** alongside silylene **128** (Scheme 21). Formation of **127** was explained by dissociation of a $\text{Si}=\text{Si}$ bond in **88** giving disilylensilylene **129** followed by cyclization. Scheschkewitz et al. have reported synthesis of cyclotrisilenes **105** and **11** via similar type intermediate **130** (Schemes 22 and Eq. 33) [28].



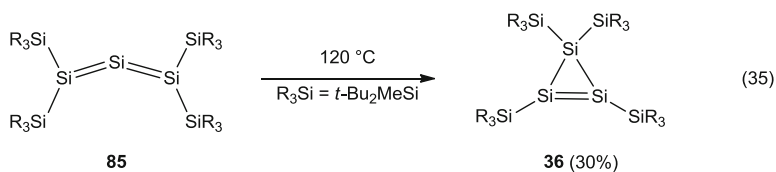
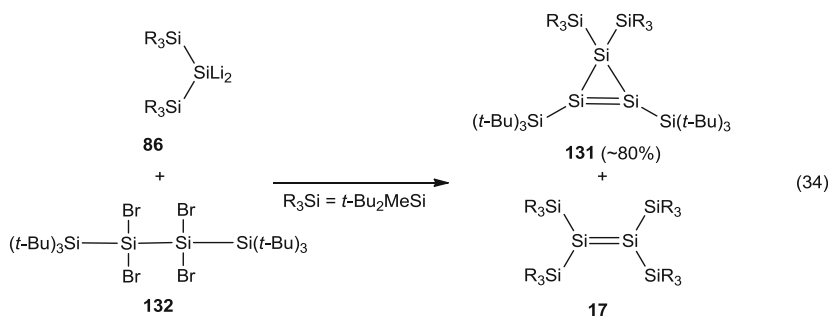
Tetrasilacyclotrisilene **131** was synthesized by reaction of 2,2-dilithiotrisilane **86** and 2,2,3,3-tetrabromotetrasilane **132** (Eq. 34) [90], and cyclotrisilene **36** [75] was obtained by thermal rearrangement of tetrasilyltrisilaallene **85**, reiterating previous observations for the corresponding tin compound [91] (Eq. 35).



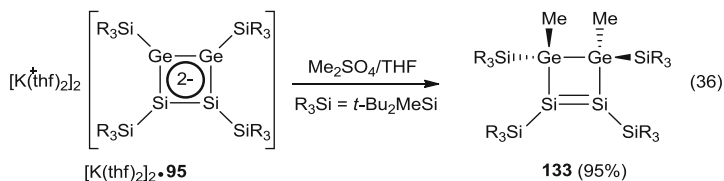
Scheme 21



Scheme 22

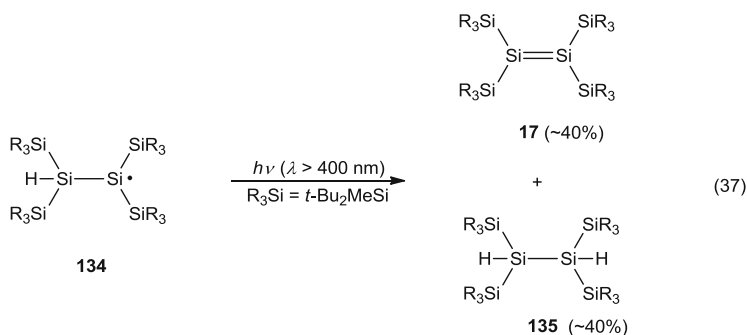


Digermadisiletene **133** was obtained by methylation of the corresponding dianion **95** (Eq. 36) [79].



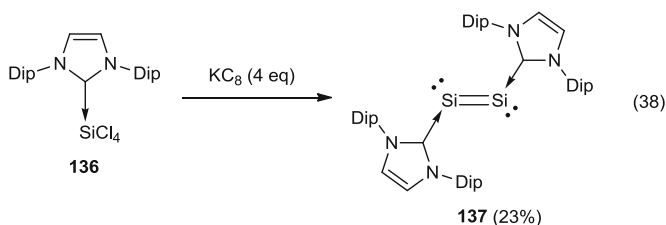
2.6.2 Disproportionation of (Hydrosilyl)silyl Radical

Apeloig et al. have found that upon irradiation, (hydrosilyl)silyl radical **134** undergoes disproportionation reaction to give tetrasilyldisilene **17** and 1,2-dihydrodisilane **135** (Eq. 37) [92].



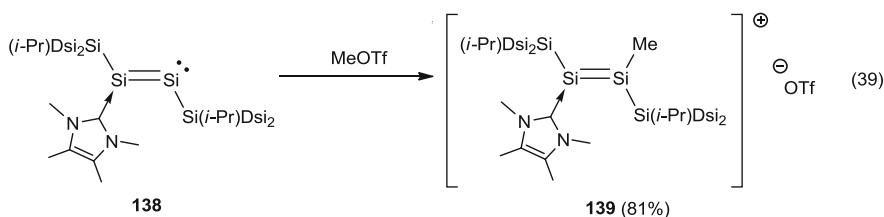
2.6.3 Donor–Coordinate Disilene-Like Compounds

Robinson et al. have shown that reductive dechlorination of NHC-coordinate silicon tetrachloride **136** with potassium graphite gave NHC₂Si₂ (**137**) as dark-red crystals in 23% yield (Eq. 38) [93].



Since formal oxidation state of silicon in **137** is zero, compound **137** is categorized as a NHC-supported disilicon(0) compound. Molecular structure, spectroscopic properties, and theoretical studies indicate that compound **137** possess significant Si=Si double-bond character. Two carbene ligands are almost perpendicular to the Si=Si unit in **137**, indicating very small conjugative interactions between Si=Si and NHC. The Si=Si bond distance of **137**, 2.2294(11) Å, is slightly longer than typical Si=Si double bond but within the reported range of Si=Si bond distances (2.14–2.29 Å). The ^{29}Si resonance of **137** in C_6D_6 appeared at 224.5 ppm in the unsaturated silicon region. The $\pi(\text{Si}=\text{Si}) \rightarrow \pi^*(\text{Si}=\text{Si})$ transition band was observed at 466 nm in THF.

Disilyne **19** forms a complex with a NHC (**138**), which reacted with MeOTf to give NHC-coordinate disilenylium cation **139** (Eq. 39) [94].

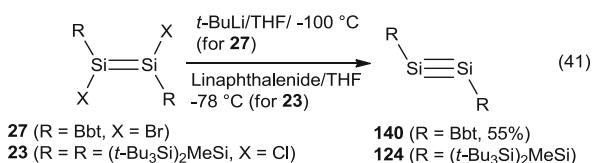
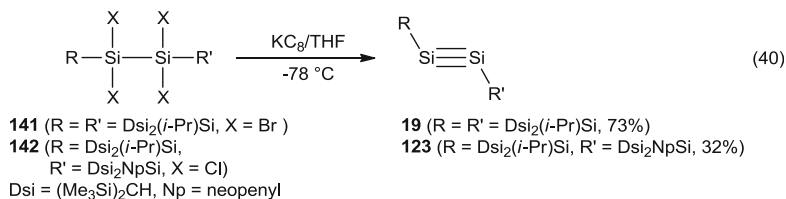


The ^{29}Si NMR signals of Si=Si bond of **138** in THF- d_8 appeared at 28.7 (NHC–Si=Si) and 276.3 ppm (NHC–Si=Si). The UV–vis spectrum of **138** shows an absorption band at 409 nm with a shoulder (ca. 440 nm). The former is assigned to the HOMO \rightarrow LUMO transition [$\pi(\text{Si}=\text{Si}) \rightarrow \pi^*(\text{Si}=\text{Si})$] and the shoulder is assigned to HOMO–1 to LUMO transition [$n(\text{Si}) \rightarrow \pi^*(\text{Si}=\text{Si})$]. The Si=Si bond length of 2.1989(6) Å in **138** is in the typical region of disilenes. The three-coordinate silicon atom has planar geometry with the sum of the bond angles of 359.16°. The torsion angle of the Si_4 chain is 165.12(2)°, which indicates that the two $\text{SiDsi}_2(i\text{-Pr})$ groups are positioned in *trans*-fashion and a lone-pair of electrons resides on the two-coordinate silicon atom. In contrast, the ^{29}Si NMR signals of Si=Si bond in **139** appeared at 54.0 (NHC–Si=Si) and 168.8 ppm (NHC–Si=Si). In the solid state, no significant interactions between the skeletal silicon atoms of **139** and the triflate anion are found. No Si=Si bond elongation is observed after the addition of the methyl group to **138**; the Si=Si bond length of 2.192(2) Å in **139** is typical of a Si=Si double bond. The UV–vis spectrum of **139** in THF has an absorption band at 408 nm assignable to $\pi(\text{Si}=\text{Si}) \rightarrow \pi^*(\text{Si}=\text{Si})$ transition.

Reaction of **138** with ZnCl_2 gave the corresponding adduct of **138**· ZnCl_2 , where ZnCl_2 coordinated to the silicon atom with a lone pair of electrons. The two silyl groups on the unsaturated silicon atoms are arranged in the *cis*-orientation owing to the interaction between the NHC and ZnCl_2 moieties.

2.7 Stable Disilynes

Because silicon–silicon triply bonded compounds, disilynes, have two (different) $\pi(\text{Si}=\text{Si})$ bonds at the same silicon atoms [5, 19–24], disilynes may be also regarded as formally belonging to the class of functional disilenes. Stable silyl- and aryl-substituted disilynes **19**, **123**, **140**, and **124** were synthesized by reductive dehalogenation of the corresponding tetrahalodisilanes (Eq. 40) [16, 89] or by reduction of 1,2-dihalodisilenes (Eq. 41) [14, 15, 38].



All reported stable disilynes (RSi≡SiR) have *trans*-bent geometry with shorter Si≡Si bonds. The $d(\text{Si}\equiv\text{Si})$ are 2.0622(9), 2.0569(12), and 2.108(5) Å for **19**, **123**, and **140**, respectively, being markedly shorter than that of disilenes. The R–Si–Si angles amount to 137.44(4)° for **19**, 138.78(5)° (*i*-PrDsi₂Si side) and 137.89(5)° (NpDsi₂Si side) for **123**, and 133.0(3)° for **140**. Unsaturated ²⁹Si NMR signal of diaryldisilyne **140** is observed at 16.7 ppm, while that of bisilyldisilyne **19** is found at much lower field, at 89.9 ppm. Interestingly, the ²⁹Si chemical shift is sensitive to the geometry around Si≡Si bond; in compound **123**, an unsymmetrically substituted bisilyldisilyne, the triply bonded ²⁹Si nucleus bearing a *i*-PrDsi₂Si group resonates at 62.6 ppm, whereas that with a NpDsi₂Si group is low-field shifted to 106.3 ppm. For detailed discussion of silicon–silicon triple bond in disilyne, please see the comprehensive reviews on disilynes [5, 19–24].

3 Reactivity

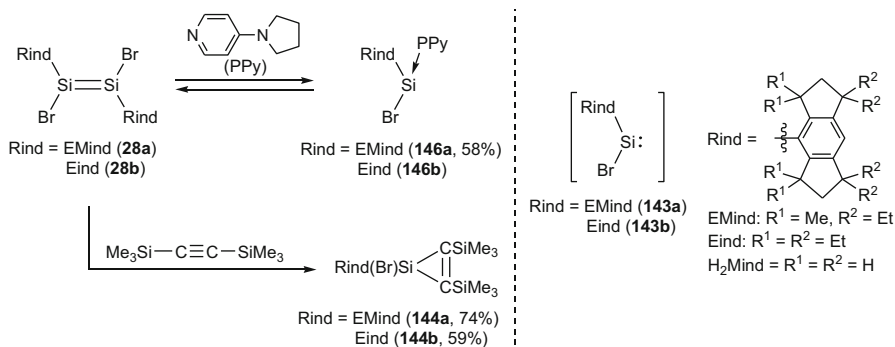
Because the fundamental reactivity of stable disilenes and disilynes has been well documented in the several comprehensive reviews, this chapter focuses on the reactions of stable functional disilenes together with new reactions of disilenes that have been found after 2004.

3.1 Unimolecular Reactions

3.1.1 Dissociation into Two Silylenes

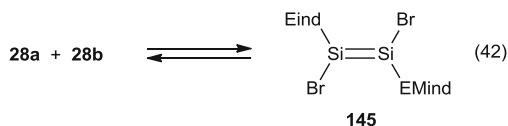
Dissociation of Si=Si double bond into two silylenes is one of the fundamental unimolecular reactions. Dissociation of functional disilenes should be important because it works as a “masked” silylene to provide highly reactive functional silylenes that should be useful for new building block for unsaturated silicon compounds. According to the CGMT (Carter–Goddard–Malrieu–Trinquier) model [40–42], which is generally accepted as a theoretical model for description of the Group 14 double bonds, the bond dissociation energy (BDE) of the Si=Si double bond in disilenes depends on the singlet–triplet energy gap of the corresponding silylene (ΔE_{st}): $BDE = E_{\sigma} + E_{\pi} - 2\Delta E_{st}$ where E_{σ} and E_{π} are σ bond and π bond energies of Si=Si double bond, respectively. Silylenes with electronegative and π -donating substituents such as halogen, NR_2 , and OR are calculated to have larger ΔE_{st} , and the corresponding disilenes are predicted to have smaller BDE [95]. Although facile dissociations of Si=Si double bond into two silylenes have already been extensively discussed in the previous comprehensive reviews [2, 4], functional disilenes provide new insight into the dissociation of the Si=Si double bond.

1,2-Dibromodisilenes **28a** and **28b** dissociate into the corresponding arylbromo-silylenes **143a** and **143b**, which is confirmed by trapping reaction with bis(trimethylsilyl)acetylene giving the corresponding [1+2] adducts **144** (Scheme 23) and the crossover reaction of disilenes **28a** and **28b** giving unsymmetrical disilene **145** (Eq. 42) [39]. Although arylbromosilylenes **143a** and **143b** are not observed spectroscopically, equilibrium between disilenes and silylene–PPy complexes **146a** and **146b** were observed in the presence of 4-pyrrolidinopyridine (PPy) with equilibrium constants K_{eq} of $350 M^{-1}$ for R = Eind and $0.64 M^{-1}$ for R = EMind. Silylene–PPy complex **146a** was isolated in crystalline form. Facile dissociation of the 1,2-dibromodisilenes was supported by DFT calculations. The bond dissociation enthalpy (BDE) of the Si=Si double bond in (H₂Mind)

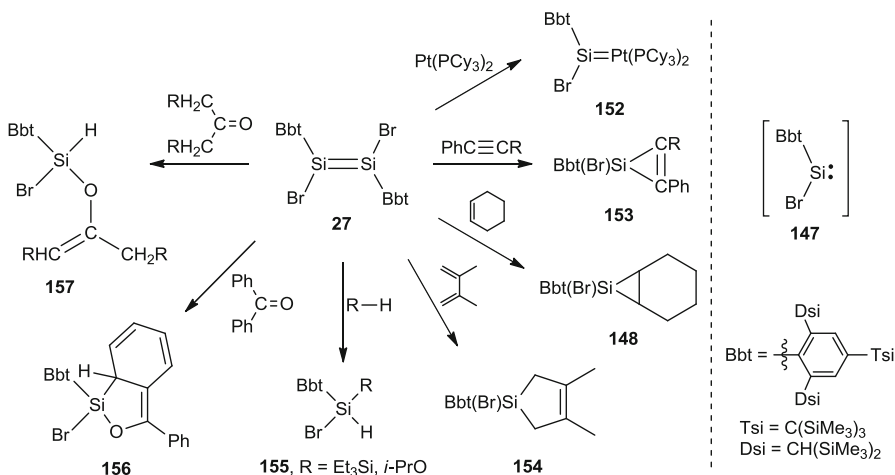


Scheme 23

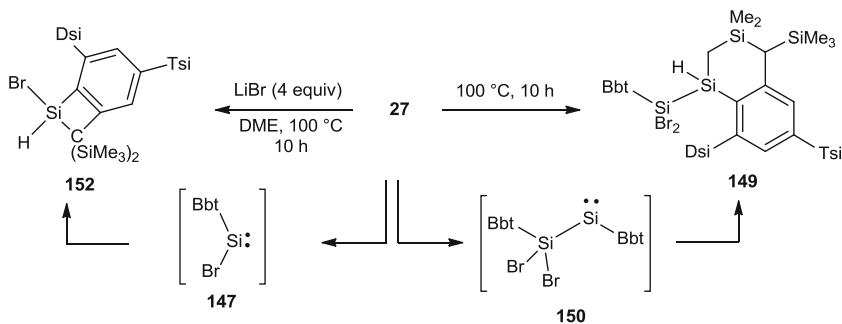
$\text{BrSi}=\text{Si}(\text{H}_2\text{Mind})\text{Br}$ of $19.2 \text{ kcal mol}^{-1}$ at the B3LYP/6-31G(d,p) level is lower than those of $(\text{H}_2\text{Mind})\text{PhSi}=\text{SiPh}(\text{H}_2\text{Mind})$ ($34.0 \text{ kcal mol}^{-1}$) and $\eta^1\text{-Cp}^*\{(\text{Me}_3\text{Si})_2\text{N}\}\text{Si}=\text{Si}\{\text{N}(\text{SiMe}_3)_2\}(\eta^1\text{-Cp}^*)$ **44** ($23.2 \text{ kcal mol}^{-1}$). Electronic effects of electronegative and π -donative bromo substituents would be responsible for these results as mentioned in the previous paragraph [95].



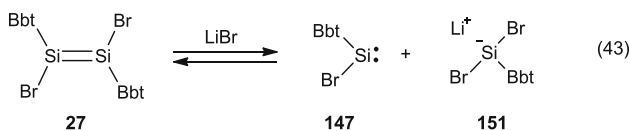
Sasamori, Tokitoh, and coworkers found that lithium bromide promotes the dissociation of Si=Si double bond of 1,2-dibromodisilene $\text{Bbt}(\text{Br})\text{Si}=\text{SiBbt}(\text{Br})$ (**27**). Disilene **27** reacted with excess amount of various reagents at room temperature in benzene to give products identical to the products of $\text{Bbt}(\text{Br})\text{Si}:$ (**147**) instead of simple trapping products of disilene **27** (Scheme 24) [96]. Interestingly, the presence of lithium bromide accelerates the formation of the silylene adducts. For instance, while disilene **27** reacts with cyclohexene (6 equiv) in DME at room temperature for 24 h to give silacyclopropane **148** quantitatively, this reaction was completed in the presence of excess lithium bromide (10 equiv) within only 7 min. Furthermore, thermolysis of disilene **27** in the absence of lithium bromide in C_6D_6 at 100°C for 10 h gave **149**, an intramolecular insertion product of disilene **27** that would result from 1,2-bromine migration across the Si=Si double bond followed by C–H insertion of the resulting aryl(dibromosilyl)silylene **150**. In contrast, thermolysis of **27** in the presence of 4 equiv of lithium bromide gave **152**, the intramolecular insertion product of $\text{Bbt}(\text{Br})\text{Si}:$ (**147**) (Scheme 25). The silylene-like reactivity of disilene **27** is proposed to be due to a trace amount of lithium bromide that promotes dissociation of disilene **27** into silylene **147** and silylenoid **151**, although both **147** and **151** have not been observed spectroscopically (Eq. 43).



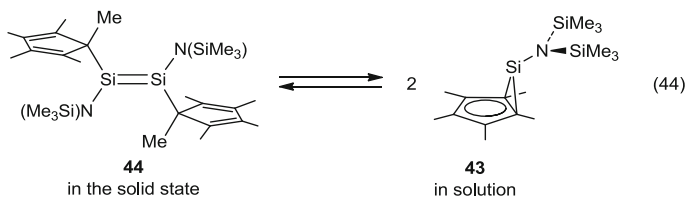
Scheme 24



Scheme 25

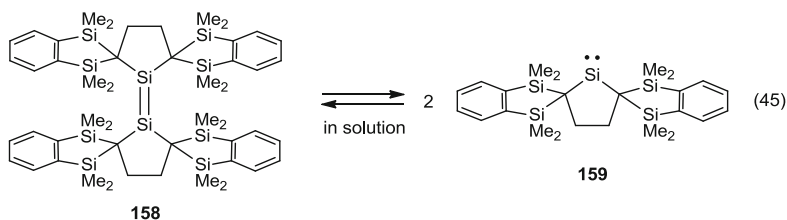


Jutzi found reversible phase-dependent transformation between disilene **44** and divalent silicon compound **43** (Eq. 44) [49]. Compound **43** is a colorless oil and it exists as a monomeric form in solution. Upon crystallization it slowly dimerizes to give yellow crystals of disilene **44**. When disilene **44** dissolved in organic solvents, a colorless solution of **43** was again obtained. This phenomena is explained by different stereoelectronic and steric effects exerted by the pentamethylcyclopentadienyl groups in **44** and **43**, unspecified lattice effects in the solid-state structure of **44**, a small energy difference between **44** and **43**, a low activation energy for the equilibrium process, and the gain in entropy upon monomer formation.



Very recently tetraalkyldisilene **158** is found to equilibrate with the corresponding dialkylsilylene **159** in solution (Eq. 45) [97]. The equilibrium in solution was observed by NMR and UV-vis spectroscopies, and the thermodynamic parameters of the equilibrium were estimated to be $\Delta H = 36 \pm 3 \text{ kJ mol}^{-1}$ and $\Delta S = 170 \pm 15 \text{ J mol}^{-1} \text{ K}^{-1}$. Notable structural characteristics of **158** include the long $\text{Si}=\text{Si}$ distance of $2.252(3) \text{ \AA}$ and the twist angle of 22.6° . The three-coordinate silicons adopt a slightly pyramidalized geometry with the *trans*-bent angle β of 17.5° . The $\text{Si}=\text{Si}$ distance is near the longer end of the reported range [$2.132(2)$ - $2.2890(14) \text{ \AA}$]. These structural features can be rationalized by

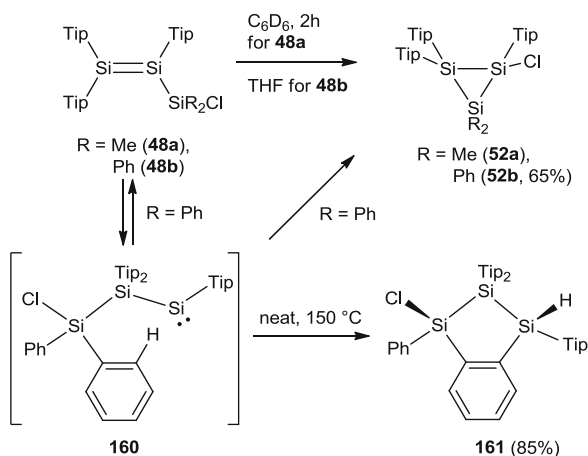
the severe steric repulsion between the silylene moieties. The ^{29}Si NMR spectrum of **158** at -80°C in toluene- d_8 showed the resonance of sp^2 -silicon appeared at 123.3 ppm. Analysis of the percent buried volume ($\%V_{\text{bur}}$), a measure of the steric demand around the central silicon, showed that the flexible steric bulkiness of the alkyl substituent in **158** and **159** allows the reversible dimerization and the isolation of both species.



Dissociation of $\text{Si}=\text{Si}$ double bond in tetrasiladiene **88** gave cyclotrisilene **127** (Scheme 21, Sect. 2.6.1).

3.1.2 1,2-Migration Giving Silylsilylene

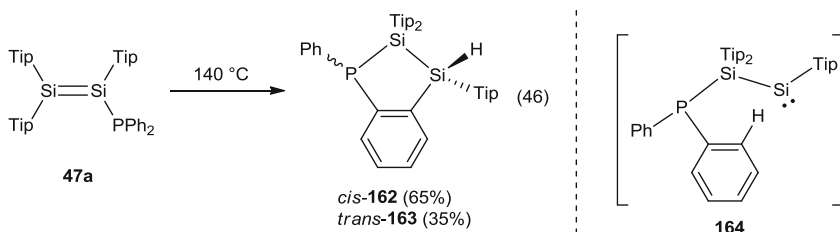
Disilene–disilanylsilylene rearrangement ($\text{R}_2\text{Si}=\text{SiR}(\text{SiR}'_3) \rightarrow [(\text{R}'_3\text{Si})\text{R}_2\text{Si}]\text{RSi}$) through 1,2-silyl migration was found for reactions of transient and stable disilenes. In Sect. 2.6, ring expansion reactions of silylenecyclotetrasilane to cyclopentasilene were explained by a stepwise disilene–disilanylsilylene rearrangement. In some isomerization reactions of silyl-substituted disilenes, the disilene–disilanylsilylene rearrangement seems to be involved. For instance, chlorosilyl-substituted disilene **48b** isomerizes to the corresponding chloro-substituted cyclotrisilane **52b**, which was



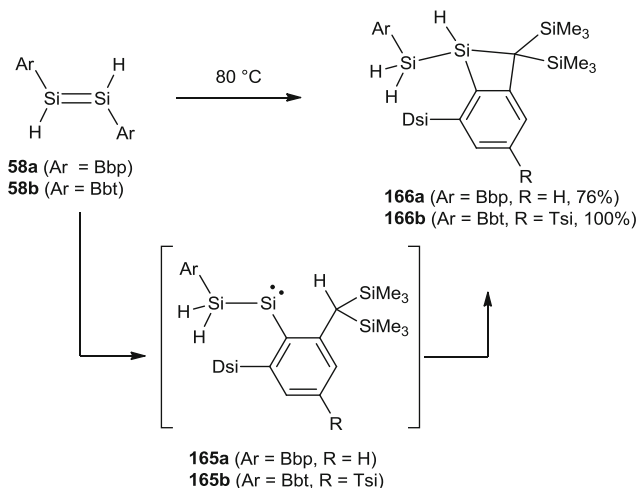
Scheme 26

explained by 1,2-migration of chlorosilyl group over Si=Si double bond giving a disilanyldisilene **160** followed by Si–Cl insertion reaction of the resulting silylene (Scheme 26). When the reaction was performed at 150°C without solvent, trisilaindane **161**, which was explained by a C–H insertion reaction of disilanyl-silylene **160**, was obtained [53].

Upon heating phosphinyl-substituted disilene **47a**, similar phosphadisilaindanes **162** and **163** were obtained probably resulting from 1,2-migration giving disilanyl-silylene **164** followed by insertion of the silylene into one ortho C–H bond of one of phenyl group on the phosphinyl substituent (Eq. 46) [43].



A similar migration was also found in 1,2-dihydrodisilenes **58** (Scheme 27).

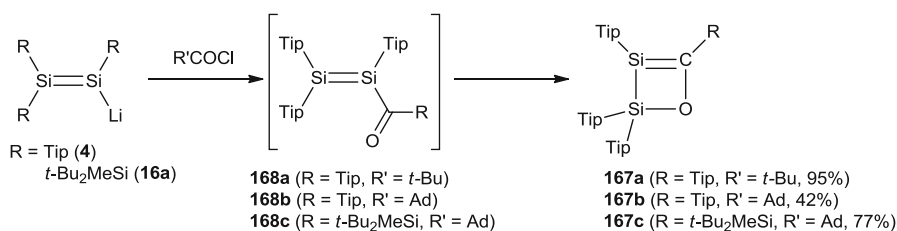


Scheme 27

3.2 Bimolecular Reactions

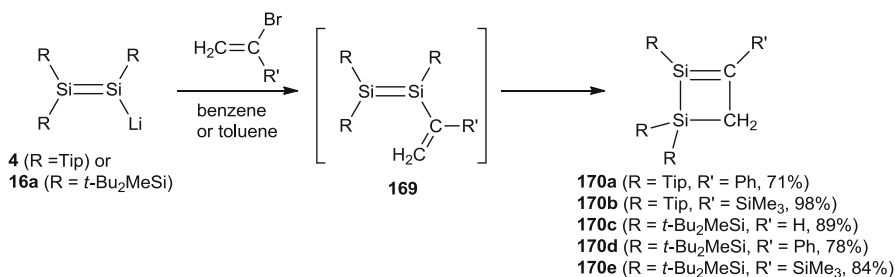
3.2.1 Electrophilic Substitution: Reactions of Disilenides with Electrophiles

In Sect. 2, various reactions of disilenides with electrophiles giving a variety of new disilenes have been mentioned. Reactions of disilenides with some ketones gave new unsaturated silicon compounds via multistep reactions. For instance, reactions of disilenides **4** and **16a** with carboxylic acid chlorides gave cyclic silenes **167a–c**. Formation of new silenes **167a–c** was explained by initial formation of acyl disilenes **168a–c**, which were not observed even at low temperatures, followed by [2+2] cyclization (Scheme 28) [98, 99].



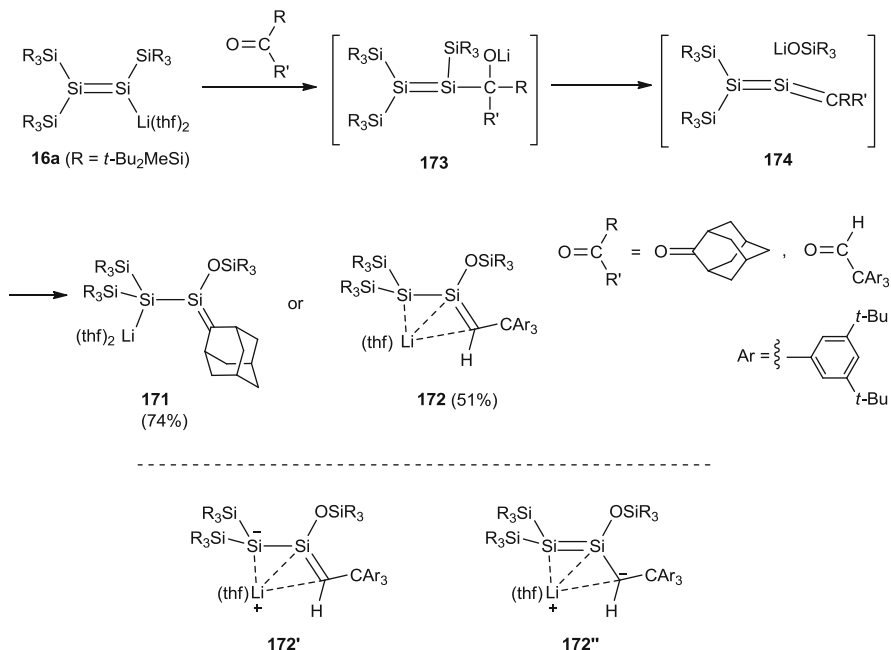
Scheme 28

Similar stepwise addition–cyclization reactions giving silene derivatives were found in the reaction of disilenide with vinyl halides (Scheme 29) [99, 100].



Scheme 29

Silyl-substituted disilenide **16a** undergoes sila-Peterson-type reactions. Reaction of **16a** with adamantanone gave a silyl-anion-substituted silene (1,2-disilaallyl anion) **171** in 74% yield (Scheme 30) [98]. When triarylacetaldehyde was used, similar reaction occurred to give the corresponding silene **172** in 51% yield [99]. Formation mechanism of silenes **171** and **172** can involve nucleophilic addition of sp² silyl anion of disilenide to the carbonyl carbon giving **173** followed by



Scheme 30

elimination of siloxylithium to give 1,2-disilaallene **174**. Because of less steric hindrance of the disilaallenes, the resulting siloxylithium adds to the Si=Si double bond of **174** to give the silenes.

Interestingly, structure of **172** in solution changes depending on the solvents. In THF-*d*₈, **172** exists as η^1 -fashion similar to **171**. In toluene-*d*₈ and in the solid state, **172** exists as a η^3 -disilaallyllithium structure having an intramolecular interaction between lithium and Si=C moiety. According to the structural features of **172** including shorter Si=C bond length [1.755(2) Å] and typical Si-Si bond length [2.3356(8) Å], resonance structure **172'** is favored to **172''**.

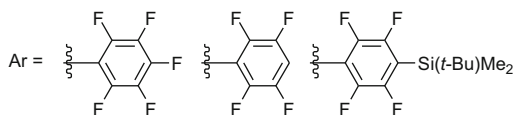
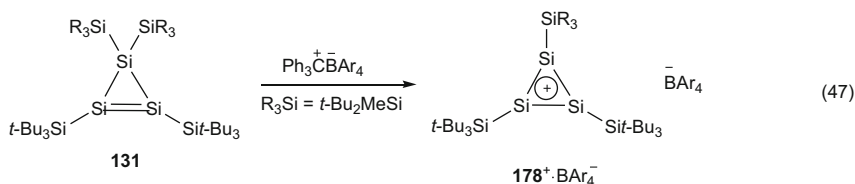
3.2.2 Nucleophilic Substitution: Reactions of Halodisilenes with Nucleophiles

As shown in Sect. 2.3.1, reactions of halodisilenes with nucleophiles are very useful methods to introduce various substituents to the sp² silicons in disilenes similar to the reactions of disilenides with electrophiles. Although the mechanism of the substitution reactions remains open, addition-elimination process where 1,2-addition of alkyl (or aryl) metal species (R'-M) toward Si=Si double bond followed by 1,2-elimination of metal halides MX is proposed as a possible mechanism because facile 1,2-addition of alkyllithium to the Si=Si double bond of

The one-electron oxidation of disilene **17** results in 2.1% stretching (2.307(2) Å) and more twisting (64.9°) of Si=Si double bond compared with those of neutral disilene **17** (2.2598(18) Å and 54.5°) and a nearly planar geometry around both three-coordinate silicon atoms [104]. The highly twisted geometry is explained by effective $\sigma[\text{Si}(\text{sp}^2)-\text{Si}(\text{sp}^3)]-\pi$ hyperconjugation and supported by elongation of $\sigma[\text{Si}(\text{sp}^2)-\text{Si}(\text{sp}^3)]$ and theoretical calculations on model compounds [103]. The EPR spectrum of **175** shows a singlet signal ($g = 2.0049$) accompanied by a doublet satellite signal due to ^{29}Si nuclei of the double bond. The hyperfine coupling constant (hfcc) of 2.30 mT is less than half that of related three-coordinate silyl radical (*t*-Bu₂MeSi)₃Si[•] (5.80 mT) [105], suggesting that the unpaired electron is delocalized over three-coordinate silicon atoms. One-electron reduction similarly results in 3.6% elongation (2.341(5) Å) and much more twisting (88°) of the Si–Si double bond. However, the geometry around one of the three-coordinate silicon atom is nearly planar and that of the other silicon atoms is considerably pyramidalized, which shows that the former silicon atom has a radical character, while the other silicon atom has a silyl anion character. Accordingly, the EPR spectrum of **176** shows a rapid spin exchange between two three-coordinate silicon atoms on the EPR timescale. At higher temperature, **176** shows a singlet signal ($g = 2.0061$) accompanied by a doublet satellite signal with hfcc of 2.45 mT, while at 120 K the hfcc of the satellite signal is 4.50 mT indicating the rapid spin exchange in contrast to delocalization observed in cation radical **175** [104].

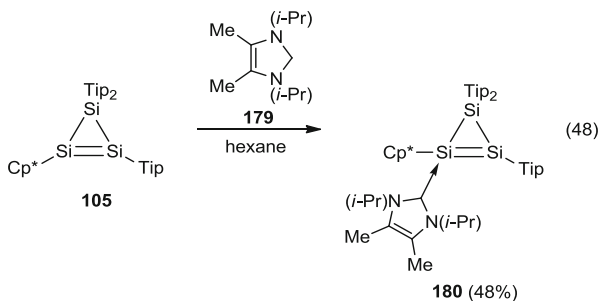
Interestingly, when disilene **17** was oxidized by Et₃Si⁺ instead of Ph₃C⁺, cyclotrasilylium cation **177**⁺ was obtained instead of radical cation of **17** [106] (Scheme 31). Although the mechanism for the formation of **177**⁺ remains open, possible mechanism was proposed to involve abstraction of methyl group by Et₃Si (C₆H₆), cyclization, and migration of silyl substituent. X-ray analysis shows that **177**⁺ exists as a free silylium ion and the four-membered ring are folded with the fold angle of 28(2)°. The geometry around each of the three-coordinate silicon atoms is almost planar and the distances between the unsaturated silicon atoms of 2.2266(10) and 2.2187(10) Å are intermediate between Si=Si bond distances and Si–Si single-bond distances. The ^{29}Si resonances due to the terminal silicon atoms in the cationic part (δ_{Si} 286.8) are low-field shifted compared to that of the central silicon atom (δ_{Si} 183.8). The structural parameters, ^{29}Si resonances, and theoretical calculations are consistent with a trisilaallyl cation character.

Silyl-substituted cyclic disilene **131** undergoes elimination of the substituents upon oxidation to give the corresponding delocalized silyl cations. Cyclotrisilene **131** reacts with trityl cation in toluene and gave the corresponding silicon version of cyclopropenylium cation, cyclotrisilylium cations **178**⁺ (Eq. 47). In the single crystals of **178**⁺TSFPB[−] (TSFPB[−] = B[−]{C₆F₄-4-[SiMe₂(*t*-Bu)]₄), the closest distance between the ring silicon atoms of **178**⁺ and F atoms in TSFPB is 6.017 (9) Å, which is out of the range of a significant interaction and indicates that **178** is a free silyl cation. The Si–Si distances in the three-membered ring of 2.211(2)–2.221(3) Å are intermediate between the Si=Si double bond [2.1612(8) Å] and the Si–Si single bond [2.3694(8) and 2.3762(8) Å] of cyclotrisilene **131**. The geometry around the three-coordinate silicon atoms in the three-membered ring is almost planar, strongly suggesting that **178**⁺ is a persilaaromatic compound.

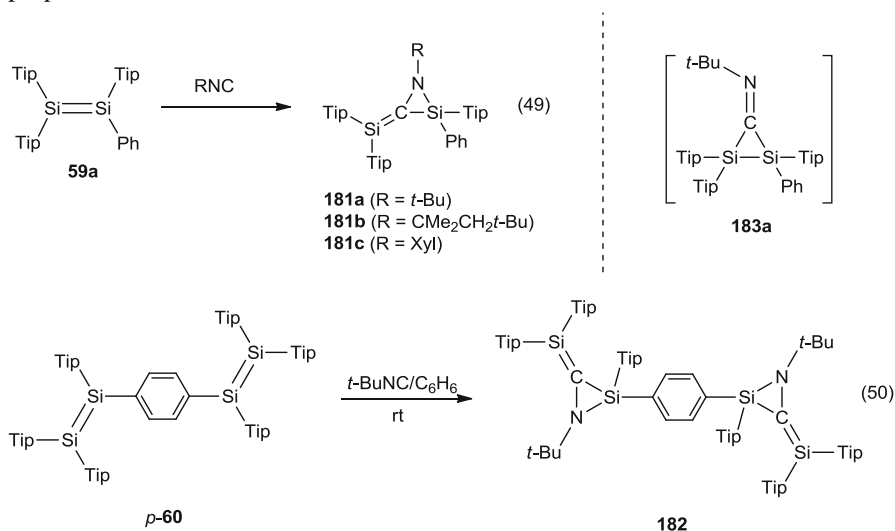


3.2.4 Coordination of Lewis Bases

Because of the low-lying LUMO of disilenes, the Si=Si double bond in disilenes are attacked by various nucleophiles such as water, alcohols, and amines. Recently, Scheschkewitz found that *N*-heterocyclic carbenes (NHC) can reversibly coordinate to the three-coordinate silicon atom of disilene [28]. Reaction of cyclotrisilene **105** with imidazol-2-ylidene **179** in hexane gave 1:1 adduct **180** as red crystals in 48% yield (Eq. 48). X-ray analysis shows that carbene **179** coordinates to the Cp*-substituted unsaturated silicon atom which are predicted to be positively charged. The Si-C(NHC) distance of 1.9843(14) Å is relatively long compared with those of **138** [1.9221(16) Å] [94] and **137** [1.9271(15) Å] [93]. Coordination of the carbene results in elongation of the Si=Si double bond [2.2700(5) Å; calculated Si=Si distance of **105** is 2.13362 Å] and pyramidalization of double-bond silicon atoms with the sums of the bond angles of 317° at Si(Cp*)(NHC) and 340° at Si(Tip). The ²⁹Si resonances of the unsaturated silicon nuclei [−85.6 ppm for Si(Cp*)(NHC) and −61.5 ppm for Si(Tip)] and ¹³C resonance of the unsaturated carbon nucleus (161.4 ppm) in **180** are considerably upfield shifted by complexation compared with those of **105** (57.7 ppm and 37.1 ppm) and free **179** (205.7 ppm). A variable temperature NMR study shows that **180** dissociates into **105** and **179** in solution and the free energy for the dissociation process at 298 K is estimated to be 9 kJ mol^{−1}.



In a related work, very recently Scheschkewitz and coworkers have found the reversible reactions of disilenes **59a** and *p*-**60** with isocyanides giving disilamethyleneaziridine derivatives **181a–c** and **182** as shown in Eqs. (49) and (50) [107]. During formation of **181a**, [1+2] cycloadduct, disilacyclopropanimine **183a** was observed at low temperature by NMR spectroscopy. On the basis of DFT calculations, a donor–acceptor complex of **59a** and *t*-BuNC similar to **180** is proposed as a transition state.

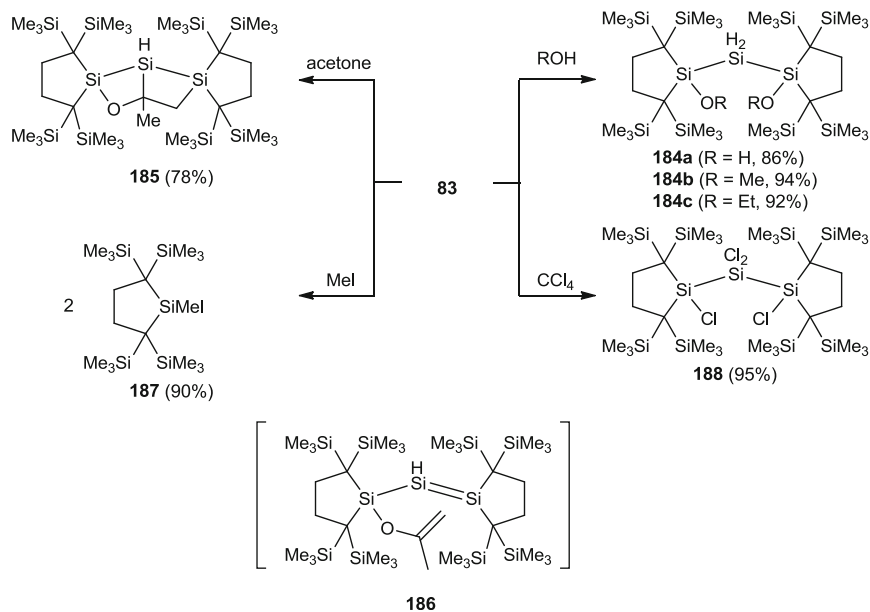


Marschner have observed the formation of adduct of tetrasilylidisilene (Me₃Si)(*i*-Pr₃Si)Si=Si(SiMe₃)(Si*i*-Pr₃) (see compound **193** in Table 1) with KF and CeF [108].

3.2.5 Addition Reactions with Two or More Si=Si Double Bonds

Although simple 1,2-addition reactions across Si=Si double bond have been well summarized in nice reviews of disilenes, addition toward compounds with two or more Si=Si double bond such as trisiladiene (trisilaallene) and tetrasiladiene provides further insight into the addition toward multiple bonds with silicon.

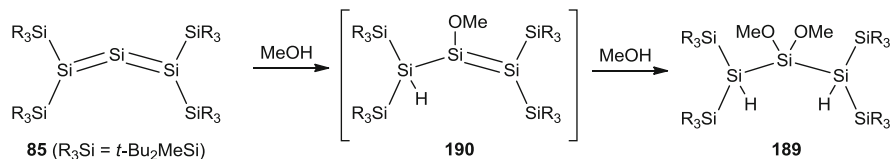
Trisilaallene **83** bearing two cumulative Si=Si double bonds reacted with ROH (R = H, Me, Et) gave the corresponding adduct **184a–c** where ROH groups are connected at the terminal silicon atoms (Scheme 32) [109]. The regioselective formation of **184a–c** can be explained by a stepwise addition of ROH to a polar Si=Si double bond of **83** where terminal silicon atoms are calculated to be positively charged (R₂Si^{δ+}=Si^{δ-}=Si^{δ+}R₂). Complete chlorination of two Si=Si double bond occurred upon treatment with carbon tetrachloride to form **188**. Interestingly, **83** reacted with acetone to give bicyclic adduct **185** in good yield. Formation of **185** would be explained by the initial ene reaction of one of the Si=Si



Scheme 32

bond in **83** with acetone giving **186**, followed by [2+2] cycloaddition of the other Si=Si double bond and the C=C double bond in **186**. In the reaction with methyl iodide, 2 equiv of adduct **187**, which is formally regarded as the Si=Si bond cleavage product, are obtained.

On the other hand, the reactivity of silyl-substituted trisilaallene **85** toward alcohols is different from that of alkyl-substituted trisilaallene **83**. Trisilaallene **85** reacts with MeOH to form the 3,3-dimethoxypentasilane derivative **189** as a single product in 42% yield (Scheme 33).



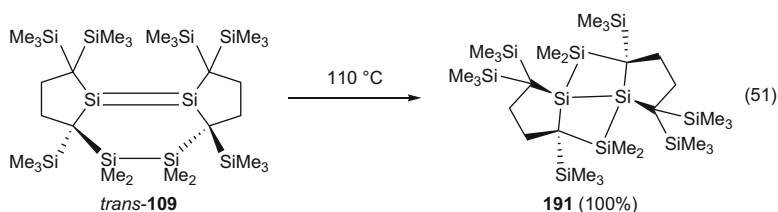
Scheme 33

The formation of **189** can be understood as a sequential addition of methanol to **85** and disilene **190**. Charge distribution of **85**_{opt} (an optimized structure of **85** at the B3LYP/6-31G(d) level, see also Sect. 2.5.1) can explain the observed regioselectivity. The calculated atomic charges (−0.36 and −0.37 for the terminal silicons and −0.08 for the central silicon atom) in **85**_{opt} suggests the charge distribution of R₂Si^{δ−}=Si^{δ+}=Si^{δ−}R₂ which reasonably leads to the formation of intermediate

190 by the initial addition of **85** with methanol. Because of a resonance structure of **190**, the second addition of **190** with methanol would afford **189**.

3.2.6 Miscellaneous

The increased diversity of disilenes enables the discovery of new, unusual, and interesting reactions. Interestingly, *trans*-**109** isomerized stereospecifically to tetracyclic compound **191** in 100% yield upon heating at 110 °C in xylene-*d*₁₀ or in the solid state (Eq. 51) [85]. The activation parameters for the isomerization are $\Delta H^\ddagger = 19.0 \pm 1.2 \text{ kcal mol}^{-1}$ and $\Delta S^\ddagger = -21 \pm 3 \text{ kcal mol}^{-1}$. The largely negative ΔS^\ddagger may rule out multistep mechanisms involving cleavage of the Si–Si bond or the Si=Si bond. Stereospecific formation of tetracyclic compound **191** and the activation parameters show that this isomerization is an unprecedented symmetry-allowed thermal [2s+2a] intramolecular cycloaddition between Si=Si double bond and Si–Si single bond.



4 Outlook

In this decade, the diversity of the structure and reactivity of disilenes have dramatically increased, and stable disilenes began to be used as unique π electron units for functional materials, e.g., in electroluminescent devices. This indicates that disilenes as well as other unsaturated silicon compounds are evolving from fundamentally interesting molecules to useful and unique π electron units. Further efforts to exploit the feature of silicon π electron compounds are anticipated not only to establish deeper understanding of structure, bonding, reactivity, and functionality of the multiply bonded compounds of main group elements but also in order to contribute to the development of brand-new functional materials such as nanostructured materials, molecular catalysts for useful transformation reactions, small molecule activators, and organic–inorganic hybrid materials.

Table 1 (continued)

| | | | | Metric parameters around Si=Si bond | | UV-vis | Reference | | | |
|-----------------------------------|----------------|------------------|-----------------------------------|--|--|---|----------------------------|--|--------------------------------|-----------------------|
| R ¹ | R ² | R ³ | R ⁴ | $\delta(\text{Si})$ in C ₆ D ₆ ^d at rt | $d(\text{Si}=\text{Si})/\text{\AA}$ | <i>trans</i> -Bent angle, β /deg | Twist angle τ /deg | $\lambda_{\text{max}}/\text{nm}$ (ϵ) in hexane ^d at rt | Habit (mp/°C) | Reference (CCDC#) |
| Si(<i>i</i> -Pr)Dsi ₂ | H | NPh ₂ | Si(<i>i</i> -Pr)Dsi ₂ | 46d | 66.6 (¹ <i>J</i> (Si,H) = 160 Hz, Si ³), 136.4 (Si ⁴) | 14.5 (Si ³) | | 339 (2250), 440 (4430) | Orange crystals (161) | [51] (CCDC-770876) |
| Tip | Tip | Tip | PPh ₂ | 47a | 96.5 (² <i>J</i> (Si,P)=77 Hz, Si ³), 54.4 (¹ <i>J</i> (Si,P)= 116 Hz, Si ⁴) | | | 423 (18380) | Orange crystals (135) | [43] |
| Tip | Tip | Tip | P(<i>i</i> -Pr) ₂ | 47b | 96.6 (br. ² <i>J</i> (Si,P) = ca. 60 Hz, Si ³), 53.2 (¹ <i>J</i> (Si,P) = 118 Hz, Si ⁴) | | | | Orange-yellow solid | [43] |
| Tip | Tip | Tip | PCy ₂ | 47c | 95.4 (br. ² <i>J</i> (Si,P) = ca. 60 Hz, Si ³), 52.5 (br., ¹ <i>J</i> (Si,P) = ca. 115 Hz, Si ⁴), 98.8 (² <i>J</i> (Si,P) = 89 Hz, Si ³), 53.0 (¹ <i>J</i> (Si,P) = 133 Hz, Si ⁴) | 8.9 (Si ³), 7.7 (Si ⁴) | 1.8 | 416 (18970) | Orange crystals (140) | [43] (CCDC-768711) |
| Tip | Tip | Tip | P(<i>t</i> -Bu) ₂ | 47d | | | | | Orange-yellow solid | [43] |
| Tip | Tip | Tip | SiMe ₂ Cl | 48a | 103.0 (Si ³), 39.9 (Si ⁴) | | | | Orange crystals | [53] |
| Tip | Tip | Tip | SiPh ₂ Cl | 48b^a | ¹ <i>J</i> (Si,Si) = 123 Hz 109.1 (Si ³) 35.5 (Si ⁴) ¹ <i>J</i> (Si,Si) = 120 Hz | 17.3 (Si ³), 25.0 (Si ⁴), 7.1, 8.2, | | 427(24800) | Orange crystals (134, dec.) | [53] (CCDC-691791) |

Table 1 (continued)

| | | R ¹ R ² R ³ R ⁴ Si ^a =Si ^b | | $\delta(\text{Si})$ in C ₆ D ₆ ^d at rt | Metric parameters around Si=Si bond | | | UV-vis $\lambda_{\text{max}}/\text{nm}$ (ϵ) in hexane ^e at rt | Habit (mp/°C) | Reference (CCDC#) |
|------|--------|---|---|--|---|--|---|--|---|-----------------------|
| | | | | | $d(\text{Si}=\text{Si})/\text{\AA}$ | <i>trans</i> -Bent angle β/deg | Twist angle τ/deg | | | |
| Tip | Tip | Tip | Ph | 59a | 2.175(1) | 22.0 (Si ^a), 22.8 (Si ^b) | 1.5 | 439 (19000) | Bright-yellow crystals (156–157, dec.) | [59] (CCDC-643816) |
| Tip | Tip | Tip | 4-FC ₆ H ₄ | 59b ^b | 2.1468(8), 2.1536(8), 2.1417(8), 2.1462(8) | 4.9 (Si ^{a1}), 2.9 (Si ^{b1}), 15.8 (Si ^{a2}), 9.3 (Si ^{b2}), 1.3 (Si ^{a3}), 8.1 (Si ^{b3}), 1.4 (Si ^{a4}), 1.8 (Si ^{b4}) | 1.5, 2.6, 2.7, 0.9 | 437 (16800) | Orange crystals (143–145, dec.) | [60] (CCDC-821133) |
| Tip | Tip | Tip | 4-ClC ₆ H ₄ | 59c | 2.1735(4) | 15.8 (Si ^a), 23.8 (Si ^b) | 1.3 | 445 (19200) | Orange crystals (145–147, dec.) | [60] (CCDC-821134) |
| Tip | Tip | Tip | 4-BrC ₆ H ₄ | 59d | 2.1707(5) | 16.2 (Si ^a), 24.5 (Si ^b) | 0.4 | 447 (16200) | Orange crystals (143–145, dec.) | [60] (CCDC-821135) |
| Tip | Tip | Tip | 4-IC ₆ H ₄ | 59e | 70.7 (Si ^a), 56.8 (Si ^b) | | | | No isolation | [60] |
| Tip | Tip | Tip | 4-SiMe ₂ C ₆ H ₄ | 59g | 71.5 (Si ^a), 56.5 (Si ^b) | | | | | [60] |
| Eind | Ph | Ph | Eind | 62 | 2.1593(16) | 2.7 | 0 | 461 (24000) | Orange powder (286–290, dec.) | [17] (CCDC-673565) |
| Eind | 2-Naph | 2-Naph | Eind | 67a ^c | 2.1623(18) | 5.4 [<i>s</i> -cis], 15.2 [<i>s</i> -trans] | 0 [<i>s</i> -cis], [<i>s</i> -trans] | 504 (25000) [THF] | Red powder (282–285) | [62] |

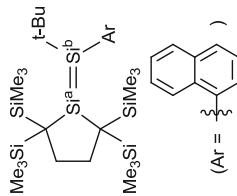
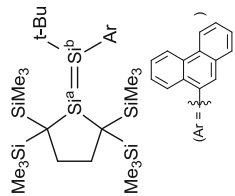
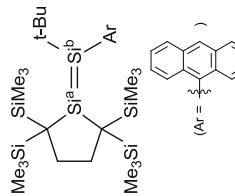
2.1667
(12)
[*s*-trans]

| Eind | M ₂ F] | M ₂ F] | Eind | 67b^c | 60.4 | 2.149(5) [s-cis], 2.1531 (13) [s-trans] | 4.3 [s-cis], 4.4 [s-trans] | 0 [s-cis, s-trans] | 510 (30000) [THF] | Red powder (284–287) | [62] |
|---|----------------------|---|---|-----------------------------|---|---|--|-----------------------|---|---------------------------------------|------------------------|
| Tip | Fc | Fc | Tip | 68a | 72.6 | 2.1733(15) [s-trans] | 27.9 | 0 | 332 (5900), 427 (24000) | Red crystals (160–163) | [65] |
| Tip | Rc | Rc | Tip | 68b | 70.6 | 2.1851(12) | 32.3 | 0 | 340 (5000), 430 (22000) | Light-yellow crystals (180–183) | [66] (CCDC-712630) |
| Bbt | M ₂ SiC≡C | M ₂ SiC≡C | Bbt | 69a | 44.6 | 2.202(2) | 8.9 | 0 | 437 (24000) | Yellow crystals (251, dec.) | [67] (CCDC-770194) |
| Bbt | PhC≡C | PhSiC≡C | Bbt | 69b | 42.6 | 2.1871(10) | 11.3 | 0 | 469 (31000) | Orange crystals (280–282) | [67] (CCDC-770195) |
| NHC | Lone pair | Lone pair | NHC | 137 | 224.5 | 2.2294(11) | | 0 | 466 [THF] | Dark-red block crystals | [93] (CCDC-687305) |
| Si(<i>i</i> -Pr) ₂ Dsi ₂ | NHC | Lone pair | Si(<i>i</i> -Pr) ₂ Dsi ₂ | 138 | 28.7 (Si ^a), 276.3 (Si ^b) [THF- <i>d</i> ₆] | 2.1989(6) | 9.2 (Si ^a) | | 300 (14000), 409 (10000), 440 (sh, 6000) | Brown crystals (141–142 dec.) | [94] (CCDC-829664) |
| Si(<i>i</i> -Pr) ₂ Dsi ₂ | NHC | Si(<i>i</i> -Pr) ₂ Dsi ₂ | ZnCl ₂ | 138 ZnCl₂ | 66.9 (Si ^a), 190.8 (Si ^b) [THF- <i>d</i> ₆] | 2.2006(13) | 4.9 (Si ^a), 17.7 (Si ^b) | 15.5 | 425 (4400) [THF] | Yellow solid (144–146, dec.) | [94] (CCDC-829665) |
| Eind | Br | Br | EMind | 145 | 71.6, 74.8 | | | | | Exist only in solution | [39] |
| EMind | Ph | Ph | EMind | 192 | 65.0 | | | | 451 (24000) | Yellow solid (336–338) | [39] |
| Si(<i>i</i> -Pr) ₃ | SiMe ₃ | SiMe ₃ | Si(<i>i</i> -Pr) ₃ | 193 | 147.1 | 2.1967(11) | 11.9 | 0 | | Orange crystals | [108] (CCDC-661271) |

^aCrystallographically two independent molecules exist^bCrystallographically four independent molecules exist^c*s-cis* and *s-trans* isomers exist in the same position^dUnless otherwise noted

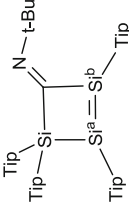
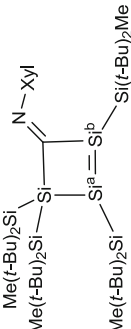
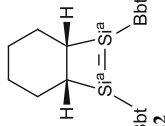
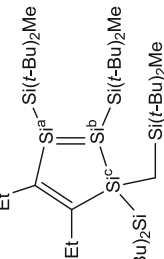
Table 2 Properties and structural parameters of cyclic disilenes

| Compound | ²⁹ Si NMR $\delta(\text{Si})$ in C_6D_6 at rt | Metric parameters around Si=Si bond | | | UV-vis $\lambda_{\text{max}}/\text{nm}$ (ϵ) in hexane ^b at rt | Habit (mp/ $^{\circ}\text{C}$) | Reference (CCDC#) |
|----------|--|-------------------------------------|---|--|---|------------------------------------|----------------------|
| | | $d(\text{Si}=\text{Si})/\text{\AA}$ | <i>trans</i> -Bent angle/deg | RSi=SiR/deg and others | | | |
| | 42.5 (Si ^a) ¹ J(Si ^a , Si) = 21.1 Hz | 2.118(1) | 9.1 | 413 (4912) | Red crystalline solid (156–157) | [28] (CCDC- 872266) | |
| | 95.1 (Si ^a), 195.0 (Si ^b) | | | 291 (8100), 454 (5900) | Orange-red crystals (173–174) | [45] | |
| | 100.8 (Si ^a), 192.1 (Si ^b) | 2.1706(12) | 0.4 (Si ^a), 2.7 (Si ^b) | 294(4000), 320(2800), 463 (3200) | Orange-red crystals (164–166) | [45] (CCDC- 691557) | |
| | 105.2 (¹ J(²⁹ Si, ^{117/119} Sn) = 458/479 Hz, Si ^b), 92.5 (² J(²⁹ Si, ^{117/119} Sn) = 218/228 Hz, Si ^a) | | | | Yellow | [27] | |

| | | | | | | | |
|--|--|--|---|---------------------------------------|---|---|---------------------------|
|  <p>65a</p> | 131.8 (Si ^a), 97.7 (Si ^b) | 2.1943 (14) major 2.189(6) minor (disordered) | 2.2 (Si ^a), 23.8 (Si ^b) (major), 6.6 (Si ^a), 33.8 (Si ^b) (minor) | τ : 0.0 (major), 11.7 (minor) | 287 (8700), 342 (6500), 376 (9800) [3-MIP] | Yellow crystals (167–168, dec.) | [30] (CCDC- 732656) |
|  <p>65b</p> | 132.4 (Si ^a), 99.6 (Si ^b) | 2.209(2) | 12.9 (Si ^a), 26.7 (Si ^b) | τ : 0.7 | 304 (16100), 343 (8500), 378 (11700) [3-MIP] | Yellow crystals (192–194, dec.) | [30] (CCDC- 732657) |
|  <p>65c</p> | 123.2 (Si ^a), 85.6 (Si ^b) | 2.1754(12) | 6.9 (Si ^a), 11.4 (Si ^b) | τ : 1.0 | 525(420), 394 (19400), 373 (18900), 354 (16600) [3-MIP] | Blue-purple crystals (196–197, dec.) | [30] (CCDC- 732658) |

(continued)

Table 2 (continued)

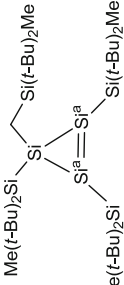
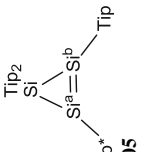
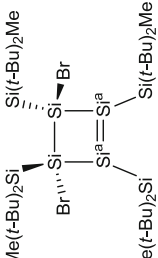
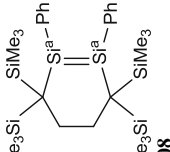
| Compound | ²⁹ Si NMR δ(Si) in C ₆ D ₆ ^b at rt | Metric parameters around Si=Si bond | | | UV-vis λ _{max} /nm (ε) in hexane ^b at rt | Habit (mp ^c /C) | Reference (CCDC#) |
|---|---|--|---|----------------------------|--|---|---------------------------|
| | | d(Si=Si)/Å | <i>trans</i> -Bent angle/deg | RSi=SiR/deg and others | | | |
|  | 82.8, 131.6 | 2.1505(6) | 5.7 (Si ^a), 5.3 (Si ^b) | Dihedral: 7.3 τ: 0.9 | 402 | Orange crystals (176) | [68] |
|  | 165.1, 173.9 | 2.1975(7) | 1.7 (Si ^a), 14.0 (Si ^b) | Dihedral: 28.5 τ: 18.2 | 455 (11000) | Dark-red crystals (175–176) | [68] |
|  | 92.3 (Si ^a) | 2.213(3) | 28.9, 26.4 | τ: 42.8 | 272 (44000), 419 (16000) | Orange-red crystals (> 118, decolorized) | [73] |
|  | 95.6 (Si ^b), 166.4 (Si ^a) | 2.1808(5) Si ^b -Si ^c : 2.3520(5) Si ^a -C: 1.8947(16) C=C: 1.367(2) | 23.8 (Si ^a), 30.3 (Si ^b) | Dihedral: 59.5, τ: 30.4 | 287 (7150), 363 (2250), 493 (6180) | Red crystals (152–154) | [37] (CCDC- 736896) |

70

71

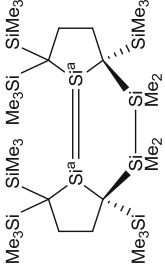
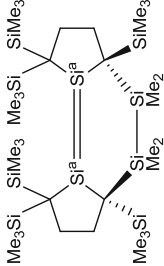
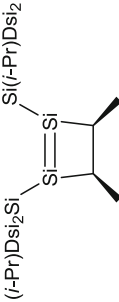
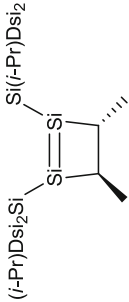
82

97

| | | | | |
|--|--|--|--|------|
|  <p>Me(<i>t</i>-Bu)₂Si—Si(<i>t</i>-Bu)₂Me Si^a=Si^a Si^a—C—C—C—Si^a Me(<i>t</i>-Bu)₂Si</p> <p>99</p> | 122.8 (Si ⁱⁱⁱ) | 274 (12700), 373 (1030), 407 (1370), 457 (2060) | Bright-orange crystals (159–161) | [80] |
|  <p>Tip₂ Si Si^a=Si^b—C—C—C—Si^a Cp* Tip</p> <p>105</p> | 37.1 (Si ^b) 57.7 (Si ^{iv}) [1,2-dimethoxyethane- <i>d</i> ₁₀] | | Orange oil | [28] |
|  <p>Me(<i>t</i>-Bu)₂Si—Si(<i>t</i>-Bu)₂Me Brⁱⁱⁱ—Si—C—C—C—Si^a Brⁱⁱⁱ—Si—C—C—C—Si^a Me(<i>t</i>-Bu)₂Si</p> <p>106</p> | 141.4 (Si ^{iv}) | 432 (3300), 326 (4700), 288 (5400), 277 (47 000). | Yellow crystals (153–155) | [83] |
|  <p>Me₃Si—SiMe₃—C—C—C—Si^a—Ph Me₃Si—SiMe₃—C—C—C—Si^a—Ph Me₃Si—SiMe₃—C—C—C—Si^a—Ph</p> <p>108</p> | 100.9 (Si ^{iv}) | 427 (8400) | Yellow crystals (>100, dec.) (CCDC- 785603) | [84] |
| | 2.1595(9) | | | |
| | 13.3, 19.1 | | | |
| | Dihedral: 32.0 τ : 15.1 | | | |

(continued)

Table 2 (continued)

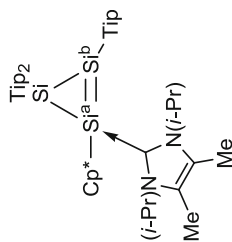
| Compound | ^{29}Si NMR $\delta(\text{Si})$ in C_6D_6 at rt | Metric parameters around Si=Si bond | | | UV-vis $\lambda_{\text{max}}/\text{nm}$ (ϵ) in hexane ^b at rt | Habit (mp/ $^\circ\text{C}$) | Reference (CCDC#) |
|--|---|-------------------------------------|---------------------------------|---------------------------------|---|---------------------------------------|---------------------------|
| | | $d(\text{Si}=\text{Si})/\text{\AA}$ | <i>trans</i> -Bent angle/deg | RSi=SiR/deg and others | | | |
|  <i>cis</i> - 109 | 128.1 (Si ^{iv}) | 2.1767(6) | 3.9, 12.4, | τ : 3.9 | 433 (8580), 353 (12800) | Yellow crystals (208, dec.) | [85] (CCDC- 609693) |
|  <i>trans</i> - 109 | 135.9 (Si ^{iv}) | 2.2687(7) | 32.9, 0.9 | τ : 42.5 | 517 (4800), 334 (6830). | Red-purple crystals (182, dec.) | [85] (CCDC- 609692) |
|  <i>cis</i> - 111 | 156.0 | | | | 234 (21880), 420 (6040) | Yellow crystals (161, dec.) | [69] |
|  <i>trans</i> - 111 | 152.1 | 2.1632(10) | 13.8, 10.9 | Dihedral: 32.2 τ : 15.8 | 237 (15490), 422 (5320) | Yellow crystals (164, dec.) | [69] (CCDC- 655096) |

| | | | | | | |
|------------|--|--|--------------------------------|--|-------------------------------|-----------------------|
| <p>112</p> | 167.4 | <i>cis</i> -Bent 1.6 | τ : 16.7 | 288 (7850) 328 (8230) 468 (14600) | Orange crystals (336) | [86] |
| <p>113</p> | 162.2 (Si ^a), 136.7 (Si ^b) | 16.9 (Si ^b), 15.0 (Si ^a) | τ : 11.7 | | Orange crystals (< 0 dec.) | [87] (CCDC-810606) |
| <p>115</p> | 150.2 (Si ^a) | 5.3, 3.1 | Dihedral: 13.6 τ : 8.8 | 448 (9100), 335 (3800), 284 (6400) | Yellow crystals (207) | [87] (CCDC-810607) |
| <p>118</p> | 70.0 (Si ^a), 130.1 (Si ^b) | | | | | [89] |
| <p>125</p> | | | | | | |

(continued)

Table 2 (continued)

| Compound | ^{29}Si NMR $\delta(\text{Si})$ in C_6D_6 at τ | Metric parameters around Si=Si bond | | | UV-vis $\lambda_{\text{max}}/\text{nm}$ (ϵ) in hexane ^b at rt | Habit (mp/ $^\circ\text{C}$) | Reference (CCDC#) |
|----------|---|---|--|---|---|-------------------------------------|---------------------------|
| | | $d(\text{Si}=\text{Si})/\text{\AA}$ | <i>trans</i> -Bent angle/deg | RSi=SiR/deg and others | | | |
| | 142.9 (Si^{II}) | 2.1428(5) | 11.8, 0.0 | Dihedral: 8.6 τ : 4.3 | 391 (4400), 277 (10800) | Yellow crystals (156–158) | [77] (CCDC- 665966) |
| | 97.4 (Si^{II}) | 2.1612(8) | 0.4, 4.9 | Dihedral: 4.8 τ : 2.4 | 472 (500), 302 (1700), 264 (3900) | Orange-red crystals (213–216) | [90] (CCDC- 279877) |
| | 167.6 (Si^{II}) | Molecule 1: 2.1874(12) Molecule 2: 2.195 | Molecule 1: 14.8, 20.3 Molecule 2: 15.1, 20.7 | Molecule 1: Dihedral: 47.7 τ : 19.1 Molecule 2: Dihedral: 48.1, τ : 21.5 | 441 (2890), 388 (1160), 337 (820) | Orange crystals (175–177) | [79] (CCDC- 623571) |
| | 123.3 (Si^{II}) [toluene- d_6 , 193 K] | 2.252(3) | 17.5 | τ : 22.6 | 441, 371, 335 [3-MP, 83K] | Orange-red crystals | [97] |



180

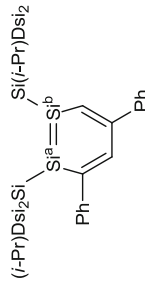
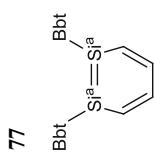
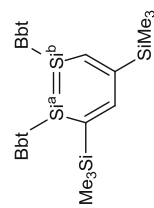
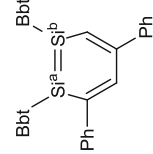
^aCrystallographically two independent molecules exist^bUnless otherwise noted

Red crystals
[28]
(CCDC-
869292)

-85.9 (Tip-Si), -85.6
(Si^a), -61.5 (Si^b)
[toluene-*d*₆]
2.2700(5)

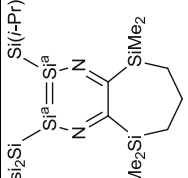
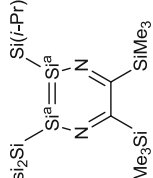
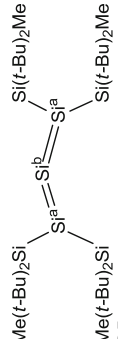
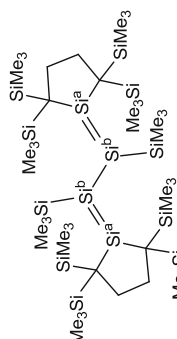
Table 3 Properties and structural parameters of disilenes with conjugative units

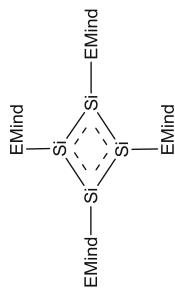
| Compound | ²⁹ Si NMR | | Metric parameters around Si=Si bond | | UV-vis $\lambda_{\text{max}}/\text{nm}$ (ϵ) in hexane ^b at rt | Habit (mp/°C) | Reference (CCDC#) |
|-------------|---|--|--|--|---|--|---------------------------|
| | $\delta(\text{Si})$ in C_6D_6 ^b at rt | $d(\text{Si}=\text{Si})/\text{\AA}$ | <i>trans</i> -Bent angle/deg | RSi=SiR'/deg and others | | | |
| | 56.8 (Si ^a), 70.7 (Si ^b) ¹ J(Si, Si) = 150.0 Hz | 2.1674(8) | 16.5 (Si ^b) 19.3 (Si ^a) | τ : 3.9 Dihedral angle with phenylene: 38.9(1) | 508 (27000) | Red crystals (~190, dec.) | [59] (CCDC- 643817) |
| p-60 | | | | | | | |
| | 54.6 (Si ^a), 72.9 (Si ^b) ¹ J(Si, Si) = 148.4 Hz | 2.1914(9) 2.1861(9) | 26.7 (Si ^{a1}) 20.2 (Si ^{b1}) 26.7 (Si ^{a2}) 20.4 (Si ^{b2}) | τ : 0.0, 0.5 Dihedral angle with phenylene 44.0, 47.7 | 450 (39000) | Orange crystals (162) | [5] (CCDC- 821136) |
| m-60 | | | | | | | |
| | Hardly soluble | 2.156(2) | 0.7 (Si ^b), 2.7 (Si ^a) | τ : 1.7 Dihedral angle with termi- nal phenyl 0.3 and 3.8 | 543 (30000), | Purple-red crystals (>255, dec.) | [17] (CCDC- 673566) |
| 61 | | | | | | | |
| | 99.2 (Si ^a) ¹ H NMR: 8.47 (s, 2H) | 2.2018(18) Endocyclic C-Si: 1.799(5) and 1.804(4) | 3.4, 4.3 | τ : 6.0 Dihedral angle: 13.1 | 246 (2548), 313 (745), 382 (240), 427 (116) | Yellow crystals (142, dec.) | [69] (CCDC- 655097) |
| 62 | | | | | | | |

| | | | |
|--|--|--|--|
|  <p>$(i\text{-Pr})\text{Dsi}_2\text{Si}^a\text{=Si}^b\text{Si}(i\text{-Pr})\text{Dsi}_2$</p> | <p>99.4 (Si^a), 106.8 (Si^b) ¹H NMR: 8.01 (s, 1H), 8.61 (s, 1H)</p> | <p>12.1, 13.7</p> | <p>Yellow crystals [69] (52 was not purified because of contamination of 51)</p> |
| <p>77</p>  <p>79a</p> | <p>57.1 (Si^a) ¹H NMR: 7.61–7.68 (m, 2H), 7.72–7.79 (m, 2H)</p> | <p>2.2334(7) Endocyclic C–Si: 1.8047 (19) and 1.806(2)</p> | <p>Light-yellow crystals (CCDC-768830) (317–318, dec.)</p> |
|  <p>79b</p> | <p>64.1, 65.4 ¹H NMR: 8.28 (s, 1H), 8.35 (s, 1H)</p> | <p>Dihedral angle: 45.6, τ: 21.3</p> | <p>Orange-yellow crystals (179, dec.) [70]</p> |
|  <p>79c</p> | <p>55.0, 61.7 ¹H NMR: 8.21 (d, ⁴J = 2.2 Hz, 1H), 8.26 (d ⁴J = 2.2 Hz, 1H)</p> | <p>378 (11000)</p> | <p>Orange, obtained as crude mixture [70]</p> |

(continued)

Table 3 (continued)

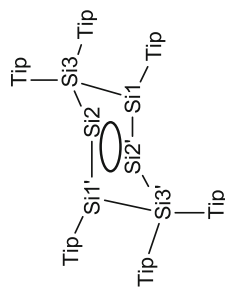
| Compound | ²⁹ Si NMR δ(Si) in C ₆ D ₆ at rt | Metric parameters around Si=Si bond | | UV-vis λ _{max} /nm (ε) in hexane ^b at rt | Habit (mp/°C) | Reference (CCDC#) |
|---|---|--|--|---|-----------------------------------|---------------------------|
| | | d(Si=Si)/Å | trans-Bent angle/deg | | | |
|  80 | 54.0 (Si ^a) | 2.2531(16) | 21.5, 21.4 | 269 (13500), 312 (10100), 403 (8000), 431 (10200), 465 (sh, 2400), 500 (sh, 1500) | Deep-red crystals (112–115) | [72] (CCDC- 734039) |
|  81 | 40.2 (Si ^a) | Endocyclic Si–N 1.679(4), 1.678(4) | τ: 49.7 Dihedral: 83.3 | | Dark-red oil | [71] |
|  82 | 44.6 (Si ^a), 418.5 (Si ^b) | | | 400 (3400) | Red solid (100–101) | [75] |
|  88^a | 210.2 (Si ¹), 9.3 (Si ^{1b}) | Molecule 1: 2.1980(16) 2.2168(16) 2.3400 (15) [Si ^b –Si ^{1b}] Molecule 2: 2.2045(16) 2.2157(17) 2.3423 (15) [Si ^b –Si ^{1b}] | Molecule 1: 0.2 (Si ^{1a}) 12.3 (Si ^{1b}) 15.3 (Si ^{1c}) 34.7 (Si ^{1b}) Molecule 2: 12.9 (Si ^{1c}) 24.4 (Si ^{1b}) 9.0 (Si ^{1a}) 24.8 (Si ^{1b}) | 438 (2600), 363 (700), 299 (1200), [3-MP, rt] 510 (1200), 430 (4400), 355 (1600), 297 (2800), 244 (5600), [3-MP, 77 K] | Red crystals (100, dec.) | [77] (CCDC- 665965) |



91

448 (29000),
271 (70000)
Orange crystals [78]
(CCDC-
786049)

-52, -50,
300.308
[solid-state
CP/MAS]
2.2671(8),
2.2846(8),
2.2877(8),
2.2924(8)



103

623 (642)
Dark-green
blocks
(>216)
[81]
(CCDC-
745661)

-84.8,
+124.6,
-89.3
2.3375(5)
(Si1-Si3),
2.3581(5)
(Si2-Si3),
2.3275(5)
(Si1-Si2),
2.3034(5)
(Si1-Si2')

^aCrystallographically two independent molecules exist

^bUnless otherwise noted

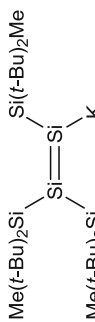
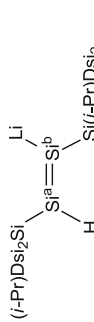
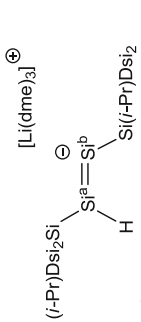
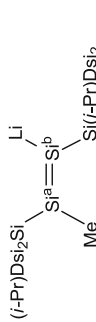
Table 4 Properties and structural parameters of charged disilenes and related compounds

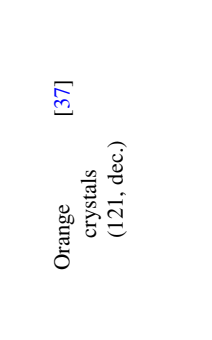
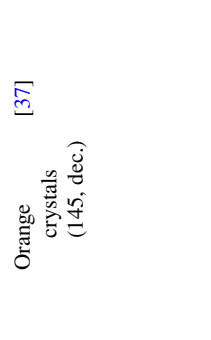
| Compound | Metric parameters around Si=Si bond | | | | UV-vis $\lambda_{\text{max}}/\text{nm}$ (ϵ) in hexane ^a at rt | Habit (mp/ $^{\circ}\text{C}$) | Reference (CCDC#) |
|--------------|---|--|---|--|---|-------------------------------------|---------------------------|
| | ²⁹ Si NMR $\delta(\text{Si})$ in C_6D_6 at π | <i>trans</i> - Bent angle/deg | RSi=SiR/deg and others | $d(\text{Si}^{\text{a}}=\text{Si}^{\text{b}})/\text{\AA}$ | | | |
| | 111.3 (Si ^a), 59.5 (Si ^b) | 11.8 (Si ^a), 4.3 (Si ^b) | RSi=SiR/deg and others τ : 6.8 | 2.1824(5) Mg-Si: 2.5587(6) | 425 (4193) | Yellow crystals (203, dec.) | [25] (CCDC- 876918) |
| 5 | 94.46 (Si ^b), 90.16 (Si ^a) [THF- <i>d</i> ₈] | 14.6, 16.7 (Si ^b), 8.1, 11.8 (Si ^a) | τ : 4.4, 4.6 | 2.1721(12), 2.1696(11) Cu-Si: 2.2412(8), 2.2458(8) | 476 (31127), 371 [THF] 462, 384 [hexane] | Deep-red crystals (176, dec.) | [25] (CCDC- 876919) |
| 6 | 107.05 (Si ^b), 57.48 (Si ^a) [THF- <i>d</i> ₈] | | | | 468 (28728), 356 [hexane] | Red solid (204, dec.) | [25] |
| 7 | 152.5 (Si ^b), 116.8 (Si ^a) | 6.1 (Si ^a), 5.5 (Si ^b) | τ : 4.3 | 2.2144(7), Si ^b -Zr: 2.7611(6) | 715 (approx. 7000), 416 (approx. 3000) | Green solid | [26] |
| 8 | | | | | | | |

| | | | | | |
|-------------------|---|--|---|-----------------------------|---|
| <p>9</p> | <p>−44.4 (Si^a), 134.5, 143.9</p> | <p>Si^a–Si^b: 2.362(1) Si^b–Si^c: 2.198(1) Si^a–Mg: 2.625(1) Si^c–Mg: 2.552(1)</p> | <p>4.3 (Si^b), 9.4 (Si^c)</p> | <p>415 (3200) [pentane]</p> | <p>Orange blocks [27] (209, dec.) (CCDC-288946)</p> |
| <p>12</p> | <p>126.4, 144.9</p> | <p>2.2117(13) Si–K: 3.4398 (14), 3.5236 (14)</p> | <p>Yellow crystals</p> | <p>[30] (CCDC-732659)</p> | |
| <p>14b</p> | <p>78.2, 145.9 [C₇D₈]</p> | <p>2.2114 (10)</p> | <p>[32]</p> | <p>[32]</p> | |
| <p>16a</p> | <p>77.6 (Si^a), 328.4 (Si^b) ⁷LiNMR: −0.6 [THF-<i>d</i>₆]</p> | <p>2.1983(18) Si–Li: 2.598(9)</p> | <p>Red crystals (159–161)</p> | <p>[33]</p> | |
| <p>16b</p> | <p>79.5 (Si^a), 325.6 (Si^b) [THF-<i>d</i>₆]</p> | <p>2.1983(18) Si–Li: 2.598(9)</p> | <p>Red crystals (158–159)</p> | <p>[33]</p> | |

(continued)

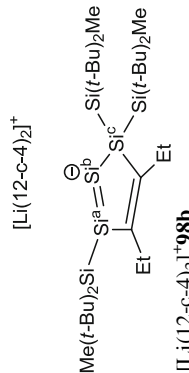
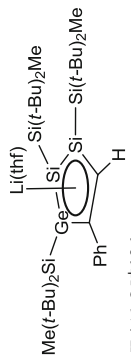
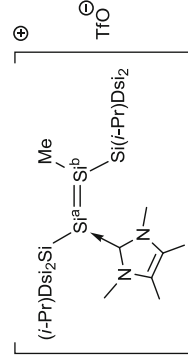
Table 4 (continued)

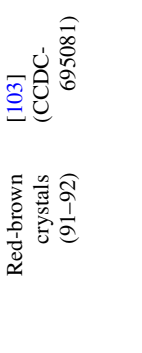
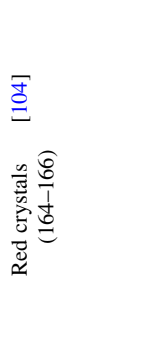

| Compound | Metric parameters around Si=Si bond | | | UV-vis $\lambda_{\text{max}}/\text{nm}$ (ϵ) in hexane ^a at rt | Habit (mp/ $^{\circ}\text{C}$) | Reference (CCDC#) |
|---|--|-------------------------------------|--|---|------------------------------------|----------------------|
| | ²⁹ Si NMR $\delta(\text{Si})$ in C_6D_6 ^a at rt | <i>trans</i> - Bent angle/deg | RSi=SiR/deg and others | | | |
|  | 81.7 (Si ^a), 323.1 (Si ^b) [THF- <i>d</i> ₈] | | | Red crystals (155–156) | [33] | |
| 16c  | 124.7 (Si ^a), 165.0 (Si ^b) ¹ H NMR: 7.10 (s, 1H, SiH) ⁷ Li NMR: 0.86. | | 268 (3380), 302 (1430), 390 (5540) | Red crystals (92, dec.) | [35] | |
| 20a  | | | | | [35] (CCDC- 638830) | |
| 20b  | 114.1 (Si ^b), 143.4 (Si ^a) [THF- <i>d</i> ₈], | | | Red | [36] | |

| | | | | | |
|--|--|--|---|---|--|
| $\left[\begin{array}{c} \text{Li} \\ \text{Si}^{\text{a}} \\ \text{Si}^{\text{b}} \\ \text{Si}^{\text{c}} \\ \text{Si}^{\text{d}} \end{array} \right]^{\ominus} \cdot$ <p>⊕ [K(dme)₄]</p> <p>22</p> | <p>ESR parameters: g-factor = 1.99962, $a(^{29}\text{Si}^{\text{a}})$ = 3.92 mT, $a(^{29}\text{Si}^{\text{b}}) = 2.24$ mT, $a(^1\text{H}_\gamma) = 0.23$ mT [MeTHF]</p> | <p>2.1728(14)</p> | <p>$\text{Si}^{\text{b}}\text{--Si}^{\text{c}}\text{--Si}^{\text{d}}\text{--Si}^{\text{a}}$: 177.7 $A(\text{Si}^{\text{a}}\text{Si}^{\text{c}}\text{Si}^{\text{d}})$: 112.84(6) 113.97(6)</p> | <p>237 (14800), 292 (4890), 403 (2040), 713 (50) [hexane]</p> | <p>Dark-brown crystals (121, dec.) 638831)</p> |
|  <p>[Li(thf)]⁺ 98a</p> | <p>22.0 (Si^b), 29.9 (Si^a) ⁷Li NMR: -5.8 [toluene-<i>d</i>₈]</p> | <p>Si^a–Si^b: 2.2508 (10), 2.2438 (10)</p> | <p>276 (8520), 361 (1540), 490 (4400)</p> | <p>Orange crystals (121, dec.)</p> | <p>Orange crystals (145, dec.)</p> |
|  <p>[Li(t-Bu)₂CO]⁺ 98a</p> | <p>SiC: 1.844(3), 1.829(3) C–C: 1.418(4)</p> | | | | |

(continued)

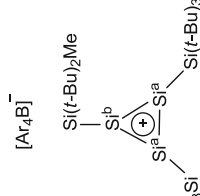
Table 4 (continued)

| Compound | Metric parameters around Si=Si bond | | | UV-vis $\lambda_{\text{max}}/\text{nm}$ (ϵ) in hexane ^a at rt | Habit (mp/ $^{\circ}\text{C}$) | Reference (CCDC#) |
|---|--|--|---|---|--|---------------------------|
| | ²⁹ Si NMR $\delta(\text{Si})$ in C_6D_6 at rt | <i>trans</i> - Bent angle/deg | RSi=SiR/deg and others | | | |
|  <p>$[\text{Li}(12\text{-c-}4)_2]^+$ 98b</p> | -28.0 (Si ^c), 134.9 (Si ^b or Si ^a), 145.0 (Si ^b or Si ^a) ⁷ Li NMR: -2.1 [toluene- <i>d</i> ₈] | | | 347(2620), 489 (5230) | Orange crystals (139, dec.) | [37] |
|  <p>$[\text{Li}(\text{thf})]^+$ 101</p> | Skeletal silicon: 54.4, 69.1 ⁷ Li NMR -5.4 [toluene- <i>d</i> ₈] 97.4 and 104.9 ⁷ Li NMR: -0.6 [THF- <i>d</i> ₈] | 2.2403(7) Si-Ge: 2.3220(5) Si-C: 1.8269 (18) | | 375 (4050), 474 (4020) | Bright-orange plates (135, dec.) | [79] (CCDC- 288755) |
|  <p>$[\text{Li}(12\text{-c-}4)_2]^+$ 139</p> | 54.0 (Si ^a), 168.8 (Si ^b) | 2.192(2) | 8.5 (Si ^a), 5.8 (Si ^b) | 251 (23000), 275 (25000), 408 (3600) [hexane] | Yellow crystals (143-145, dec.) | [110] |

| | | | |
|--|---|---|-------------------------------------|
| <p>TPFPB⁻</p>  <p>Me(<i>t</i>-Bu)₂Si=Si(<i>t</i>-Bu)₂Me</p> <p>Me(<i>t</i>-Bu)₂Si=Si(<i>t</i>-Bu)₂Me</p> <p>175</p> | <p>ESR parameters: <i>g</i>-factor = 2.0049, $a(^{29}\text{Si}^{\text{IV}}) = 2.30 \text{ mT}$ [C₆H₅F]</p> <p>τ: 64.9</p> <p>427 (2300)</p> | <p>Red-brown crystals (91–92)</p> | <p>[103] (CCDC- 695081)</p> |
| <p>[Li(thf)₄]⁺</p>  <p>Me(<i>t</i>-Bu)₂Si=Si(<i>t</i>-Bu)₂Me</p> <p>Me(<i>t</i>-Bu)₂Si=Si(<i>t</i>-Bu)₂Me</p> <p>176</p> | <p>ESR parameters: <i>g</i>-factor = 2.0061, $a(^{29}\text{Si}^{\text{IV}}) = 2.45 \text{ mT}$ [MeTHF]</p> <p>τ: 88</p> <p>291 (11600), 436(2100) [THF]</p> | <p>Red crystals (164–166)</p> | <p>[104]</p> |
| <p>TPFPB⁻</p>  <p>Me(<i>t</i>-Bu)₂Si=Si(<i>t</i>-Bu)₂Me</p> <p>177</p> | <p>ESR parameters: $183.8 (\text{Si}^{\text{I}}),$ $286.8 (\text{Si}^{\text{II}})$</p> <p>Si^I–Si^{II}; 2.2266 (10), 2.2187 (10) Si^{Ia}...Si^{Ia} 2.8066 (10)</p> | <p>Red-brown crystals (98–99)</p> | <p>[106] (CCDC- 714254)</p> |

(continued)

Table 4 (continued)

| Compound | ²⁹ Si NMR δ(Si) in C ₆ D ₆ ^a at rt | Metric parameters around Si=Si bond | | | UV-vis λ _{max} /nm (ε) in hexane ^a at rt | Habit (mp/°C) | Reference (CCDC#) |
|--|---|---|-------------------------------------|---------------------------|--|------------------------------------|---------------------------|
| | | d(Si=Si)/Å | <i>trans</i> - Bent angle/deg | RSi=SiR/deg and others | | | |
| [A ₄ B] ⁻ | 284.6 (Si ^a) 288.1 (Si ^b) [toluene-d ₈] | Si ^a -Si ^a : 2.221(3) Si ^a -Si ^b : 2.218(3), 2.211(3) | | | | Yellow solid (240–242, dec.) | [90] (CCDC- 279878) |
|  (<i>t</i> -Bu) ₃ Si 178 | | | | | | | |

^aUnless otherwise noted

References

1. West R, Fink MJ, Michl J (1981) Tetramesityldisilene, a stable compound containing a silicon-silicon double bond. *Science* 214:1343–1344
2. Okazaki R, West R (1996) Chemistry of stable disilenes. *Adv Organomet Chem* 39:231–273
3. Weidenbruch M (2001) Recent advances in the chemistry of silicon-silicon multiple bonds. In: Rappoport Z, Apeloig Y (eds) *Chemistry of organic silicon compounds*, vol 3. Wiley, Chichester, pp 391–428
4. Kira M, Iwamoto T (2006) Progress in the chemistry of stable disilenes. *Adv Organomet Chem* 54:73–148
5. Lee VY, Sekiguchi A (2010) Heavy analogs of alkenes, 1,3-dienes, allenes and alkynes: Multiply bonded derivatives of Si, Ge, Sn and Pb. In: *Organometallic compounds of low-coordinate Si, Ge, Sn and Pb: from phantom species to stable compounds*. Wiley, Chichester, pp 199–334. doi:10.1002/9780470669266.ch5
6. Abersfelder K, Scheschkewitz D (2010) Synthesis of homo- and heterocyclic silanes via intermediates with Si=Si bonds. *Pure Appl Chem* 82(3):595–602
7. Kira M (2012) Bonding and structure of disilenes and related unsaturated group-14 element compounds. *Proc Jpn Acad Ser B* 88(5):167–191
8. Sekiguchi A, Maruki I, Ebata K, Kabuto C, Sakurai H (1991) High-pressure synthesis, structure and novel photochemical reactions of 7,7,8,8-tetramethyl-7,8-disila bicyclo[2.2.2] octa-2,5-diene. *J Chem Soc Chem Commun* 341–343
9. Kira M, Iwamoto T, Kabuto C (1996) The first stable cyclic disilene: hexakis(trialkylsilyl) tetrasilacyclobutene. *J Am Chem Soc* 118:10303–10304
10. Weidenbruch M, Willms S, Saak W, Henkel G (1997) Hexaaryltetrasilene-1,3-diene: a molecule with conjugated Si-Si double bonds. *Angew Chem Int Ed Engl* 1997(36):2503–2504
11. Iwamoto T, Tamura M, Kabuto C, Kira M (2000) A stable bicyclic compound with two Si=Si double bonds. *Science* 290(5491):504–506
12. Ishida S, Iwamoto T, Kira M (2003) A stable silicon-based allene analogue with a formally sp-hybridized silicon atom. *Nature* 421:725–727
13. Scheschkewitz D (2004) A silicon analogue of vinylolithium: structural characterization of a disilene. *Angew Chem Int Ed* 43(22):2965–2967
14. Wiberg N, Niedermayer W, Fischer G, Nöth H, Suter M (2002) Synthesis, structure and dehalogenation of the disilene RClSi=SiClR [R = (*t*Bu₃Si)₂MeSi]. *Eur J Inorg Chem* 1066–1070
15. Wiberg N, Vasisht SK, Fischer G, Mayer P (2004) Disilynes. III A relatively stable disilyne RSi≡SiR (R = SiMe(Si*t*Bu₃)₂). *Z Anorg Allg Chem* 630(12):1823–1828
16. Sekiguchi A, Kinjo R, Ichinohe M (2004) A stable compound containing a silicon-silicon triple bond. *Science* 305(5691):1755–1777
17. Fukawaza A, Li Y, Yamaguchi S, Tsuji H, Tamao K (2007) Coplanar oligo(*p*-phenylenedisilylene)s based on the octaethyl-substituted *s*-hydrindacenyl group. *J Am Chem Soc* 129:14164–14165
18. Scheschkewitz D (2011) The versatile chemistry of disilene: disila analogues of vinyl anions as synthons in low-valent silicon chemistry. *Chem Lett* 40(1):2–11
19. Sekiguchi A, Ichinohe M, Kinjo R (2006) The chemistry of disilyne with a genuine Si–Si triple bond: synthesis, structure, and reactivity. *Bull Chem Soc Jpn* 79(6):825–832
20. Power PP (2007) Bonding and reactivity of heavier group 14 element alkyne analogues. *Organometallics* 26:4362–4372
21. Sekiguchi A (2008) Disilyne with a silicon-silicon triple bond: a new entry to multiple bond chemistry. *Pure Appl Chem* 80(3):447–457
22. Power PP (2010) Main-group elements as transition metals. *Nature* 463(7278):171–177
23. Fischer RC, Power PP (2010) π -Bonding and the lone pair effect in multiple bonds involving heavier main group elements: developments in the new millennium. *Chem Rev* 110:3877–3923

24. Asay M, Sekiguchi A (2012) Recent developments in the reactivity of stable disilynes. *Bull Chem Soc Jpn* 85(12):1245–1261
25. Cowley MJ, Abersfelder K, White AJ, Majumdar M, Scheschkewitz D (2012) Transmetallation reactions of a lithium disilenide. *Chem Commun* 48(52):6595–6597
26. Nguyen T-I, Scheschkewitz D (2005) Activation of a Si=Si bond by η^1 -coordination to a transition metal. *J Am Chem Soc* 127:10174–10175
27. Abersfelder K, Guclu D, Scheschkewitz D (2006) An unsaturated α , ω -dianionic oligosilane. *Angew Chem Int Ed* 45(10):1643–1645
28. Leszczynska K, Abersfelder K, Mix A, Neumann B, Stammeler HG, Cowley MJ, Jutzi P, Scheschkewitz D (2012) Reversible base coordination to a disilene. *Angew Chem Int Ed* 51(27):6785–6788
29. Watanabe H, Takeuchi K, Fukawa N, Kato M, Goto M, Nagai Y (1987) Air-stable tetrakis (2,4,6-trisopropylphenyl)disilene. Direct synthesis of disilene from dihalomonosilane. *Chem Lett* 16:1341–1344
30. Iwamoto T, Kobayashi M, Uchiyama K, Sasaki S, Nagendran S, Isobe H, Kira M (2009) Anthryl-substituted trialkyldisilene showing distinct intramolecular charge-transfer transition. *J Am Chem Soc* 2009:3156–3157
31. Ichinohe M, Sanuki K, Inoue S, Sekiguchi A (2004) Disilynyllithium from tetrasila-1,3-butadiene: a silicon analogue of a vinylolithium. *Organometallics* 23:3088–3090
32. Ichinohe M, Sanuki K, Inoue S, Sekiguchi A (2006) Tetrasila-1,3-butadiene and its transformation to disilynyl anions. *Silicon Chem* 3(3–4):111–116
33. Inoue S, Ichinohe M, Sekiguchi A (2005) Disilynyl anions derived from reduction of tetrakis (di-*tert*-butylmethylsilyl)disilene with metal naphthalene through a disilene dianion intermediate: synthesis and characterization. *Chem Lett* 34(11):1564–1565
34. Kira M, Iwamoto T, Yin D, Maruyama T, Sakurai H (2001) Novel 1,2-dilithiodisilanes derived from reduction of stable tetrakis(trialkylsilyl)disilenes with lithium metal. *Chem Lett* 2001:910–911
35. Kinjo R, Ichinohe M, Sekiguchi A (2007) An isolable disilyne anion radical and a new route to the disilenide ion upon reduction of a disilyne. *J Am Chem Soc* 129:26–27
36. Yamaguchi T, Ichinohe M, Sekiguchi A (2010) Addition of methylolithium to disilyne $\text{RSi}\equiv\text{SiR}$ ($\text{R} = \text{Si}^i\text{Pr}[\text{CH}(\text{SiMe}_3)_2]$), giving a disilynyllithium, and its unexpected isomerization to a disilacyclopropylsilyllithium. *New J Chem* 34(8):1544–1546
37. Yasuda H, Lee VY, Sekiguchi A (2009) Si_3C_2 -rings: from a nonconjugated trisilacyclopentadiene to an aromatic trisilacyclopentadienide and cyclic disilenide. *J Am Chem Soc* 131:6352–6353
38. Sasamori T, Hironaka K, Sugiyama Y, Takagi N, Nagase S, Hosoi Y, Furukawa Y, Tokitoh N (2008) Synthesis and reactions of a stable 1,2-diaryl-1,2-dibromodisilene: a precursor for substituted disilenes and 1,2-diaryldisilyne. *J Am Chem Soc* 130:13856–13857
39. Suzuki K, Matsuo T, Hashizume D, Tamao K (2011) Room-temperature dissociation of 1,2-dibromodisilenes to bromosilylenes. *J Am Chem Soc* 133(49):19710–19713
40. Carter EA, Goddard WA III (1986) Relation between singlet-triplet gaps and bond energies. *J Phys Chem* 90:998–1001
41. Trinquier G, Malrieu J-P (1987) Nonclassical distortions at multiple bonds. *J Am Chem Soc* 109:5303–5315
42. Malrieu J-P, Trinquier G (1989) Trans bending at double bonds. Occurrence and extent. *J Am Chem Soc* 111:5916–5921
43. Hartmann M, Haji-Abdi A, Abersfelder K, Haycock PR, White AJ, Scheschkewitz D (2010) Synthesis, characterisation and complexation of phosphino disilenes. *Dalton Trans* 39(39):9288–9295
44. Takeuchi K, Ichinohe M, Sekiguchi A (2012) A new disilene with π -accepting groups from the reaction of disilyne $\text{RSi}\equiv\text{SiR}$ ($\text{R} = \text{Si}^i\text{Pr}[\text{CH}(\text{SiMe}_3)_2]$) with isocyanides. *J Am Chem Soc* 134(6):2954–2957

45. Lee VY, Miyazaki S, Yasuda H, Sekiguchi A (2008) Isomeric metamorphosis: Si₃E (E = S, Se, and Te) bicyclo[1.1.0]butane and cyclobutene. *J Am Chem Soc* 2758–2759
46. Michalczyk MJ, West R, Michl R (1984) Cis and trans isomers of disilenes: photochemical and thermal interconversions. *J Am Chem Soc* 106:821–822
47. Schmedake TA, Haaf M, Apeloig Y, Müller T, Bukalov S, West R (1999) Reversible transformation between a diaminosilylene and a novel disilene. *J Am Chem Soc* 9479–9480
48. Jutzi P, Mix A, Rummel B, Schoeller WW, Neumann B, Stammler HG (2004) The (Me₅C₅)Si⁺ cation: a stable derivative of HSi⁺. *Science* 305(5685):849–851
49. Jutzi P, Mix A, Neumann B, Rummel B, Schoeller WW, Stammler HG, Rozhenko AB (2009) Reversible transformation of a stable monomeric silicon(II) compound into a stable disilene by phase transfer: experimental and theoretical studies of the system {[Me₃Si₂N](Me₅C₅)Si}_n with n = 1, 2. *J Am Chem Soc* 131:12137–12143
50. Khan S, Sen SS, Roesky HW, Kratzert D, Michel R, Stalke D (2010) One pot synthesis of disilatricycloheptene analogue and Jutzi's disilene. *Inorg Chem* 49(20):9689–9693
51. Takeuchi K, Ikoshi M, Ichinohe M, Sekiguchi A (2010) Addition of amines and hydroborane to the disilyne RSi≡SiR (R = SiPr[CH(SiMe₃)₂]₂) giving amino- and boryl-substituted disilenes. *J Am Chem Soc* 132:930–931
52. Takeuchi K, Ikoshi M, Ichinohe M, Sekiguchi A (2011) Silicon version of enamines: amino-substituted disilenes by the reactions of the disilyne RSi≡SiR (R = SiPr[CH(SiMe₃)₂]₂) with amines. *J Organomet Chem* 696(6):1156–1162
53. Abersfelder K, Scheschkewitz D (2008) Synthesis of trisila analogues of allyl chlorides and their transformations to chlorocyclotrisilanes, cyclotrisilanides, and a trisilaindane. *J Am Chem Soc* 130:4114–4121
54. Abersfelder K, Nguyen T-I, Scheschkewitz D (2009) Stannyl-substituted disilenes and a disilastannirane. *Z Anorg Allg Chem* 635(13–14):2093–2098
55. Takeuchi K, Ichinohe M, Sekiguchi A (2011) Hydroboration of disilyne RSi≡SiR (R = SiPr[CH(SiMe₃)₂]₂), giving boryl-substituted disilenes. *Organometallics* 30(7):2044–2050
56. Inoue S, Ichinohe M, Sekiguchi A (2008) An isolable boryl-substituted disilene from the reaction of an sp²-type silyl anion with haloboranes: synthesis and characterization. *Chem Lett* 37(10):1044–1045
57. Agou T, Sugiyama Y, Sasamori T, Sakai H, Furukawa Y, Takagi N, Guo JD, Nagase S, Hashizume D, Tokitoh N (2012) Synthesis of kinetically stabilized 1,2-dihydrodisilenes. *J Am Chem Soc* 134(9):4120–4123
58. Wiberg N, Niedermayer W, Nöth H, Markus W (2001) On the way to a disilyne -Si≡Si-: formation of RHSi=SiHR and indication of the intermediate formation of RSi≡SiR (R = SiH(SiⁱBu₃)₂). *Z Anorg Allg Chem* 627:1717–1722
59. Bejan I, Scheschkewitz D (2007) Two Si-Si double bonds connected by a phenylene bridge. *Angew Chem Int Ed* 46(30):5783–5786
60. Jeck J, Bejan I, White AJP, Nied D, Breher F, Scheschkewitz D (2010) Transfer of a disilynyl moiety to aromatic substrates and lateral functional group transformation in aryl disilenes. *J Am Chem Soc* 2010(132):17306–17315
61. Brown HC, Okamoto Y (1958) Electrophilic substituent constants. *J Am Chem Soc* 80:4979–4987
62. Kobayashi M, Matsuo T, Fukunaga T, Hashizume D, Fueno H, Tanaka K, Tamao K (2010) Air-stable, room-temperature emissive disilenes with π-extended aromatic groups. *J Am Chem Soc* 132:15162–15163
63. Matsuo T, Kobayashi M, Tamao K (2010) π-Conjugated disilenes stabilized by fused-ring bulky “Rind” groups. *Dalton Trans* 39(39):9203–9208
64. Tamao K, Kobayashi M, Matsuo T, Furukawa S, Tsuji H (2012) The first observation of electroluminescence from di(2-naphthyl)disilene, an Si=Si double bond-containing π-conjugated compound. *Chem Commun* 48(7):1030–1032
65. Sasamori T, Yuasa A, Hosoi Y, Furukawa Y, Tokitoh N (2008) 1,2-Bis(ferrocenyl)disilene: a multistep redox system with an Si=Si double bond. *Organometallics* 27:3325–3327

66. Yuasa A, Sasamori T, Hosoi Y, Furukawa Y, Tokitoh N (2009) Synthesis and properties of stable 1,2-bis(metallocenyl)disilenes: novel d- π conjugated systems with a Si=Si double bond. *Bull Chem Soc Jpn* 82(7):793–805
67. Sato T, Mizuhata Y, Tokitoh N (2010) 1,2-Dialkynyldisilenes: silicon analogues of (*E*)-enediyne. *Chem Commun* 46(24):4402–4404
68. Ohmori Y, Ichinohe M, Sekiguchi A, Cowley MJ, Huch V, Scheschkewitz D (2013) Functionalized cyclic disilenes via ring expansion of cyclotrisilenes with isocyanides. *Organometallics* 32(6):1591–1594
69. Kinjo R, Ichinohe M, Sekiguchi A, Takagi N, Sumimoto M, Nagase S (2007) Reactivity of a disilyne $\text{RSi}\equiv\text{SiR}$ ($\text{R} = \text{SiPr}[\text{CH}(\text{SiMe}_3)_2]$) toward π -bonds: stereospecific addition and a new route to an isolable 1,2-disilabenzene. *J Am Chem Soc* 129:7766–7767
70. Han JS, Sasamori T, Mizuhata Y, Tokitoh N (2010) Reactivity of an aryl-substituted silicon-silicon triple bond: 1,2-disilabenzenes from the reactions of a 1,2-diaryldisilyne with alkynes. *Dalton Trans* 39(39):9238–9240
71. Takeuchi K, Ichinohe M, Sekiguchi A (2008) Reactivity of the disilyne $\text{RSi}\equiv\text{SiR}$ ($\text{R} = \text{SiPr}[\text{CH}(\text{SiMe}_3)_2]$) toward silylcyanide: two pathways to form the bis-adduct $[\text{RSiSiR}(\text{CNSiMe}_3)_2]$ with some silaketenimine character and a 1,4-diaza-2,3-disilabenzene analogue. *J Am Chem Soc* 130:16848–16849
72. Takeuchi K, Ichinohe M, Sekiguchi A, Guo J-D, Nagase S (2010) Reactivity of the disilyne $\text{RSi}\equiv\text{SiR}$ ($\text{R} = \text{SiPr}[\text{CH}(\text{SiMe}_3)_2]$) toward bis(silylcyanide) forming a 1,4-diaza-2,3-disilabenzene analog. *J Phys Org Chem* 390–394
73. Han JS, Sasamori T, Mizuhata Y, Tokitoh N (2010) Reactivity of an aryl-substituted silicon-silicon triple bond: reactions of a 1,2-diaryldisilyne with alkenes. *J Am Chem Soc* 132: 2546–2547
74. Wakita K, Tokitoh N, Okazaki R, Takagi N, Nagase S (2000) Crystal structure of a stable silabenzene and its photochemical valence isomerization into the corresponding silabenzvalene. *J Am Chem Soc* 122(23):5648–5649
75. Tanaka H, Inoue S, Ichinohe M, Driess M, Sekiguchi A (2011) Synthesis and striking reactivity of an isolable tetrasilyl-substituted trisilaallene. *Organometallics* 30(13):3475–3478
76. Schäfer A, Weidenbruch M, Müller T, Pravinkumar K, Becker JY (2009) Electrochemical properties of a disilene, a tetrasila-1,3-butadiene, and their germanium analogues. *Chem Eur J* 15(34):8424–8428
77. Uchiyama K, Nagendran S, Ishida S, Iwamoto T, Kira M (2007) Thermal and photochemical cleavage of Si=Si double bond in tetrasila-1,3-diene. *J Am Chem Soc* 129:10638–10639
78. Suzuki K, Matsuo T, Hashizume D, Fueno H, Tanaka K, Tamao K (2011) A planar rhombic charge-separated tetrasilacyclobutadiene. *Science* 331(6022):1306–1309
79. Lee VY, Takanashi K, Kato R, Matsuno T, Ichinohe M, Sekiguchi A (2007) Heavy analogues of the 6π -electron anionic ring systems: cyclopentadienide ion and cyclobutadiene dianion. *J Organomet Chem* 692(13):2800–2810
80. Lee VY, Yasuda H, Sekiguchi A (2007) Interplay of $E_nE'_{n-3}C$ valence isomers ($E, E' = \text{Si}, \text{Ge}$): bicyclo[1.1.0]butanes with very short bridging bonds and their isomerization to alkyl-substituted cyclopropenes. *J Am Chem Soc* 129:2436–2437
81. Abersfelder K, White AJ, Rzepa HS, Scheschkewitz D (2010) A tricyclic aromatic isomer of hexasilabenzene. *Science* 327(5965):564–566
82. Leszczynska K, Abersfelder K, Majumdar M, Neumann B, Stammmer HG, Rzepa HS, Jutzi P, Scheschkewitz D (2012) The Cp^*Si^+ cation as a stoichiometric source of silicon. *Chem Commun* 48(63):7820–7822
83. Takanashi K, Lee VY, Ichinohe M, Sekiguchi A (2006) A (tetrasilacyclobutadiene) tricarbonyliron complex $[(\eta^4\text{-}(\text{tBu}_2\text{MeSi})_4\text{Si}_4)\text{Fe}(\text{CO})_3]$: the silicon cousin of petit's (cyclobutadiene)tricarbonyliron complex $[(\eta^4\text{-H}_4\text{C}_4)\text{Fe}(\text{CO})_3]$. *Angew Chem Int Ed* 45(20): 3269–3272
84. Abe T, Iwamoto T, Kira M (2010) A stable 1,2-disilacyclohexene and its 14-electron palladium(0) complex. *J Am Chem Soc* 132:5008–5009

85. Tanaka R, Iwamoto T, Kira M (2006) Fused tricyclic disilenes with highly strained Si-Si double bonds: addition of a Si-Si single bond to a Si-Si double bond. *Angew Chem Int Ed* 45(38):6371–6373
86. Kobayashi H, Iwamoto T, Kira M (2005) A stable fused bicyclic disilene as a model for silicon surface. *J Am Chem Soc* 127:15376–15377
87. Iwamoto T, Furiya Y, Kobayashi H, Isobe H, Kira M (2010) Synthesis and facile ring expansion of silylenecyclotetrasilane. *Organometallics* 29(8):1869–1872
88. Iwamoto T, Kabuto C, Kira M (1999) The first stable cyclotrisilene. *J Am Chem Soc* 121:886–887
89. Murata Y, Ichinohe M, Sekiguchi A (2010) Unsymmetrically substituted disilyne $\text{Dsi}_2^i\text{PrSi-Si}\equiv\text{Si-SiNpDsi}_2$ (Np = CH_2^tBu): synthesis and characterization. *J Am Chem Soc* 132: 16768–16770
90. Ichinohe M, Igarashi M, Sanuki K, Sekiguchi A (2005) Cyclotrisilylenylium ion: the persilaaromatic compound. *J Am Chem Soc* 127:9978–9979
91. Wiberg N, Lerner H-W, Vasisht S-K, Wagner S, Karaghiosoff K, Nöth H, Ponikvar W (1999) Tetrasupersilyl-tristannaallene and -tristannacyclopropene ($t\text{Bu}_3\text{Si}$) $_4\text{Sn}_3$ –isomers with the shortest Sn=Sn double bonds to date. *Eur J Inorg Chem* 1211–1218
92. Molev G, Tumanskii B, Sheberla D, Botoshansky M, Bravo-Zhivotovskii D, Apeloig Y (2009) Isolable photoreactive polysilyl radicals. *J Am Chem Soc* 131:11698–11700
93. Wang Y, Xie Y, Wei P, King RB, Schaefer HF 3rd, von RSP, Robinson GH (2008) A stable silicon(0) compound with a Si=Si double bond. *Science* 321(5892):1069–1071
94. Yamaguchi T, Sekiguchi A, Driess M (2010) An *N*-heterocyclic carbene-disilyne complex and its reactivity toward ZnCl_2 . *J Am Chem Soc* 132:14061–14063
95. Kami M, Apeloig Y (1990) Substituent effects on the geometries and energies of the Si=Si double bond. *J Am Chem Soc* 112:8589–8590
96. Han JS, Sasamori T, Mizuhata Y, Tokitoh N (2012) Evidence for LiBr-assisted generation of a silylene from a 1,2-diaryl-1,2-dibromodisilene. *Chem Asian J* 7(2):298–300
97. Abe T, Tanaka R, Ishida S, Kira M, Iwamoto T (2012) New isolable dialkylsilylene and its isolable dimer that equilibrate in solution. *J Am Chem Soc* 134(49):20029–20032
98. Inoue S, Ichinohe M, Sekiguchi A (2007) Conversion of a disilene into a silene: silyl-anion-substituted silene by a sila-Peterson-type reaction from an sp^2 -type silyl anion. *Angew Chem Int Ed* 46(18):3346–3348
99. Tanaka H, Inoue S, Ichinohe M, Sekiguchi A (2009) An (η^3 -disilaallyl)lithium derivative: interconversion of π -allyl-type bonding and η^1 coordination to a silyllithium fragment. *Organometallics* 28(23):6625–6628
100. Bejan I, Inoue S, Ichinohe M, Sekiguchi A, Scheschkewitz D (2008) 1,2-Disilacyclobut-2-enes: donor-free four-membered cyclic silenes from reaction of disilenes with vinylbromides. *Chem Eur J* 14(24):7119–7122
101. Kira M, Iwamoto T (2000) Stable cyclic and acyclic persilyldisilenes. *J Organomet Chem* 611:236–247
102. Ichinohe M, Kinjo R, Sekiguchi A (2003) The first stable methyl-substituted disilene: synthesis, crystal structure, and regioselective MeLi addition. *Organometallics* 22:4621–4623
103. Inoue S, Ichinohe M, Sekiguchi A (2008) The isolable cation radical of disilene: synthesis, characterization, and a reversible one-electron redox system. *J Am Chem Soc* 6078–6079
104. Sekiguchi A, Inoue S, Ichinohe M, Arai Y (2004) Isolable anion radical of blue disilene ($t\text{Bu}_2\text{MeSi}$) $_2\text{Si}=\text{Si}(\text{SiMe}t\text{Bu}_2)_2$ formed upon one-electron reduction: synthesis and characterization. *J Am Chem Soc* 126:9626–9629
105. Sekiguchi A, Fukawa T, Nakamoto M, Lee VY, Ichinohe M (2002) Isolable silyl and germyl radicals lacking conjugation with π -bonds: synthesis, characterization, and reactivity. *J Am Chem Soc* 124:9865–9869
106. Inoue S, Ichinohe M, Yamaguchi T, Sekiguchi A (2008) A free silylium ion: a cyclotetrasilenylium ion with allylic character. *Organometallics* 27:6056–6058

107. Majumdar M, Huch V, Bejan I, Meltzer A, Scheschkewitz D (2013) Reversible, complete cleavage of Si=Si double bonds by isocyanide insertion. *Angew Chem Int Ed* 52(12): 3516–3520
108. Zirmgast M, Flock M, Baumgartner J, Marschner C (2008) Formation of formal disilene fluoride adducts. *J Am Chem Soc* 130:17460–17470
109. Iwamoto T, Abe T, Ishida S, Kabuto C, Kira M (2007) Reactions of trisilaallene and 2-germadisilaallene with various reagents. *J Organomet Chem* 692(1–3):263–270
110. Yamaguchi T, Asay M, Sekiguchi A (2012) $[(\text{Me}_3\text{Si})_2\text{CH}]_2\text{iPrSi}(\text{NHC})\text{Si}=\text{Si}(\text{Me})\text{Si}(\text{Pr})[\text{CH}(\text{SiMe}_3)_2]_2]^+$: a molecule with disilyl cation character. *J Am Chem Soc* 134(2): 886–889

Recent Advances in the *N*-Heterocyclic Carbene-Supported Chemistry of Silicon

Eric Rivard

Abstract This review serves to highlight recent developments in the use of *N*-heterocyclic carbene donors to stabilize reactive bonding environments involving silicon.

Keywords Inorganic bonding · *N*-heterocyclic carbenes · Silicon

Contents

| | | |
|---|---|-----|
| 1 | Introduction | 204 |
| 2 | Early Coordination Chemistry Between <i>N</i> -Heterocyclic Carbenes and Silicon-Based Substrates Followed by the Landmark Discovery of a Disilene, Si ₂ , Complex | 205 |
| 3 | Trapping Silicon(II) Halides and Hydrides in the Form of Stable Adducts | 208 |
| 4 | Versatile Chemistry of Donor-Stabilized SiCl ₂ | 212 |
| 5 | Silicon Heterocycles: New Directions in Inorganic Bonding | 215 |
| 6 | Multiply Bonded Silenes and Silynes | 217 |
| 7 | New Synthetic Strategies Involving Silylated Carbenes and Silylimidazolium Cations .. | 221 |
| 8 | Summary and Future Directions | 222 |
| | References | 223 |

Abbreviations

| | |
|------|---|
| Ad | Adamantyl |
| aNHC | Abnormal <i>N</i> -heterocyclic carbene |
| Ar' | 2,6-Tipp ₂ C ₆ H ₃ |
| Ar* | 2,6-Mes ₂ C ₆ H ₃ |
| CAAC | Cyclicalkyl(amino)carbene |
| Cp | Cyclopentadienyl |

E. Rivard (✉)
Department of Chemistry, University of Alberta, 11227 Saskatchewan Dr., Edmonton, AB,
Canada T2G 2G2
e-mail: erivard@ualberta.ca

| | |
|-------------------|--|
| Cp* | Pentamethylcyclopentadienyl |
| DFT | Density functional theory |
| Dipp | Diisopropylphenyl = 2,6- ⁱ Pr ₂ C ₆ H ₃ |
| Dsi | CH(SiMe ₃) ₂ |
| EWG | Electron withdrawing group |
| ImMe ₄ | [(MeCNMe) ₂ C:] |
| IPr | [(HCNDipp) ₂ C:] |
| LA | Lewis acid |
| LB | Lewis base |
| Mes | Mesityl = 2,4,6-Me ₃ C ₆ H ₂ |
| Mu | Muonium |
| NBO | Natural bond order |
| NHC | <i>N</i> -heterocyclic carbene |
| OTf | Triflate = O ₃ SCF ₃ ⁻ |
| SIPr | [(H ₂ CNDipp) ₂ C:] |
| Tipp | Triisopropylphenyl = 2,4,6- ⁱ Pr ₃ C ₆ H ₂ |
| Xyl | Xylyl = 2,6-Me ₂ C ₆ H ₃ |

1 Introduction

The chemistry of silicon has an important role in establishing conceptual connections between the chemical principles associated with its well-known congener, carbon, and the often vastly different bonding and reactivity pathways observed amongst other “inorganic” main group elements [1]. For example, C–C multiple bonding is a prominent feature of organic chemistry, whereas the formation of stable multiple bonds between silicon requires steric protection of the weaker and more reactive Si–E π -bonds (E = element) in the form of bulky substituents at silicon ([2–6]; for a recent report of a stable Ge=O double bond, see [7]). Despite numerous efforts to prepare compounds with Si–Si multiple bonds in the condensed phase, this goal was only achieved in 1981 when West reported the landmark synthesis of Mes₂Si=SiMes₂ (Mes = 2,4,6-Me₃C₆H₂) [8]. This report was followed two decades later by two nearly concurrent syntheses of stable disilynes ArSi≡SiAr (Ar = sterically encumbered aryl group) by the groups of Wiberg and Sekiguchi [9, 10], while Kira and coworkers reported the elegant preparation of inorganic allene analogues including R'Si=Si=SiR' [R' = (Me₃Si)₂CCH₂CH₂C(SiMe₃)₂] [11, 12]. These species were important in further advancing the concept of *kinetic stabilization* wherein hindered substituents are used to create a protective steric cradle about reactive inorganic multiple bonds and/or low-coordinate environments [13]. As more hindered ligands were developed and new molecular archetypes could be isolated in the condensed phase, it was noted that inorganic bonding exhibited unusual features

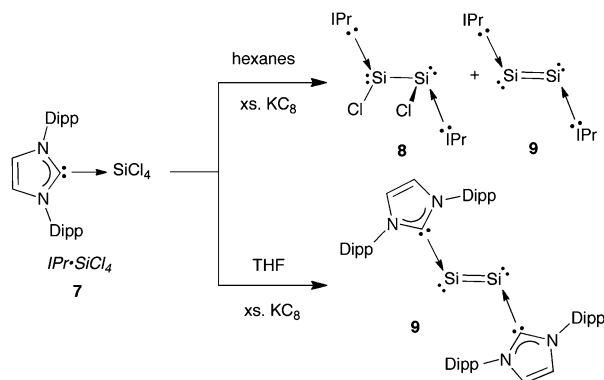
relative to bonding motifs involving carbon. For example, *trans*-bending is often observed within the inorganic Group 14 alkene (R_2MMR_2) and alkynes ($RMMR$) derivatives ($M=Si-Pb$) [14–16], and more recently these low-coordinate species, as well as tetrelenes ($R_2M:$), have been shown to activate small molecules such as dihydrogen under mild conditions [17–19] (a chemical transformation that otherwise usually requires d-orbital assistance from transition metal centers).

A more recent addition to the synthetic toolkit of main group chemists is the use of strongly electron donating *N*-heterocyclic carbenes (NHCs) [20–23] to stabilize reactive molecular entities [24–26]. The primary role of these ligands is to donate electron density into low-lying LUMO states that would normally be involved in molecular decomposition processes. Furthermore, synthetic routes are available which place steric bulk within NHC ligands in close proximity to the molecular unit being sequestered, thus providing added kinetic stabilization of reactive bonding modes such as inorganic π -bonds. Recent examples of species isolated using this strategy include: HBBH [27], B_2 [28], BH [29], and the Group 15 element allotropes P_x [30–32] and As_2 [33].

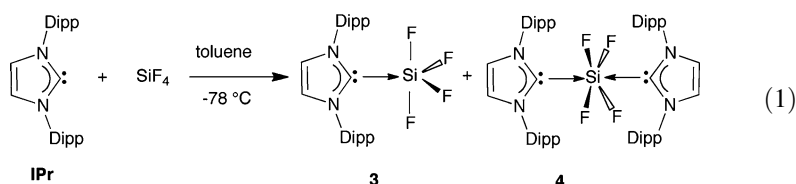
This review article seeks to document the vigorous scientific activity with regard to using *N*-heterocyclic carbene donors to intercept silicon-based species with formal oxidation states ranging from +4 to 0. A concurrent goal of this review is to highlight the new bonding environments that have been uncovered using this methodology and to provide insight into how the inorganic chemistry of silicon has advanced as a result of the use of NHCs as ligands. Due to the modular nature of many of the chemical syntheses of NHCs, a wide array of these ligands are readily available for scientific exploration with salient examples discussed in this review article listed below (Chart 1). It should also be mentioned that the NHC–Si bonding in these species is largely regarded as being dative in nature [34] (as illustrated by $C_{NHC} \rightarrow Si$ bonding descriptors), however in some species, significant C–Si π -bonding can be present due to concurrent $Si \rightarrow C_{NHC}$ π -backdonation.

2 Early Coordination Chemistry Between *N*-Heterocyclic Carbenes and Silicon-Based Substrates Followed by the Landmark Discovery of a Disilene, Si_2 , Complex

The discovery of stable NHCs by Arduengo [20] spawned a new era in synthetic inorganic chemistry. Amongst the early pioneers in the field of NHC-main group chemistry was Kuhn [35] who reported the first stable adducts between the carbenes $ImMe_2R_2$ ($R = Me, Et$ and tPr) and the silicon(IV) halides $SiCl_4$, Ph_2SiCl_2 , and Me_2SiCl_2 [36]. These reactions (Scheme 1) afforded thermally stable 1:1 molecular adducts with trigonal bipyramidal geometries at Si with the NHC ligands occupying equatorial sites. The Si–C bond length in the crystallographically investigated complex $ImMe_2Et_2 \cdot SiCl_4$ (**1a**) was determined to be 1.911(7) Å, which lies at the longer end of the typical Si–C single bond length range of 1.87–1.92 Å [13].



Scheme 2 Synthesis of $\text{IPr}\cdot\text{ClSi-SiCl}\cdot\text{IPr}$ (**8**) and $\text{IPr}\cdot\text{Si=Si}\cdot\text{IPr}$ (**9**)



In 2008, Robinson and coworkers reported a key breakthrough in the field of NHC-silicon chemistry. Following the successful isolation of a stable diborene(2) complex $\text{IPr}\cdot\text{HB=BH}\cdot\text{IPr}$ (**5**) via the reduction of $\text{IPr}\cdot\text{BBr}_3$ (**6**) with KC_8 [27], Robinson later investigated analogous chemistry with Group 14 halides [38]. Specifically, when $\text{IPr}\cdot\text{SiCl}_4$ (**7**) was combined with excess KC_8 as a reducing agent in hexanes, a mixture containing the novel low-oxidation state silicon species $\text{IPr}\cdot\text{ClSi-SiCl}\cdot\text{IPr}$ (**8**) and $\text{IPr}\cdot\text{Si=Si}\cdot\text{IPr}$ (**9**) was obtained. The disilene complex **9** was then isolated in pure form via fractional crystallization; a higher isolated yield of **9** (23%) could be obtained when the reduction chemistry was conducted in THF (Scheme 2).

The dark red dichlorodisilylene adduct $\text{IPr}\cdot\text{ClSi-SiCl}\cdot\text{IPr}$ (**8**) has a crystallographically determined Si-Si bond length of 2.393(3) Å which is only slightly longer than the Si-Si bond length in elemental silicon (ca. 2.36 Å), while each Si center in **8** displays pyramidalized geometries consistent with the presence of stereochemically active lone pairs. The disilene adduct $\text{IPr}\cdot\text{Si=Si}\cdot\text{IPr}$ (**9**) crystallized with a *gauche* $\text{C}_{\text{IPr}}\text{-Si-Si-C}_{\text{IPr}}$ arrangement in the solid state with $\text{C}_{\text{IPr}}\text{-Si-Si}$ angles of $93.37(5)^\circ$ and a short Si-Si bond length of 2.2294(11) Å; the Si-Si bond length in **9** lies within the expected range for Si-Si double bonds [2.15–2.29 Å] [2, 13]. The bonding in **9** was examined by density functional theory and these calculations support the presence of a Si-Si π -bond while the remaining Si-Si and Si- C_{IPr} σ -bonds were found to be largely of p-orbital character at Si (>80%), which explains the nearly orthogonal geometric relationship between these bonds. Accordingly the lone pairs present at the Si centers in **9** have significant s-character (73%) [38]. In the absence of donor molecules, the Si_2 unit has been shown to adopt a highly reactive triplet ground state [39], thus the interaction

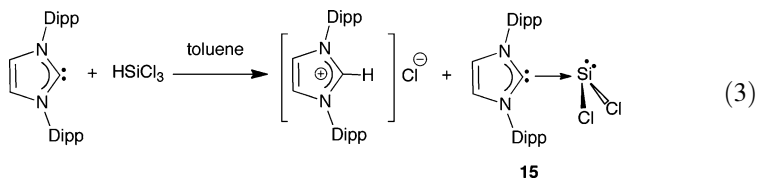
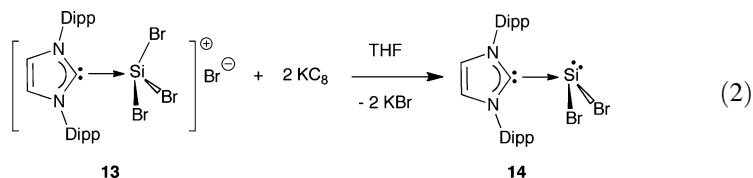
of two IPr groups leads to pairing of electrons to yield a singlet $:\text{Si}=\text{Si}:$ unit. The Jones group has been quite active in the field of main group element carbene chemistry [40] and reported the synthesis of the heavier group 14 element digermene $\text{IPr}\cdot\text{Ge}=\text{Ge}\cdot\text{IPr}$ (**10**) [41] and distannene $\text{IPr}\cdot\text{Sn}=\text{Sn}\cdot\text{IPr}$ (**11**) [42] analogues via the reduction of the element (II) dihalide adducts $\text{IPr}\cdot\text{ECl}_2$ (E = Ge and Sn) [41, 43] with the mild Mg(I) reducing agents $[\{(\text{Aryl}^i\text{Nacnac})\text{Mg}\}_2]$ ($\text{Aryl}^i\text{Nacnac} = [(\text{Aryl}^i\text{NCMe})_2\text{CH}]$, Aryl = Dipp or Mes) [44, 45]. Attempts to prepare the Ge_2 and Sn_2 adducts **10** and **11** by treating $\text{IPr}\cdot\text{ECl}_2$ (E = Ge and Sn) with common reducing agents such as KC_8 , Na, or K led to the extrusion of Ge and Sn metal in place of forming the desired dimetallene adducts. As with **9**, the heavier Group 14 element analogues adopt *trans*-bent geometries with E–E double bonds. The stabilization of a new silicon allotrope, Si_2 , in the form of a stable complex represents an exciting development in main group chemistry which has charioted much of the further chemistry described in this review.

3 Trapping Silicon(II) Halides and Hydrides in the Form of Stable Adducts

Continuing with the theme of low-coordinate silicon chemistry, the study of Si(II) dihalides in the gas phase and under cryogenic conditions [46] has industrial relevance given the likely presence of SiF_2 during the plasma etching of elemental silicon [47] and the role of transient SiCl_2 during the high temperature synthesis of high purity silicon via the reaction of HSiCl_3 with H_2 [48]. Unfortunately attempts to isolate pure SiX_2 species results in either oligomerization or disproportionation to give SiX_4 and silicon metal. It should be mentioned, however, that in 1986 Jutzi and coworkers successfully prepared the stable Si(II) complex Cp^*_2Si (**12**) ($\text{Cp}^* = \eta^5\text{-Me}_5\text{C}_5$) [49] which prefaced the later isolation of cyclic *N*-heterocyclic silylenes featuring two-coordinate Si(II) centers [50, 51]. Recent developments in the chemistry of *N*-heterocyclic silylenes are summarized by Burgert and Driess in a different chapter of this volume.

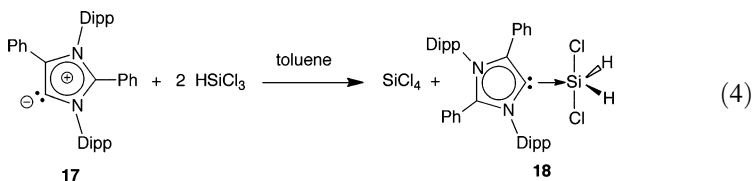
It is important within the context of this review to mention that transient SiCl_2 has been generated under mild conditions and delivered to various substrates. For example, the group of Karsch investigated the dehydrohalogenation of HSiCl_3 using amines as bases to afford SiCl_2 in situ [52]. Later, du Mont and his research team reported the use of $\text{Me}_3\text{Ge-SiCl}_3$ as a chemical source of SiCl_2 [53]. These important discoveries, when taken with the abovementioned reduction of $\text{IPr}\cdot\text{SiCl}_4$ (**7**) to $\text{IPr}\cdot\text{Si}=\text{Si}\cdot\text{IPr}$ (**9**), implied that the Si(II) dihalide complex, $\text{IPr}\cdot\text{SiCl}_2$, might be isolated in pure form under suitable synthetic conditions. Consequently the groups of Roesky and Filippou independently targeted the preparation of adducts of the general form $\text{IPr}\cdot\text{SiX}_2$ (X = halogen) via parallel strategies. For example, Filippou and coworkers generated the stable Si(II) bromide adduct $\text{IPr}\cdot\text{SiBr}_2$ (**14**) in 48% yield by treating the Si(IV) bromide salt $[\text{IPr}\cdot\text{SiBr}_3]\text{Br}$ (**13**) with two

equivalents of KC_8 in THF [54] (2). The Roesky group used a carbene-induced dehydrohalogenation reaction to generate $\text{IPr}\cdot\text{SiCl}_2$ (**15**) in high yield (78%) via the treatment of IPr with HSiCl_3 [55] (3); the imidazolium salt $[\text{IPrH}]\text{Cl}$ generated in the reaction can be separated by filtration and regenerated into free IPr via treatment with $\text{K}[\text{O}^t\text{Bu}]$ [56].

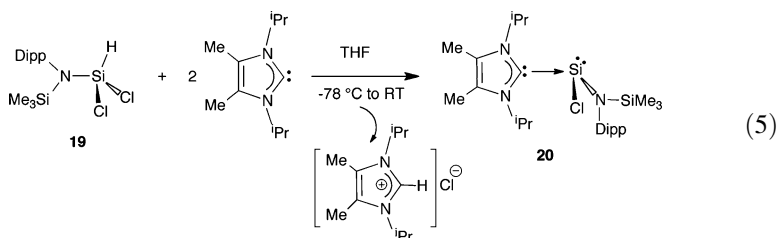


$\text{IPr}\cdot\text{SiBr}_2$ (**14**) is a yellow moisture-sensitive solid that is soluble in arene and ethereal solvents. The $\text{Si}-\text{C}_{\text{IPr}}$ distance in **14** is 1.989(3) Å (by X-ray crystallography) while the adjacent $\text{Si}-\text{Br}$ bonds [2.3493(11) Å *avg.*] are elongated with respect to those found in gas phase SiBr_2 [2.245(3) Å] due to an increase in coordination number at silicon [57]. The isotropic solid state $^{29}\text{Si}\{\text{H}\}$ NMR chemical shift for **14** matched well the value found in C_6D_6 solution indicating a lack of significant intermolecular interactions in between $\text{IPr}\cdot\text{SiBr}_2$ units (as corroborated by X-ray crystallography) [54]. Roesky's $\text{Si}(\text{II})$ dichloride adduct $\text{IPr}\cdot\text{SiCl}_2$ (**15**) exhibits similar overall structural parameters as **14**, with an experimentally identical $\text{Si}-\text{C}_{\text{IPr}}$ distance of 1.985(4) Å and a significantly pyramidalized Si center [bond angle sum at Si = 290.71(19) $^\circ$] [55]. Roesky and coworkers have explored the chemical reactivity of $\text{IPr}\cdot\text{SiCl}_2$ (**15**) in great detail, and these studies will be highlighted later in this review.

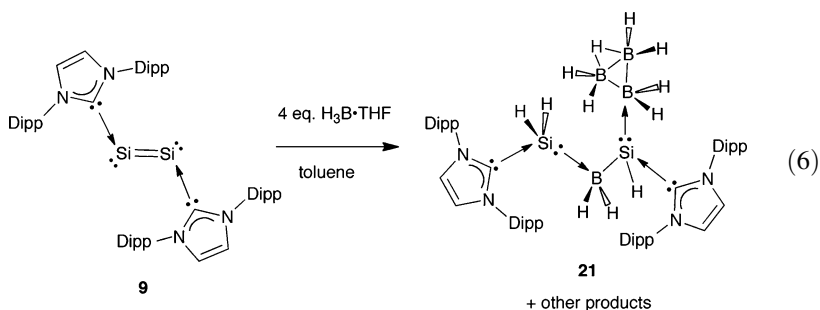
More recently, Roesky reported the reaction of NHCs with H_2SiCl_2 [58]. In the case of the hindered donor, IPr , loss of HCl did not occur (as was the case for HSiCl_3), but instead the formation of the 2:1 adduct $\text{IPr}\cdot\text{H}_2\text{SiCl}_2\cdot\text{IPr}$ (**16**) was noted. Interestingly, when the abnormal carbene **17** was combined with HSiCl_3 , a dismutation reaction transpired to give the 1:1 adduct **18** and SiCl_4 as products (4). In a separate study, IPr was reacted with the formal $\text{Si}(\text{III})$ halide dimer $\text{Cl}_3\text{Si}-\text{SiCl}_3$, resulting in clean disproportionation chemistry to afford $\text{IPr}\cdot\text{SiCl}_4$ and $\text{IPr}\cdot\text{SiCl}_2$ [59].



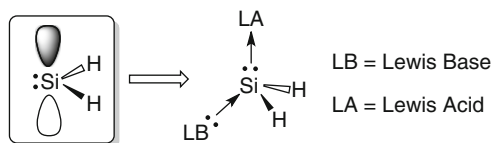
In chemistry which parallels the synthesis of $\text{IPr}\cdot\text{SiCl}_2$ (**15**), Cui and coworkers synthesized the novel amidochlorosilylene adduct $\text{ImMe}_2'\text{Pr}_2\cdot\text{Si}[\text{N}(\text{Dipp})\text{SiMe}_3]\text{Cl}$ (**20**) from the dehydrohalogenation of $[(\text{Me}_3\text{Si})\text{DippN}]\text{SiHCl}_2$ (**19**) with excess $\text{ImMe}_2'\text{Pr}_2$ (**5**) [60]. The same research team explored related carbene-induced dehydrohalogenation chemistry to yield stable *N*-heterocyclic silylenes from parent halohydrides LSiHCl (L = dianionic ligand) [61]. This general route obviates the need for harsh reductants, however, insertion of a backbone positioned C–H group on the *N*-heterocyclic carbene into the silylene generated was occasionally noted.



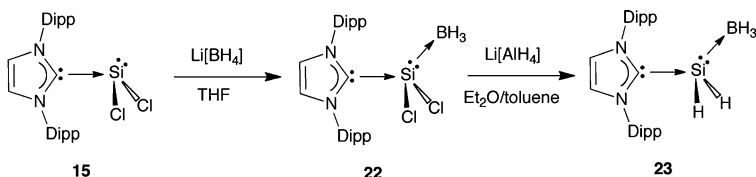
Another synthetic target that was explored within the context of carbene-stabilization was the parent silylene, SiH_2 . Parent silylene has been generated from the photoirradiation of PhSiH_3 with an ArF exciplex laser at 186 nm and studied by spectroscopic means [62]. As silylene adopts a singlet ground state, dual donor–acceptor (or Lewis base–Lewis acid) coordination appeared to be a viable route towards intercepting this species in the condensed phase (Scheme 3). Added interest in this research stems from the role SiH_2 has as an intermediate in the chemical vapor deposition of silicon metal from SiH_4 at high temperatures [63]. The first formal donor–acceptor complex of SiH_2 , $\text{IPr}\cdot\text{SiH}_2\cdot\text{BH}_2\text{-SiH}(\text{B}_3\text{H}_7)\cdot\text{IPr}$ (**21**), was reported in 2011 as a product in 30% yield from the borane-induced Si–Si bond cleavage of the disilene adduct $\text{IPr}\cdot\text{Si}=\text{Si}\cdot\text{IPr}$ (**9**) (6) [64].



In pursuit of a more direct method, Roesky and coworkers reacted $\text{IPr}\cdot\text{SiCl}_2$ (**15**) with the hydride source $\text{Li}[\text{BH}_4]$ with the intention of forming $\text{IPr}\cdot\text{SiH}_2\cdot\text{BH}_3$ (**22**); however, conducting this reaction in THF yielded the borane-capped Si(II) dichloride complex $\text{IPr}\cdot\text{SiCl}_2\cdot\text{BH}_3$ (**22**) [65] (with formal extrusion of LiH).



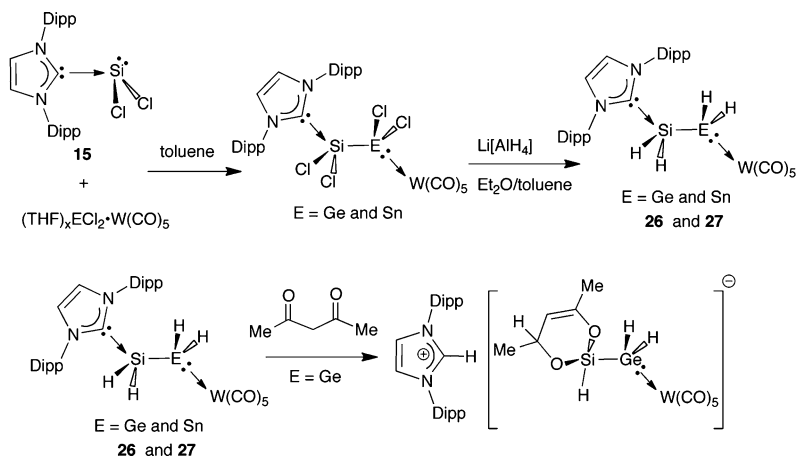
Scheme 3 Singlet structure of SiH₂ and donor–acceptor complexation protocol



Scheme 4 Overall synthetic route towards the silylene adduct IPr•SiH₂•BH₃ (**23**)

Later the Rivard group noted that the hydride source Li[AlH₄] converted IPr•SiCl₂•BH₃ (**22**) into IPr•SiH₂•BH₃ (**23**) when short reaction times coupled with an Et₂O/toluene solvent mixture were employed [66] (Scheme 4); prolonged reaction times led to the formation of copious amounts of the known alane adduct IPr•AlH₃ [67], presumably via a carbene exchange reaction between **23** and the AlH₃ byproduct. Based on the energies of the frontier orbitals in the EH₂ series (E = Si, Ge, Sn and Pb), SiH₂ is predicted to be both the strongest Lewis base and Lewis acid in the series, and concurrently IPr•SiH₂•BH₃ (**23**) is stable in refluxing toluene and only decomposes at ca. 230°C in the solid state under N₂ [66]. For comparison, the previously reported Ge(II) congener IPr•GeH₂•BH₃ (**24**) [43] decomposes completely in refluxing toluene to yield IPr•BH₃ and Ge metal (with H₂ evolution). The tin analogue IPr•SnH₂•BH₃ could not be isolated [68] and the use of the strongly Lewis acidic group W(CO)₅ was required to stabilize the Sn(II) dihydride in the form of the complex IPr•SnH₂•W(CO)₅ (**25**) [68].

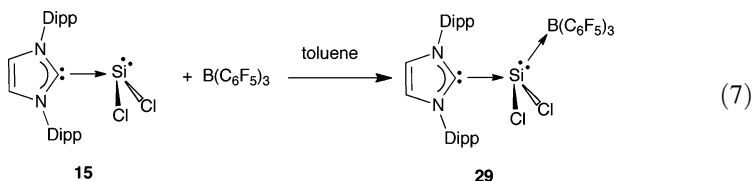
This general donor–acceptor strategy was also used by the Rivard group to access the inorganic ethylene adducts IPr•H₂Si–GeH₂•W(CO)₅ (**26**) and IPr•H₂Si–SnH₂•W(CO)₅ (**27**) [69]. The synthetic route used to prepare **26** and **27** is outlined in Scheme 5 and relies upon the strong nucleophilic character of the Si center in Roesky's silylene adduct IPr•SiCl₂ (**15**) to form the core Si–Ge and Si–Sn linkages by displacing THF from (THF)_xEC1₂•W(CO)₅ (E = Ge and Sn; x = 1 and 2). The nature of the Si–E bonding within these species is currently under investigation; however, IPr•H₂Si–GeH₂•W(CO)₅ (**26**) reacts cleanly with acetylacetonate, demonstrating the hydridic nature of the Si–H bonds (Si^{δ+}–H^{δ-}) and the lability of the terminal C_{IPr}–Si linkage in **26** [69] (Scheme 5). In later work from the same group, the Si(II) hydride IPr•SiH(BH₃)-NHDipp (**28**) was prepared in modest yield from the reaction of the stable Si(II) amide adduct IPr•Si(Cl)NHDipp with excess Li[BH₄] in diethyl ether solvent; compound **28** can be formally regarded as a donor–acceptor adduct of the silyleneamide, HSi(NHDipp) [70].



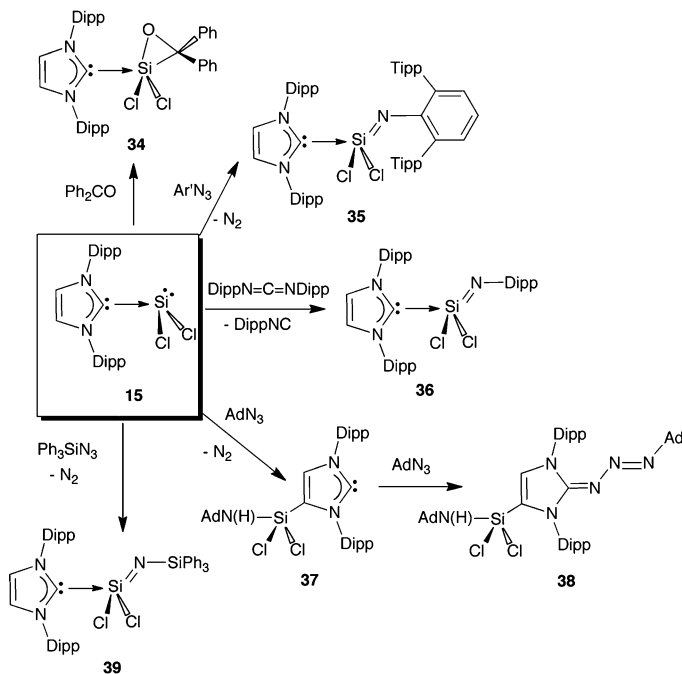
Scheme 5 Synthesis of the heavy ethylene adducts $\text{IPr}\cdot\text{H}_2\text{Si-EH}_2\cdot\text{W}(\text{CO})_5$ (E = Ge and Sn; 26 and 27) and hydrosilylation chemistry

4 Versatile Chemistry of Donor-Stabilized SiCl_2

The Roesky group has investigated the chemistry of $\text{IPr}\cdot\text{SiCl}_2$ (**15**) in great depth and due to Roesky's recent review of his work in this area [71], only a brief selection of this chemistry will be presented here. A common reactivity thread that arises largely from Roesky's work is the nucleophilicity and redox activity of the lone pair at silicon in **15**. For example, the dual electrophilic and nucleophilic character of the SiCl_2 unit was first demonstrated via the synthesis of the donor–acceptor complex $\text{IPr}\cdot\text{SiCl}_2\cdot\text{B}(\text{C}_6\text{F}_5)_3$ (**29**) [72] (7).



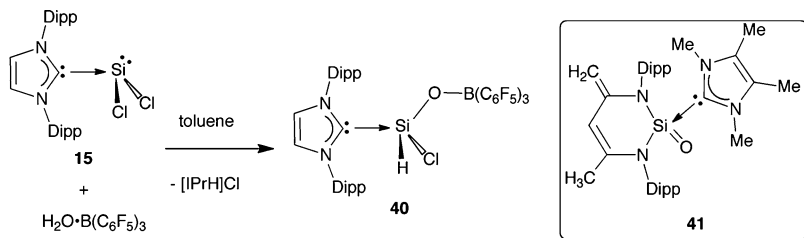
In addition, $\text{IPr}\cdot\text{SiCl}_2$ has been shown to be an effective two-electron donor to a wide range of mid-to-late transition metal complexes as exemplified by the synthesis of complexes such as $[(\text{IPr}\cdot\text{SiCl}_2)_2\text{Ni}(\text{CO})_2]$ (**30**) [73], $[(\text{IPr}\cdot\text{SiCl}_2)_2\text{Co}(\text{CO})_3]^+[\text{CoCl}_3(\text{THF})]^-$ (**31**) [74], $[(\text{IPr}\cdot\text{SiCl}_2)\text{V}(\text{CO})_3\text{Cp}]$ (**32**) [75], and the Rh(I) salt *all-trans*- $[(\text{IPr}\cdot\text{SiCl}_2)_2\text{Rh}(\text{CO})_2]^+[\text{Rh}(\text{CO})_2\text{Cl}_2]^-$ (**33**) by the Rivard group [66]. Moreover Roesky and coworkers have discovered that efficient [1 + 2] cycloaddition chemistry can transpire between $\text{IPr}\cdot\text{SiCl}_2$ (**15**) and Ph_2CO [76] to give **34** (Scheme 6), which highlights the ability of the silicon center in **15** to act both as an electrophile and as a nucleophile in reacting with benzophenone. Further redox chemistry involving $\text{IPr}\cdot\text{SiCl}_2$ (**15**) was uncovered by the same group as



Scheme 6 Representative chemistry of $\text{IPr}\cdot\text{SiCl}_2$ (**15**); Ad = adamantyl; Dipp = 2,6- $i\text{-Pr}_2\text{C}_6\text{H}_3$; Tipp = 2,4,6- $i\text{-Pr}_3\text{C}_6\text{H}_2$

various stable Si(IV) imine complexes were formed by the oxidative coupling of **15** with hindered arylazides [77], such as $\text{Ar}'\text{N}_3$ ($\text{Ar}' = 2,6\text{-Tipp}_2\text{C}_6\text{H}_3$; Tipp = 2,4,6- $i\text{-Pr}_3\text{C}_6\text{H}_2$) [78] (e.g., the synthesis of $\text{IPr}\cdot\text{SiCl}_2=\text{NAr}'$ (**35**) in Scheme 6). An alternate route to an imine complex with a less hindered aryl group at nitrogen was found via the cleavage of the carbodiimide $\text{DippN}=\text{C}=\text{NDipp}$ with **15** to give the known isonitrile DippNC : and $\text{IPr}\cdot\text{SiCl}_2=\text{NDipp}$ (**36**) as products [77]. When compound **15** was combined with adamantyl azide, AdN_3 , the stepwise formation of the NHC backbone activated product **37** and the oxidized triazine **38** was noted [77]. Silylazides, such as Ph_3SiN_3 , also participate in clean oxidation chemistry with **15** to give stable silylamido adducts [78] (e.g., **39**; Scheme 6).

A novel donor–acceptor complex featuring a silicon(IV) oxo bonding environment, $\text{IPr}\cdot\text{SiHCl}(\text{O})\cdot\text{B}(\text{C}_6\text{F}_5)_3$ (**40**), was prepared recently [79]. This formal silaformyl chloride complex was obtained from the condensation reaction between $\text{IPr}\cdot\text{SiCl}_2$ (**15**) and the arylfluoroborane hydrate adduct $\text{H}_2\text{O}\cdot\text{B}(\text{C}_6\text{F}_5)_3$ in toluene (Scheme 7); the HCl produced in this reaction was sequestered by IPr to form the insoluble imidazolium salt $[\text{IPrH}]\text{Cl}$. The Si–O distance in **40** is 1.568(15) Å and is almost 0.03 Å longer with respect to the Si–O bond length in Driess's silanone adduct **41** [80]. Theoretical studies show that some Si–O π -bond character exists in **40**; however, the extremely large polarization (96% towards Si based on NBO analysis) suggests that this bonding interaction is still considerably reduced with respect to free $\text{HClSi}=\text{O}$ where the

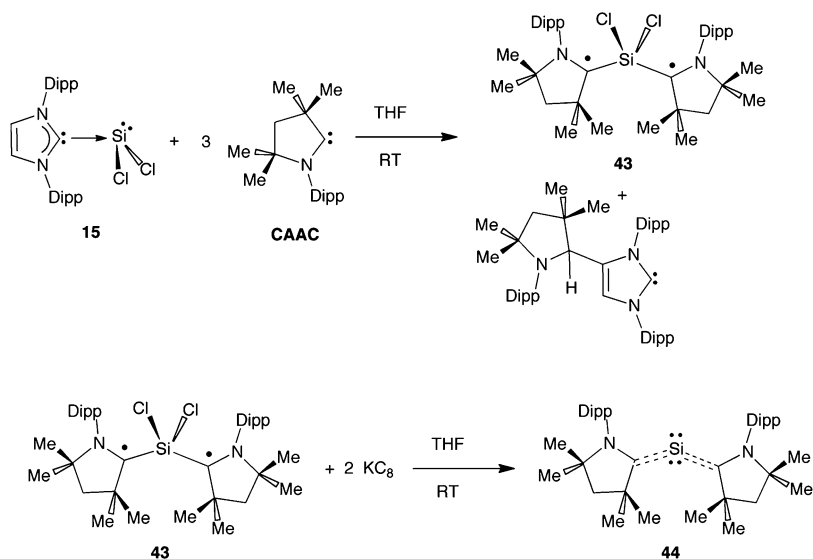


Scheme 7 Synthesis of $\text{IPr}\cdot\text{HSiCl}(\text{O})\cdot\text{B}(\text{C}_6\text{F}_5)_3$ (**40**) and structure of Driess' silanone adduct **41**

π -bonding component is polarized 80% towards Si. Notably, the calculated $C_{\text{IPr}}\text{--Si}$ bond dissociation energy in **40** was 51.1 kcal/mol (77.9 kcal/mol when corrected for dispersion effects) [79].

A nice addition of the field of main group chemistry is the use of muons as hydrogen radical surrogates to probe LUMO states via $\text{E}\text{--}\mu\text{u}$ bond forming chemistry (E = main group element; μu = muonium). In a study by Percival et al. $\text{IPr}\cdot\text{SiCl}_2$ (**15**) was irradiated with muons to give the radical species $\text{IPr}\cdot\text{Si}\mu\text{Cl}_2$ (**42**) with considerable unpaired electron density located at the carbene carbon, as supported by muon spin resonance (μSR) spectroscopy and theoretical calculations [81]. Along the similar theme of carbene-supported radicals, a very interesting combined experimental and theoretical study by the groups of Roesky, Tkach, Stalke, and Frenking appeared in early 2013 concerning the synthesis of the novel silane $\text{L}^\cdot\text{--SiCl}_2\text{--L}^\cdot$ (**43**) diradical (L = CAAC) [82]. The synthesis of **43** was accomplished via ligand exchange chemistry between the $\text{Si}(\text{II})$ dihalide adduct $\text{IPr}\cdot\text{SiCl}_2$ (**15**) with excess CAAC (Scheme 8), and **43** was isolated as a dark blue solid, along with a lighter blue polymorph. These species are exceedingly reactive to air, however are quite thermally stable under inert atmosphere (decomposition noted at 172–173 and 185–186°C for each polymorph). Some broadening of the $^{13}\text{C}\{^1\text{H}\}$ NMR resonances of **43** was noted in solution pointing towards the possible presence of unpaired electron density in **43**. SQUID magnetometry was performed on a sample containing both polymorphs and the residual magnetism observed was interpreted as arising from the presence of a diamagnetic (strongly antiferromagnetic singlet state) along with a weakly ferromagnetically coupled spin system. EPR spectroscopic analysis supported the presence of minor quantities of spin carriers in solution, but failed to detect the characteristic half-field signal of a triplet state. In fact, detailed theoretical studies indicate a small energetic preference (3–5 kcal/mol) for a singlet state in **43** over a triplet state [82].

In a subsequent report, the same research groups detailed the reduction of **43** with two equivalents of KC_8 to give the moderately air-stable silylone complex $\text{L}\cdot\text{Si}\cdot\text{L}$ **44** (L = CAAC) as a blue-black solid in a 95% yield (Scheme 8) [83]. The $\text{Si}\text{--}\text{C}$ bonds in **44** [1.8411(18) Å] are similar to those found in the diradical precursor **43** [1.8469(2) Å *avg.*] [81] and are significantly shortened with respect to the dative $\text{Si}\text{--}\text{C}$ linkage found in $\text{IPr}\cdot\text{SiCl}_2$ [1.985(4) Å] [55]. The $\text{C}\text{--}\text{Si}\text{--}\text{C}$ bond

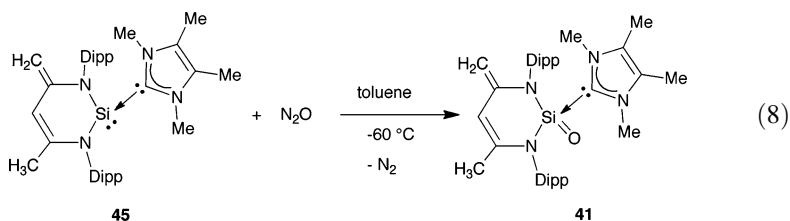


Scheme 8 Synthesis of the diradical silane **43** and its conversion into the silylone adduct **44**

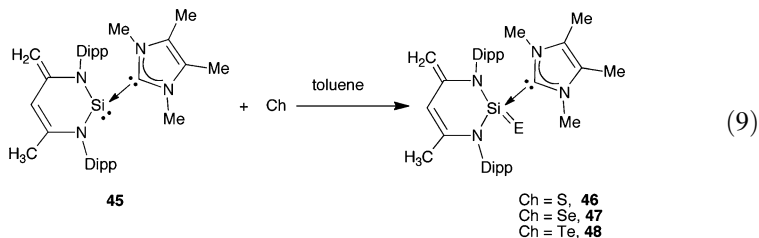
angles in **44** average to $117.44(11)^\circ$ which is narrower than the corresponding angles in Kira's bent silaallenes [ca. 135°] wherein formal Si=Si=Si bonding environments are present [11, 12]. Theoretical studies support the presence of significant Si→C π -backbonding to give a three-center C–Si–C π -manifold, along with an energetically accessible directional non-bonding orbital at silicon (HOMO – 1). Further support for a silylone structure stems from the calculation of two significantly positive successive proton affinity values for **44** (272.2 and 186.7 kcal/mol) [82]. Future reactivity studies will no doubt provide further insight into the bonding and reactivity in this formal bis(CAAC) adduct of a Si(0) atom.

5 Silicon Heterocycles: New Directions in Inorganic Bonding

A longstanding goal of silicon research is to isolate a stable monomeric analogue of the ubiquitous ketone molecular class (e.g., $R_2Si=O$), a repeat unit of economically important polysiloxanes. With the recent impressive advances in ligand design, compounds which exhibit Si–O π -bond character have been isolated [84], with the isolation of a three-coordinate silanone (R_2SiO) with an unsupported Si=O double bond now within synthetic reach [84–86]. An important step towards isolating a silanone in a bottleable form appeared in 2009 when the group of Driess synthesized the NHC-stabilized silanone **41** via the mild oxidation of the carbene-bound silylene **45** with excess N_2O [80] (8).

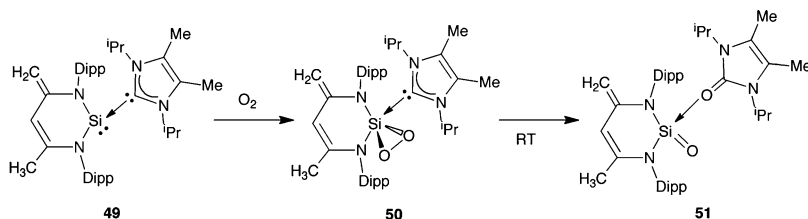


The Si–O distance in **41** was determined to be 1.541(2) Å [80] while the C_{NHC}–Si dative interaction [1.930(2) Å] is the same within experimental error as the C_{IPr}–Si bond length in IPr•Si=Si•IPr (**9**) [1.927(2) Å] [38]. The short Si–O interaction in **41** was accompanied by compressed Si–N bonds [1.748(3) *avg.*] and suggests that considerable zwitterionic character (Si⁺–O[−]) is present in this bonding framework in place of an unperturbed Si=O double bond. Furthermore, a significantly pyramidalized geometry is present at Si in **41**, presumably due to donation of carbene electron density into a Si–O π* orbital ([80]; for a theoretical bonding analysis of four-coordinate, base-stabilized silanoic ester analogues, see [87]). The generality of this stabilization method was further demonstrated by Driess and coworkers with the synthesis of the silachalcone adducts **46–48** via direct reaction of **45** with elemental S, Se, and Te, respectively [88] (9).



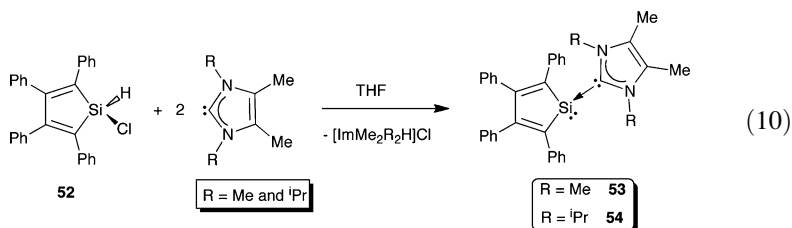
When the ImMe₂^{*i*}Pr₂ silylene adduct **49** was treated with dioxygen, the unusual carbene-supported dioxasilirane **50** was obtained (Scheme 9) [89]. Upon storing **50** in toluene at room temperature, a clean oxo transfer reaction transpired to form the *N*-heterocyclic ketone-bound silanone complex **51** (Scheme 9). The formal insertion of an oxo unit into a Si–C linkage is reminiscent of the transformation of metastable dioxasiliranes R₂SiO₂ into silanoic esters RSi(O)OR [90]. The O–O distances in the dioxasilirane **50** is 1.510(3) Å and is in the range expected for organodioxiranes [91]. Expanded Si–O distances in **50** [1.682(2)–1.693(2) Å] were noted in **50** relative to those calculated for donor-free dioxasiliranes R₂SiO₂ (1.632–1.678 Å; [92]) due to the increase in coordination number at the silicon center in **50** [89].

Carbene-stabilized silacyclopentadienylidenes ImMe₂R₂•Si(C₄Ph₄) (R = Me and ^{*i*}Pr; **53** and **54**) were prepared as orange-red or orange-yellow solids by Cui and coworkers via the dehydrohalogenation of HSi(Cl)C₄Ph₄ **52** (10) [93]. The presence of a stereochemically active lone pair in **54** was confirmed by X-ray crystallography, and revealed a highly pyramidalized geometry about the Si center.



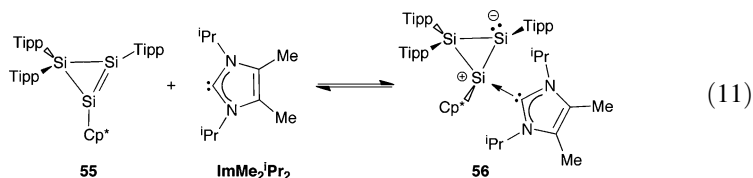
Scheme 9 Synthesis of the dioxasilirane **50** and thermal cleavage of the SiO₂ heterocycle [89]

In compound **54**, the central aryl ring of the ImMe₂^{*i*}Pr₂ donor lies nearly orthogonal to the silicon heterocycle (91.8° between the planes) in line with electron donation from a carbene carbon lone pair into an orbital of high p-character on Si (91% according to DFT calculations) [93]. Silicon heterocycle ring-expansion and insertion chemistry was also reported between **54** and unsaturated substrates such as aldehydes and alkynes [94].

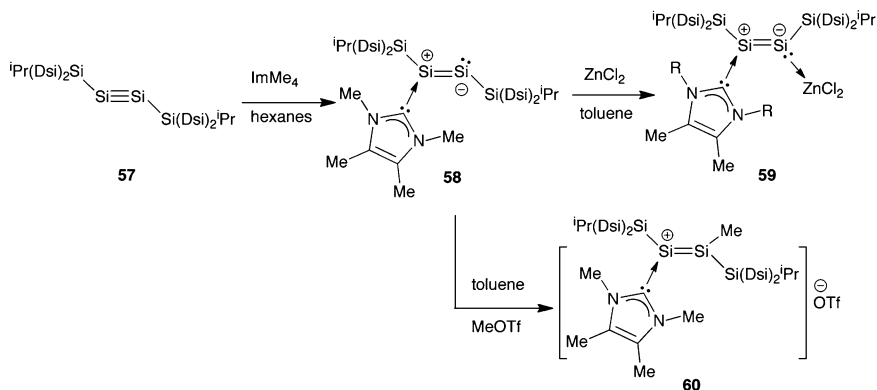


6 Multiply Bonded Silenes and Silynes

The groups of Scheschkewitz and Jutzi reported a joint research endeavor which described the reversible coordination of ImMe₂^{*i*}Pr₂ with the heterocyclic disilene Tipp₂SiSi(Cp*)=SiTipp **55** to form **56** [95] (11). The endocyclic Si=Si bond in **56** [2.2700(5) Å] is longer than the calculated Si=Si distance for the base-free Si₃ ring in **55** indicating donation of the electron density from the carbene into a Si–Si π* orbital. Moreover, substantial pyramidalization of the Si center adjacent to the carbene-bound Si was noted due to the acquisition of non-bonding (lone pair) character upon coordination of the NHC [95].

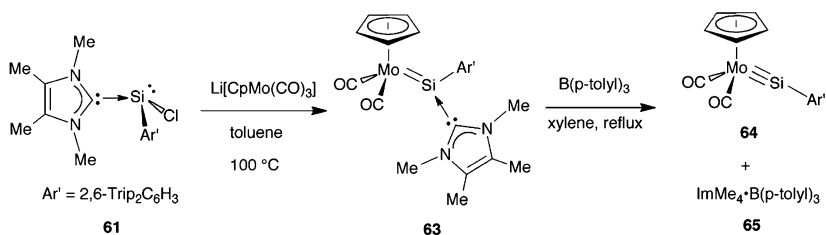


Sekiguchi and Driess also investigated the chemistry between the *N*-heterocyclic carbene ImMe_4 and the disilyne $(^i\text{PrDsi}_2\text{Si})\text{Si}\equiv\text{Si}(\text{Dsi}_2^i\text{Pr})$ [$\text{Dsi}=\text{CH}(\text{SiMe}_3)_2$] (**57**) (Scheme 10) [96, 97]. When the stable disilyne **57** was combined with ImMe_4 in hexanes, the stable 1:1 adduct [$\text{ImMe}_4\cdot(^i\text{PrDsi}_2\text{Si})\text{Si}=\text{Si}(\text{Dsi}_2^i\text{Pr})$] (**58**) was obtained as an air- and moisture-sensitive brown solid [96]. The $\text{C}_{\text{NHC}}\text{-Si}$ linkage [1.9211(16) Å] in **58** was found to be similar in value as the $\text{C}_{\text{IPr}}\text{-Si}$ bond in Robinson's adduct $\text{IPr}\cdot\text{Si}=\text{Si}\cdot\text{IPr}$ (**9**) [1.9271(15) Å] [28], while the central Si-Si distance in **58** is elongated by ca. 0.13 Å relative to the disilyne precursor **57** [2.0622(9) Å] [10], thus the Si-Si interaction in **58** was formulated as a Si=Si double bond. In addition, coordination of ImMe_4 to **57** increases the nucleophilicity of one of the Si atoms and enables the synthesis of the ZnCl_2 complex, $\text{ImMe}_4\cdot(^i\text{PrDsi}_2\text{Si})\text{Si}=\text{Si}(\text{Dsi}_2^i\text{Pr})\cdot\text{ZnCl}_2$ (**59**) [96]; interestingly, a *cis* arrangement of the hindered $-\text{Si}(\text{Dsi}_2^i\text{Pr})$ substituents is present in the solid state. To further illustrate the Lewis basic character of the two-coordinate silylene center in **58**, this adduct was combined with the alkylating agent MeOTf ($\text{OTf} = \text{F}_3\text{CSO}_3^-$) to generate the novel disilyl cation [$\text{ImMe}_4\cdot(^i\text{PrDsi}_2\text{Si})\text{Si}=\text{Si}(\text{Dsi}_2^i\text{Pr})\text{Me}$] $^+$ as a triflate salt (**60**) [97] (Scheme 10).



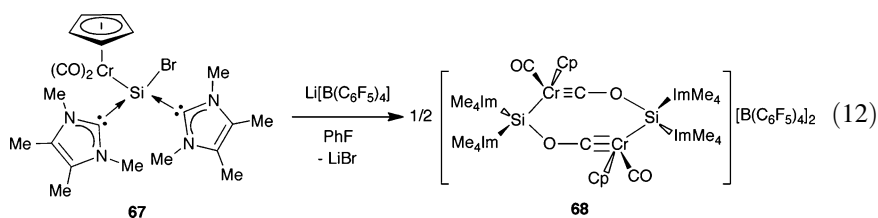
Scheme 10 Synthesis and representative chemistry of [$\text{ImMe}_4\cdot(^i\text{PrDsi}_2\text{Si})\text{Si}=\text{Si}(\text{Dsi}_2^i\text{Pr})$] (**58**)

The use of NHCs as protecting groups or masking agents for chemical transformations is another emerging aspect of modern main group chemistry. Soon after the discovery of SiX_2 adducts ($\text{X} = \text{Br}$ and Cl) of IPr in 2009 [54, 55], the Filippou group synthesized the arylchlorosilylene and germylene complexes $\text{ImMe}_4\cdot\text{ECl}(\text{Ar}')$ [$\text{E} = \text{Si}$ and Ge , (**61**) and (**62**); $\text{Ar}' = 2,6\text{-Tipp}_2\text{C}_6\text{H}_3$] [98]. The stable Si(II) adduct **61** was then reacted with $\text{Li}[\text{Mo}(\text{CO})_2\text{Cp}]$ in hot toluene (100°C) to

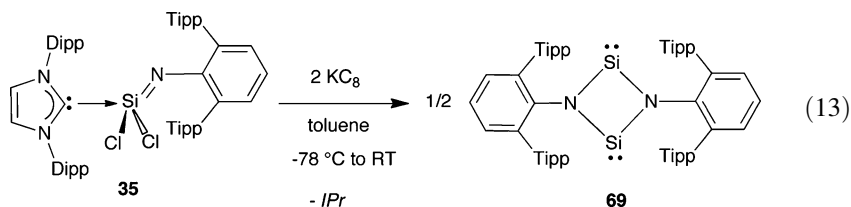


Scheme 11 Generation of the metallosilyne **64** via carbene-bound Si(II) reagents

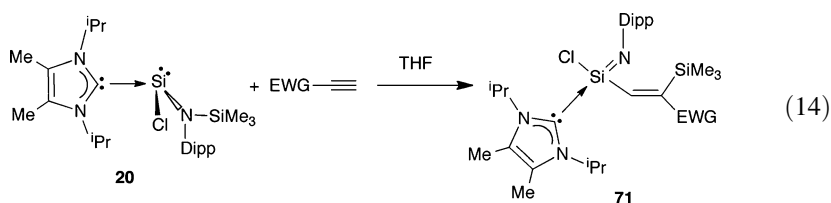
yield the carbene-sequestered metallosilene $[\text{CpMo}(\text{CO})_2=\text{Si}(\text{Ar}')\cdot\text{ImMe}_4]$ (**63**) as a dark-brown solid [99]. Removal of the silicon-bound carbene was possible via treatment of **63** with the Lewis acid $\text{B}(\text{p-tolyl})_3$ to yield the base-free metallosilyne $[\text{CpMo}(\text{CO})_2\equiv\text{SiAr}']$ (**64**) along with $\text{ImMe}_4\cdot\text{B}(\text{p-tolyl})_3$ (**65**) as a byproduct (Scheme 11). Removal of the carbene from **63** to form the metallosilyne $[\text{CpMo}(\text{CO})_2\equiv\text{SiAr}']$ (**64**) resulted in a contraction of the Mo–Si distance from 2.3452(8) Å *avg.* in **63** to 2.2241(7) Å in **64**, with a concomitant widening of the Mo–Si–C_{Ar'} angle from 145.32(8)° *avg.* to 173.49(8)° [99]. These metric parameters support the presence of Mo–Si triple bonding in **64** while IR spectroscopic analysis revealed that Mo–CO π -backbonding is stronger in this complex than in the alkyldiyne congener $[\text{CpMo}(\text{CO})_2\equiv\text{C}(\text{Xyl})]$; $\text{Xyl} = 2,6\text{-Me}_2\text{C}_6\text{H}_3$] [100]. It should be reiterated that the success of the synthetic protocol outlined in Scheme 11 relies entirely upon the ability of NHCs to stabilize low-oxidation state Si(II) species, such as $\text{Ar}'\text{SiCl}$. Filippou and coworkers expanded upon this novel study to prepare the chromium complex $[\text{CpCr}(\text{CO})_2=\text{SiBr}\cdot\text{SiPr}]$ (**66**) ($\text{SiPr} = [(\text{H}_2\text{CNDipp})_2\text{C}]$), which undergoes NHC-substitution chemistry to yield the metallosilene adduct $[\text{CpCr}(\text{CO})_2\text{-Si}(\text{ImMe}_2\text{Pr}_2)_2\text{Br}]$ (**67**) [101]; removal of a bromide from the Si center in **67** was accomplished with $\text{Li}[\text{B}(\text{C}_6\text{F}_5)_4]$ to give the unusual chromium alkyldiyne dimer **68** (12) [101].



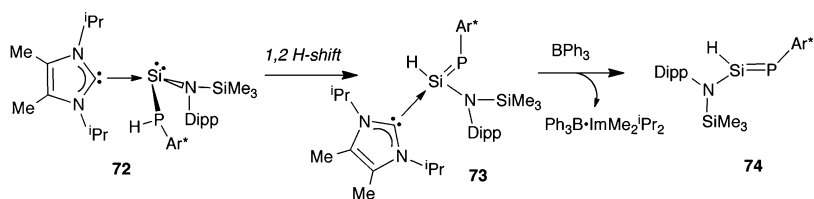
In a conceptually related fashion, the Si(IV)imido adduct $\text{IPr}\cdot\text{SiCl}_2=\text{NAr}'$ (**35**) [102] was reduced with KC_8 to give the silaisonitrile dimer $(:\text{SiNAr}')_2$ (**69**) as a yellow crystalline solid in a 21% yield (13) [103]. The two terphenyl ligands in **69** form a steric pocket which surrounds the Si_2N_2 core and intraring Si–N single bonds of 1.755(1) Å *avg.* were determined by X-ray crystallography. Calculated Laplacian distributions support the presence of a lone pair of electrons at each Si center, and accordingly, Staudinger type reactivity between **69** and Me_3SiN_3 was noted to form the oxidized silimine $\text{Me}_3\text{SiN}=\text{Si}(\mu\text{-NAr}')_2\text{Si}=\text{NSiMe}_3$ (**70**) [103].



The regiospecific silylation of electron deficient alkynes with $\text{ImMe}_2^i\text{Pr}_2\cdot\text{SiCl}[\text{N}(\text{Dipp})\text{SiMe}_3]$ (**20**) was reported by the Cui group [104] (14). The resulting products $\text{ImMe}_2^i\text{Pr}_2\cdot\text{SiCl}=\text{NDipp}[\text{CH}=\text{C}(\text{SiMe}_3)\text{EWG}]$; EWG = electron withdrawing group) **71** were generated in high yield and conversion of these species into the synthetically useful trimethoxysilyl-olefins was possible upon treatment with excess methanol [104].



The same group prepared the amidophosphidosilylene adduct $\text{ImMe}_2^i\text{Pr}_2\cdot\text{Si}(\text{PAr}^*\text{H})[\text{NDipp}(\text{SiMe}_3)]$ [$\text{Ar}^* = 2,6\text{-Mes}_2\text{C}_6\text{H}_3$] (**72**) from the salt elimination reaction between **20** and $\text{Li}[\text{PHAr}^*]$ [105]. Compound **72** underwent a 1,2 hydrogen shift process under ambient conditions to afford a rare example of a silaphosphene $\text{ImMe}_2^i\text{Pr}_2\cdot(\text{H})\text{Si}=\text{PAr}^*[\text{NDipp}(\text{SiMe}_3)]$ (**73**) (as indicated in Scheme 12). The base-free analogue $(\text{H})\text{Si}=\text{PAr}^*[\text{NDipp}(\text{SiMe}_3)]$ (**74**) was then generated via removal of the *N*-heterocyclic carbene $\text{ImMe}_2^i\text{Pr}_2$ via complexation with BPh_3 . Compound **74** was structurally authenticated by X-ray crystallography, and this study revealed the presence of a short $\text{P}=\text{Si}$ multiple bond [2.0718(6) Å] and second-order perturbation theory identified a significant $\text{N}-\text{Si}$ negative hyperconjugative interaction between the lone pair on N and the low-lying $\text{Si}-\text{P}$ π^* orbital in **74** [105].

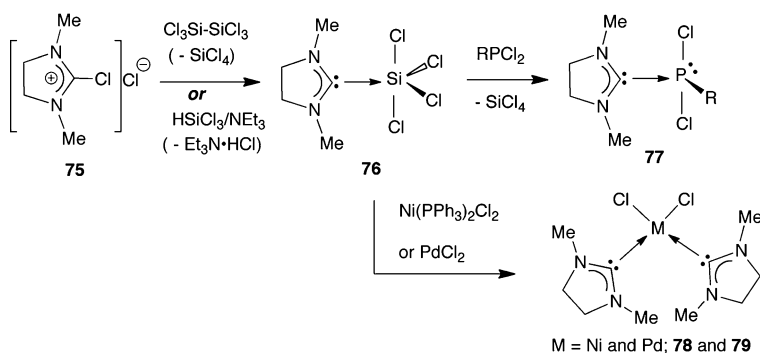


Scheme 12 Synthesis of the silaphosphene adduct **73** and generation of the free silaphosphene **74** via decomplexation chemistry

7 New Synthetic Strategies Involving Silylated Carbenes and Silylimidazolium Cations

Although hindered NHCs, such as IPr, are in general straightforward to prepare, their lighter analogues show greater thermal instability and are often synthesized via reduction of their corresponding thiones $\text{NHC}=\text{S}$ with potassium metal in refluxing THF [22]. An interesting method of generating carbenes that avoids either the isolation of free carbenes or the use of pyrophoric reagents was reported recently by the Rösenthaller group [106]. For example, the stable adduct $\text{SiMe}_2\cdot\text{SiCl}_4$ (**76**) could be synthesized from the commercially available chloroimidazolium salt **75** and later used to transfer carbene (SiMe_2) to both main group element and transition metal (Ni or Pd) centers (Scheme 13).

Weigand and coworkers have explored *C*-silylated imidazolium salts, such as $[\text{ImMe}_2^i\text{Pr}_2\text{-SiMe}_3]\text{OTf}$ (**80**), as mild carbene delivery agents to yield various cationic and dicationic phosphorus (III) adducts via ClSiMe_3 elimination chemistry. A nice illustration of this concept was the high yielding reaction between PCl_3 and two equivalents of **80** at 50°C under sonication to give the formal PCl_2^{2+} dication as a bis(carbene) adduct $[(\text{ImMe}_2^i\text{Pr}_2)_2\text{PCl}](\text{OTf})_2$ (**81**) [32] (15).

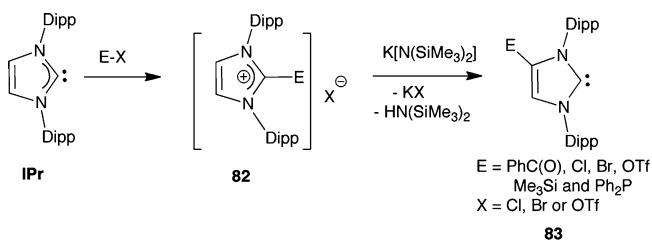


Scheme 13 $\text{SiImMe}_2\cdot\text{SiCl}_4$ (**76**) as a useful carbene transfer reagent



An often encountered, and generally undesired, ligand activation process that transpires with carbenes bearing unsubstituted olefinic backbones (e.g. IPr) is insertion chemistry involving the exposed C–H groups along the heterocyclic backbone [107]. Placement of alkyl groups at the 4- and 5-positions of the carbene

ring does mitigate this side-reaction at the expense of more difficult NHC syntheses. The Bertrand group used backbone C–H activation to their advantage, and devised a general and rapid method to functionalize the 4- and 5-positions of the readily available carbene, IPr [108] (Scheme 14). In this general procedure, the carbenic center of IPr is first functionalized with various electrophiles to yield a family of precursor imidazolium salts [IPr-E]X (E=PhC(O), Cl, Br, OTf, Me₃Si, and PPh₂; X = Cl, Br, or OTf) (**82**). Upon treatment of these salts with the hindered base K[N(SiMe₃)₂] a formal migration of the electrophilic group from the N–C–N carbon to the olefin backbone transpired generating a nucleophilic carbene site in the process (**83**). This procedure can be adapted to generate asymmetrically disubstituted NHCs (at the 4- and 5-positions) in moderate to high yields [108].



Scheme 14 Synthesis of backbone-functionalized IPr analogues

8 Summary and Future Directions

This review article hopefully conveys the rapid growth and general excitement associated with the use of NHCs as ligands in modern silicon chemistry. As a result of this new paradigm in chemical synthesis, a variety of novel reactive species that were previously elusive to synthetic chemists [109] could now be intercepted as stable complexes. Not only can fundamentally intriguing species, such as SiCl₂, Si₂, and H₂SiGeH₂, be handled under ambient conditions (in the form of stable adducts with NHCs), these encapsulated species readily participate in subsequent chemistry anticipated for the free species due to the labile nature of the dative C_{NHC}–Si bonds. It is conceivable that this stabilization strategy could be used to generate new chemical reagents for the controlled synthesis of silicon nanostructures or clusters upon thermolysis chemistry (e.g., starting from metastable SiH₂ adducts such as IPr•SiH₂•BH₃ (**23**) [66]). The recent synthesis of the first stable bis-carbene silylone complex CAAC•Si•CAAC (**44**) [83] should also be seen as a sign that the search for new bonding environments involving silicon will not abate any time soon. Although not specifically mentioned in this review, NHCs are being used as catalysts in organosilicon chemistry and as initiators for the ring-opening polymerization of cyclic siloxanes [110]. In this light, more advances in NHC-mediated bond forming chemistry involving silicon-based substrates can be expected in the near future.

References

1. Rappoport Z, Apeloig Y (1988) Chemistry of organosilicon compounds, vol 2. Wiley, Chichester
2. Power PP (1999) π -Bonding and the lone pair effect in multiple bonding between heavier main group elements. *Chem Rev* 99:3463–3504
3. Fischer RC, Power PP (2010) π -Bonding and the lone pair effect in multiple bonds involving heavier main group elements: developments in the new millennium. *Chem Rev* 110:3877–3923
4. Weidenbruch M (2003) From a cyclotrisilane to a cyclotriplumbane: low coordination and multiple bonding in group 14 chemistry. *Organometallics* 22:4348–4360
5. Mizuhata Y, Sasamori T, Tokitoh N (2009) Stable heavier carbene analogues. *Chem Rev* 109:3479–3511
6. Asay M, Jones C, Driess M (2011) *N*-Heterocyclic carbene analogues with low-valent group 13 and group 14 elements: synthesis, structures, and reactivities of a new generation of multitolerant ligands. *Chem Rev* 111:354–396
7. Li L, Fukawa T, Matsuo T, Hashizume D, Fueno H, Tanaka K, Tamao K (2012) A stable germanone as the first isolated heavy ketone with a terminal oxygen atom. *Nat Chem* 4:361–365
8. West R, Fink M, Michl J (1981) Tetramesityldisilene, a stable compound containing a silicon–silicon double bond. *Science* 214:1343–1344
9. Wiberg N, Niedermayer W, Fischer G, Nöth, H, Suter M (2002) Synthesis, structure and dehalogenation of the disilene $\text{RCiSi}=\text{SiClR}$ [$\text{R} = (\text{tBu}_3\text{Si})_2\text{MeSi}$]. *Eur J Inorg Chem* 1066–1070
10. Sekiguchi A, Kinjo R, Ichinohe M (2004) A stable compound containing a silicon–silicon triple bond. *Science* 305:1755–1757
11. Ishida S, Iwamoto T, Kabuto C, Kira M (2003) A stable silicon-based allene analogue with a formally *sp*-hybridized silicon atom. *Nature* 421:725–727
12. Kira M (2010) An isolable dialkylsilylene and its derivatives. A step toward comprehension of heavy unsaturated bonds. *Chem Commun* 2893–2903
13. Ya Lee V, Sekiguchi A (2010) Organometallic compounds of low-coordinate Si, Ge, Sn and Pb: from phantom species to stable compounds. Wiley, Hoboken
14. Power PP (2003) Silicon, germanium, tin and lead analogues of acetylenes. *Chem Commun* 2091–2101
15. Power PP (2007) Bonding and reactivity of heavier group 14 element alkyne analogues. *Organometallics* 26:4362–4372
16. Rivard E, Power PP (2007) Multiple bonding in heavier element compounds stabilized by bulky terphenyl ligands. *Inorg Chem* 46:10047–10064
17. Spikes GH, Fettinger JC, Power PP (2007) Facile activation of dihydrogen by an unsaturated heavier main group compound. *J Am Chem Soc* 127:12232–12233
18. Power PP (2011) Interaction of multiple bonded and unsaturated heavier main group compounds with hydrogen, ammonia, olefins, and related molecules. *Acc Chem Res* 44:627–637
19. Protchenko AV, Birjkumar KH, Dange D, Schwarz AD, Vidovic D, Jones C, Kaltsoyannis N, Mountford P, Aldridge S (2012) A stable two-coordinate acyclic silylene. *J Am Chem Soc* 134:6500–6503
20. Arduengo AJ III, Harlow RL, Kline M (1991) A stable crystalline carbene. *J Am Chem Soc* 113:361–363
21. Arduengo AJ III (1999) Looking for stable carbenes: the difficulty in starting anew. *Acc Chem Res* 32:913–921
22. Kuhn N, Kratz T (1993) Synthesis of imidazol-2-ylidenes by reduction of imidazole-2(3H)-thiones. *Synthesis* 561–562

23. Martin D, Melaimi M, Soleilhavoup M, Bertrand G (2011) A brief survey of our contribution to stable carbene chemistry. *Organometallics* 30:5304–5313
24. Wang Y, Robinson GH (2009) Unique homonuclear multiple bonding in main group compounds. *Chem Commun* 5201–5213
25. Wang Y, Robinson GH (2011) Carbene stabilization of highly reactive main-group molecules. *Inorg Chem* 50:12326–12337
26. Kuhn N, Al-Sheikh A (2005) 2,3-Dihydroimidazol-2-ylidenes and their main group element chemistry. *Coord Chem Rev* 249:829–857
27. Wang Y, Quillian B, Wei P, Wannere CS, Xie Y, King RB, Schaefer HF III, Schleyer PVR, Robinson GH (2007) A stable neutral diborene containing a BB double bond. *J Am Chem Soc* 129:12412–12413
28. Braunschweig H, Dewhurst RD, Hammond K, Mies J, Radacki K, Vargas A (2012) Ambient-temperature isolation of a compound with a boron-boron triple bond. *Science* 336:1420–1422
29. Kinjo R, Donnadiou B, Ali Celik M, Frenking G, Bertrand G (2011) Synthesis and characterization of a neutral tricoordinate organoboron isoelectronic with amines. *Science* 333:610–613
30. Masuda JD, Schoeller WW, Donnadiou B, Bertrand G (2007) NHC-mediated aggregation of P₄: isolation of a P₁₂ cluster. *J Am Chem Soc* 129:14180–14181
31. Back O, Kuchenbeiser G, Donnadiou B, Bertrand G (2009) Nonmetal-mediated fragmentation of P₄: isolation of P₁ and P₂ bis(carbene) adducts. *Angew Chem Int Ed* 48:5530–5533
32. Weigand JJ, Feldmann K–O, Henne FD (2010) Carbene-stabilized phosphorus(III)-centered cations [LPX₂]⁺ and [L₂PX]²⁺ (L = NHC; X = Cl, CN, N₃). *J Am Chem Soc* 132:16321–16323
33. Abraham MY, Wang Y, Xie Y, Wei P, Schaefer HF III, Schleyer PVR, Robinson GH (2010) Carbene stabilization of diarsenic: from hypervalency to allotropy. *Chem Eur J* 16:432–435
34. Haaland A (1989) Covalent versus dative bonds to main group metals, a useful distinction. *Angew Chem Int Ed Engl* 28:992–1007
35. Kuhn N, Henkel G, Kratz T, Kreutzberg J, Boese R, Maulitz AH (1993) Derivate des Imidazols, VI. Stabile carben–borane. *Chem Ber* 126:2041–2045
36. Kuhn N, Kratz T, Bläser D, Boese R (1995) Derivates des Imidazols, XIII. Carben-Komplexe des Siliciums und Zinns. *Chem Ber* 128:245–250
37. Ghadwal RS, Sen SS, Roesky HW, Tavcar G, Merkel S, Stalke D (2009) Neutral penta- and hexacoordinate *N*-heterocyclic carbene complexes derived from SiX₄ (X = F, Br). *Organometallics* 28:6374–6377
38. Wang Y, Xie Y, Wei P, King RB, Schaefer HF III, Schleyer PVR, Robinson GH (2008) A stable silicon(0) compound with a Si=Si double bond. *Science* 321:1069–1071
39. Li S, Van Zee RJ, Weltner W (1994) Magneto-infrared spectra of the Si₂, Ge₂, and Sn₂ molecules in rare-gas matrices. *J Chem Phys* 100:7079–7086
40. Jones C (2001) The stabilization and reactivity of indium trihydride complexes. *Chem Commun* 2293–2298
41. Sidiropoulos A, Jones C, Stasch A, Klein S, Frenking G (2009) *N*-Heterocyclic carbene stabilized digermanium(0). *Angew Chem Int Ed* 48:9701–9704
42. Jones C, Sidiropoulos A, Holzmann N, Frenking G, Stasch A (2012) An *N*-heterocyclic carbene adduct of diatomic tin, :Sn=Sn: *Chem Commun* 48:9855–9857
43. Thimer KC, Al-Rafia SMI, Ferguson MJ, McDonald R, Rivard E (2009) Donor/acceptor stabilization of Ge(II) dihydride. *Chem Commun* 7119–7121
44. Green SP, Jones C, Stasch A (2007) Stable magnesium(I) compounds with Mg–Mg bonds. *Science* 318:1754–1757
45. Bonyhady SJ, Jones C, Nembenna S, Stasch A, Edwards AJ, McIntyre GJ (2010) β-Diketiminato-stabilized magnesium(I) dimers and magnesium(II) hydride complexes: synthesis, characterization, adduct formation, and reactivity studies. *Chem Eur J* 16:938–955
46. Timms PL (1973) Chemistry of boron and silicon subhalides. *Acc Chem Res* 6:118–123
47. Urry G (1970) Systematic synthesis in the polysilane series. *Acc Chem Res* 3:306–312

48. Sirtl E, Reuschel K (1964) Über die Reduktion von Chlorosilanen mit Wasserstoff. *Z Anorg Allg Chem* 332:113–123
49. Jutzi P, Kanne D, Krüger C (1986) Decamethylsilicocene-synthesis and structure. *Angew Chem Int Ed Engl* 25:164
50. Denk M, Lennon R, Hayashi R, West R, Belyakov AV, Verne HP, Haaland A, Wagner M, Metzler N (1994) Synthesis and structure of a stable silylene. *J Am Chem Soc* 116:2691–2692
51. Haaf M, Schmedake TA, West R (2000) Stable silylenes. *Acc Chem Res* 33:704–714
52. Karsch HH, Bienlein F, Sladek A, Heckel M, Burger K (1995) New method for the synthesis of silaheterocycles and the first pentacoordinate silanol. *J Am Chem Soc* 117:5160–5161
53. du Mont W-W, Gust T, Seppälä E, Wismach C, Jones PG, Ernst L, Grunenberg J, Marsmann HC (2002) Unusual P=C bond cleavage by double dichlorosilylene transfer from trichlorosilyltrimethylgermane to *P*-phosphanyl phosphalkenes. *Angew Chem Int Ed* 41:3829–3832
54. Filippou AC, Chernov O, Schnakenburg G (2009) SiBr₂(Idipp): a stable *N*-heterocyclic carbene adduct of dibromosilylene. *Angew Chem Int Ed* 48:5687–5690
55. Ghadwal RS, Roesky HW, Merkel S, Henn J, Stalke D (2009) Lewis base stabilized dichlorosilylene. *Angew Chem Int Ed* 48:5683–5686
56. Jafarpour L, Stevens ED, Nolan SP (2000) A sterically demanding nucleophilic carbene: 1,3-bis(2,6-diisopropylphenyl)imidazol-2-ylidene). Thermochemistry and catalytic application in olefin metathesis. *J Organomet Chem* 606:49–54
57. Hargittai I, Schultz G, Tremmel J, Kagramanov ND, Maltsev AK, Nefedov OM (1983) Molecular structure of silicon dichloride and silicon dibromide from electron diffraction combined with mass spectrometry. *J Am Chem Soc* 105:2895–2896
58. Pratap Singh A, Ghadwal RS, Roesky HW, Holstein JJ, Dittrich B, Demers J-P, Chevelkov V, Lange A (2012) Lewis base mediated dismutation of trichlorosilane. *Chem Commun* 48:7574–7576
59. Ghadwal RS, Pröpper K, Dittrich B, Jones PG, Roesky HW (2011) Neutral pentacoordinate silicon fluorides derived from amidinate, guanidinate, and triazapentadienate ligands and base-induced disproportionation of Si₂Cl₆ to stable silylenes. *Inorg Chem* 50:358–364
60. Cui H, Cui C (2011) Silylation of *N*-heterocyclic carbene with aminochlorosilane and -disilane: dehydrogenation vs. Si–Si bond cleavage. *Dalton Trans* 40:11937–11940
61. Cui H, Shao Y, Li X, Kong L, Cui C (2009) Dehydrochlorination to silylenes by *N*-heterocyclic carbenes. *Organometallics* 28:5191–5195
62. Gaspar PP, Holten D, Konieczny S, Corey JY (1987) Laser photolysis of silylene precursors. *Acc Chem Res* 20:329–336
63. Jasinski JM, Gates SM (1991) Facile synthesis of a rare silicon chemical vapor deposition one step at a time: fundamental studies of silicon hydride chemistry. *Acc Chem Res* 24:9–15
64. Abraham MY, Wang Y, Xie Y, Wei P, Schaefer HF III, Schleyer PVR, Robinson GH (2011) Cleavage of carbene-stabilized disilicon. *J Am Chem Soc* 133:8874–8876
65. Azhakar A, Tavcar G, Roesky HW, Hey J, Stalke D (2011) Synthesis of a rare chlorosilylene-BH₃ adduct. *Eur J Inorg Chem* 475–477
66. Al-Rafia SMI, Malcolm AC, McDonald R, Ferguson MJ, Rivard E (2012) Efficient generation of stable adducts of Si(II) dihydride using a donor-acceptor approach. *Chem Commun* 48:1308–1310
67. Baker RJ, Davies AJ, Jones C, Kloth M (2002) Structural and spectroscopic studies of carbene and *N*-donor ligand complexes of group 13 hydrides and halides. *J Organomet Chem* 656:203–210
68. Al-Rafia SMI, Malcolm AC, Liew SK, Ferguson MJ, Rivard E (2011) Stabilization of the heavy methylene analogues, GeH₂ and SnH₂, within the coordination sphere of a transition metal. *J Am Chem Soc* 133:777–779
69. Al-Rafia SMI, Malcolm AC, McDonald R, Ferguson MJ, Rivard E (2011) Trapping the parent inorganic ethylenes H₂SiGeH₂ and H₂SiSnH₂ in the form of stable adducts at ambient temperature. *Angew Chem Int Ed* 50:8354–8357

70. Al-Rafia SMI, McDonald R, Ferguson MJ, Rivard E (2012) Preparation of stable low-oxidation-state group 14 element amidohydrides and hydride-mediated ring-expansion chemistry of *N*-heterocyclic carbenes. *Chem Eur J* 18:13810–13820
71. Roesky HW (2013) Chemistry of low valent silicon. *J Organometal Chem.* doi:10.1016/j.jorganchem.2012.08.025
72. Ghadwal RS, Roesky HW, Merkel S, Stalke D (2010) Ambiphilicity of dichlorosilylene in a single molecule. *Chem Eur J* 16:85–88
73. Tavcar G, Sen SS, Azhakar R, Thorn A, Roesky HW (2010) Facile syntheses of silylene nickel carbonyl complexes from Lewis base stabilized chlorosilylenes. *Inorg Chem* 49:10199–10202
74. Li J, Merkel S, Henn J, Meindl K, Döring A, Roesky HW, Ghadwal RS, Stalke D (2010) Lewis-base-stabilized dichlorosilylene: a two-electron σ -donor ligand. *Inorg Chem* 49:775–777
75. Ghadwal RS, Azhakar R, Pröpper K, Holstein JJ, Dittrich B, Roesky HW (2011) *N*-Heterocyclic carbene stabilized dichlorosilylene transition-metal complexes of V(I), Co(I), and Fe(0). *Inorg Chem* 50:8502–8508
76. Ghadwal RS, Sen SS, Roesky HW, Granitzka M, Kratzert D, Merkel S, Stalke D (2010) Convenient access to monosilicon epoxides with pentacoordinate silicon. *Angew Chem Int Ed* 49:3952–3955
77. Ghadwal RS, Roesky HW, Granitzka M, Stalke D (2010) A facile route to functionalized *N*-heterocyclic carbenes (NHCs) with NHC base-stabilized dichlorosilylene. *J Am Chem Soc* 132:10018–10020
78. Samuel PP, Azhakar R, Ghadwal RS, Sen SS, Roesky HW, Granitzka M, Matussek J, Herbst-Irmer R, Stalke D (2012) Stable silaimines with three- and four-coordinate silicon atoms. *Inorg Chem* 51:11049–11054
79. Ghadwal RS, Azhakar R, Roesky HW, Pröpper K, Dittrich B, Goedecke C, Frenking G (2012) Donor-acceptor stabilized silaformyl chloride. *Chem Commun* 48:8186–8188
80. Xiong Y, Yao S, Driess M (2009) An isolable NHC-supported silanone. *J Am Chem Soc* 131:7562–7563
81. Percival PW, Brodovitch JC, Mozafari M, Mitra A, West R, Ghadwal RS, Azhakar R, Roesky HW (2011) Free radical reactivity of mono- and dichlorosilylene with muonium. *Chem Eur J* 17:11970–11973
82. Chandra Mondal K, Roesky HW, Schwarzer MC, Frenking G, Tkach I, Wolf H, Kratzert D, Herbst-Irmer R, Niepötter B, Stalke D (2013) Conversion of a singlet silylene to a stable biradical. *Angew Chem Int Ed* 52:1801–1805
83. Chandra Mondal K, Roesky HW, Schwarzer MC, Frenking G, Niepötter B, Wolf H, Herbst-Irmer R, Stalke D (2013) A stable singlet biradicaloid siladicalbene: $(L)_2Si$. *Angew Chem Int Ed* 52:2963–2967
84. Yao S, Xiong Y, Driess M (2011) Zwitterionic and donor-stabilized *N*-heterocyclic silylenes (NHSis) for metal-free activation of small molecules. *Organometallics* 30:1748–1767
85. Okazaki R, Tokitoh N (2000) Heavy ketones, the heavier element congeners of a ketone. *Acc Chem Res* 33:625–630
86. Steele AR, Kipping FS (1929) Some derivatives of tri-*p*-tolylsilicane. *J Chem Soc* 357–358
87. Epping JD, Yao S, Karni M, Apeloig Y, Driess M (2010) Si=X multiple bonding with four-coordinate silicon? Insights into the nature of the Si=O and Si=S double bonds in stable silanoic esters and related thioesters: a combined NMR spectroscopic and computational study. *J Am Chem Soc* 132:5443–5455
88. Yao S, Xiong Y, Driess M (2010) *N*-Heterocyclic carbene (NHC)-stabilized silanechalcogenones: $NHC \rightarrow Si(R)_2 = E$ ($E = O, S, Se, Te$). *Chem Eur J* 16:1281–1288
89. Xiong Y, Yao S, Müller R, Kaupp M, Driess M (2010) From silicon(II)-based dioxygen activation to adducts of elusive dioxasilanes and sila-ureas stable at room temperature. *Nat Chem* 2:577–580
90. Patyk A, Sander W, Gauss J, Cremer D (1989) Dimethyldioxasilirane. *Angew Chem Int Ed Engl* 28:898–900
91. Sander W, Schroeder, Muthusamy S, Kirschfeld, Kappert W, Boese R, Kraka E, Sosa C, Cremer D (1997) Dimesityldioxirane. *J Am Chem Soc* 119:7265–7270

92. Sawwan N, Greer A (2007) Rather exotic types of cyclic peroxides: heteroatom dioxiranes. *Chem Rev* 107:3247–3285
93. Gao Y, Zhang J, Hu H, Cui C (2010) Base-stabilized 1-silacyclopenta-2,4-dienylidenes. *Organometallics* 29:3063–3065
94. Gao Y, Hu H, Cui C (2011) The reactivity of a silacyclopentadienylidene towards aldehydes: silole ring expansion and the formation of base-stabilized silacyclohexadienones. *Chem Eur J* 17:8803–8806
95. Leszczynska K, Abersfelder K, Mix A, Neumann B, Stammer H-G, Cowley MJ, Jutzi P, Scheschkewitz D (2012) Reversible base coordination to a disilene. *Angew Chem Int Ed* 51:6785–6788
96. Yamaguchi T, Sekiguchi A, Driess M (2010) An *N*-heterocyclic carbene-disilyne complex and its reactivity toward $ZnCl_2$. *J Am Chem Soc* 132:14061–14063
97. Yamaguchi T, Asay M, Sekiguchi A (2012) $[(Me_3Si)_2CH]_2PrSi(NHC)Si=Si(Me)Si^+Pr[CH(SiMe_3)_2]_2^+$: a molecule with disilynyl cation character. *J Am Chem Soc* 134:886–889
98. Filippou AC, Chernov O, Blom B, Stumpf KW, Schnakenburg G (2010) Stable *N*-heterocyclic carbene adducts of arylchlorosilylenes and their germanium homologues. *Chem Eur J* 16:2866–2872
99. Filippou AC, Chernov O, Stumpf KW, Schnakenburg G (2010) Metal-silicon triple bonds: the molybdenum silylydne complex $[Cp(CO)_2Mo\equiv Si-R]$. *Angew Chem Int Ed* 49:3296–3300
100. Dossett SJ, Hill AF, Jeffery JC, Marken F, Sherwood P, Stone FGA (1988) Chemistry of polynuclear metal complexes with bridging carbene or carbyne ligands. *J Chem Soc Dalton Trans* 2453–2465
101. Filippou AC, Chernov O, Schnakenburg G (2011) Chromium-silicon multiple bonds: the chemistry of terminal *N*-heterocyclic carbene-stabilized halosilylydne ligands. *Chem Eur J* 17:13574–13583
102. Ghadwal RS, Roesky HW, Schulzke C, Granitzka M (2010) *N*-Heterocyclic carbene stabilized dichlorosilanimine $IPr\cdot Cl_2Si=NR$. *Organometallics* 29:6329–6333
103. Ghadwal RS, Roesky HW, Pröpper K, Dittrich B, Klein S, Frenking G (2011) A dimer of silaisonitrile with two-coordinate silicon atoms. *Angew Chem Int Ed* 50:5374–5378
104. Cui H, Ma B, Cui C (2012) Metal-free, stereospecific bis-silylation of functionalized alkynes with NHC-supported silylamino-silylene. *Organometallics* 31:7339–7342
105. Cui H, Zhang J, Cui C (2013) 2-Hydro-2-aminophosphasilene with *N*-Si-P π conjugation. *Organometallics* 32:1–4
106. Böttcher T, Bassil BS, Zhechkov L, Heine T, Rösenthaller G-V (2013) $(NHC^{Me})SiCl_4$: a versatile carbene transfer reagent-synthesis from silicochloroform. *Chem Sci* 4:77–83
107. Bates JJ, Kennepohl P, Gates DP (2009) Abnormal reactivity of an *N*-heterocyclic carbene (NHC) with a phosphalkene: a route to a 4-phosphino-substituted NHC. *Angew Chem Int Ed* 48:9844–9847
108. Mendoza-Espinoza D, Donnadiou B, Bertrand G (2010) Synthesis of 4- and 4,5-functionalized imidazol-2-ylidenes from a single 4,5-unsubstituted imidazol-2-ylidene. *J Am Chem Soc* 132:7264–7265
109. Young NA (2013) Main group coordination chemistry at low temperatures: a review of matrix isolated group 12 to group 18 complexes. *Coord Chem Rev* 257:956–1010
110. Fuchter MJ (2010) *N*-Heterocyclic carbene mediated activation of tetravalent silicon compounds: a critical evaluation. *Chem Eur J* 16:12286–12294

Index

A

Acylsilanes, 24
Alkynyldisilenes, 144
Alkynylsilanes, 6
Amidophosphidosilylene, 220
Aminosilanides, 17
Aminosilyldisilylene, 137
Arylchlorosilylenes, 100, 218
Aryldisilenes, 27, 138, 141
Aryltrialkylidisilenes, 27

B

Benzil, 94
Benzophenone, 94, 212
Bicycloheptasilane, 79
Bicyclooctasilane, 79
Bicyclooctasil-1(5)-ene, 154
Bicyclopentasilane, 72
Bis(acylsilane), 24
Bis(diisopropylamino)silylene, 110
Bis(disilynyl) cuprate, 29
Bis(hydrosilyl)palladium, 109
Bis(silenide) mercury, 24, 27
Bis(silyloxy)silanes, 18
Bis(silyl)zinc, 9
Bis(trimethylsilyl)acetylene, 21, 160
Bis(tri-tert-butylsilyl)silylene, 110
Bis(zincate), 10
Bond dissociation energy (BDE), 160, 214
Boratasilene, 7
Borylsilanes, 6
Bromosilanes, 13, 21, 103, 134, 140, 144, 149

C

Cages, strained, 72
Calcium bicyclobutandiide, 33
Carbenes, N-heterocyclic, 87, 100, 158, 169, 203
Catalysis, 85
CGMT (Carter–Goddard–Malrieu–Trinquier) model, 134, 160
Chalcogen activation, carbocyclic silylene, 106
Chalcogenatrisilabicyclobutanes, 136
Chlorosilanes, 5, 10
Cluster compounds, 25, 35, 49
Cubanes, 9, 51
Cyclobutadiene, 33, 74
Cyclohexasilanyl bromide, 79
Cyclopentasilene, 163
Cyclopropenylsilanes, 108
Cyclosilanes, 4
Cyclotetrasiladienes, 149
Cyclotrisilanes, 29, 58, 71, 163
Cyclotrisilenes, 32, 117, 131, 136, 145, 150, 155, 218

D

Decamethylsilicocene, 4, 115
Decasilaadamantane, 79
Diadamantylsilane, 26
Dialkylsilylene tetrakis(trimethylsilyl)silacyclopentane-1,1-diyl, 103
Dialkyltetrachlorodisilane, 147
Diaminosilylene, 136
Diaryl-1,2-dibromodisilenes, 134, 160

- Diaryldisilanes/silenes, 141
 Diaryldisilyne, 159
 3,4-Dibromocyclotetrasilene, 152
 Dibromodisilenes, 134, 160
 Dichlorodisiladigermetane, 149
 Diethylaminosilanes, 17
 Digermadisilacyclobutadiene, 149
 Digermadisiletene, 157
 Dihalosilylenoids, 20
 Dihydriddisilenes, 140
 1,4-Dihydro-1,2-disilettes, 31
 Dihydrosilanes, 5
 Dihydrotrisilastannete, 32
 Dilithio silane aggregates, 24
 Dilithiosilanes, 22, 147
 Dilithiotetrasilanes, 27
 Dilithiotrisilane, 27
 Dilithium silandiide, 21
 Dimetallatetrasilanes, 27
 Dimetallo-disilanes, 132
 Dioxasilranes, 216
 Dioxasilolanes, 21
 Diphenylsilane, 7
 Disilabenzenes, 146
 Disilacyclobutenes, 153
 Disilacyclopentadienes, 150
 Disilacyclopropanimine, 170
 Disila-2-gallataallen anions, 22
 Disila-1-germatricyclopentane, 74
 Disila-2-indataallen anions, 22
 Disilamethyleneaziridines, 170
 Disilanes, 7, 10, 17, 23, 27, 52, 72, 79, 129, 141, 147, 157, 159
 Disilapentalene, 26
 2,3-Disilapyrazines, 146
 Disilastannacyclopropane, 139
 Disilene–disilanyl-silylene rearrangement, 163
 Disilenes, 125
 alkyl-substituted, 27, 103
 amino-substituted, 136
 aryl-substituted, 27, 30
 boryl-substituted, 139
 conjugated, 147
 cyano-substituted, 135
 cyclic, 152
 heteroatom-substituted, 133
 hydrogen-substituted, 140
 metal-substituted (metal disilenides), 27, 28, 130
 phosphino-substituted, 136
 pseudohalogen-substituted, 134
 silyl-substituted, 19, 28, 30, 32, 154
 Disilenides, 27, 28, 125, 129, 130
 Disilynes, 25, 28, 125, 129–133, 139, 140, 146, 153, 155, 218
 stable, 159
 Dismutational aromaticity, 76, 152
 Di(tert-butyl)tetrachlorodisilane, 53
 Di(tert-butyl)tetrahalodigermane, 53
 Dizinc silanes, 24
 Dodecahedrane, 51
 Donor–coordinate disilene-like compounds, 157
- E**
 Ehnysilyl anion, 31
 Ethynylsilanes, 6
- F**
 β -Fluorosilyl anion, 18
- G**
 Gallataallene, 23
 Germadisilacyclopentadiene, 35, 151
 Germadisilacyclopentasilanide, 35, 151
 Germanium clusters, 49
 Germatrisilacyclobutadiene, 33
- H**
 Halodisilenes, 166
 Hexagermaoctahedrane, 79
 Hexagermaprismanes, 58, 68
 Hexamesitylcyclotrigermane, 73
 Hexasilabenzenes, 32, 151
 Hexasilaprismanes, 49, 58, 68
 Hydridodibromosilanes, 140
 (Hydrosilyl)silyl radical, disproportionation, 157
 Hypersilyl lithium, 14
 α,ω -(Hypersilyl)silanes, 4
- I**
 Imidazol-2-ylidene, 169
 Indataallene, 23
- L**
 1-Lithio-1,2-bissilyldisilene, 141
 Lithiosilanes, 7
 Lithium cyclotrisilanides, 29
 Lithium dimethyl(phenyl)silane, 12

Lithium disilene, 28–32, 130
Lithium hexamethyldisilazane, 17, 137
Lithium hydridodisilene, 132
Lithium (phenyl)silanides, 8
Lithium α -(*tert*-butoxy)silanides, 18

M

Magnesium silylenoid, 21
Magnesium trisilapropene-1,3-diide, 32, 131
Magnesium trisilene-1,3-diide, 32, 131
Mercury bis(acylsilane), 24
Mercury bis(silene), 27
Metallosilyne, 219
Methoxysilyl anion, 17
Monosilanyl anions, 4

N

Naphthalenides, alkali metal, 27, 32, 33, 53, 132, 151
Neopentasilane, 5
NHC-stabilized, 101
Nonasilicides, 36

O

Octagermacubanes, 51, 61
Octasilacubanes, 49, 51, 61, 79
Octasilacuneane, 79
Oligosilanyl anions, 4
Oligosilyl anions, perhydrogenated, 4
Organic lightemitting diodes (OLED), 144
Organodilithiosilane, geminal, 22
Organodioxiranes, 216
Organosilicon compounds, Friedel–Crafts, 3
Oxadisilettes, 31
2-Oxa-silacyclopentene, 108

P

Pentagermapropellane, 73
Pentamethyldiethylenetriamine, 8
Pentaprismane, 52
Pentasilan[*n*]staffanes, 72
Pentasilatricyclopentane, 74
Pentasilicide dianion, 36
Phenylenetetrasiladiene, 30, 141–143
Phenylpentasilane, 5
Phosphadisilaindanes, 164
Phosphasilene, 23, 220
Polygermane cages, 78
Polysilane, 49

Polysilicon cages, 78
Potassium tetrasilatetrahedranide, 34
Propellanes, 73, 76

S

Silaborene, 23
Silacyclopentadienylenes, carbene-stabilized, 216
Silacyclopentenes, 20
Silacyclopropane, 20, 161
Silacycloprenenides, 30
Silafuorene anion, 26
Silaindene dianion, 26
Silaketenimines, 107
 α,ω -Silandiides, 4
Silaphosphene, 220
Silarenes, 107
Silylsilyl anion, 31
Siliconoid, 34
Silicon–silicon double bond, see: Disilenes
Silicon–silicon triple bonds, see: Disilynes
Silole monoanion/dianion, 25
Siloxiranes, 108
Silyl anions (silanides), 1
 chiral, 10
 zwitterionic, 14
Silylazides, 213
Silyl dianions, 22
Silylenecycloctetrasilane, 154, 163
Silylenes, 85
 acyclic, 85
 π and/or σ -coordinated ligands, 114
 base-stabilised, 85, 100
 σ -bonded substituents, 110
 carbocyclic, 85, 102
 π -coordinated, 85
 N-heterocyclic, 85
 phosphorus ylide-stabilised, 103
Silylenoids, 1, 17
Silyl enol ether, 108
Silyl(ethynyl)silanes, 6
Silylenes, 26
Silylimidazolium cations, 221
Silyliumylidene, 92, 115
Silylsilylene, 1,2-migration, 163
Silylzinc compounds, 9
Silynes, 26
 multiply bonded, 217
Small molecule bond activation, 85
Sparteine, 13
Spirosilanes, 26
Stannyldisilenes, 30

T

Tetraalkyldisilenes, 125, 162
Tetraalkyltrisilaallene, 147
Tetraaryldisilenes, 30, 141
Tetrabromocycloctetrasilane, 149, 152
Tetrabromodisilane, 52, 59
Tetrabromotetrasilane, 155
Tetrachlorodisilane, 23
Tetrachlorotetra-*t*-butylcycloctetrasilane, 79
Tetragermatetrahedranes, 59
Tetrahedranes, 9, 25, 34, 49, 51, 59, 60, 69
Tetrasilabenzobenzvalene, 75
Tetrasilabicyclobutane, 74
Tetrasilabutadiene, 23, 25, 27, 28, 130, 148
Tetrasilacyclobutenide, 31, 32
Tetrasiladistyrylbenzene, 30, 141–143
Tetrasilanes, 7, 10, 18
Tetrasilatetrahedranes, 9, 25, 34, 49,
59, 69
Tetrasilicide tetraanion, 36
Tetrasilylcycloctetrasilene, 155
Tetrasilyldiaryltetrasiladiene, 132
Tetrasilyldisilene, 19, 28, 154
Tetrasilyltrisilaallene, 155, 170
Thexyl octagermacubane, 55
Triaryldisilenides, 29–32, 130, 141
Triaryltrichlorocycloctetrasilane, 151

Tribromomonosilane, 52
Trimethylgermylsilane, 11
Trisilaallene, 23, 147, 155, 170, 204
Trisilaallyl chlorides, 29
Trisilabicyclobutane, 150
Trisilacyclopentadienide, 35
Trisilacyclopropanides, 30
Trisiladienes (trisilaallenes), 147
Trisilanes, 7, 17, 23, 29, 129
Trisilastannete, 32
Trisilyldisilenides, 28
Tris(methoxysilyl) ethers, 15
Tris(silyl)zincate, 10
Trityl tetrakis[3,5-bis(trifluoromethyl)phenyl]
borate, 69

Z

Zincates, 9, 10
Zinc bis(disilynyl)
29
Zinc bis(silanide), 16
Zinc disilenides, 130
Zinc silanide, 25
Zintl anions, 35, 51
Zintl phases, 35
Zirconium disilenides, 29, 130